frontiers | Research Topics

Volume II: Novel molecular mechanisms and innovative therapeutic approaches for age-associated diseases

Edited by
Leming Sun, Zhen Fan and Zhe-Sheng Chen

Published in
Frontiers in Molecular Biosciences
Frontiers in Bioengineering and Biotechnology

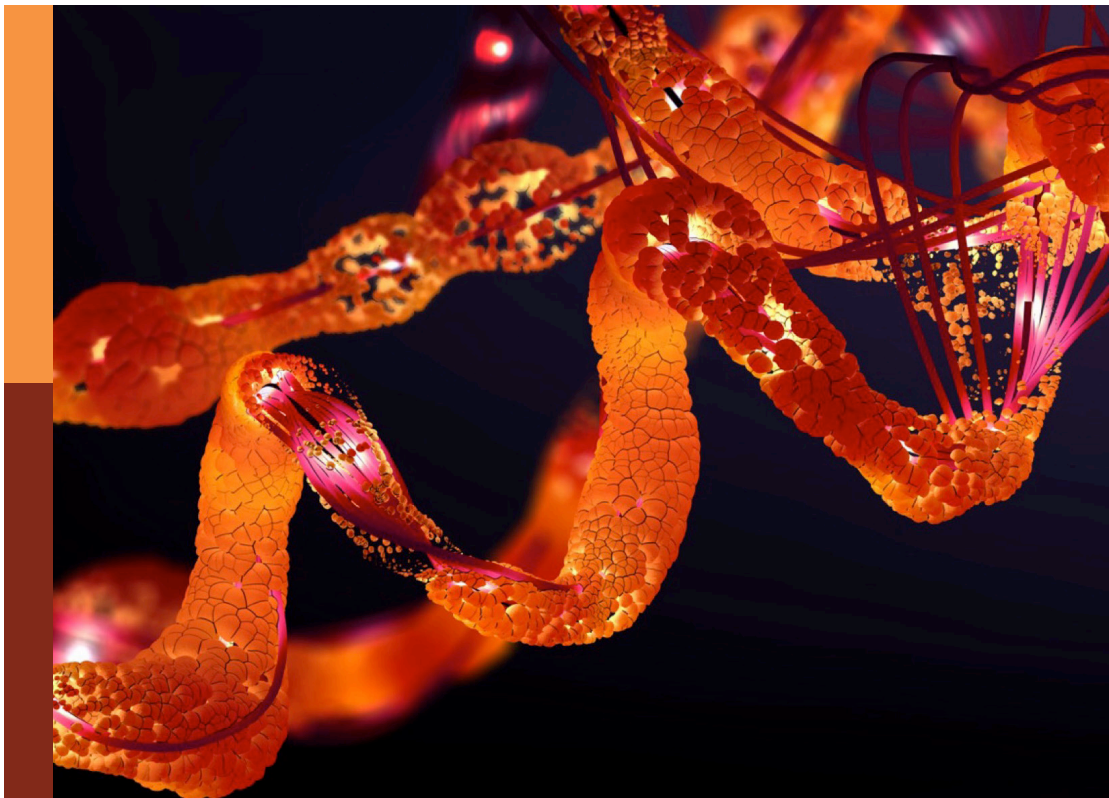

ISSN 1664-8714
ISBN 978-2-83251-121-3
DOI 10.3389/978-2-83251-121-3

About Frontiers

Frontiers is more than just an open access publisher of scholarly articles: it is a pioneering approach to the world of academia, radically improving the way scholarly research is managed. The grand vision of Frontiers is a world where all people have an equal opportunity to seek, share and generate knowledge. Frontiers provides immediate and permanent online open access to all its publications, but this alone is not enough to realize our grand goals.

Frontiers journal series

The Frontiers journal series is a multi-tier and interdisciplinary set of open-access, online journals, promising a paradigm shift from the current review, selection and dissemination processes in academic publishing. All Frontiers journals are driven by researchers for researchers; therefore, they constitute a service to the scholarly community. At the same time, the *Frontiers journal series* operates on a revolutionary invention, the tiered publishing system, initially addressing specific communities of scholars, and gradually climbing up to broader public understanding, thus serving the interests of the lay society, too.

Dedication to quality

Each Frontiers article is a landmark of the highest quality, thanks to genuinely collaborative interactions between authors and review editors, who include some of the world's best academicians. Research must be certified by peers before entering a stream of knowledge that may eventually reach the public - and shape society; therefore, Frontiers only applies the most rigorous and unbiased reviews. Frontiers revolutionizes research publishing by freely delivering the most outstanding research, evaluated with no bias from both the academic and social point of view. By applying the most advanced information technologies, Frontiers is catapulting scholarly publishing into a new generation.

What are Frontiers Research Topics?

Frontiers Research Topics are very popular trademarks of the *Frontiers journals series*: they are collections of at least ten articles, all centered on a particular subject. With their unique mix of varied contributions from Original Research to Review Articles, Frontiers Research Topics unify the most influential researchers, the latest key findings and historical advances in a hot research area.

Find out more on how to host your own Frontiers Research Topic or contribute to one as an author by contacting the Frontiers editorial office: frontiersin.org/about/contact

Volume II: Novel molecular mechanisms and innovative therapeutic approaches for age-associated diseases

Topic editors

Leming Sun — Northwestern Polytechnical University, China

Zhen Fan — Tongji University, China

Zhe-Sheng Chen — St. John's University, United States

Citation

Sun, L., Fan, Z., Chen, Z.-S., eds. (2023). *Volume II: Novel molecular mechanisms and innovative therapeutic approaches for age-associated diseases*. Lausanne: Frontiers Media SA. doi: 10.3389/978-2-83251-121-3

Table of contents

frontiers in Molecular Biosciences

REVIEW
published: 27 January 2022
doi: 10.3389/fmolb.2022.848105

PIWI-Interacting RNAs (piRNAs): Promising Applications as Emerging Biomarkers for Digestive System Cancer

Aiting Cai[1†], Yuhao Hu[1†], Zhou Zhou[1], Qianyi Qi[1], Yixuan Wu[1], Peixin Dong[2], Lin Chen[3*] and Feng Wang[1*]*

[1]*Department of Laboratory Medicine, Affiliated Hospital of Nantong University, Nantong, China,* [2]*Department of Obstetrics and Gynecology, Hokkaido University School of Medicine, Hokkaido University, Sapporo, Japan,* [3]*Department of Gastroenterology and Laboratory Medicine, Nantong Third Hospital Affiliated to Nantong University, Nantong, China*

OPEN ACCESS

Edited by:
Zhe-Sheng Chen,
St. John's University, United States

Reviewed by:
Fukang Sun,
Shanghai Jiao Tong University, China
Francisco Arenas-Huertero,
Children's Hospital of Mexico Federico Gómez, Mexico

***Correspondence:**
Peixin Dong
dpx1cn@gmail.com
Lin Chen
xiaobei227@sina.com
Feng Wang
richardwangf@163.com

†These authors have contributed equally to this work

Specialty section:
This article was submitted to Molecular Diagnostics and Therapeutics, a section of the journal Frontiers in Molecular Biosciences

Received: *04 January 2022*
Accepted: *12 January 2022*
Published: *27 January 2022*

Citation:
Cai A, Hu Y, Zhou Z, Qi Q, Wu Y, Dong P, Chen L and Wang F (2022) PIWI-Interacting RNAs (piRNAs): Promising Applications as Emerging Biomarkers for Digestive System Cancer. Front. Mol. Biosci. 9:848105. doi: 10.3389/fmolb.2022.848105

PIWI-interacting RNAs (piRNAs) are a novel type of small non-coding RNAs (sncRNAs), which are 26–31 nucleotides in length and bind to PIWI proteins. Although piRNAs were originally discovered in germline cells and are thought to be essential regulators for germline preservation, they can also influence gene expression in somatic cells. An increasing amount of data has shown that the dysregulation of piRNAs can both promote and repress the emergence and progression of human cancers through DNA methylation, transcriptional silencing, mRNA turnover, and translational control. Digestive cancers are currently a major cause of cancer deaths worldwide. piRNAs control the expression of essential genes and pathways associated with digestive cancer progression and have been reported as possible biomarkers for the diagnosis and treatment of digestive cancer. Here, we highlight recent advances in understanding the involvement of piRNAs, as well as potential diagnostic and therapeutic applications of piRNAs in various digestive cancers.

Keywords: Piwi-interacting RNA, cancer biomarker, diagnosis, prognosis, digestive system cancer, therapeutic target

1 INTRODUCTION

Cancer is the leading cause of death and a serious public health problem in China (Zeng et al., 2018; Feng et al., 2019). In 2018, half of the newly diagnosed cancers in China were in the digestive system (Zeng et al., 2018; Feng et al., 2019). More than one-third of all deaths were related to the digestive tract (Zeng et al., 2018; Feng et al., 2019). According to the Global Cancer Burden report, three of the top five most common cancers are digestive system cancers: hepatocellular carcinoma (HCC), gastric cancer (GC), and colorectal cancer (CRC) (Bray et al., 2018). Therefore, timely detection and standardized treatment are particularly critical. Studies have confirmed the key role of non-coding RNAs (ncRNAs) in mediating human carcinogenesis (ENCODE Project Consortium, 2012). PIWI-interacting RNAs (piRNAs) are the least studied sncRNAs and participate in epigenetic and retrotransposon post-transcriptional gene silencing by interacting with PIWI proteins (Xiao and Ke, 2016; Ozata et al., 2019). piRNAs were first identified in germ cell lines and their expression was also confirmed in somatic tissues (Girard et al., 2006; Martinez et al., 2015). piRNA precursors are transcribed from piRNA clusters, modified in the cytoplasm, and transported into the nucleus, where

piRNAs form complexes with PIWI proteins (Zhang et al., 2018). Some studies have shown that abnormally expressed piRNAs are closely related to a variety of malignancies (Yin and Lin, 2007; Ku and Lin, 2014). This article focuses on the regulatory role of piRNAs and PIWIs in digestive system cancers and discusses the potential clinical applications of piRNAs in digestive cancer diagnosis and treatment.

2 ORIGIN AND FUNCTION OF PIWI-INTERACTING RNAS

2.1 PIWI-Interacting RNAs and PIWI

piRNAs have the following six characteristics: 1) piRNAs are approximately 26–31 nucleotides in length, whereas microRNAs and siRNAs have lengths of 21–23 nucleotides. piRNAs are independent of the Dicer enzyme and are produced by a single-stranded precursor (Weng et al., 2019). 2) The majority of piRNA clusters in somatic cells are unidirectional, whereas the majority of germline piRNA clusters are dual-stranded (Yamanaka et al., 2014). 3) The majority of mature primary piRNAs contain uridine at the 5′ end, and the 3′ ends of piRNAs are uniquely methylated 2-OH structures (Hirakata and Siomi, 2016). 4) piRNAs are unevenly distributed among various genomic sequences, including exons, introns, and repeat sequences (Aravin et al., 2006; Girard et al., 2006; Grivna et al., 2006). 5) piRNAs are derived not only from the transposons themselves but also from the flanking genomic sequences (Aravin et al., 2006; Girard et al., 2006; Grivna et al., 2006). 6) piRNAs are not degraded in circulation and are stably expressed in body fluids (Yang et al., 2015; Freedman et al., 2016).

piRNAs have been detected in somatic cells and germ cells of mammals (mice and humans), Drosophila (Kawamura et al., 2008), Caenorhabditis elegans (Batista et al., 2008), and zebrafish (Houwing et al., 2008). Argonaute proteins are divided into the AGO subfamily and PIWI subfamily. PIWI proteins are mainly expressed in the germline and human tumors (Höck and Meister, 2008). The human PIWI protein subfamily consists of PIWIL1, PIWIL2, PIWIL3 and PIWIL4 (Höck and Meister, 2008). piRNAs are essential in many stages of spermatogenesis, and PIWIs are necessary to maintain the function of reproductive system stem cells (Weng et al., 2019). The absence of piRNAs can lead to pathogenic effects in the reproductive system, such as birth defects and infertility (Weng et al., 2019).

2.2 Biological Formation of PIWI-Interacting RNAs

piRNAs can be classified into three derived sources: lncRNAs, mRNAs, and transposons (Cheng et al., 2019). Most in-depth research has focused on the transposon source of piRNAs. piRNAs are produced from single-stranded precursors, and Dicer enzymes are not required. piRNA biogenesis has little in common with siRNA and miRNA biogenesis (Cheng et al., 2019). The biogenesis of piRNAs involves two pathways: primary amplification and secondary amplification (also described as a ping-pong amplification loop) (Cheng et al., 2019).

Several proteins, including RNA polymerase II, the Rhino-Deadlock- Cutoff complex (RDC complex), Moonshiner (Moon), TATA-box binding protein (TBP)-related factor 2 (TRF2), three prime repair exonuclease (TREX), and 56-kDa U2AF-associated protein (UAP56), are involved in the transcription of piRNA precursors in the nucleus (Aravin et al., 2006; Girard et al., 2006; Weng et al., 2019; Wu et al., 2020). RNA polymerase II is first recruited to piRNA clusters, and the RDC complex then helps to promote transcription. Moon interacts with the RDC complex and TRF2 to enhance transcription start. TREX prevents R-loop formation, and UAP56 inhibits dual-strand cluster splicing. After nuclear transport, piRNA precursors are resolved by the RNA helicase Armitage (Armi), and precursors are processed into pre-piRNAs by the endonuclease Zucchini (Zuc). Then, pre-piRNAs are loaded onto the PIWI proteins (PIWI and Aubergine), trimmed by an exonuclease Nibbler and methylated by the Hen1 methyltransferase.

In secondary amplification, primary piRNAs are stimulated through the catalysis of the AGO3 and Aubergine (Aub) proteins, finally producing mature piRNAs (Wu et al., 2020). Aub is loaded with piRNAs and this complex recognizes and cleaves complementary RNAs (such as transposon mRNAs or transcripts derived from the opposite strand of the same piRNA cluster). This cleavage produces the 5′ end of a new piRNA, which is subsequently loaded into AGO3 and induces the cleavage of complementary RNA. This results in a new piRNA that is identical in sequence to the piRNA that initiated the cycle (Wu et al., 2020). With repeated cutting, piRNA production is amplified. Therefore, generating a large number of piRNAs in a short time is called the ping-pong loop (Zhang et al., 2011). The piRNAs generated by the ping-pong loop are mature piRNAs. Once mature piRNAs or piRNA/PIWI protein complexes are formed, they can bind to target genes in the nucleus to silence or delay target gene transcription (Luteijn and Ketting, 2013).

2.3 Biological Functions of PIWI-Interacting RNAs

2.3.1 piRNAs and Transposon Silencing

In piRNA biogenesis, piRNA clusters are located in transposon elements. Thus, piRNAs are thought to be involved in transposon silencing through epigenetic mechanisms (DiGiacomo et al., 2013). Transposable elements shift and replicate by inserting themselves into the genome (Tóth et al., 2016). Improper insertion of transposable elements may lead to genomic mutations, such as chromosome deletion, duplication, and rearrangement (Hedges and Deininger, 2007). The activation of transposable elements will affect the integrity of the genome, which is very important for the transmission of genetic information. The activation of transposable elements can also damage DNA and lead to meiosis arrest, which in turn affects the growth and development of stem cells. The over-activation of transposable elements is potentially highly pathogenic and is quite harmful to the organisms (Vagin et al., 2006). piRNAs maintain genomic integrity by silencing

transposons (Fu and Wang, 2014; Lin et al., 2021). It has been proved that piRNAs interact with PIWI subfamily proteins, resulting in the development of the piRNA-induced silencing complex (piRISC), which detects and silences complementary sequences at the transcriptional (TGS) and post-transcriptional (PTGS) levels (Czech et al., 2018; Cheng et al., 2019). In the TGS, gene expression is suppressed by altering the chromosome. PTGS works through mRNA destabilization and mRNA translation inhibition (Liu et al., 2004; Phay et al., 2018).

2.3.2 PIWI-Interacting RNAs and DNA Methylation

DNA methylation is a type of DNA chemical modification and refers to the process of selectively adding S-Adenosyl-l-methionine (SAM) to specific bases by DNA methyltransferase (DNMT) (Pan et al., 2018). In the piRNA-PIWIL1 pathway, the activation of PIWIL1 can lead to a global loss of hypomethylation and specific regional changes in hypermethylation (Litwin et al., 2017). Hypomethylation can promote mitotic recombination and lead to chromosome deletion, ectopic rearrangement, and rearrangement (Sciamanna et al., 2011). Hypermethylation mostly occurs in the CpG islands of the promoter region. Under the regulation of DNMT, tumor suppressor genes can be inactivated, and transcription can be suppressed. The PIWI-piRNA pathway contributes to tumorigenesis through this mechanism (Yan et al., 2015). DNA methylation is also a critical mechanism leading to transposon silencing (Weng et al., 2019).

2.3.3 PIWI-Interacting RNAs and mRNA

After transcription, piRNAs have a function similar to that of microRNAs. They can induce mRNA degradation (Pek et al., 2012; Yu et al., 2019), thus hindering protein synthesis (Dai et al., 2020). The piRNA-mediated mRNA degradation can occur through two major mechanisms: either by the slicing of mRNA by PIWI or via a deadenylation-dependent mechanism (Rouget et al., 2010; Zhang et al., 2015). piRNAs and microRNAs are both important non-coding small RNAs, and they regulate gene expression. Whether piRNAs have a function similar to that of microRNAs requires further investigation.

2.3.4 Workflow for PIWI-Interacting RNA Discovery and Analysis

In general, a piRNA of interest can be extracted from non-piRNA molecules using high-throughput approaches (such as RNA-sequencing or microarray analysis). Multiple piRNA databases have been established for piRNA annotation. Northern blotting, *in situ* hybridization, and reverse transcription-quantitative polymerase chain reaction (RT-qPCR) are frequently used for experimental validation of piRNAs. The functional effect of a circRNA can be examined after piRNA silencing with shRNA or piRNA antisense inhibitor, or lentiviral vector/piRNA mimic-mediated piRNA overexpression. *In vitro* and *in vivo* assays provide essential insights into the piRNA's function in tumor cells. Finally, the molecules interacting with the piRNA (proteins and RNAs) could be identified using RNA binding protein immune-precipitation (RIP) experiments and luciferase reporter assays, respectively (Cheng et al., 2019; Huang et al., 2021; Liu et al., 2021) (**Figure 1**).

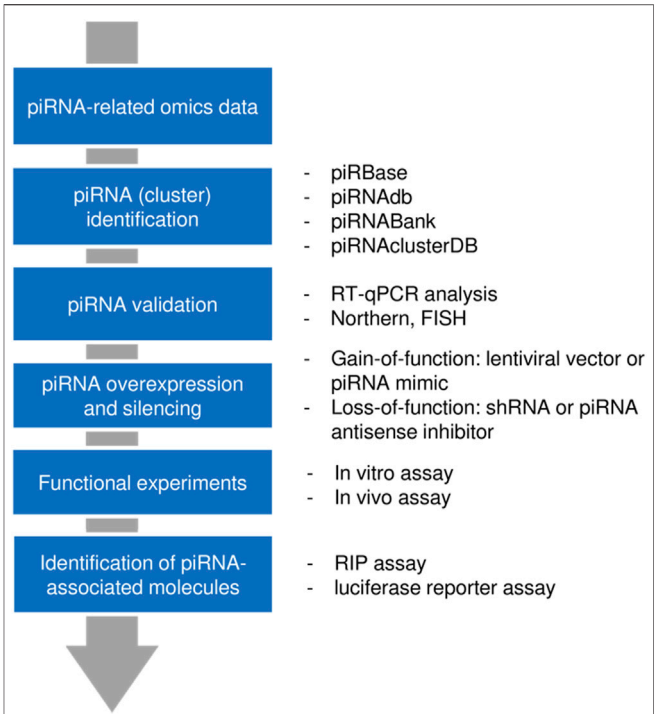

FIGURE 1 | Workflow for piRNA discovery and analysis. First, a candidate piRNA was identified from a pool of RNAs through high-throughput approaches. After validation, gain-of-function or loss-of-function models were generated and the functional impact of a piRNA was assessed. By using pulldown assay or reporter assay, those molecules that interact with piRNAs (proteins or RNAs) could be determined.

3 PIWI-INTERACTING RNAS IN DIGESTIVE SYSTEM CANCERS

The dysregulation of piRNA expression has been associated with various diseases, especially tumors and reproductive system diseases (Liu et al., 2019). piRNAs have pro-cancer or anti-cancer functions in cancer initiation, progression, and metastasis (Guo et al., 2020). piRNAs not only affect the growth, apoptosis, and invasion of tumor cells but also control cancer cell metastasis (Liu et al., 2018; Shen et al., 2018). In breast cancer, the levels of piR-4987 are positively correlated with lymph node metastasis (Huang et al., 2013). In addition, piR-823 expression is 2-fold higher in poorly differentiated colorectal cancer (CRC) tissues than in well/moderately-differentiated CRC tissues (Sabbah et al., 2021). The upregulation of piR-823 is associated with the presence of distant metastasis in gastric cancer (GC) patients (Cui et al., 2011).

Cancers of the digestive system include HCC, GC, CRC, pancreatic cancer, esophageal cancer, and biliary tract cancer. There is increasing evidence to support a strong association between piRNAs, PIWI proteins, and digestive system cancers

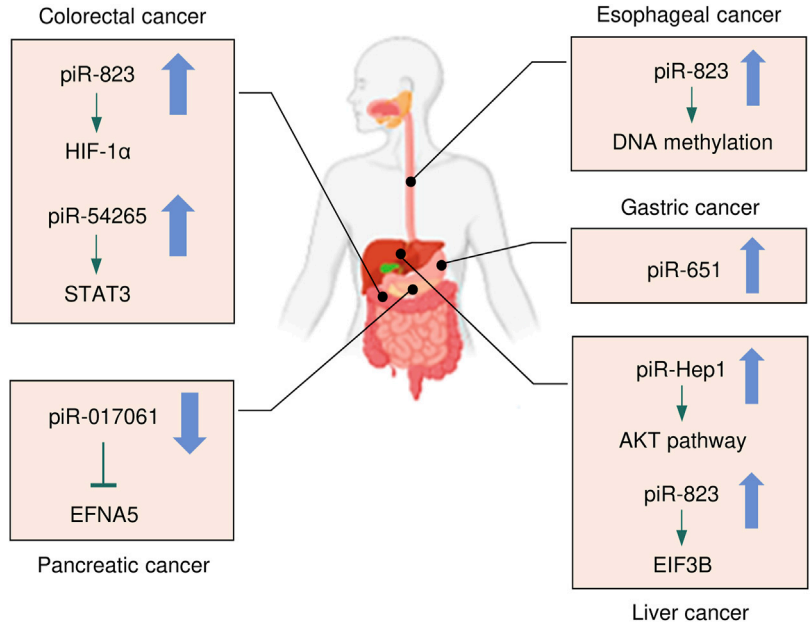

FIGURE 2 | The expression and underlying mechanisms of piRNAs in digestive system cancers. Oncogenic and anti-oncogenic piRNAs and their influence on the downstream pathways in digestive system cancers are shown. The up arrow indicates oncogenic piRNAs that are upregulated in digestive system cancers, while the down arrow suggests tumor-suppressive piRNAs that are downregulated in digestive system cancers.

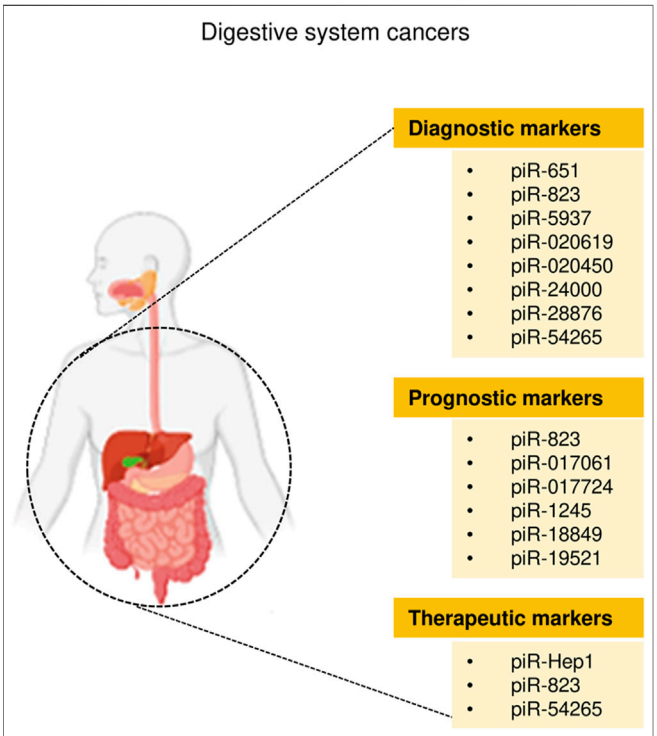

FIGURE 3 | The clinical application of piRNAs in digestive system cancers.

(Cui et al., 2011; Sabbah et al., 2021). The aberrant piRNA expression affects the tumorigenesis and progression of digestive system cancers (**Figures 2**, **3**). The current understanding of piRNAs and PIWI proteins in major digestive system cancers has been summarized in **Table 1**.

3.1 PIWI-Interacting RNAs and Hepatocellular Carcinoma

HCC is one of the most common malignancies worldwide and is the second leading cause of death in men (Islami et al., 2017). Chronic infection accounts for more than 78% of liver cancer cases in China (Islami et al., 2017). From 2013 to 2021, the incidence of liver cancer has increased in both men and women (Ryerson et al., 2016). With no obvious symptoms or characteristics in the early stage, the onset of liver cancer can go undetected. Most patients are already in the middle or late stage when they are first diagnosed. Therefore, it is particularly important to explore biomarkers that could be utilized in the early diagnosis and treatment of HCC.

Rizzo et al. (2016) applied small RNA sequencing technology to analyze piRNA expression patterns in different stages of liver disease. Changes in piRNA expression profiles can distinguish HCC tissue from liver cirrhosis (Rizzo et al., 2016). The Wilcoxon-Mann-Whitney test was used to evaluate the difference in piRNAs in various patterns of liver disease. The specific expression of piRNAs in tumors has been revealed. For example, piR-020498 is upregulated in high-grade dysplastic nodules and advanced HCC but is nearly undetectable in nodules of other degrees. Additionally, piR-013306 is overexpressed only in HCC. These results showed that piRNAs are involved in the progression of HCC and show specific expression in each stage (**Table 2**). The presence of

TABLE 1 | Summary of piRNAs and PIWI proteins in digestive system cancers.

Cancer type	piRNA	Expression	Biomarker utility	Source	Detection method	Ref
HCC	piR-Hep1	Upregulation	Promotes cell viability, motility, invasiveness, and activates the AKT pathway; therapeutic target	Cell lines, tissue	RT-qPCR, RNA sequencing, northern blotting	Law et al. (2013)
	PIWIL2/ PIWIL4	Upregulation	Prognostic biomarker	Tissue	Tissue chips, immunofluorescence staining	Zeng et al. (2017)
Hepatic fibrosis	piR-823	Upregulation	Binds to EIF3B to activate HSCs via upregulating TGF-β1	Activated HSCs	RT-qPCR, CCK-8, BrdU, RNA pull-down, liquid chromatography-mass spectrometry assay	Tang et al. (2018)
CRC	piR-017724	Downregulation	Prognostic biomarker	Tissue	RT-qPCR, RNA sequencing	Qu et al. (2019)
	piR-18849	Upregulation	Prognostic biomarker; positively correlated with lymph node metastasis and tumor grade	Tissue	RT-qPCR, RNA sequencing	Yin et al. (2019)
	piR-19521	Upregulation	Prognostic biomarker; negatively correlates with the degree of tumor differentiation	Tissue	RT-qPCR, RNA sequencing	Yin et al. (2019)
	PIWIL1	Upregulation	Prognostic biomarker; correlates with tumor differentiation degree, infiltration depth, lymphovascular invasion, lymph node metastasis and TNM stage	Tissue	Kaplan-Meier method, Cox's proportional hazards model, IHC and RT-qPCR	Sun et al. (2017)
	piR-5937	Downregulation	Diagnostic biomarker; decreased with advanced clinical stage	Blood serum	RT-qPCR	Vychytilova-Faltejskova et al. (2018)
	piR-28876	Downregulation	Diagnostic biomarker; decreased with advanced clinical stage	Blood serum	RT-qPCR	Vychytilova-Faltejskova et al. (2018)
	piR-020619	Upregulation	Diagnostic biomarker	Serum	RT-qPCR, ROC curve analysis	Wang et al. (2020)
	piR-020450	Upregulation	Diagnostic biomarker	Serum	RT-qPCR, ROC curve analysis I	Wang et al. (2020)
	piR-823	Upregulation	Inhibits the ubiquitination of HIF-1α by up-regulating the G6PD, up-regulates the glucose consumption of carcinoma cells and inhibits intracellular ROS; prognostic and therapeutic biomarker	Cell lines, tissues	RT-qPCR, CCK-8, invasion, apoptosis, glucose consumption assay, detection of intracellular ROS and half-life of G6PD	Feng et al. (2020)
	piR-823	Upregulation	Upregulates phosphorylation and transcriptional activity of HSF1; therapeutic target	Cell lines, tissue	CCK-8, cell cycle, colony formation, apoptosis, luciferase reporter, RIP assay	Yin et al. (2017)
	piR-24000	Upregulation	Diagnostic biomarker	Tissue	RT-qPCR	Iyer et al. (2020)
	piR-54265	Upregulation	Forms PIWIL2/STAT3/ p-SRC complex to activate STAT3 signaling; therapeutic target	Cell line, tissue, animal	Cell viability, colony formation, apoptosis, invasion, migration, RIP assay, animal experiments	Mai et al. (2018)
	piR-54265	Upregulation	Diagnostic biomarker	Tissue, serum	RT-qPCR	Mai et al. (2020)
	piR-1245	Upregulation	Prognostic biomarker	Cell lines, tissue	MTT, colony formation, invasion, migration, apoptosis assay	Weng et al. (2018)

(Continued on following page)

TABLE 1 | (*Continued*) Summary of piRNAs and PIWI proteins in digestive system cancers.

Cancer type	piRNA	Expression	Biomarker utility	Source	Detection method	Ref
GC	PIWIL1/2	Upregulation	Prognostic biomarker	Tissue	IHC	Wang et al. (2012)
	piR-651	Upregulation	Diagnostic biomarker	Peripheral blood	RT-qPCR	Cui et al., 2011
	piR-823	Upregulation	Diagnostic biomarker	Peripheral blood	RT-qPCR	Cui et al., 2011
	piR-651	Upregulation	Inhibits cell proliferation; diagnostic biomarker	Cell lines, tissue	MTT assay, cell cycle analysis, RT-qPCR	Cheng et al. (2011)
	PIWIL1	Upregulation	Prognostic biomarker	Cell lines, tissue	Wound-healing, invasion, cell proliferation assay	Gao et al. (2018)
	piR-823	Downregulation	Therapeutic target	Cell lines, tissue,	MTT, tumorigenicity assay	Cheng et al. (2012)
Pancreatic cancer	piR-017061	Downregulation	Inhibits cancer cell growth; prognostic biomarker	Cell lines, Tissue	Cell viability, colony formation assay, RT-qPCR	Müller et al. (2015), Xie et al. (2021)
Esophageal squamous cell carcinoma	piR-823	Upregulation	Induce DNA methylation, diagnostic biomarker	Tissue	RT-qPCR	Su et al. (2020)
	PIWIL1	Upregulation	Prognostic biomarker	Tissue	RT-qPCR, western blot, IHC	He et al. (2009)
Cholangiocarcinoma and gallbladder carcinoma	Exosomal piRNAs		Diagnostic biomarker	Blood	Exosome separation and RNA isolation, RNA sequencing and mapping	Gu et al. (2020)

TABLE 2 | Changes of piRNA expression during human liver carcinogenesis.

	Low-grade dysplastic nodules	High-grade dysplastic nodules	Early hepatocellular carcinoma	Progressed hepatocellular carcinoma
piR-001078, -001207, -001346, -017061, -017295, -019420, -020450	✓	✓	✓	✓
piR-001170, -016975, -017724, -019951, -020828, -020829	✓	✓	✓	✓
piR-020498	✗	✓	✓	✓
piR-013306	✗	✗	✗	✓

✓: Presence; ✗: Absence.

piRNA molecules was detected in all samples of HCC, verifying the involvement of these piRNAs in liver carcinogenesis.

Currently, the specific mechanisms by which piRNAs act in HCC remain unclear. Previous studies have indicated that piRNAs, such as piR-Hep1 (Law et al., 2013) and piR-823 (Tang et al., 2018), are closely linked with the occurrence and development of HCC. A novel piRNA, piR-Hep1, was identified through large-scale parallel sequencing (Law et al., 2013). When compared to normal cells, HCC cells have a 12-fold higher expression of piR-Hep1 (Law et al., 2013). Silencing of piR-Hep1 inhibited the proliferation, migration, and invasion ability of HCC cells (Law et al., 2013). Downregulation of piR-Hep1 also reduced the level of AKT phosphorylation (Nakanishi et al., 2005; Whittaker et al., 2010; Law et al., 2013). Interestingly, the expression of PIWIL2 was positively correlated with the level of piR-Hep1 in HCC tissues, implying that piR-Hep1 might mediate the PI3K/AKT pathway by binding to PIWIL2, thus playing a role in the function of HCC recurrence and progression. Hence, piR-Hep1 may represent a new therapeutic target for HCC.

The expression of piR-823 is significantly upregulated in activated hepatic stellate cells (HSCs), and the overexpression of piR-823 can promote HSC proliferation and the production of α-SMA and COL1a1. The binding of piR-823 with eukaryotic initiation factor 3B (EIF3B) activates HSCs in liver fibrogenesis by increasing transforming growth factor-β1 (TGF-β1) (Tang et al., 2018). Therefore, blockade of piR-823 might be a new strategy to treat liver fibrosis, a major risk factor for HCC.

The role of piRNAs is affected and regulated by their binding protein (Ding et al., 2018). RNA-binding proteins are also inextricably linked with HCC. Li et al. (2020) found that RNA-binding proteins help transform the physiological microenvironment into the tumor microenvironment by regulating protein synthesis, thus initiating the biogenesis of secondary mouse HCC. PIWIL1 (also known as HIWI) is a member of the PIWI subfamily. Studies have shown that PIWIL1 is highly expressed in HCC tissue and HCC cells (MHCC97L and MHCC97H) (Xie et al., 2015). The downregulation of PIWIL1, mediated by shRNA, restrains the proliferation and migration of HCC cells (Xie et al., 2015). The

expression of PIWIL1 was positively associated with HCC tumor size and metastasis and negatively associated with the survival rate (Zhao et al., 2012). After the knockdown of PIWIL1, the proliferation, invasion, and metastasis of HCC cells were suppressed (Zhao et al., 2012). Therefore, PIWIL1 may be a latent biomarker or therapeutic target for HCC. Zeng et al. (2017) investigated the cellular localization and expression of the molecular chaperones PIWIL2 and PIWIL4. The authors found that the co-expression of PIWIL2 and PIWIL4 could be employed as an indicator of poor prognosis and malignancy in HCC. The above findings indicated that both piRNAs and PIWI proteins are associated with the occurrence and development of HCC, and they have the potential to be used as novel biomarkers for HCC (**Figures 2**, **3**).

3.2 PIWI-Interacting RNAs and Colorectal Cancer

CRC has the third-highest cancer incidence and second-highest cancer mortality worldwide. It is among the top five mortality-causing cancers worldwide (Bray et al., 2018). The incidence of CRC has significantly increased in recent years (Chen et al., 2016; Bray et al., 2018). The detection efficiency of CRC is low, and early screening is hampered by complicated techniques, expensive costs, and the highly invasive nature of CRC. Therefore, many patients are diagnosed at an advanced stage. Because there is currently no effective treatment for CRC, the prognosis of CRC patients is very poor (Carethers and Jung, 2015). Consequently, it is urgent to find more reliable and useful predictive biomarkers for the early identification and diagnosis of CRC.

Many studies have indicated that piRNAs are involved in the process and development of CRC. The high expression level of piR-823 is positively correlated with the proliferation of CRC cells (Yin et al., 2017). piR-823 has been shown to recruit HSF1, a common transcription factor that upregulates heat shock proteins to exert its phosphorylation and transcriptional activity (Yin et al., 2017). This recruitment ability of piR-823 contributes to colon tumorigenesis (Yin et al., 2017). Additionally, CRC patients with high expression levels of piR-823 have a poorer prognosis than patients with low expression levels (Yin et al., 2017). High levels of piR-823 have been associated with poor treatment outcomes in patients with stage II and stage III CRCs. Furthermore, piR-823 was shown to enhance glucose-6-phosphate dehydrogenase (G6PD) expression to promote glucose consumption in CRC cells and downregulate the content of intracellular reactive oxygen species (ROS) by suppressing the ubiquitination of hypoxia-inducible factor-1α (HIF-1α) (Feng et al., 2020). In addition, the level of piR-54265 in CRC tissues was found to be higher than that in non-tumor tissues, and its expression was inversely correlated with the survival of patients with CRC (Mai et al., 2018). piR-54265 binds to PIWIL2 and forms the PIWIL2/STAT3/phosphorylated-SRC complex, thus promoting CRC metastasis and chemoresistance (Mai et al., 2018), suggesting that piR-54265 might be a hopeful therapeutic target for CRC. In another study, the level of piR-54265 in CRC patients decreased sharply after surgical treatment but then increased after tumor recurrence (Mai et al., 2020). Moreover, piR-54265 has shown significant specificity in the serum of patients with CRC (Mai et al., 2020). Therefore, serum piR-54265 holds the potential as a biomarker for monitoring of CRC.

Similarly, piR-1245 is overexpressed in CRC tissues, and regulates CRC cell survival by modulating the expression of tumor suppressor genes (Weng et al., 2018). Patients with high piR-1245 expression had markedly shortened overall survival times (Weng et al., 2018). By establishing a predictive group of piRNAs, previous studies have found that 5 piRNA molecules (Qu et al., 2019), piR-020619/piR-020450 (Wang et al., 2020), or piR-5937/piR-28876 (Vychytilova-Faltejskova et al., 2018) have stronger diagnostic potential when compared with the traditional marker CEA. The diagnostic potential of piRNAs also showed higher sensitivity and specificity. The expression of piR-017724 (Qu et al., 2019) and PIWIL1 (Sun et al., 2017) in serum was positively correlated with the overall survival and progression-free survival, suggesting that piR-017724 and PIWIL1 are independent prognostic factors in CRC. The overexpression of piR-18849 is connected to the degree of tumor differentiation and lymph node metastasis in CRC patients (Yin et al., 2019). Thus, piR-18849 may act as a potential therapeutic target for CRC and as an index to judge patient prognosis. The high piR-24000 expression is notably correlated with the phenotype of invasive CRC, including poor differentiation, distant metastasis, and advanced stage (Iyer et al., 2020). Furthermore, ROC analysis has indicated that there is an observable diagnostic ability of piR-24000 to distinguish CRC patients from healthy subjects (Iyer et al., 2020). Taken together, dysregulation of piRNAs is closely implicated in multiple signaling pathways that regulate the development and progression of CRC, and they could be critical diagnostic and prognostic biomarkers and vital therapeutic targets for CRC (**Figures 2**, **3**). However, the investigation of piRNAs in CRC is preliminary, and the role of piRNAs and their underlying mechanisms require further in-depth study.

3.3 PIWI-Interacting RNA and Gastric Cancer

GC is among the top 5 most common malignant tumors worldwide and is the third highest cause of mortality (Bray et al., 2018). The incidence of early gastric cancer has been extremely high, and the radical cure probability of patients with early GC is relatively higher than that of patients with advanced GC (Bray et al., 2018). Patients with advanced GC often have a poor prognosis. Therefore, there is an urgent need for developing new GC markers that can assess the progression of GC and forecast treatment outcomes.

Studies of piRNA profiles have found that piRNAs are abundant in the human stomach (Lin et al., 2019). Transcript analysis of healthy gastric tissues and GC samples identified that nearly half of piRNAs were upregulated in GC samples (Martinez et al., 2016). This implies that piRNAs might impact the pathogenesis of GC. piR-651 is more abundant in GC tissues than in non-cancer tissues, and downregulation of piR-651

inhibits the growth of GC cells (Cheng et al., 2011). The level of piR-823 is reduced in GC cell lines and GC tissues, and overexpression of piR-823 suppresses GC cell growth (Cheng et al., 2012). Experiments in nude mice demonstrated that piR-823 has a tumor-suppressive effect *in vivo* (Cheng et al., 2012). In another study, a ROC curve analysis has shown that the peripheral blood level of piR-823 was a valuable biomarker for differentiating GC patients from healthy controls (Cui et al., 2011). The high PIWIL2 expression was associated with shorter overall survival of GC patients (Wang et al., 2012). PIWIL1 is highly expressed in GC cell lines, and preventing PIWIL1 expression was shown to suppress the malignant behavior of GC cells (Gao et al., 2018). Overall, piRNAs and PIWI proteins could be used as new biomarkers for GC screening, GC diagnosis, and prognosis prediction, and targeted therapy (**Figures 2**, **3**).

3.4 PIWI-Interacting RNA and Pancreatic Cancer

Pancreatic cancer is the eighth most prevalent cancer in women and the 10th most common cancer in men (Chen et al., 2016). Pancreatic cancer is a highly malignant digestive tract cancer and is difficult to diagnose and treat. The expression of piR-017061 is downregulated in pancreatic cancer tissues than in normal tissues with a fold change of 2.3 (Müller et al., 2015). piR-017061 attenuates the development and growth of pancreatic cancer cells by cooperating with PIWIL1 to facilitate *EFNA5* mRNA degradation (Xie et al., 2021). These preliminary findings indicated that piR-017061 should be further investigated as a clinical marker of pancreatic cancer.

3.5 PIWI-Interacting RNA and Esophageal Cancer

Esophageal carcinoma is the sixth leading cause of death in humans, and its incidence is rapidly rising (Pennathur et al., 2013; Smyth et al., 2017). Overexpression of piR-823 was detected in esophageal cancer tissues, and the levels of piR-823 were positively correlated with the risk of lymph node metastasis (Su et al., 2020). Using ROC curve analysis, piR-823 was identified as a valuable biomarker for differentiating esophageal cancer from normal controls (Su et al., 2020). In addition, the expression of piRNA-823 and DNMT3B were positively associated with each other, indicating that piRNA-823 might play an oncogenic function in esophageal cancer by inducing aberrant DNA methylation via DNMT3B (Su et al., 2020). A higher amount of PIWIL1 protein expression in the cytoplasm of esophageal cancer cells is correlated to higher histological grade, advanced tumor stage, and poorer overall survival (He et al., 2009). More comprehensive research is required to understand the specific mechanisms of piR-823 in esophageal cancer.

3.6 PIWI-Interacting RNA and Biliary Tract Cancer

Biliary tract cancer arises from epithelial cells lining the biliary tract. Plasma exosomal piRNAs can be either significantly upregulated or downregulated in these patients (Gu et al., 2020). The levels of piR-10506469 were significantly increased in plasma exosomes from cholangiocarcinoma malign cholangiocarcinoma or gallbladder carcinoma patients compared with healthy individuals (Gu et al., 2020). Furthermore, the expression of piR-10506469 and piR-20548188 were significantly reduced after surgery (Gu et al., 2020). Thus, these piRNAs might serve as potential biomarkers of cholangiocarcinoma and gallbladder carcinoma.

4 THERAPEUTIC APPROACHES USING PIWI-INTERACTING RNAS

The potential of piRNAs to affect numerous downstream pathways can bring a significant impact on the molecular and functional landscape of cancer cells, promoting attempts to create future therapies that specifically target piRNAs (Jacovetti et al., 2021). Numerous preclinical research employing piRNA-based therapeutic compounds has already demonstrated outstanding results in terms of the capacity of piRNAs to influence the malignant features of HCC, CRC and GC cells (Cheng et al., 2012; Law et al., 2013; Mai et al., 2018) (**Figure 2**). The silencing of piR-Hep1 with a locked nucleic acid inhibitor inhibited cell viability, motility, and invasiveness in HCC cells (Law et al., 2013). In CRC cells, piR-54265 acts as an oncogenic piRNA, and overexpression of piR-54265 activates STAT3 signaling, consequently enhancing the proliferation, metastasis, and chemoresistance of CRC cells (Mai et al., 2018). Knockdown of piR-54265 using shRNA was associated with the inhibition of invasive ability and colony-forming capacity as well as attenuation of tumor growth in nude mice (Mai et al., 2018). Treatment with a specific chemically modified piR-54265 inhibitor significantly suppressed the growth and metastasis of implanted tumors in mice, and improved the sensitivity of CRC cells to 5-FU *in vivo* (Mai et al., 2018). These findings suggest that piR-Hep1 and piR-54265 could be druggable targets for the effective treatment of digestive cancers, and that combined chemotherapy with a piR-54265 inhibitor could be a viable future treatment option for CRC (**Figure 3**).

On the other hand, the restoration of tumor-suppressive piRNA could be considered another tool to achieve significant anti-tumor effects. For instance, lentiviral vector-mediated overexpression of piR-36712 in breast cancer cells suppressed malignant phenotypes and had a synergistic anti-tumor effect when combined with chemotherapy agents (Tan et al., 2019). Moreover, piR-823 mimics could significantly inhibit the growth of GC cells both *in vitro* and *in vivo* (Cheng et al., 2012). This observation suggests that piR-823 is a possible therapeutic target in digestive cancers (**Figure 3**).

5 FUTURE PERSPECTIVES

piRNAs have gradually attracted increasing attention since they were first discovered in animal germ cells in 2006. Although several studies have demonstrated a relationship between piRNAs and cancer biology, their roles and the respective regulatory mechanisms require further exploration. The following questions remain open for investigation:

1) How to precisely quantify piRNAs? Different piRNA expressions have been reported in cancer and adjacent normal tissues. However, the molecular features of adjacent normal tissues might be similar to that of cancer tissues (Krishnan and Damaraju, 2018). As a result, using surrounding normal tissues as a reference might lead to erroneous interpretation of piRNA expression. Normal tissues collected from healthy individuals may serve as a better control for comparison with tumor tissues (Krishnan and Damaraju, 2018).
2) How are piRNA transcripts generated in human cancer cells? HSP83/Shu is believed to play a role in the PIWI loading step, and HSP90 and its co-chaperone FKBP6 are required for the secondary piRNA biogenesis (Ishizu et al., 2012). However, most of our knowledge comes from Drosophila germline cells (Wu et al., 2020), and the exact mechanisms underlying piRNA biogenesis in human tumor cells remain largely unknown.
3) What are the mechanisms by which piRNAs exert their functions? Currently, the underlying mechanisms that account for the biological functions of piRNAs in tumor cells are still unclear. Upregulation of PIWI protein was a frequent event in many tumor types (Dong et al., 2021). Even in the absence of piRNAs, PIWI could interact with other molecules to induce tumorigenesis, cancer metastasis, and chemoresistance through piRNA-independent pathways (Dong et al., 2021). piRNA-interacting partners can be detected by high-throughput experimental approaches (Huang et al., 2021).
4) Do genetic variants alter the functions of the mature piRNAs, leading to their deregulation and the carcinogenic process? Single-nucleotide polymorphisms (SNPs) and insertion-deletion (INDELs) are of particular clinical importance due to their ability to impair gene functions (Karki et al., 2015). Some SNP variants in piRNA sequences have been associated with an increased risk of cancer development (Fu et al., 2015). Thus, it would be crucial to explore the effects of these genetic variations on piRNA functions and the development of digestive system cancers.
5) What are the roles of piRNAs in cancer stemness? The emerging roles of piRNAs in mediating cancer stem cell (CSC)-like properties have been observed (Su et al., 2021). It has been demonstrated that piR-823 was significantly upregulated in the ALDH-positive breast CSCs, and piR-823 confers stem-like properties to breast cancer cells by activating the Wnt signaling pathway (Ding et al., 2021). In clear cell renal carcinoma cells, piR-31115 induces epithelial-mesenchymal transition (EMT) via decreasing E-cadherin expression and increasing mesenchymal markers (Vimentin and Snail) (Du et al., 2021). These results suggest that the expression of certain piRNAs is required for the initiation and maintenance of CSCs, and the roles of piRNAs in gastrointestinal CSCs deserve further investigation.

6 CONCLUSION

At present, the approaches for the early diagnosis of major digestive system cancers are limited, and the prognosis of patients with digestive system cancers is still poor. Therefore, there is an urgent need to find more accurate and convenient clinical biomarkers that can assist in the diagnosis and treatment of these diseases. Growing evidence suggests that some individual piRNAs (such as piR-823 and piR-54265) modulate the occurrence, progression, and chemoresistance in multiple digestive cancers (such as HCC, CRC and GC) (**Figure 2**). However, the roles of dysregulated PIWI-piRNA pathway in digestive cancers have not been thoroughly investigated. Additional in-depth research will help to clarify the specific mechanisms by which piRNAs affect digestive system cancers. In conclusion, piRNAs represent new candidate diagnostic/prognostic biomarkers for digestive system cancers, as well as possible targets for future cancer therapy (**Figure 3**).

AUTHOR CONTRIBUTIONS

FW conceived the project and supervised the writing. AC and YH searched the literature and wrote the article. ZZ, QQ, YW made subsequent amendments. LC and PD revised the manuscript. All authors are involved in the revision and approved the final version of the manuscript.

FUNDING

This work was supported by the National Natural Science Foundation of China (81873978), the Key Project of Social Development in Jiangsu Province (BE2019691), the Chinese Postdoctoral Science Foundation (2018M642298), the Project of Jiangsu Commission of Health (Z2020011), and the Postdoctoral Research Funding Project of Jiangsu Province (2021K012A).

REFERENCES

Aravin, A., Gaidatzis, D., Pfeffer, S., Lagos-Quintana, M., Landgraf, P., Iovino, N., et al. (2006). A Novel Class of Small RNAs Bind to MILI Protein in Mouse Testes. *Nature* 442 (7099), 203–207. doi:10.1038/nature04916

Batista, P. J., Ruby, J. G., Claycomb, J. M., Chiang, R., Fahlgren, N., Kasschau, K. D., et al. (2008). PRG-1 and 21U-RNAs Interact to Form the piRNA Complex Required for Fertility in *C. elegans*. *Mol. Cell* 31 (1), 67–78. doi:10.1016/j.molcel.2008.06.002

Bray, F., Ferlay, J., Soerjomataram, I., Siegel, R. L., Torre, L. A., and Jemal, A. (2018). Global Cancer Statistics 2018: GLOBOCAN Estimates of Incidence and Mortality Worldwide for 36 Cancers in 185 Countries. *CA Cancer J. Clin.* 68 (6), 394–424. doi:10.3322/caac.21492

Carethers, J. M., and Jung, B. H. (2015). Genetics and Genetic Biomarkers in Sporadic Colorectal Cancer. *Gastroenterology* 149 (5), 1177–1190. doi:10.1053/j.gastro.2015.06.047

Chen, W., Zheng, R., Baade, P. D., Zhang, S., Zeng, H., Bray, F., et al. (2016). Cancer Statistics in China, 2015. *CA: A Cancer J. Clinicians* 66 (2), 115–132. doi:10.3322/caac.21338

Cheng, J., Deng, H., Xiao, B., Zhou, H., Zhou, F., Shen, Z., et al. (2012). piR-823, a Novel Non-coding Small RNA, Demonstrates *In Vitro* and *In Vivo* Tumor Suppressive Activity in Human Gastric Cancer Cells. *Cancer Lett.* 315 (1), 12–17. doi:10.1016/j.canlet.2011.10.004

Cheng, J., Guo, J.-M., Xiao, B.-X., Miao, Y., Jiang, Z., Zhou, H., et al. (2011). piRNA, the New Non-coding RNA, is Aberrantly Expressed in Human Cancer Cells. *Clinica Chim. Acta* 412 (17–18), 1621–1625. doi:10.1016/j.cca.2011.05.015

Cheng, Y., Wang, Q., Jiang, W., Bian, Y., Zhou, Y., Gou, A., et al. (2019). Emerging Roles of piRNAs in Cancer: Challenges and Prospects. *Aging* 11 (21), 9932–9946. doi:10.18632/aging.102417

Cui, L., Lou, Y., Zhang, X., Zhou, H., Deng, H., Song, H., et al. (2011). Detection of Circulating Tumor Cells in Peripheral Blood from Patients with Gastric Cancer Using piRNAs as Markers. *Clin. Biochem.* 44 (13), 1050–1057. doi:10.1016/j.clinbiochem.2011.06.004

Czech, B., Munafò, M., Ciabrelli, F., Eastwood, E. L., Fabry, M. H., Kneuss, E., et al. (2018). piRNA-Guided Genome Defense: From Biogenesis to Silencing. *Annu. Rev. Genet.* 52, 131–157. doi:10.1146/annurev-genet-120417-031441

Dai, P., Wang, X., and Liu, M.-F. (2020). A Dual Role of the PIWI/piRNA Machinery in Regulating mRNAs during Mouse Spermiogenesis. *Sci. China Life Sci.* 63 (3), 447–449. doi:10.1007/s11427-020-1632-5

DiGiacomo, M., Comazzetto, S., Saini, H., DeFazio, S., Carrieri, C., Morgan, M., et al. (2013). Multiple Epigenetic Mechanisms and the piRNA Pathway Enforce LINE1 Silencing during Adult Spermatogenesis. *Mol. Cell* 50 (4), 601–608. doi:10.1016/j.molcel.2013.04.026

Ding, D., Liu, J., Midic, U., Wu, Y., Dong, K., Melnick, A., et al. (2018). TDRD5 Binds piRNA Precursors and Selectively Enhances Pachytene piRNA Processing in Mice. *Nat. Commun.* 9 (1), 127. doi:10.1038/s41467-017-02622-w

Ding, X., Li, Y., Lü, J., Zhao, Q., Guo, Y., Lu, Z., et al. (2021). piRNA-823 Is Involved in Cancer Stem Cell Regulation through Altering DNA Methylation in Association with Luminal Breast Cancer. *Front. Cel Dev. Biol.* 9, 641052. doi:10.3389/fcell.2021.641052

Dong, P., Xiong, Y., Konno, Y., Ihira, K., Xu, D., Kobayashi, N., et al. (2021). Critical Roles of PIWIL1 in Human Tumors: Expression, Functions, Mechanisms, and Potential Clinical Implications. *Front. Cell Dev. Biol.* 9, 656993. doi:10.3389/fcell.2021.656993

Du, X., Li, H., Xie, X., Shi, L., Wu, F., Li, G., et al. (2021). piRNA-31115 Promotes Cell Proliferation and Invasion via PI3K/AKT Pathway in Clear Cell Renal Carcinoma. *Dis. Markers* 2021, 1–8. doi:10.1155/2021/6915329

ENCODE Project Consortium (2012). An Integrated Encyclopedia of DNA Elements in the Human Genome. *Nature* 489 (7414), 57–74. doi:10.1038/nature11247

Feng, J., Yang, M., Wei, Q., Song, F., Zhang, Y., Wang, X., et al. (2020). Novel Evidence for Oncogenic piRNA-823 as a Promising Prognostic Biomarker and a Potential Therapeutic Target in Colorectal Cancer. *J. Cell Mol. Med.* 24 (16), 9028–9040. doi:10.1111/jcmm.15537

Feng, R.-M., Zong, Y.-N., Cao, S.-M., and Xu, R.-H. (2019). Current Cancer Situation in China: Good or Bad News from the 2018 Global Cancer Statistics?. *Cancer Commun.* 39 (1), 22. doi:10.1186/s40880-019-0368-6

Freedman, J. E., Gerstein, M., Mick, E., Rozowsky, J., Levy, D., Kitchen, R., et al. (2016). Diverse Human Extracellular RNAs are Widely Detected in Human Plasma. *Nat. Commun.* 7, 11106. doi:10.1038/ncomms11106

Fu, A., Jacobs, D. I., Hoffman, A. E., Zheng, T., and Zhu, Y. (2015). PIWI-interacting RNA 021285 is Involved in Breast Tumorigenesis Possibly by Remodeling the Cancer Epigenome. *Carcin* 36 (10), 1094–1102. doi:10.1093/carcin/bgv105

Fu, Q., and Wang, P. J. (2014). Mammalian piRNAs. *Spermatogenesis* 4, e27889. doi:10.4161/spmg.27889

Gao, C.-l., Sun, R., Li, D.-h., and Gong, F. (2018). PIWI-Like Protein 1 Upregulation Promotes Gastric Cancer Invasion and Metastasis. *Ott* 11, 8783–8789. doi:10.2147/OTT.S186827

Girard, A., Sachidanandam, R., Hannon, G. J., and Carmell, M. A. (2006). A Germline-specific Class of Small RNAs Binds Mammalian Piwi Proteins. *Nature* 442 (7099), 199–202. doi:10.1038/nature04917

Grivna, S. T., Beyret, E., Wang, Z., and Lin, H. (2006). A Novel Class of Small RNAs in Mouse Spermatogenic Cells. *Genes Dev.* 20 (13), 1709–1714. doi:10.1101/gad.1434406

Gu, X., Wang, C., Deng, H., Qing, C., Liu, R., Liu, S., et al. (2020). Exosomal piRNA Profiling Revealed Unique Circulating piRNA Signatures of Cholangiocarcinoma and Gallbladder Carcinoma. *Acta Biochim. Biophys. Sin.* 52 (5), 475–484. doi:10.1093/abbs/gmaa028

Guo, B., Li, D., Du, L., and Zhu, X. (2020). piRNAs: Biogenesis and Their Potential Roles in Cancer. *Cancer Metastasis Rev.* 39 (2), 567–575. doi:10.1007/s10555-020-09863-0

He, W., Wang, Z., Wang, Q., Fan, Q., Shou, C., Wang, J., et al. (2009). Expression of HIWI in Human Esophageal Squamous Cell Carcinoma is Significantly Associated with Poorer Prognosis. *BMC Cancer* 9, 426. doi:10.1186/1471-2407-9-426

Hedges, D. J., and Deininger, P. L. (2007). Inviting Instability: Transposable Elements, Double-Strand Breaks, and the Maintenance of Genome Integrity. *Mutat. Res.* 616 (1–2), 46–59. doi:10.1016/j.mrfmmm.2006.11.021

Hirakata, S., and Siomi, M. C. (2016). piRNA Biogenesis in the Germline: From Transcription of piRNA Genomic Sources to piRNA Maturation. *Biochim. Biophys. Acta Gene Regul. Mech.* 1859 (1), 82–92. doi:10.1016/j.bbagrm.2015.09.002

Höck, J., and Meister, G. (2008). The Argonaute Protein Family. *Genome Biol.* 9 (2), 210. doi:10.1186/gb-2008-9-2-210

Houwing, S., Berezikov, E., and Ketting, R. F. (2008). Zili Is Required for Germ Cell Differentiation and Meiosis in Zebrafish. *EMBO J.* 27 (20), 2702–2711. doi:10.1038/emboj.2008.204

Huang, G., Hu, H., Xue, X., Shen, S., Gao, E., Guo, G., et al. (2013). Altered Expression of piRNAs and Their Relation with Clinicopathologic Features of Breast Cancer. *Clin. Transl. Oncol.* 15 (7), 563–568. doi:10.1007/s12094-012-0966-0

Huang, S., Yoshitake, K., and Asakawa, S. (2021). A Review of Discovery Profiling of PIWI-Interacting RNAs and Their Diverse Functions in Metazoans. *Int. J. Mol. Sci.* 22 (20), 11166. doi:10.3390/ijms222011166

Ishizu, H., Siomi, H., and Siomi, M. C. (2012). Biology of PIWI-Interacting RNAs: New Insights Into Biogenesis and Function Inside and Outside of Germlines. *Genes Dev.* 26 (21), 2361–2373. doi:10.1101/gad.203786.112

Islami, F., Chen, W., Yu, X. Q., Lortet-Tieulent, J., Zheng, R., Flanders, W. D., et al. (2017). Cancer Deaths and Cases Attributable to Lifestyle Factors and Infections in China, 2013. *Ann. Oncol.* 28 (10), 2567–2574. doi:10.1093/annonc/mdx342

Iyer, D. N., Wan, T. M.-H., Man, J. H.-W., Sin, R. W.-Y., Li, X., Lo, O. S.-H., et al. (2020). Small RNA Profiling of piRNAs in Colorectal Cancer Identifies Consistent Overexpression of piR-24000 that Correlates Clinically with an Aggressive Disease Phenotype. *Cancers* 12 (1), 188. doi:10.3390/cancers12010188

Jacovetti, C., Bayazit, M. B., and Regazzi, R. (2021). Emerging Classes of Small Non-Coding RNAs With Potential Implications in Diabetes and Associated Metabolic Disorders. *Front. Endocrinol.* 12, 670719. doi:10.3389/fendo.2021.670719

Karki, R., Pandya, D., Elston, R. C., and Ferlini, C. (2015). Defining "Mutation" and "Polymorphism" in the Era of Personal Genomics. *BMC Med. Genomics* 8, 37. doi:10.1186/s12920-015-0115-z

Kawamura, Y., Saito, K., Kin, T., Ono, Y., Asai, K., Sunohara, T., et al. (2008). Drosophila Endogenous Small RNAs Bind to Argonaute 2 in Somatic Cells. *Nature* 453 (7196), 793–797. doi:10.1038/nature06938

Krishnan, P., and Damaraju, S. (2018). The Challenges and Opportunities in the Clinical Application of Noncoding RNAs: The Road Map for miRNAs and piRNAs in Cancer Diagnostics and Prognostics. *Int. J. Genom.* 2018, 1–18. doi:10.1155/2018/5848046

Ku, H.-Y., and Lin, H. (2014). PIWI Proteins and Their Interactors in piRNA Biogenesis, Germline Development and Gene Expression. *Natl. Sci. Rev.* 1 (2), 205–218. doi:10.1093/nsr/nwu014

Law, P. T.-Y., Qin, H., Ching, A. K.-K., Lai, K. P., Co, N. N., He, M., et al. (2013). Deep Sequencing of Small RNA Transcriptome Reveals Novel Non-Coding RNAs in Hepatocellular Carcinoma. *J. Hepatol.* 58 (6), 1165–1173. doi:10.1016/j.jhep.2013.01.032

Li, G., Ni, A., Tang, Y., Li, S., and Meng, L. (2020). RNA Binding Proteins Involved in Regulation of Protein Synthesis to Initiate Biogenesis of Secondary Tumor in Hepatocellular Carcinoma in Mice. *PeerJ* 8, e8680. doi:10.7717/peerj.8680

Lin, X., Xia, Y., Hu, D., Mao, Q., Yu, Z., Zhang, H., et al. (2019). Transcriptome-Wide piRNA Profiling in Human Gastric Cancer. *Oncol. Rep.* 41 (5), 3089–3099. doi:10.3892/or.2019.7073

Lin, Y., Zheng, J., and Lin, D. (2021). PIWI-Interacting RNAs in Human Cancer. *Semin. Cancer Biol.* 75, 15–28. doi:10.1016/j.semcancer.2020.08.012

Litwin, M., Szczepańska-Buda, A., Piotrowska, A., Dzięgiel, P., and Witkiewicz, W. (2017). The Meaning of PIWI Proteins in Cancer Development. *Oncol. Lett.* 13 (5), 3354–3362. doi:10.3892/ol.2017.5932

Liu, J., Carmell, M. A., Rivas, F. V., Marsden, C. G., Thomson, J. M., Song, J.-J., et al. (2004). Argonaute2 Is the Catalytic Engine of Mammalian RNAi. *Science* 305 (5689), 1437–1441. doi:10.1126/science.1102513

Liu, J., Zhang, S., and Cheng, B. (2018). Epigenetic Roles of PIWI-Interacting RNAs (piRNAs) in Cancer Metastasis (Review). *Oncol. Rep.* 40 (5), 2423–2434. doi:10.3892/or.2018.6684

Liu, Y., Dou, M., Song, X., Dong, Y., Liu, S., Liu, H., et al. (2019). The Emerging Role of the piRNA/piwi Complex in Cancer. *Mol. Cancer* 18 (1), 123. doi:10.1186/s12943-019-1052-9

Liu, Y., Li, A., Xie, G., Liu, G., and Hei, X. (2021). Computational Methods and Online Resources for Identification of piRNA-Related Molecules. *Interdiscip. Sci. Comput. Life Sci.* 13 (2), 176–191. doi:10.1007/s12539-021-00428-5

Luteijn, M. J., and Ketting, R. F. (2013). PIWI-interacting RNAs: From Generation to Transgenerational Epigenetics. *Nat. Rev. Genet.* 14 (8), 523–534. doi:10.1038/nrg3495

Mai, D., Ding, P., Tan, L., Zhang, J., Pan, Z., Bai, R., et al. (2018). PIWI-interacting RNA-54265 is Oncogenic and a Potential Therapeutic Target in Colorectal Adenocarcinoma. *Theranostics* 8 (19), 5213–5230. doi:10.7150/thno.28001

Mai, D., Zheng, Y., Guo, H., Ding, P., Bai, R., Li, M., et al. (2020). Serum piRNA-54265 is a New Biomarker for Early Detection and Clinical Surveillance of Human Colorectal Cancer. *Theranostics* 10 (19), 8468–8478. doi:10.7150/thno.46241

Martinez, V. D., Enfield, K. S. S., Rowbotham, D. A., and Lam, W. L. (2016). An Atlas of Gastric PIWI-Interacting RNA Transcriptomes and Their Utility for Identifying Signatures of Gastric Cancer Recurrence. *Gastric Cancer* 19 (2), 660–665. doi:10.1007/s10120-015-0487-y

Martinez, V. D., Vucic, E. A., Thu, K. L., Hubaux, R., Enfield, K. S. S., Pikor, L. A., et al. (2015). Unique Somatic and Malignant Expression Patterns Implicate PIWI-Interacting RNAs in Cancer-type Specific Biology. *Sci. Rep.* 5, 10423. doi:10.1038/srep10423

Müller, S., Raulefs, S., Bruns, P., Afonso-Grunz, F., Plötner, A., Thermann, R., et al. (2015). Next-Generation Sequencing Reveals Novel Differentially Regulated mRNAs, lncRNAs, miRNAs, sdRNAs and a piRNA in Pancreatic Cancer. *Mol. Cancer* 14, 94. doi:10.1186/s12943-015-0358-5

Nakanishi, K., Sakamoto, M., Yamasaki, S., Todo, S., and Hirohashi, S. (2005). Akt Phosphorylation is a Risk Factor for Early Disease Recurrence and Poor Prognosis in Hepatocellular Carcinoma. *Cancer* 103 (2), 307–312. doi:10.1002/cncr.20774

Ozata, D. M., Gainetdinov, I., Zoch, A., O'Carroll, D., and Zamore, P. D. (2019). PIWI-Interacting RNAs: Small RNAs with Big Functions. *Nat. Rev. Genet.* 20 (2), 89–108. doi:10.1038/s41576-018-0073-3

Pan, Y., Liu, G., Zhou, F., Su, B., and Li, Y. (2018). DNA Methylation Profiles in Cancer Diagnosis and Therapeutics. *Clin. Exp. Med.* 18 (1), 1–14. doi:10.1007/s10238-017-0467-0

Pek, J. W., Patil, V. S., and Kai, T. (2012). piRNA Pathway and the Potential Processing Site, the Nuage, in the Drosophila Germline. *Dev. Growth Differ.* 54 (1), 66–77. doi:10.1111/j.1440-169x.2011.01316.x

Pennathur, A., Gibson, M. K., Jobe, B. A., and Luketich, J. D. (2013). Oesophageal Carcinoma. *Lancet* 381 (9864), 400–412. doi:10.1016/S0140-6736(12)60643-6

Phay, M., Kim, H. H., and Yoo, S. (2018). Analysis of piRNA-Like Small Non-coding RNAs Present in Axons of Adult Sensory Neurons. *Mol. Neurobiol.* 55 (1), 483–494. doi:10.1007/s12035-016-0340-2

Qu, A., Wang, W., Yang, Y., Zhang, X., Dong, Y., Zheng, G., et al. (2019). A Serum piRNA Signature as Promising Non-invasive Diagnostic and Prognostic Biomarkers for Colorectal Cancer. *Cancer Manag. Res.* 11, 3703–3720. doi:10.2147/CMAR.S193266

Rizzo, F., Rinaldi, A., Marchese, G., Coviello, E., Sellitto, A., Cordella, A., et al. (2016). Specific Patterns of PIWI-Interacting Small Noncoding RNA Expression in Dysplastic Liver Nodules and Hepatocellular Carcinoma. *Oncotarget* 7 (34), 54650–54661. doi:10.18632/oncotarget.10567

Rouget, C., Papin, C., Boureux, A., Meunier, A.-C., Franco, B., Robine, N., et al. (2010). Maternal mRNA Deadenylation and Decay by the piRNA Pathway in the Early Drosophila Embryo. *Nature* 467 (7319), 1128–1132. doi:10.1038/nature09465

Ryerson, A. B., Eheman, C. R., Altekruse, S. F., Ward, J. W., Jemal, A., Sherman, R. L., et al. (2016). Annual Report to the Nation on the Status of Cancer, 1975-2012, Featuring the Increasing Incidence of Liver Cancer. *Cancer* 122 (9), 1312–1337. doi:10.1002/cncr.29936

Sabbah, N. A., Abdalla, W. M., Mawla, W. A., AbdAlMonem, N., Gharib, A. F., Abdul-Saboor, A., et al. (2021). piRNA-823 is a Unique Potential Diagnostic Non-Invasive Biomarker in Colorectal Cancer Patients. *Genes* 12 (4), 598. doi:10.3390/genes12040598

Sciamanna, I., Vitullo, P., Curatolo, A., and Spadafora, C. (2011). A Reverse Transcriptase-Dependent Mechanism is Essential for Murine Preimplantation Development. *Genes* 2 (2), 360–373. doi:10.3390/genes2020360

Shen, S., Yu, H., Liu, X., Liu, Y., Zheng, J., Wang, P., et al. (2018). PIWIL1/piRNA-DQ593109 Regulates the Permeability of the Blood-Tumor Barrier via the MEG3/miR-330-5p/RUNX3 Axis. *Mol. Ther. Nucleic Acids* 10, 412–425. doi:10.1016/j.omtn.2017.12.020

Smyth, E. C., Lagergren, J., Fitzgerald, R. C., Lordick, F., Shah, M. A., Lagergren, P., et al. (2017). Oesophageal Cancer. *Nat. Rev. Dis. Primers* 3, 17048. doi:10.1038/nrdp.2017.48

Su, J.-F., Concilla, A., Zhang, D.-z., Zhao, F., Shen, F.-F., Zhang, H., et al. (2021). PIWI-interacting RNAs: Mitochondria-Based Biogenesis and Functions in Cancer. *Genes Dis.* 8 (5), 603–622. doi:10.1016/j.gendis.2020.09.006

Su, J.-F., Zhao, F., Gao, Z.-W., Hou, Y.-J., Li, Y.-Y., Duan, L.-J., et al. (2020). piR-823 Demonstrates Tumor Oncogenic Activity in Esophageal Squamous Cell Carcinoma through DNA Methylation Induction via DNA Methyltransferase 3B. *Pathol. Res. Pract.* 216 (4), 152848. doi:10.1016/j.prp.2020.152848

Sun, R., Gao, C.-l., Li, D.-h., Li, B.-j., and Ding, Y.-h. (2017). Expression Status of PIWIL1 as a Prognostic Marker of Colorectal Cancer. *Dis. Markers* 2017, 1–7. doi:10.1155/2017/1204937

Tan, L., Mai, D., Zhang, B., Jiang, X., Zhang, J., Bai, R., et al. (2019). PIWI-interacting RNA-36712 Restrains Breast Cancer Progression and Chemoresistance by Interaction with SEPW1 Pseudogene SEPW1P RNA. *Mol. Cancer* 18 (1), 9. doi:10.1186/s12943-019-0940-3

Tang, X., Xie, X., Wang, X., Wang, Y., Jiang, X., and Jiang, H. (2018). The Combination of piR-823 and Eukaryotic Initiation Factor 3 B (EIF3B) Activates Hepatic Stellate Cells via Upregulating TGF-β1 in Liver Fibrogenesis. *Med. Sci. Monit.* 24, 9151–9165. doi:10.12659/MSM.914222

Tóth, K. F., Pezic, D., Stuwe, E., and Webster, A. (2016). The piRNA Pathway Guards the Germline Genome Against Transposable Elements. *Adv. Exp. Med. Biol.* 886, 51–77. doi:10.1007/978-94-017-7417-8_4

Vagin, V. V., Sigova, A., Li, C., Seitz, H., Gvozdev, V., and Zamore, P. D. (2006). A Distinct Small RNA Pathway Silences Selfish Genetic Elements in the Germline. *Science* 313 (5785), 320–324. doi:10.1126/science.1129333

Vychytilova-Faltejskova, P., Stitkovcova, K., Radova, L., Sachlova, M., Kosarova, Z., Slaba, K., et al. (2018). Circulating PIWI-Interacting RNAs piR-5937 and piR-28876 Are Promising Diagnostic Biomarkers of Colon Cancer. *Cancer*

Epidemiol. Biomarkers Prev. 27 (9), 1019–1028. doi:10.1158/1055-9965.EPI-18-0318

Wang, Y., Liu, Y., Shen, X., Zhang, X., Chen, X., Yang, C., et al. (2012). The PIWI Protein Acts as a Predictive Marker for Human Gastric Cancer. *Int. J. Clin. Exp. Pathol.* 5 (4), 315–325.

Wang, Z., Yang, H., Ma, D., Mu, Y., Tan, X., Hao, Q., et al. (2020). Serum PIWI-Interacting RNAs piR-020619 and piR-020450 Are Promising Novel Biomarkers for Early Detection of Colorectal Cancer. *Cancer Epidemiol. Biomarkers Prev.* 29 (5), 990–998. doi:10.1158/1055-9965.EPI-19-1148

Weng, W., Li, H., and Goel, A. (2019). Piwi-interacting RNAs (piRNAs) and Cancer: Emerging Biological Concepts and Potential Clinical Implications. *Biochim. Biophys. Acta Rev. Cancer* 1871 (1), 160–169. doi:10.1016/j.bbcan.2018.12.005

Weng, W., Liu, N., Toiyama, Y., Kusunoki, M., Nagasaka, T., Fujiwara, T., et al. (2018). Novel Evidence for a PIWI-Interacting RNA (piRNA) as an Oncogenic Mediator of Disease Progression, and a Potential Prognostic Biomarker in Colorectal Cancer. *Mol. Cancer* 17 (1), 16. doi:10.1186/s12943-018-0767-3

Whittaker, S., Marais, R., and Zhu, A. X. (2010). The Role of Signaling Pathways in the Development and Treatment of Hepatocellular Carcinoma. *Oncogene* 29 (36), 4989–5005. doi:10.1038/onc.2010.236

Wu, X., Pan, Y., Fang, Y., Zhang, J., Xie, M., Yang, F., et al. (2020). The Biogenesis and Functions of piRNAs in Human Diseases. *Mol. Ther. Nucleic Acids* 21, 108–120. doi:10.1016/j.omtn.2020.05.023

Xiao, Y., and Ke, A. (2016). PIWI Takes a Giant Step. *Cell* 167 (2), 310–312. doi:10.1016/j.cell.2016.09.043

Xie, J., Xing, S., Shen, B.-Y., Chen, H.-T., Sun, B., Wang, Z.-T., et al. (2021). PIWIL1 Interacting RNA piR-017061 Inhibits Pancreatic Cancer Growth via Regulating EFNA5. *Hum. Cell* 34 (2), 550–563. doi:10.1007/s13577-020-00463-2

Xie, Y., Yang, Y., Ji, D., Zhang, D., Yao, X., and Zhang, X. (2015). Hiwi Downregulation, Mediated by shRNA, Reduces the Proliferation and Migration of Human Hepatocellular Carcinoma Cells. *Mol. Med. Rep.* 11 (2), 1455–1461. doi:10.3892/mmr.2014.2847

Yamanaka, S., Siomi, M. C., and Siomi, H. (2014). piRNA Clusters and Open Chromatin Structure. *Mobile DNA* 5, 22. doi:10.1186/1759-8753-5-22

Yan, H., Wu, Q.-L., Sun, C.-Y., Ai, L.-S., Deng, J., Zhang, L., et al. (2015). piRNA-823 Contributes to Tumorigenesis by Regulating *De Novo* DNA Methylation and Angiogenesis in Multiple Myeloma. *Leukemia* 29 (1), 196–206. doi:10.1038/leu.2014.135

Yang, X., Cheng, Y., Lu, Q., Wei, J., Yang, H., and Gu, M. (2015). Detection of Stably Expressed piRNAs in Human Blood. *Int. J. Clin. Exp. Med.* 8 (8), 13353–13358.

Yin, H., and Lin, H. (2007). An Epigenetic Activation Role of Piwi and a Piwi-Associated piRNA in Drosophila melanogaster. *Nature* 450 (7167), 304–308. doi:10.1038/nature06263

Yin, J., Jiang, X. Y., Qi, W., Ji, C. G., Xie, X. L., Zhang, D. X., et al. (2017). piR-823 Contributes to Colorectal Tumorigenesis by Enhancing the Transcriptional Activity of HSF 1. *Cancer Sci.* 108 (9), 1746–1756. doi:10.1111/cas.13300

Yin, J., Qi, W., Ji, C. G., Zhang, D. X., Xie, X. L., Ding, Q., et al. (2019). Small RNA Sequencing Revealed Aberrant piRNA Expression Profiles in Colorectal Cancer. *Oncol. Rep.* 42 (1), 263–272. doi:10.3892/or.2019.7158

Yu, Y., Xiao, J., and Hann, S. S. (2019). The Emerging Roles of PIWI-Interacting RNA in Human Cancers. *Cancer Manag. Res.* 11, 5895–5909. doi:10.2147/CMAR.S209300

Zeng, G., Zhang, D., Liu, X., Kang, Q., Fu, Y., Tang, B., et al. (2017). Co-Expression of Piwil2/Piwil4 in Nucleus Indicates Poor Prognosis of Hepatocellular Carcinoma. *Oncotarget* 8 (3), 4607–4617. doi:10.18632/oncotarget.13491

Zeng, H., Chen, W., Zheng, R., Zhang, S., Ji, J. S., Zou, X., et al. (2018). Changing Cancer Survival in China during 2003-15: A Pooled Analysis of 17 Population-Based Cancer Registries. *Lancet Glob. Health* 6 (5), e555–e567. doi:10.1016/S2214-109X(18)30127-X

Zhang, P., Kang, J.-Y., Gou, L.-T., Wang, J., Xue, Y., Skogerboe, G., et al. (2015). MIWI and piRNA-Mediated Cleavage of Messenger RNAs in Mouse Testes. *Cell Res.* 25 (2), 193–207. doi:10.1038/cr.2015.4

Zhang, Y., Liu, W., Li, R., Gu, J., Wu, P., Peng, C., et al. (2018). Structural Insights into the Sequence-Specific Recognition of Piwi by Drosophila Papi. *Proc. Natl. Acad. Sci. USA* 115 (13), 3374–3379. doi:10.1073/pnas.1717116115

Zhang, Z., Xu, J., Koppetsch, B. S., Wang, J., Tipping, C., Ma, S., et al. (2011). Heterotypic piRNA Ping-Pong Requires Qin, a Protein with Both E3 Ligase and Tudor Domains. *Mol. Cell* 44 (4), 572–584. doi:10.1016/j.molcel.2011.10.011

Zhao, Y.-M., Zhou, J.-M., Wang, L.-R., He, H.-W., Wang, X.-L., Tao, Z.-H., et al. (2012). HIWI is Associated with Prognosis in Patients with Hepatocellular Carcinoma After Curative Resection. *Cancer* 118 (10), 2708–2717. doi:10.1002/cncr.26524

Conflict of Interest: The authors declare that the research was conducted in the absence of any commercial or financial relationships that could be construed as a potential conflict of interest.

Publisher's Note: All claims expressed in this article are solely those of the authors and do not necessarily represent those of their affiliated organizations, or those of the publisher, the editors and the reviewers. Any product that may be evaluated in this article, or claim that may be made by its manufacturer, is not guaranteed or endorsed by the publisher.

frontiers in Molecular Biosciences

REVIEW
published: 11 February 2022
doi: 10.3389/fmolb.2022.842399

Mutations of CX46/CX50 and Cataract Development

Yumeng Shi[1], *Xinbo Li*[2]* *and Jin Yang*[1]*

[1]Key Laboratory of Visual Impairment and Restoration of Shanghai, Department of Ophthalmology and Visual Science, Eye Ear Nose and Throat Hospital of Fudan University, Shanghai, China, [2]Casey Eye Institute, Oregon Health and Science University, Portland, OR, United States

Cataract is a common disease in the aging population. Gap junction has been considered a central component in maintaining homeostasis for preventing cataract formation. Gap junction channels consist of connexin proteins with more than 20 members. Three genes including GJA1, GJA3, and GJA8, that encode protein Cx43 (connexin43), Cx46 (connexin46), and Cx50 (connexin50), respectively, have been identified in human and rodent lens. Cx46 together with Cx50 have been detected in lens fiber cells with high expression, whereas Cx43 is mainly expressed in lens epithelial cells. Disrupted expression of the two connexin proteins Cx46 and Cx50 is directly related to the development of severe cataract in human and mice. In this review article, we describe the main role of Cx46 and Cx50 connexin proteins in the lens and the relationship between mutations of Cx46 or Cx50 and hereditary cataracts. Furthermore, the latest progress in the fundamental research of lens connexin and the mechanism of cataract formation caused by lens connexin dysfunction are summarized. Overall, targeting connexin could be a novel approach for the treatment of cataract.

Keywords: gap junction, Cx46, Cx50, cataract, lens microcirculation, oxidative stress

OPEN ACCESS

Edited by:
Zhe-Sheng Chen,
St. John's University, United States

Reviewed by:
Pranjal Sarma,
University of Cincinnati, United States
Jie Chen,
Affiliated Eye Hospital of Wenzhou Medical University, China

***Correspondence:**
Jin Yang
jin_yang@fudan.edu.cn
Xinbo Li
lixinb@ohsu.edu

Specialty section:
This article was submitted to Molecular Diagnostics and Therapeutics, a section of the journal Frontiers in Molecular Biosciences

Received: *23 December 2021*
Accepted: *12 January 2022*
Published: *11 February 2022*

Citation:
Shi Y, Li X and Yang J (2022) Mutations of CX46/CX50 and Cataract Development. Front. Mol. Biosci. 9:842399. doi: 10.3389/fmolb.2022.842399

INTRODUCTION

Cataract is the opacity of lens and the most important cause of low vision and blindness worldwide. Cataract can be divided into metabolic cataract, age-related cataract, congenital cataract and others. With the increase of the elderly population, there are more and more aged-related cataract. Congenital cataract is the main cause of blindness in children, exerting a dramatic impact on their quality of life. Therefore, the prevention and treatment of cataract is particularly important. Lens homeostasis is critical to its transparency, and its imbalance can lead to cataract.

The lens is a biconvex transparent tissue situated between the iris and the vitreous, composed of a single layer of epithelial cells under the anterior capsule and the enormous lens fibers differentiated from epithelial cells (Ruan et al., 2020). Epithelial cells at the lens equator region migrate laterally toward the equator, where they transform into differentiating fiber cells and finally turn into mature fiber cells through extensive cell elongation. The lens is able to transmit light via the contraction or relaxation of the ciliary muscle and focus light onto the retina (Summers et al., 2021). In order to increase light transmission and minimize light scattering, various organelles including the Golgi apparatus, endoplasmic reticulum, and nucleus are degraded in the differentiating lens fibroblasts (Brennan et al., 2018; Brennan et al., 2021). In addition, lens crystallins are at high concentration in the lens to enable appropriate refractive ability that aids in light transmission and focusing (Cvekl and Eliscovich, 2021).

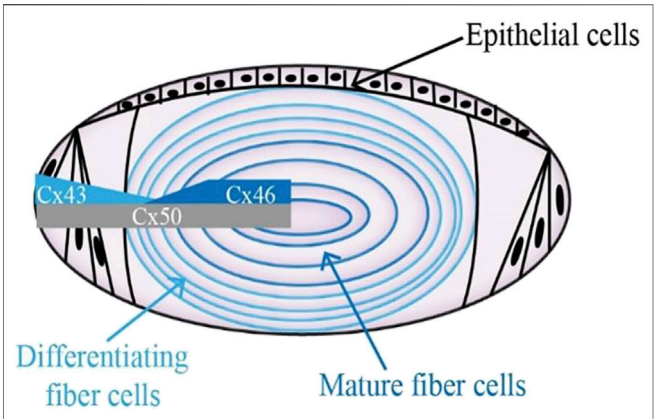

FIGURE 1 | Diagram showing the distribution of connexin hemichannels in the lens. Connexin isoform Cx43 is mainly expressed in the anterior epithelial layer. Cx46 can be found in the differentiating lens fibroblasts and mature lens fibroblasts. The expression of Cx50 stays the course of entire lens development.

Gap junction channels are critical in regulating the lens microcirculation system, which is crucial for the motion of the ions and other medium to maintain lens homeostasis (Brink et al., 2020; Valiunas et al., 2019; Valiunas and White, 2020). Moreover, gap junctional communication is a way to maintain normal lens fiber cells physiology and tissue functions (Van Campenhout et al., 2021). Gap junction channels facilitate these processes by permitting the selective passage of ions and other molecules, forming both electrical and biochemical coupling between cells. Gap junction channels are assembled by the coaxial alignment of two hemichannels. Six connexin molecules oligomerize into a hemichannel (also called connexon) (Beyer and Berthoud, 2014). Connexins are a family of structurally related transmembrane proteins in humans with approximately 20 members. Every single connexin protein consists of four transmembrane domains (T1-T4), two extracellular loops (EL1, EL2) with a cytoplasmic loop (IL), and cytoplasmic N-terminal and C-terminal components (Figueroa et al., 2019; Mese et al., 2007; Sánchez et al., 2019). Three connexins presented in the lens are α1 (Cx43), α3 (Cx46), and α8 (Cx50), which are encoded by three genes: Gja1, Gja3, and Gja8, respectively (Yue et al., 2021; Ping et al., 2021). In the layer of lens epithelial cells, abundant expression of Cx43 could be detected, whereas Cx46 is exclusively present in the lens fiber cell, where its expression corresponds with fiber cell differentiation, and Cx50 is widely expressed in both lens epithelial and fiber cells (**Figure 1**) (Paul et al., 1991; Delvaeye et al., 2018; Ceroni et al., 2019; Tong et al., 2021). Although the pathogenesis of cataracts is not yet fully clear (Davison, 2020; Hashemi et al., 2020; Shiels and Hejtmancik, 2021; Taylan Sekeroglu and Utine, 2021), a number of studies have shown that disruption of lens connexin hemichannels proteins Cx46 and Cx50 expression are associated with cataract formation (White et al., 1998; Chang et al., 2002; Addison et al., 2006; Xia et al., 2006a).

CX46 AND CX50 IN CATARACT FORMATION

Mutations of Cx46 and Cx50 Identified in Human and Rodents With Cataracts

More than 40 different mutations associated with cataractogenesis have been identified in the gene region of GJA3 and GJA8 in human pedigrees (**Table 1**). The first variant P-to-S transition at site 88 in Cx50 was identified in a British family with zonular pulverulent or "dust-like" cataracts (Mese et al., 2007). Subsequently, two mutations in the GJA3 gene have also been reported in different families with inherited congenital cataracts (Mackay et al., 1999).

More variants of these two connexin hemichannels have been reported in families in recent years. A heterozygous G-to-A substitution in the exon region of GJA3 gene was detected and resulted in the replacement of Asp with Gly at the N-terminus of Cx46 protein in a Chinese family with congenital nuclear pulverulent and posterior polar cataract (Rees et al., 2000). Another Cx46 variant, R76H, was identified in a large Australian cataract pedigree with zonular pulverulent cataract by using linkage analysis (Ping et al., 2021). Most of these mutations in the Cx46 protein are present in the N-terminal, the first transmembrane, and extracellular domains. One missense mutation N188T and another frameshift mutation at the position S380Qfs of Cx46 gene were found to be related to hereditary autosomal dominant cataract in two different Chinese families (Paul et al., 1991; Li et al., 2004). In addition, a missense mutation in the Cx46 coding region occurred in a Chinese cataract pedigree, giving rise to the dysfunction of the Cx46 protein, which might be potentially linked to the development of congenital nuclear cataract. Methionine substituted for valine at site 44 (V44M) in the Cx46 gene is responsible for that mutation (Chen et al., 2017).

Similar to Cx46, numerous mutations of the Cx50 gene have been identified. The first Cx50 mutation from a British family with zonular pulverulent cataract was identified at the second transmembrane domain of the encoded gene (Mese et al., 2007). Subsequently, Glu48Lys was the second recognized mutation reported in a three-generation Pakistani family (Berry et al., 1999). A missense variation V64G of Cx50 conserved residues in a Chinese family occurred at the phylogenetically conserved extracellular loop1 (Sharan et al., 2005). The autosomal dominant lamellar pulverulent cataract from a four-generation British family is associated with two mutations located at P88S and P88Q of GJA8, resulting from a 262C > A transition (Arora et al., 2006). In addition, an insertion mutation at codon 203 of GJA8 was mapped in a southern Indian family with autosomal recessive cataract, producing a functionally null allele and the subsequent reduction of transmembrane domain, cytoplasmic domain, and the second extracellular domain, and was different from the vast majority of mutations recognized with dominant features (Ponnam et al., 2007). Recently, a new variation at site 166 (c.166A > C) in Cx50 coding region was confirmed by the comprehensive screening by next-generation sequencing in a Mauritanian family with

TABLE 1 | Summary of Cx46 and Cx50 mutants associated with cataract formation.

Mutation	Cataract type	Family origin	References
Human Cx46			
N63S	zonular pulverulent	British	Mackay et al. (1999)
P187L	nuclear pulverulent	Chinese	Rees et al. (2000)
R76H	zonular pulverulent	Australian	Ping et al. (2021)
N188T	nuclear pulverulent	Chinese	Li et al. (2004)
V44M	nuclear	Chinese	Chen et al. (2017)
Human Cx50			
P88S	zonular pulverulent	British	Mese et al. (2007)
E48K	zonular nuclear pulverulent	Pakistani	Berry et al. (1999)
V64G	nuclear	Chinese	Sharan et al. (2005)
P88S, P88Q	lamellar pulverulent	British	Arora et al. (2006)
T56P	nuclear	Mauritanian	Hadrami et al. (2019)
S217P	perinuclear	Chinese	Li et al. (2019)
Rat Cx46			
E42K	nuclear	Cataract rat strain	Yoshida et al. (2005)
Mouse Cx50			
A47A	nuclear	No2 cataract mouse	Steele et al. (1998)
V64A	nuclear and zonular cataract and microphthalmia	Mouse Aey5 generated by ENU	Graw et al. (2001)
G22R	microphthalmia and dense cataract	Lop10 mutation cataract mice	Chang et al. (2002)
S50P	whole cataract and small eye	ENU mutagenesis	Xia et al. (2006b)
Rat Cx50			
R340W	cataract	UPL rat strain	Yamashita et al. (2002)

congenital nuclear cataracts (Hadrami et al., 2019). Moreover, a novel missense mutation of c.217T > C in a four-generation Chinese family with autosomal dominant congenital cataract (ADCC) was identified, resulting from a serine-to-proline interchange at residue 73 of the Cx50 gene (Li et al., 2019).

In addition to humans, mutations of Cx46 and Cx50 in homozygous mice can cause cataracts. Targeted deletion of GJA3 and GJA8 genes in mice can develop into a dominant or semi-dominant cataract pattern. Abundant mutations have been reported in mice. A single A-to-C transversion within codon 47 was amplified and sequenced in the Cx50 protein-coding regions in No2 cataractous mouse, resulting in congenital hereditary cataracts (Steele et al., 1998). Furthermore, an ethylnitrosourea mutagenesis screen analysis revealed a new cataract mutation, Val-to-Ala interchange at codon 64 of Cx50, in mice with phenotypically hereditary congenital cataracts (Graw et al., 2001). Lens opacity 10 (Lop10) mutation at chromosome 3 and a missense single transversion (G-to-C) in the Cx50 coding region was identified in a mouse that developed microphthalmia with dense cataracts, resulting in Gly-to-Arg substitution at codon 22 (Chang et al., 2002). Moreover, another variant S50P in the Cx50 protein was reported to be associated with smaller lens (Xia et al., 2006b). Apart from mice, connexin mutations have also been detected in rats with cataracts. A C-to-T transversion located at codon 340 in the Cx50 genes was strongly associated with the development of cataracts in the Upjohn Pharmaceuticals Limited (UPL) rat model (Yamashita et al., 2002). A missense mutation at site E42K in the coding region of Cx46 from rats with congenital nuclear cataracts was reported (Yoshida et al., 2005). Only a few mutations in rodents have been utilized for the investigation of gap junction channel, and therefore it is necessary for us to broaden the related studies.

The Relationship Between Connexin Hemichannels and Cataract Formation

Mathia et al. pointed out that the lens develops an internal circulation system that deliver water, ions, and solute for lens cells to replenish its lack of blood supply (Mathias et al., 2007). It allows nutrients and ions to enter the lens from both the anterior and posterior and to migrate to the center across the extracellular spaces, and unwanted metabolites to exit at the lens equator. The lens is full of plentiful and functional ion channels and transporters that support the internal circulation system. Dysfunction of the lens circulation system has been postulated to linked to cataract formation (Berthoud et al., 2020). Lens gap junctions formed by two oligomeric subunits referred to as hemichannels (also called connexons) display a critical effect on the lens internal circulation system. Both Cx46 and Cx50 form functional homomeric/homotypic gap junction channels and hemichannels. *In vitro* studies demonstrate that majority of lens connexin mutations linked to congenital cataracts will decrease coupling conductance and influence lens circulation (Gong et al., 2007; Berthoud and Ngezahayo, 2017). Most mutations of the Cx46 and Cx50 gene leading to cataracts are recognized as autosomal dominant, but several mutations that have been investigated are non-functional in terms of expression systems (Gerido et al., 2003). Apart from that, connexin variants with increased hemichannel activity could affect lens circulation through cell depolarization, which would reduce the ability of ions and other signals to migrate throughout the organ.

As previously reported, Cx50 knockout mice developed smaller eyes and lens—32 and 46% size reduction in the mass of control littermates, respectively (Gerido et al., 2003). Several studies observed that targeted deletion of GJA8 in mice led to delay in cell denucleation, indicating an important part of Cx50 in

lens fibroblast maturation and epithelial cell proliferation (Graw et al., 2001; Sellitto et al., 2004). The expression of Cx50 in place of Cx46 by gene knock-in did not rescue epithelial proliferation, implying that Cx50, but not Cx46, facilitates normal lens growth and development after growth factor stimulation (Yamashita et al., 2002; White et al., 2007; Minogue et al., 2017).

Substantial studies have revealed that knockout of Cx46 gene in mice leads to the impairment of lens transparency and the development of nuclear cataracts, probably caused by accumulation of crystallin cleavage products and production of an insoluble complex of disulfide-associated polypeptides (Gong et al., 1997). In addition, the coupling conductance was completely eliminated when the lens fiber matured, while the conductance in differentiated fibers was greatly reduced. Cx46 deletion-induced nuclear cataracts are also strongly correlated with the elevation of intracellular Ca^{2+} and corresponding change of increased protein degradation in lens fiber cells (Baruch et al., 2001). Change in gap junction communication due to mutations in the lens may be one of the important reasons for the formation of cataracts (Sharan et al., 2005; Schadzek et al., 2019).

Recent studies demonstrated that mutations in connexin hemichannels have a great impact on the function of gap junction channels. A missense mutation with an Asp-to-Ala substitution at site 47 in the first extracellular domain of Cx50 protein in No2 mice resulted in the loss of ability to produce functional gap junction channels, leading to cataractogenesis (Katai et al., 1999). A G-to-A transition mutation at position 139 was identified in the coding region of Cx50 from a family with autosomal dominant nuclear pulverulent cataracts, and also resulted in the loss of ability to generate functional gap junction channels in paired oocytes (Schadzek et al., 2019). Mixed hemichannels consisting of normal and abnormal Cx50 or Cx46 proteins in the lens displayed remarkably altered gating properties and coupling conductance, which may give rise to cataract formation. It is still unknown what the specific role of connexin hemichannels in the lens is.

POSSIBLE MECHANISMS OF CATARACTS RELATED TO LENS CONNEXIN

Lens Microcirculation and Biomineralization

It is generally known that gap junction channels could maintain the homeostasis of ocular lens by propagating lens microcirculation. Under normal conditions, the circuit of the lens microcirculation is completed when Na^+/K^+-ATPase or Na^+/Ca^{2+} exchanger and Ca^{2+}-ATPase on epithelial cells transport Na^+ and Ca^{2+} ions out of the lens when these intracellular ions are located at the surface of cell (Delamere and Tamiya, 2004; De Maria et al., 2018). Such pumps can produce low intracellular sodium and calcium concentration and form an electrochemical environment (Alvarez et al., 2001; Alvarez et al., 2003; Okafor et al., 2003). To maintain the Na^+/Ca^{2+} gradient, gap junction channels of the lens regulate circulation system through passive diffusion. Disruption of the lens microcirculation has been implicated in cataract pathogenesis. In the normal mouse lens, differentiating fiber gap junctions facilitate sodium ion flow to the equator once it enters the intercellular compartment. However, it has been found that the intercellular concentration of Na^+ becomes promoted in lenses isolated from mice expressing Cx46-and Cx50-dominant mutants (Gao et al., 2018). Moreover, loss of Cx46 causes calcium accumulation and subsequent elevation in the activity of Lp82, which is a type of Ca^{2+}-dependent protease that generate γ-crystallin cleavage products (Baruch et al., 2001; Ebihara et al., 2003). Measurement of calcium in Cx46 knockout has demonstrated that loss of intracellular coupling leads to the blockage of the efflux path to accumulate Ca^{2+} (Gao et al., 2004). There is also a hypothesis that reduction of Cx46 and Cx50 levels alter the function of gap junction channels in regulating the circulation of lens internal mediums, bringing about further changes to other major components in the lens microcirculation. These experimental evidences offer additional support that calcium displays different distribution patterns in wild-type, knockout and knock-in lens in microcirculation models.

Calcium has also been reported to be tightly related to the development of cataracts (Gerido et al., 2003). Different etiologies of cataract lenses in humans and mice contained increased Ca^{2+} (Vanden Abeele et al., 2006). Elevation of intracellular calcium concentration and corresponding elevated protein degradation in lens fibroblasts due to loss of Cx46 gene are associated with nuclear cataract formation (Liu et al., 2015). Calpain II, a kind of Ca^{2+}-dependent protease, induces the development of nuclear cataracts in Cx46 knockout lenses by cleaving crystallin proteins (Baruch et al., 2001). Proteolysis caused by calpain has also been shown to play a role in the truncation of Cx50 (Xia et al., 2006a). Gap junction coupling is also impaired due to sharply declined levels of Cx46 and Cx50 proteins and elevated total calcium concentration in cataract lens from homozygous β-crystallin S11R-mutant mice (Li et al., 2010). Abundant investigations demonstrate an important role of calmodulin (CaM) in maintaining functional gap junction channels. Increased Cx hemichannel activity is mediated by increased intercellular Ca^{2+} concentration and the activation of CaM. The voltage from oocytes expressing Cx46 G143R loses control of hemichannels, which forms a leaky gate, leading to diminish voltage-dependent ionic conductance (Li et al., 2008). A sequence of results showed that loss of cell-cell communication impairs the movement of ions such as Na^+ and Ca^+ towards the epithelium, inducing an alteration of $[Na^+]_i$ and $[Ca^+]_i$ gradient in Cx46fs380 mice lenses (Berthoud et al., 2014). These alterations lead to a vicious spiral that could ultimately exacerbate the occurrence of cataracts. Thus, extrapolation to humans shows that people suffering from severely declined levels of connexin or damaged gap junction function may develop cataracts on account of lens microcirculation disorders.

Numerous observations suggest that accumulation of insoluble calcium salts results in the development of cataracts. It probably likely that Ca^+ would precipitate due to the high concentration of more than 1 μM in the center of the lens, forming insoluble calcium salts (Berthoud et al., 2019). Moreover, using Alizarin acid staining identified immobile and

insoluble Ca^{+} in cataractous lenses from Cx46 and Cx50 knockout mice (Gao et al., 2018). These finding may be consistent with calcium oxalate or calcium carbonate crystals found in cataracts patients.

Biomineralization occurs when insoluble precipitates comprising inorganic ions deposit and form mixed particles. Impaired lens circulation in Cx46 and Cx50 knockout mice caused cataracts though Ca^{+} accumulation, precipitation, and biomineralization (Gao et al., 2013). Moreover, modification of the connexins, including via proteolysis, ubiquitination, and phosphorylation, may alter lens microcirculation and affect subsequent biomineralization in the lens (Retamal et al., 2019). The mixed deposits in cataractous lenses might comprise of aggregated non-functional proteins and precipitated Ca^{+}. Detection of the Ca^{+} values in cataractous human lenses revealed that the insoluble lens fraction contained a higher proportion of Ca^{+} than the soluble part. Lens biomineralization is probably the main reason for the development of cataracts of additional pathogenesis.

Age-dependent Truncations

It is universally acknowledged that age-related connexin modification could deteriorate the intercellular communications between lens cells. Over 90% of downregulated expression of Cx46 and Cx50 proteins has been detected in normal lens fiber cells isolated from a group of cataracts patients aged more than 50 years old (Gong et al., 2021). The expression of Cx46 and Cx50 proteins displayed age-dependent reduction, whereas Cx43 remained relatively stable in aging mice. Two mutations in the Cx46 and Cx50 code region, Cx46V139M and Cx50V275I, respectively, were identified with mild association with the development of age-related cataracts in a Chinese population (Zhou et al., 2011). These mutants show the impact on alterations in post-translational modifications (PTMs) of connexin proteins because of age of appearance of cataracts. Polymorphisms in the intronic region of the Cx50 gene and a C-to-G substitution in the code region of Cx46 gene might be linked to the formation of age-related cataracts (Liu et al., 2011; Zhou et al., 2011). Previous studies indicate that an age-dependent decrease of gap junction conductance induces alterations in the ability of ion channels and related transporters in the lens. There is a hypothesis that elimination of over 65% of connexin proteins caused by age-related modifications is responsible for the declined coupling levels in the lens.

With increasing age, truncations in the cytoplasmic loop region and N-terminal domain of Cx46 and Cx50 accumulate in the core, resulting in decreased coupling conductance (White et al., 2007). In addition, the corresponding abundance of these truncations was remarkably altered with aging of lens fiber cells, showing the highest level of truncation products in the nucleus of the oldest fiber cells and the lowest level in the outer cortex of younger, differentiating fiber cells. Previous studies in rodent lens indicated that the levels of age-related connexin hemichannel truncations in younger lenses were lower than those found in older lenses. It is likely that the PTMs of these connexins are dependent on the age of the lens (Rozema and Ní Dhubhghaill, 2020; Fan and Monnier, 2021). The epithelial cells of lens differentiate into fiber cells and the C-terminal of Cx46 and Cx50 proteins are cleaved during this process. The endogenous Cx50 truncations resulted from the enzymolysis of calpain or other proteases. Mass spectrometry analysis identified several truncation sites of Cx46 and Cx50 proteins in bovine lens. C-terminal truncation at site V284 of Cx50 induced nonfunctional hemichannels; in contrast, truncation at position TM4 had no influence on its properties (Slavi et al., 2016). Therefore, cleavage of Cx50 by calpain is able to decrease the proportion of functional connexin hemichannels, and give rise to reduced level of gap junction coupling during lens development. The calpain activity decreases with age in the Cx46 knockout lenses. C-terminal cleavage of Cx46 has no impact on coupling conductance, and ionic permeability of connexin hemichannels composed of truncated Cx46 possessed almost the same function as the full-length isoform (Fan and Monnier, 2021). However, the mechanism attributed to truncations in Cx46 and Cx50 with differentiation and aging remains to be determined.

Other factors: Oxidative Stress and Hypoxia

Oxidative stress is responsible for the production of highly reactive oxygen species (ROS) and subsequent cellular damage at protein and DNA level has been observed in cataractous lens (Babizhayev and Bozzocosta, 1994; Lin and Takemoto, 2005). To combat constant oxidative stress from the environment, ocular tissue normally produces high concentrations of reduced glutathione (GSH) and utilizes a complicated antioxidant defense system composed of superoxide dismutase (SOD) and glutathione peroxidase (GPX). It is widely recognized that GSH plays an important role in maintaining redox homeostasis and lens transparency (Ho et al., 1997; Delamere and Tamiya, 2004). Depletion of GSH in newborn mice compromise lens transparency and eventually leads to the development of cataract (Laver et al., 1993). Plentiful evidence has been gathered to inform that cataract formation can result from oxidative stress, decreased level of GSH, and the mixed protein-thiol and protein-protein disulfide bonds. Increased levels of GSH and oxidized glutathione (GSSG) have been measured in the core of lens as it ages (Lim et al., 2020). Misfold proteins caused by mutations in some of the connexins presumably deposit in the Golgi bodies or endoplasmic reticulum (ER) to trigger stress responses and ultimately damage crystalline proteins. The Cx46fs380-mutant mice exhibited reduced total levels of β-crystallins consistent with degradation, modification, and truncation of the proteins (Minogue et al., 2005). A decreased GSH level was only observed in the nucleus of homozygous Cx46fs380 lens (Jara et al., 2020). However, a single mutation of P-to-S transversion at amino acid residue 88 of human Cx50 protein resulted in cytosolic aggregates and led to decreased degradation. In addition, a higher level of GSH was observed in homozygous Cx50D47A lens about 2 months old (Jara et al., 2020). Detection of the level of GSH in the lens

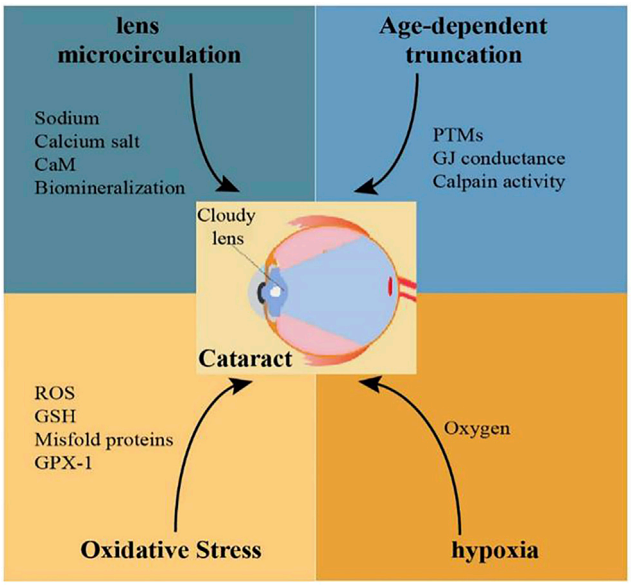

FIGURE 2 | Possible mechanisms related to Cx46 and Cx50 mutations involved in the pathogenesis of cataracts.

from connexin-knockout mice suggested that Cx46 (not Cx50) is essential for the movement of GSH from lens cortical cell to lens nuclear cell, under the condition that both Cx46 and Cx50 hemichannels assist in the transport of GSH (Serebryany et al., 2021). Mutation in the Cx46 gene region in mice led to the development of lens opacity and cataracts due to deposit of insoluble polypeptides caused by aggregation of crystallin cleavage products (Gong et al., 1997; King and Lampe, 2005; Kelly et al., 2007).

It has been suggested that targeted deletion of GPX-1 in mice can cause declined expression level of Cx46 and Cx50 together with extremely low level of coupling conductance (Wang et al., 2009). Apart from that, hydrogen peroxide was reported to keep Cx50 hemichannels open, and can assist in the movement of reductant glutathione into lens fiber cells. Both Cx50P88S and Cx50H156N mutations suppress permeability activity of Cx50 hemichannels (Shi et al., 2018). In addition, oxidative stress cause by 4-hydroxynonenal (4-HNE) can deprive the natural properties of Cx46 protein through its carbonylation (Retamal et al., 2020). These mutants ultimately induce apoptosis of lens epithelial cells and fiber cells.

A hypoxic condition is necessary for normal growth and development of the lens. Increased exposure to oxygen has been proven to be a threatening cause for the occurrence of age-related cataracts and nuclear cataracts (Brennan et al., 2020). *In vivo* studies showed that physiological hypoxia is indispensable for inhibiting cell proliferation and preserving smaller lens size (Zhao et al., 2020). Hypoxia might be a critical factor that regulate the expression and function of Cx46 in natural lens. The Cx46 promoter showed tight transcriptional responses when cultured with 1% oxygen in human lens cells (Molina and Takemoto, 2012). Further studies will be needed to elucidate the change of oxygen concentration in responding to the expression of connexin proteins in the lens.

CONCLUSION AND FUTURE DIRECTIONS

Remarkable progress and achievement have been obtained in the last few decades in our basic knowledge of the role of lens connexin hemichannels Cx46 and Cx50 in cataract formation. Connexin variants related to congenital cataracts are being identified in many regions around the world. Adequate and useful animal models have been generated for the investigation of the role of mutant connexin in lens abnormalities during cataractogenesis. The factors that mutate lens connexin in human and rodents and the mechanisms of cataract formation caused by lens connexin mutation and dysfunction could be explored in the future (**Figure 2**). Despite all the great achievements, much remains to be seen how Cx46 and Cx50 proteins are regulated in the lens under both normal and abnormal conditions. Furthermore, the clinical diagnosis, treatment and prevention based on connexin biology in cataracts are limited. Future investigations should also be arranged to develop effective therapeutic interventions against cataracts.

Mutations of Cx46 and Cx50 in human and rodents can be caused by age, oxidative stress, and hypoxia. Reduced levels of Cx46 and Cx50 proteins or these nonfunctional connexin proteins in lens fiber cells would cause disrupted lens microcirculation, and ultimately, development of cataracts.

AUTHOR CONTRIBUTIONS

JY created the whole manuscript. YS wrote the paper and XL revised the paper.

REFERENCES

Addison, P. K., Berry, V., Holden, K. R., Espinal, D., Rivera, B., Su, H., et al. (2006). A Novel Mutation in the Connexin 46 Gene (GJA3) Causes Autosomal Dominant Zonular Pulverulent Cataract in a Hispanic Family. *Mol. Vis.* 12, 791–795. doi:10.1016/j.visres.2006.01.022

Alvarez, L. J., Candia, O. A., and Polikoff, L. A. (2003). Beta-Adrenergic Stimulation of Na+-K+-2Cl− Cotransport Activity in the Rabbit Lens. *Exp. Eye Res.* 76 (1), 61–70. doi:10.1016/s0014-4835(02)00254-3

Alvarez, L. J., Candia, O. A., Turner, H. C., and Polikoff, L. A. (2001). Localization of a Na+-K+-2Cl− Cotransporter in the Rabbit Lens. *Exp. Eye Res.* 73 (5), 669–680. doi:10.1006/exer.2001.1075

Arora, A., Minogue, P. J., Liu, X., Reddy, M. A., Ainsworth, J. R., Bhattacharya, S. S., et al. (2006). A Novel GJA8 Mutation Is Associated with Autosomal Dominant Lamellar Pulverulent Cataract: Further Evidence for gap Junction Dysfunction in Human Cataract. *J. Med. Genet.* 43 (1), e2. doi:10.1136/jmg.2005.034108

Babizhayev, M., and Bozzocosta, E. (1994). Lipid Peroxide and Reactive Oxygen Species Generating Systems of the Crystalline Lens. *Biochim.*

Biophys. Acta (Bba) - Mol. Basis Dis. 1225 (3), 326–337. doi:10.1016/0925-4439(94)90014-0

Baruch, A., Greenbaum, D., Levy, E. T., Nielsen, P. A., Gilula, N. B., Kumar, N. M., et al. (2001). Defining a Link between gap junction Communication, Proteolysis, and Cataract Formation. *J. Biol. Chem.* 276 (31), 28999–29006. doi:10.1074/jbc.m103628200

Berry, V., Mackay, D., Khaliq, S., Francis, P. J., Hameed, A., Anwar, K., et al. (1999). Connexin 50 Mutation in a Family With Congenital "zonular Nuclear" Pulverulent Cataract of Pakistani Origin. *Hum. Genet.* 105 (1-2), 168–170. doi:10.1007/s004399900094

Berthoud, V. M., and Ngezahayo, A. (2017). Focus on Lens Connexins. *BMC Cell Biol.* 18 (Suppl. 1), 6. doi:10.1186/s12860-016-0116-6

Berthoud, V. M., Gao, J., Minogue, P. J., Jara, O., Mathias, R. T., and Beyer, E. C. (2020). Connexin Mutants Compromise the Lens Circulation and Cause Cataracts through Biomineralization. *Int. J. Mol Sci.* 21 (16), 5822. doi:10.3390/ijms21165822

Berthoud, V. M., Gao, J., Minogue, P. J., Jara, O., Mathias, R. T., and Beyer, E. C. (2019). The Connexin50D47A Mutant Causes Cataracts by Calcium Precipitation. *Invest. Ophthalmol. Vis. Sci.* 60 (6), 2336–2346. doi:10.1167/iovs.18-26459

Berthoud, V. M., Minogue, P. J., Yu, H., Snabb, J. I., and Beyer, E. C. (2014). Connexin46fs380 Causes Progressive Cataracts. *Invest. Ophthalmol. Vis. Sci.* 55 (10), 6639–6648. doi:10.1167/iovs.14-15012

Beyer, E. C., and Berthoud, V. M. (2014). Connexin Hemichannels in the Lens. *Front. Physiol.* 5, 20. doi:10.3389/fphys.2014.00020

Brennan, L. A., McGreal-Estrada, R., Logan, C. M., Cvekl, A., Menko, A. S., and Kantorow, M. (2018). BNIP3L/NIX Is Required for Elimination of Mitochondria, Endoplasmic Reticulum and Golgi Apparatus during Eye Lens Organelle-free Zone Formation. *Exp. Eye Res.* 174, 173–184. doi:10.1016/j.exer.2018.06.003

Brennan, L., Disatham, J., and Kantorow, M. (2020). Hypoxia Regulates the Degradation of Non-Nuclear Organelles during Lens Differentiation through Activation of HIF1a. *Exp. Eye Res.* 198, 108129. doi:10.1016/j.exer.2020.108129

Brennan, L., Disatham, J., and Kantorow, M. (2021). Mechanisms of Organelle Elimination for Lens Development and Differentiation. *Exp. Eye Res.* 209, 108682. doi:10.1016/j.exer.2021.108682

Brink, P. R., Valiunas, V., and White, T. W. (2020). Lens Connexin Channels Show Differential Permeability to Signaling Molecules. *Int. J. Mol Sci.* 21 (18), 6943. doi:10.3390/ijms21186943

Ceroni, F., Aguilera-Garcia, D., Chassaing, N., Bax, D. A., Blanco-Kelly, F., Ramos, P., et al. (2019). New GJA8 Variants and Phenotypes Highlight its Critical Role in a Broad Spectrum of Eye Anomalies. *Hum. Genet.* 138 (8-9), 1027–1042. doi:10.1007/s00439-018-1875-2

Chang, B., Wang, X., Hawes, N. L., Ojakian, R., Davisson, M. T., Lo, W., et al. (2002). A Gja8 (Cx50) point Mutation Causes an Alteration of Alpha3 Connexin (Cx46) in Semi-dominant Cataracts of Lop10 Mice. *Hum. Mol. Genet.* 11 (5), 507–513. doi:10.1093/hmg/11.5.507

Chen, L., Su, D., Li, S., Guan, L., Shi, C., Li, D., et al. (2017). The Connexin 46 Mutant (V44M) Impairs gap junction Function Causing Congenital Cataract. *J. Genet.* 96 (6), 969–976. doi:10.1007/s12041-017-0861-0

Cvekl, A., and Eliscovich, C. (2021). Crystallin Gene Expression: Insights from Studies of Transcriptional Bursting. *Exp. Eye Res.* 207, 108564. doi:10.1016/j.exer.2021.108564

Davison, J. E. (2020). Eye Involvement in Inherited Metabolic Disorders. *Ther. Adv. Ophthalmol.* 12, 2515841420979109. doi:10.1177/2515841420979109

De Maria, A., Zhao, H., and Bassnett, S. (2018). Expression of Potassium-dependent Sodium-Calcium Exchanger in the Murine Lens. *Exp. Eye Res.* 167, 18–24. doi:10.1016/j.exer.2017.11.002

Delamere, N. A., and Tamiya, S. (2004). Expression, Regulation and Function of Na,K-ATPase in the Lens. *Prog. Retin. Eye Res.* 23 (6), 593–615. doi:10.1016/j.preteyeres.2004.06.003

Delvaeye, T., Vandenabeele, P., Bultynck, G., Leybaert, L., and Krysko, D. V. (2018). Therapeutic Targeting of Connexin Channels: New Views and Challenges. *Trends Mol. Med.* 24 (12), 1036–1053. doi:10.1016/j.molmed.2018.10.005

Ebihara, L., Pal, J. D., and Pal, J. D. (2003). Effect of External Magnesium and Calcium on Human Connexin46 Hemichannels. *Biophysical J.* 84 (1), 277–286. doi:10.1016/s0006-3495(03)74848-6

Fan, X., and Monnier, V. M. (2021). Protein Posttranslational Modification (PTM) by Glycation: Role in Lens Aging and Age-Related Cataractogenesis. *Exp. Eye Res.* 210, 108705. doi:10.1016/j.exer.2021.108705

Figueroa, V. A., Jara, O., Oliva, C. A., Ezquer, M., Ezquer, F., Retamal, M. A., et al. (2019). Contribution of Connexin Hemichannels to the Decreases in Cell Viability Induced by Linoleic Acid in the Human Lens Epithelial Cells (HLE-B3). *Front. Physiol.* 10, 1574. doi:10.3389/fphys.2019.01574

Gao, J., Minogue, P. J., Beyer, E. C., Mathias, R. T., and Berthoud, V. M. (2018). Disruption of the Lens Circulation Causes Calcium Accumulation and Precipitates in Connexin Mutant Mice. *Am. J. Physiology-Cell Physiol.* 314 (4), C492–C503. doi:10.1152/ajpcell.00277.2017

Gao, J., Sun, X., Martinez-Wittinghan, F. J., Gong, X., White, T. W., and Mathias, R. T. (2004). Connections between Connexins, Calcium, and Cataracts in the Lens. *J. Gen. Physiol.* 124 (4), 289–300. doi:10.1085/jgp.200409121

Gao, J., Wang, H., Sun, X., Varadaraj, K., Li, L., White, T. W., et al. (2013). The Effects of Age on Lens Transport. *Invest. Ophthalmol. Vis. Sci.* 54 (12), 7174–7187. doi:10.1167/iovs.13-12593

Gerido, D. A., Sellitto, C., Li, L., and White, T. W. (2003). Genetic Background Influences Cataractogenesis, but Not Lens Growth Deficiency, in Cx50-Knockout Mice. *Invest. Ophthalmol. Vis. Sci.* 44 (6), 2669–2674. doi:10.1167/iovs.02-1311

Gong, X., Cheng, C., and Xia, C. H. (2007). Connexins in Lens Development and Cataractogenesis. *J. Membr. Biol.* 218 (1-3), 9–12. doi:10.1007/s00232-007-9033-0

Gong, X. D., Wang, Y., Hu, X.-B., Zheng, S.-Y., Fu, J.-L., Nie, Q., et al. (2021). Aging-Dependent Loss of GAP junction Proteins Cx46 and Cx50 in the Fiber Cells of Human and Mouse Lenses Accounts for the Diminished Coupling Conductance. *Aging.* 13 (13), 17568–17591. doi:10.18632/aging.203247

Gong, X., Li, E., Klier, G., Huang, Q., Wu, Y., Lei, H., et al. (1997). Disruption of α3 Connexin Gene Leads to Proteolysis and Cataractogenesis in Mice. *Cell.* 91 (6), 833–843. doi:10.1016/s0092-8674(00)80471-7

Graw, J., Löster, J., Soewarto, D., Fuchs, H., Meyer, B., Reis, A., et al. (2001). Characterization of a Mutation in the Lens-Specific MP70 Encoding Gene of the Mouse Leading to a Dominant Cataract. *Exp. Eye Res.* 73 (6), 867–876. doi:10.1006/exer.2001.1096

Hadrami, M., Bonnet, C., Veten, F., Zeitz, C., Condroyer, C., Wang, P., et al. (2019). A Novel Missense Mutation of GJA8 Causes Congenital Cataract in a Large Mauritanian Family. *Eur. J. Ophthalmol.* 29 (6), 621–628. doi:10.1177/1120672118804757

Hashemi, H., Pakzad, R., Yekta, A., Aghamirsalim, M., Pakbin, M., Ramin, S., et al. (2020). Global and Regional Prevalence of Age-Related Cataract: a Comprehensive Systematic Review and Meta-Analysis. *Eye.* 34 (8), 1357–1370. doi:10.1038/s41433-020-0806-3

Ho, Y.-S., Magnenat, J.-L., Bronson, R. T., Cao, J., Gargano, M., Sugawara, M., et al. (1997). Mice Deficient in Cellular Glutathione Peroxidase Develop Normally and Show No Increased Sensitivity to Hyperoxia. *J. Biol. Chem.* 272 (26), 16644–16651. doi:10.1074/jbc.272.26.16644

Jara, O., Minogue, P. J., Berthoud, V. M., and Beyer, E. C. (2020). Do Connexin Mutants Cause Cataracts by Perturbing Glutathione Levels and Redox Metabolism in the Lens? *Biomolecules.* 10 (10), 1418. doi:10.3390/biom10101418

Katai, N., Kikuchi, T., Shibuki, H., Kuroiwa, S., Arai, J., Kurokawa, T., et al. (1999). Caspaselike Proteases Activated in Apoptotic Photoreceptors of Royal College of Surgeons Rats. *Invest. Ophthalmol. Vis. Sci.* 40 (8), 1802–1807. doi:10.1007/s004170050286

Kelly, S. M., Vanslyke, J. K., and Musil, L. S. (2007). Regulation of Ubiquitin-Proteasome System-Mediated Degradation by Cytosolic Stress. *MBoC.* 18 (11), 4279–4291. doi:10.1091/mbc.e07-05-0487

King, T. J., and Lampe, P. D. (2005). Temporal Regulation of Connexin Phosphorylation in Embryonic and Adult Tissues. *Biochim. Biophys. Acta.* 1719 (1-2), 24–35. doi:10.1016/j.bbamem.2005.07.010

Laver, N. M., Robinson, W. G., Calvin, H. I., and Fu, S.-C. J. (1993). Early Epithelial Lesions in Cataracts of GSH-Depleted Mouse Pups. *Exp. Eye Res.* 57 (4), 493–498. doi:10.1006/exer.1993.1151

Li, L., Chang, B., Cheng, C., Chang, D., Hawes, N. L., Xia, C.-h., et al. (2008). Dense Nuclear Cataract Caused by the γB-Crystallin S11R Point Mutation. *Invest. Ophthalmol. Vis. Sci.* 49 (1), 304–309. doi:10.1167/iovs.07-0942

Li, L., Cheng, C., Xia, C.-h., White, T. W., Fletcher, D. A., and Gong, X. (2010). Connexin Mediated Cataract Prevention in Mice. *PLoS One.* 5 (9), e12624. doi:10.1371/journal.pone.0012624

Li, L., Fan, D.-B., Zhao, Y.-T., Li, Y., Yang, Z.-B., and Zheng, G.-Y. (2019). GJA8 Missense Mutation Disrupts Hemichannels and Induces Cell Apoptosis in Human Lens Epithelial Cells. *Sci. Rep.* 9 (1), 19157. doi:10.1038/s41598-019-55549-1

Li, Y., Wang, J., Dong, B., and Man, H. (2004). A Novel Connexin46 (GJA3) Mutation in Autosomal Dominant Congenital Nuclear Pulverulent Cataract. *Mol. Vis.* 10, 668–671. doi:10.1021/bi049306z

Lim, J. C., Grey, A. C., Zahraei, A., and Donaldson, P. J. (2020). Age-Dependent Changes in Glutathione Metabolism Pathways in the Lens: New Insights into Therapeutic Strategies to Prevent Cataract Formation-A Review. *Clin. Exp. Ophthalmol.* 48 (8), 1031–1042. doi:10.1111/ceo.13801

Lin, D., and Takemoto, D. J. (2005). Oxidative Activation of Protein Kinase Cγ through the C1 Domain. *J. Biol. Chem.* 280 (14), 13682–13693. doi:10.1074/jbc.m407762200

Liu, K., Lyu, L., Chin, D., Gao, J., Sun, X., Shang, F., et al. (2015). Altered Ubiquitin Causes Perturbed Calcium Homeostasis, Hyperactivation of Calpain, Dysregulated Differentiation, and Cataract. *Proc. Natl. Acad. Sci. USA.* 112 (4), 1071–1076. doi:10.1073/pnas.1404059112

Liu, Y., Ke, M., Yan, M., Guo, S., Mothobi, M. E., Chen, Q., et al. (2011). Association between gap junction Protein-Alpha 8 Polymorphisms and Age-Related Cataract. *Mol. Biol. Rep.* 38 (2), 1301–1307. doi:10.1007/s11033-010-0230-z

Mackay, D., Ionides, A., Kibar, Z., Rouleau, G., Berry, V., Moore, A., et al. (1999). Connexin46 Mutations in Autosomal Dominant Congenital Cataract. *Am. J. Hum. Genet.* 64 (5), 1357–1364. doi:10.1086/302383

Mathias, R. T., Kistler, J., and Donaldson, P. (2007). The Lens Circulation. *J. Membr. Biol.* 216 (1), 1–16. doi:10.1007/s00232-007-9019-y

Mese, G., Richard, G., and White, T. W. (2007). Gap Junctions: Basic Structure and Function. *J. Invest. Dermatol.* 127 (11), 2516–2524. doi:10.1038/sj.jid.5700770

Minogue, P. J., Gao, J., Zoltoski, R. K., Novak, L. A., Mathias, R. T., Beyer, E. C., et al. (2017). Physiological and Optical Alterations Precede the Appearance of Cataracts in Cx46fs380 Mice. *Invest. Ophthalmol. Vis. Sci.* 58 (10), 4366–4374. doi:10.1167/iovs.17-21684

Minogue, P. J., Liu, X., Ebihara, L., Beyer, E. C., and Berthoud, V. M. (2005). An Aberrant Sequence in a Connexin46 Mutant Underlies Congenital Cataracts. *J. Biol. Chem.* 280 (49), 40788–40795. doi:10.1074/jbc.m504765200

Molina, S. A., and Takemoto, D. J. (2012). The Role of Connexin 46 Promoter in Lens and Other Hypoxic Tissues. *Communicative Integr. Biol.* 5 (2), 114–117. doi:10.4161/cib.18715

Okafor, M., Tamiya, S., and Delamere, N. A. (2003). Sodium-calcium Exchange Influences the Response to Endothelin-1 in Lens Epithelium. *Cell Calcium.* 34 (3), 231–240. doi:10.1016/s0143-4160(03)00085-x

Paul, D. L., Ebihara, L., Takemoto, L. J., Swenson, K. I., and Goodenough, D. A. (1991). Connexin46, a Novel Lens gap junction Protein, Induces Voltage-Gated Currents in Nonjunctional Plasma Membrane of Xenopus Oocytes. *J. Cell Biol.* 115 (4), 1077–1089. doi:10.1083/jcb.115.4.1077

Ping, X., Liang, J., Shi, K., Bao, J., Wu, J., Yu, X., et al. (2021). Rapamycin Relieves the Cataract Caused by Ablation of Gja8b Through Stimulating Autophagy in Zebrafish. *Autophagy.* 17 (11), 3323–3337. doi:10.1080/15548627.2021.1872188

Ponnam, S. P. G., Ramesha, K., Tejwani, S., Ramamurthy, B., and Kannabiran, C. (2007). Mutation of the gap Junction Protein Alpha 8 (GJA8) Gene Causes Autosomal Recessive Cataract. *J. Med. Genet.* 44 (7), e85. doi:10.1136/jmg.2007.050138

Rees, M. I., Watts, P., Fenton, I., Clarke, A., Snell, R. G., Owen, M. J., et al. (2000). Further Evidence of Autosomal Dominant Congenital Zonular Pulverulent Cataracts Linked to 13q11 (CZP3) and a Novel Mutation in Connexin 46 (GJA3). *Hum. Genet.* 106 (2), 206–209. doi:10.1007/s004399900234

Retamal, M. A., Fiori, M. C., Fernandez-Olivares, A., Linsambarth, S., Peña, F., Quintana, D., et al. (2020). 4-Hydroxynonenal Induces Cx46 Hemichannel Inhibition Through its Carbonylation. *Biochim. Biophys. Acta (Bba) - Mol. Cell Biol. Lipids.* 1865 (8), 158705. doi:10.1016/j.bbalip.2020.158705

Retamal, M. A., Orellana, V. P., Arévalo, N. J., Rojas, C. G., Arjona, R. J., Alcaíno, C. A., et al. (2019). Cx46 Hemichannel Modulation by Nitric Oxide: Role of the Fourth Transmembrane helix Cysteine and its Possible Involvement in Cataract Formation. *Nitric Oxide.* 86, 54–62. doi:10.1016/j.niox.2019.02.007

Rozema, J. J., and Ní Dhubhghaill, S. (2020). Age-related Axial Length Changes in Adults: a Review. *Ophthalmic Physiol. Opt.* 40 (6), 710–717. doi:10.1111/opo.12728

Ruan, X., Liu, Z., Luo, L., and Liu, Y. (2020). The Structure of the Lens and its Associations with the Visual Quality. *BMJ Open Ophth.* 5 (1), e000459. doi:10.1136/bmjophth-2020-000459

Sánchez, A., Castro, C., Flores, D.-L., Gutiérrez, E., and Baldi, P. (2019). Gap Junction Channels of Innexins and Connexins: Relations and Computational Perspectives. *Int. J. Mol. Sci.* 20 (10), 2476. doi:10.3390/ijms20102476

Schadzek, P., Stahl, Y., Preller, M., and Ngezahayo, A. (2019). Analysis of the Dominant Mutation N188T of Human Connexin46 (hC X46) Using Concatenation and Molecular Dynamics Simulation. *FEBS Open Bio.* 9 (5), 840–850. doi:10.1002/2211-5463.12624

Sellitto, C., Li, L., and White, T. W. (2004). Connexin50 Is Essential for normal Postnatal Lens Cell Proliferation. *Invest. Ophthalmol. Vis. Sci.* 45 (9), 3196–3202. doi:10.1167/iovs.04-0194

Serebryany, E., Thorn, D. C., and Quintanar, L. (2021). Redox Chemistry of Lens Crystallins: A System of Cysteines. *Exp. Eye Res.* 211, 108707. doi:10.1016/j.exer.2021.108707

Sharan, S., Grigg, J. R., and Billson, F. A. (2005). Bilateral Naevus of Ota with Choroidal Melanoma and Diffuse Retinal Pigmentation in a Dark Skinned Person. *Br. J. Ophthalmol.* 89 (11), 1529. doi:10.1136/bjo.2005.070839

Shi, W., Riquelme, M. A., Gu, S., and Jiang, J. X. (2018). Connexin Hemichannels Mediate Glutathione Transport and Protect Lens Fiber Cells from Oxidative Stress. *J. Cell Sci.* 131 (6), jcs212506. doi:10.1242/jcs.212506

Shiels, A., and Hejtmancik, J. F. (2021). Inherited Cataracts: Genetic Mechanisms and Pathways New and Old. *Exp. Eye Res.* 209, 108662. doi:10.1016/j.exer.2021.108662

Slavi, N., Wang, Z., Harvey, L., Schey, K. L., and Srinivas, M. (2016). Identification and Functional Assessment of Age-dependent Truncations to Cx46 and Cx50 in the Human Lens. *Invest. Ophthalmol. Vis. Sci.* 57 (13), 5714–5722. doi:10.1167/iovs.16-19698

Steele, E. C., Lyon, M. F., Favor, J., Guillot, P. V., Boyd, Y., and Church, R. L. (1998). A Mutation in the Connexin 50 (Cx50) Gene Is a Candidate for the No2 Mouse Cataract. *Curr. Eye Res.* 17 (9), 883–889. doi:10.1076/ceyr.17.9.883.5144

Summers, J. A., Schaeffel, F., Marcos, S., Wu, H., and Tkatchenko, A. V. (2021). Functional Integration of Eye Tissues and Refractive Eye Development: Mechanisms and Pathways. *Exp. Eye Res.* 209, 108693. doi:10.1016/j.exer.2021.108693

Taylan Sekeroglu, H., and Utine, G. E. (2021). Congenital Cataract and its Genetics: The Era of Next-Generation Sequencing. *Turk J. Ophthalmol.* 51 (2), 107–113. doi:10.4274/tjo.galenos.2020.08377

Tong, J. J., Khan, U., Haddad, B. G., Minogue, P. J., Beyer, E. C., Berthoud, V. M., et al. (2021). Molecular Mechanisms Underlying Enhanced Hemichannel Function of a Cataract-Associated Cx50 Mutant. *Biophys. J.* 3495 (21), 00951–00956. doi:10.1016/j.bpj.2021.11.004

Valiunas, V., Brink, P. R., and White, T. W. (2019). Lens Connexin Channels Have Differential Permeability to the Second Messenger cAMP. *Invest. Ophthalmol. Vis. Sci.* 60 (12), 3821–3829. doi:10.1167/iovs.19-27302

Valiunas, V., and White, T. W. (2020). Connexin43 and Connexin50 Channels Exhibit Different Permeability to the Second Messenger Inositol Triphosphate. *Sci. Rep.* 10 (1), 8744. doi:10.1038/s41598-020-65761-z

Van Campenhout, R., Gomes, A. R., De Groof, T. W. M., Muyldermans, S., Devoogdt, N., and Vinken, M. (2021). Mechanisms Underlying Connexin Hemichannel Activation in Disease. *Int. J. Mol. Sci.* 22 (7), 3503. doi:10.3390/ijms22073503

Vanden Abeele, F., Bidaux, G., Gordienko, D., Beck, B., Panchin, Y. V., Baranova, A. V., et al. (2006). Functional Implications of Calcium Permeability of the Channel Formed by Pannexin 1. *J. Cell Biol.* 174 (4), 535–546. doi:10.1083/jcb.200601115

Wang, H., Gao, J., Sun, X., Martinez-Wittinghan, F. J., Li, L., Varadaraj, K., et al. (2009). The Effects of GPX-1 Knockout on Membrane Transport and Intracellular Homeostasis in the Lens. *J. Membr. Biol.* 227 (1), 25–37. doi:10.1007/s00232-008-9141-5

White, T. W., Gao, Y., Li, L., Sellitto, C., and Srinivas, M. (2007). Optimal Lens Epithelial Cell Proliferation Is Dependent on the Connexin Isoform Providing

gap Junctional Coupling. *Invest. Ophthalmol. Vis. Sci.* 48 (12), 5630–5637. doi:10.1167/iovs.06-1540

White, T. W., Goodenough, D. A., and Paul, D. L. (1998). Targeted Ablation of Connexin50 in Mice Results in Microphthalmia and Zonular Pulverulent Cataracts. *J. Cell Biol.* 143 (3), 815–825. doi:10.1083/jcb.143.3.815

Xia, C. H., Cheng, C., Huang, Q., Cheung, D., Li, L., Dunia, I., et al. (2006a). Absence of α3 (Cx46) and α8 (Cx50) Connexins Leads to Cataracts by Affecting Lens Inner Fiber Cells. *Exp. Eye Res.* 83 (3), 688–696. doi:10.1016/j.exer.2006.03.013

Xia, C. H., Cheung, D., DeRosa, A. M., Chang, B., Lo, W. K., White, T. W., et al. (2006b). Knock-in of Alpha3 Connexin Prevents Severe Cataracts Caused by an Alpha8 point Mutation. *J. Cell Sci.* 119 (Pt 10), 2138–2144. doi:10.1242/jcs.02940

Yamashita, S., Furumoto, K., Nobukiyo, A., Kamohara, M., Ushijima, T., and Furukawa, T. (2002). Mapping of A Gene Responsible for Cataract Formation and its Modifier in the UPL Rat. *Invest. Ophthalmol. Vis. Sci.* 43 (10), 3153–3159. doi:10.1007/s00417-002-0538-z

Yoshida, M., Harada, Y., Kaidzu, S., Ohira, A., Masuda, J., and Nabika, T. (2005). New Genetic Model Rat for Congenital Cataracts Due to a Connexin 46 (Gja3) Mutation. *Pathol. Int.* 55 (11), 732–737. doi:10.1111/j.1440-1827.2005.01896.x

Yue, B., Haddad, B. G., Khan, U., Chen, H., Atalla, M., Zhang, Z., et al. (2021). Connexin 46 and Connexin 50 gap junction Channel Properties Are Shaped by Structural and Dynamic Features of Their N-Terminal Domains. *J. Physiol.* 599 (13), 3313–3335. doi:10.1113/JP281339

Zhao, L., Wang, J., Zhang, Y., Wang, L., Yu, M., and Wang, F. (2020). Vitamin C Decreases VEGF Expression Levels via Hypoxia inducible Factor 1α Dependent and Independent Pathways in Lens Epithelial Cells. *Mol. Med. Rep.* 22 (1), 436–444. doi:10.3892/mmr.2020.11103

Zhou, Z., Wang, B., Hu, S., Zhang, C., Ma, X., and Qi, Y. (2011). Genetic Variations in GJA3, GJA8, LIM2, and Age-Related Cataract in the Chinese Population: a Mutation Screening Study. *Mol. Vis.* 17, 621–626. doi:10.1017/S0952523810000489

Conflict of Interest: The authors declare that the research was conducted in the absence of any commercial or financial relationships that could be construed as a potential conflict of interest.

Publisher's Note: All claims expressed in this article are solely those of the authors and do not necessarily represent those of their affiliated organizations, or those of the publisher, the editors and the reviewers. Any product that may be evaluated in this article, or claim that may be made by its manufacturer, is not guaranteed or endorsed by the publisher.

frontiers in Molecular Biosciences

ORIGINAL RESEARCH
published: 15 February 2022
doi: 10.3389/fmolb.2022.835508

Antrodia camphorata-Derived Antrodin C Inhibits Liver Fibrosis by Blocking TGF-Beta and PDGF Signaling Pathways

Xin-Yi Xu[1], *Yan Geng*[2]*, *Hao-Xiang Xu*[3], *Yilin Ren*[4], *Deng-Yang Liu*[4] *and Yong Mao*[5]*

[1]Institute of Cancer, Affiliated Hospital of Jiangnan University, Wuxi, China, [2]School of Life Science and Health Engineering, Jiangnan University, Wuxi, China, [3]Department of Urology, Affiliated Wuxi No. 2 Hospital of Nanjing Medical University, Wuxi, China, [4]Department of Gastroenterology, Affiliated Hospital of Jiangnan University, Wuxi, China, [5]Department of Oncology, Affiliated Hospital of Jiangnan University, Wuxi, China

Hepatic stellate cells (HSCs) play an essential role in the development of liver fibrosis. *Antrodia camphorata* (*A. camphorata*) is a medicinal fungus with hepatoprotective effect. This study investigated whether Antrodin C, an *A. camphorata*-fermented metabolite, could exert a protective role on liver fibrosis both *in vitro* and *in vivo*. The anti-fibrotic effect of Antrodin C was investigated in CFSC-8B cell (hepatic stellate cell) stimulated by transforming growth factor-β1 (TGF-β1) or platelet-derived growth factor-BB (PDGF-BB) *in vitro* and in CCl_4 induced liver fibrosis in mice. Antrodin C (50 μM) inhibited TGF-β1 or PDGF-BB stimulated CFSC-8B cell activation, migration and extracellular matrix (ECM) accumulation (all $p < 0.05$). Antrodin C (3, 6 mg/kg/d) oral administration reduced the degree of liver fibrosis induced by CCl_4 in mice. Antrodin C down-regulated the expression of α-smooth muscle actin (α-SMA) and collagen I in fibrotic livers. Furthermore, Antrodin C ameliorated alanine aminotransferase (ALT) and aspartate aminotransferase (AST) elevation in serum (all $p < 0.05$). Mechanistically, Antrodin C executes its anti-fibrotic activity through negatively modulate TGF-β1 downstream SMAD Family Member 2 (Smad2), AKT Serine/Threonine Kinase 1 (AKT), extracellular signal-regulated kinase (ERK), and P38 MAP Kinase (P38), as well as PDGF-BB downstream AKT and ERK signaling pathways. Antrodin C ameliorates the activation, migration, ECM production in HSCs and CCl_4-induced liver fibrosis in mice, suggesting that Antrodin C could serve as a protective molecule against liver fibrosis.

Keywords: liver disease, cell migration, hepatic stellate cells, extracellular matrix, cell signaling

OPEN ACCESS

Edited by:
Leming Sun,
Northwestern Polytechnical University, China

Reviewed by:
Rong-Rong He,
Jinan University, China
Yuhao Xie,
St. John's University, United States

***Correspondence:**
Yan Geng
gengyan@jiangnan.edu.cn
Yong Mao
9812015252@jiangnan.edu.cn

Specialty section:
This article was submitted to Molecular Diagnostics and Therapeutics, a section of the journal Frontiers in Molecular Biosciences

Received: *14 December 2021*
Accepted: *18 January 2022*
Published: *15 February 2022*

Citation:
Xu X-Y Geng Y, Xu H-X Ren Y, Liu D-Y and Mao Y (2022) Antrodia camphorata*-Derived Antrodin C Inhibits Liver Fibrosis by Blocking TGF-Beta and PDGF Signaling Pathways. Front. Mol. Biosci. 9:835508. doi: 10.3389/fmolb.2022.835508*

INTRODUCTION

Organ fibrosis refers to the excessive deposition of extracellular matrix (ECM) in response to chronic tissue injury (Caligiuri et al., 2021). Hepatic fibrosis is caused by various factors, such as genomic mutations, toxic chemicals, hepatitis B/C, excessive alcohol consumption, and nonalcoholic steatohepatitis (Guerra et al., 2016; George et al., 2019). Liver fibrosis are wound-healing responses generated against an insult to the liver that cause liver injury (Aydin and Akcali,

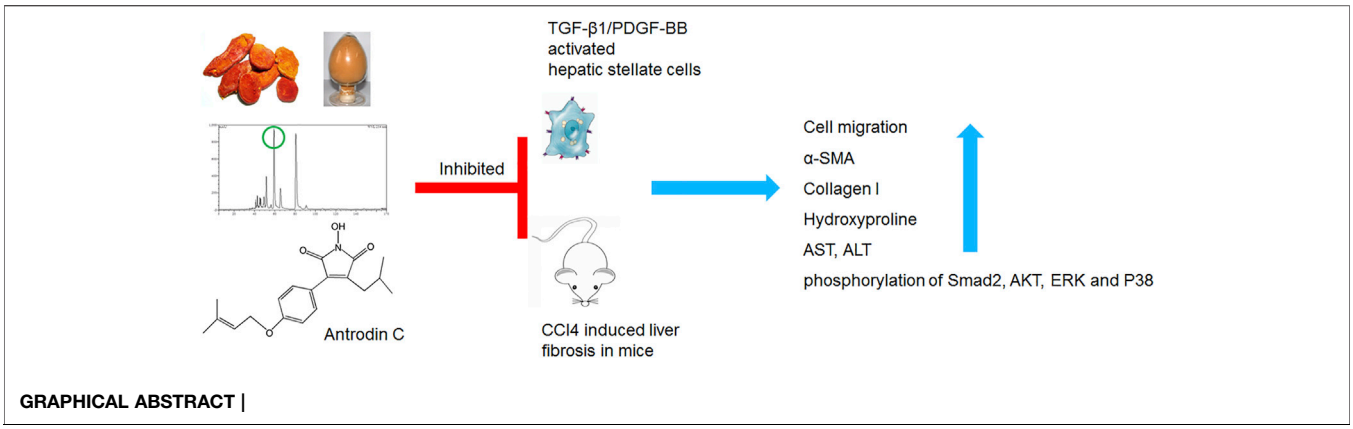

GRAPHICAL ABSTRACT |

2018). Liver fibrosis has the potential to progress to cirrhosis, liver cancer, and liver failure and its complications represent a massive health care burden worldwide (Deng et al., 2020). Aging has been considered as a risk factor for progression of fibrosis in hepatitis C and for poor outcome in alcoholic hepatitis (Goldstein et al., 2005; David and George, 2008). Therefore, it has been suggested that aging increases the susceptibility of liver fibrosis. Recent studies suggest that hepatic fibrosis could be reversible, however, its underlying mechanism remains uncertain and efficient anti-fibrotic drugs are urgently needed (Tan et al., 2021).

Hepatic stellate cells (HSCs) constitute the major mesenchymal cell type of the liver and play pivotal roles in a hepatic injury response (Dhar et al., 2020). Upon chronic liver injury, the quiescent HSCs (qHSCs) receive secreted signals and become activated HSCs (aHSCs) which express α-smooth muscle actin (α-SMA) and produce excessive extracellular matrix (ECM), including collagens and fibronectin (Jin et al., 2020; Yoon et al., 2020; Trivedi et al., 2021). Among many aberrant signaling molecules, transforming growth factor β1 (TGF-β1) and platelet-derived growth factor (PDGF) mediated signaling plays prominent roles in the transition of qHSCs into aHSCs (Kang et al., 2013).

Antrodia camphorata (also known as *Taiwanofungus camphoratus*, *Antrodia cinnamomea*) has been used as a traditional medicine or functional food for a long history in China for treating diarrhea, viral infection, diabetes mellitus liver cirrhosis, hepatoma and more (Zhenwei et al., 2021). Fermented mycelium or mycelial extract from *A. camphorata* has been found to inhibit HSCs activation *in vitro* and CCl_4 or thioacetamide induced liver fibrosis *in vivo* (Schyman et al., 2019). Two maleimide derivatives Antrodin B and Antrodin C isolated from the mycelia of *A. camphorata* inhibited the growth of Lewis lung carcinoma cells *in vitro* (Huang et al., 2019). Antrodin C inhibited breast cancer cell migration and invasion by suppressing Smad2/3 and β-Catenin signaling pathways (Kumar et al., 2015). We previously identified Antrodin B from *A. camphorata* as a novel anti-fibrotic compounds through a bioassay-guided fractionation approach (Geng et al., 2016). Antrodin C also suppressed lipopolysaccharide-induced inflammation (Lee et al., 2014). However, whether Antrodin C could inhibit HSCs activation and liver fibrosis, and the underlying mechanism remains unclear.

In this study, we isolated Antrodin C from mycelial extract of *A. camphorata* and investigated the effect and potential mechanism of Antrodin C on the aHSCs *in vitro* and CCl_4 induced liver fibrosis in mice. Together, we unraveled Antrodin C as an active compound in *A. camphorata* against liver fibrosis.

MATERIALS AND METHODS

Chemicals

3- (4, 5-dimethyl-2-thiazolyl)-2, 5-diphenyl-2H-tetrazolium bromide (MTT) (88417), silybin (S0292), SB431542 (616464), and other chemicals were purchased from Sigma-Aldrich (St. Louis, MO, United States). Recombinant Human TGF-β1 (AF-100-21C), and PDGF-BB (AF-100-14B) were purchased from PeproTech (Rocky Hill, NJ, United States). RPMI 1640 medium, fetal bovine serum (FBS), trypsin and antibiotics (penicillin and streptomycin) were purchased from Gibco (Thermofisher, USA).

Isolation and Identification of Antrodin C

The extraction and fractionation procedures were described previously (Geng et al., 2016). Briefly, the dried mycelium of *A. camphorata* was extracted in methanol and then partitioned with n-hexane (319902, Sigma-Aldrich), chloroform (288306, Sigma-Aldrich) and ethyl acetate (319902, Sigma-Aldrich). The n-hexane-soluble fraction was chromatographed on a silica gel column eluted with a gradient of n-hexane and ethyl acetate. The fraction eluted by 16% of EtOAc was further separated by a semipreparative HPLC column (Waters XBridge C18 column, Φ19 × 250 mm, 5 μm) (**Supplementary Figure S1**). The mobile phase consisted of distilled water H_2O (0.5% acetic acid) and acetonitrile (34851, Sigma-Aldrich) at 10 ml/min to obtain Antrodin C (purity > 95%). The structures of Antrodin C was analyzed by comparing their LC-MS, ^{1}H, ^{13}C NMR spectroscopic data (**Supplementary Figures S2–S4**) and compared with published data (Nakamura et al., 2004).

Cell Culture

Rat hepatic stellate cell line (CFSC-8B cells) were obtained from the cell bank of Xiangya Central Experiment Laboratory of Central South University (Changsha, China). CFSC-8B cells were cultured at 37°C in a humidified 5% CO_2 incubator and RPMI 1640 medium, supplemented with 10% FBS, 100 U/mL penicillin and 100 mg/ml streptomycin.

Cell Viability

The viability of CFSC-8B cells was quantified by the ability of living cells to reduce the yellow dye MTT to a blue formazan product. CFSC-8B cells (8×10^4 cells/mL) were seeded in a 96-well cell culture plate (Corning Incorporated, USA) and grew to 80%–90% confluence. Then the cells were incubated with Antrodin C (10–200 μM) for 24 h. The viability (% of the control) of cells treated with Antrodin C was calculated as 100% × (absorbance of treated cells/absorbance of control cells).

Cell Migration Assay

CFSC-8B cells (3×10^6 cells/mL) were seeded onto the upper chambers (8 μm pore size, Milipore, Billerica, Massachusetts, United States) with 100 μL of 0.5% FBS medium and 0.5 ml normal growth medium was added to the lower chambers as a chemoattractant in 24 well plate for 24 h. The cells left on the upper chambers were removed using a cotton swab. Then the chambers were fixed using 4% paraformaldehyde for 30 min, washed and stained 0.5% crystal violet for 30 min at 37°C. Five random views were photographed under a microscope (Nikon, Tokyo, Japan). The positive cells were counted and quantified using ImageJ. Silybin (25 μM) and SB431542 (2 μM) were used as positive controls in the assay.

Animals and CCl_4 Induced Liver Fibrosis

All animal experiments were approved by the Animal Research Committee of Jiangnan University. Male 6–8 weeks old BALB/c mice were obtained from Shanghai SLAC Laboratory Animal Co., Ltd. The animals were housed under standard conditions and fed with a normal chow diet (M01-F25-20150922034, Shanghai SLAC Laboratory Animal Co., Shanghai, China). The mice were randomly and equally divided into the CTL group, Silymarin group, CCl_4 group and two Antrodin C treatment groups (n = 6 per group). In the Antrodin C treatment groups, mice were orally administered with Antrodin C (3 or 6 mg/kg/d, formulated in 0.5% Carboxymethylcellulose sodium) daily for 2 weeks before CCl_4 injection. Silymarin was used as a positive drug control at the dose of 100 mg/kg/d daily for 2 weeks before CCl_4 injection. Then the CCl_4, Silymarin and Antrodin C groups were intraperitoneal injection CCl_4 (0.5 ml/kg, 25% solution in olive oil) twice per week, and the control group was given the same dose of olive oil. The Silymarin or Antrodin C groups were orally administered with Antrodin C or Silymarin for 4 weeks together with CCl_4 injection.

Histology Analysis

Liver tissues were embedded in paraffin and 4-μm-thick slices were cut, and placed on glass slides. Slides were stained with hematoxylin-eosin (H&E) or Sirius-red, and examined under a light microscope (Nikon, Tokyo, Japan). HE staining was performed to assess pathological changes in the liver. Sirius-red staining was performed to detect collagen deposition and was analyzed by ImageJ software (NIH, Bethsda, MD).

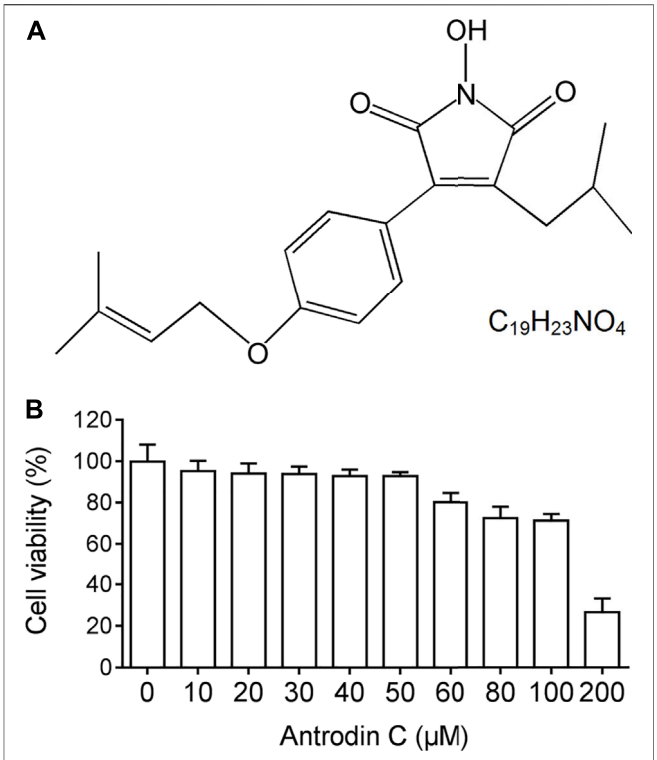

FIGURE 1 | The chemical structure and cell viability of CSFC-8B cells treated with Antrodin C **(A)** The chemical structure of Antrodin C. **(B)** Effect of Antrodin C on cell viability of CFSC-8B cells by MTT assay.

Measurement of Serum Aminotransferase Activities and Hydroxyproline Contents

The activities of alanine aminotransferase (ALT), aspartate aminotransferase (AST) in serum, and hydroxyproline contents in liver tissues were estimated spectrophotometrically using commercial diagnostic kits (Jiancheng Institute of Biotechnology, Nanjing, China).

RNA Isolation and qRT-PCR Analysis

Total RNA was extracted from mouse liver tissue or cells with Trizol reagent (Thermofisher, CA, United States). Gene expressions were measured relative to the endogenous control gene Gapdh using the comparative CT method and the sequences of specific primer pairs for α-SMA, Col1, and Col3 were described previously (Geng et al., 2016).

Western Blotting Analysis

Protein extracted from cells was resolved by SDS-polyacrylamide gel electrophoresis and transferred to PVDF membranes. Antibodies against α-SMA, GAPDH were from Sigma-Aldrich (St. Louis, MO, United States). Antibodies against Smad2,

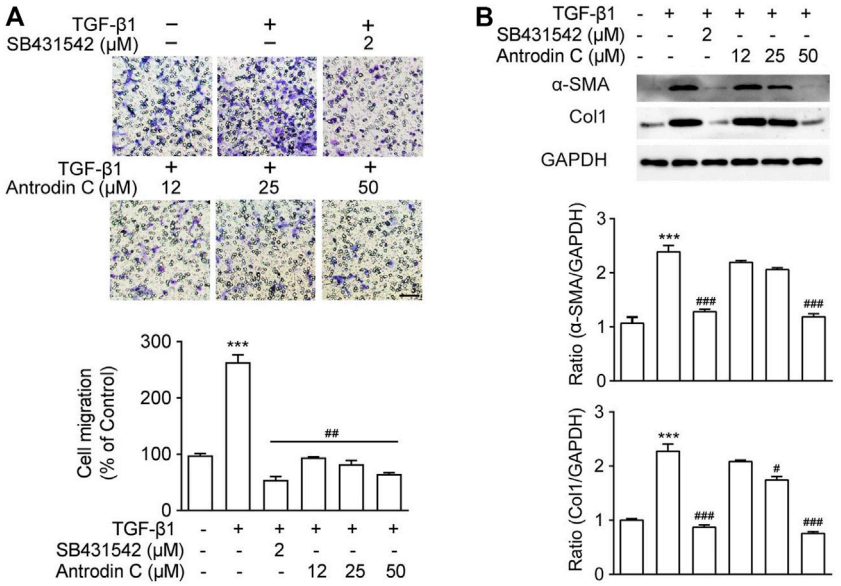

FIGURE 2 | Effects of Antrodin C on TGF-β1 induced cell migration as well as α-SMA and Col1 production in CFSC-8B cells. **(A)** Representative images of migrated CSFC-8B cells treated with or without Antrodin C (12–50 μM) and SB431542 in the presence or absence of TGF-β1. The data were normalized to % of migrated control cells. Scale bar, 100 μm. **(B)** Western blot analysis of α-SMA and Col1 expression. GAPDH was used as an internal control. Data represent mean ± SD (n = 3), ***p < 0.001 compared with control; #p < 0.05, ##p < 0.01, ###p < 0.001 compared with cells treated with TGF-β1 only.

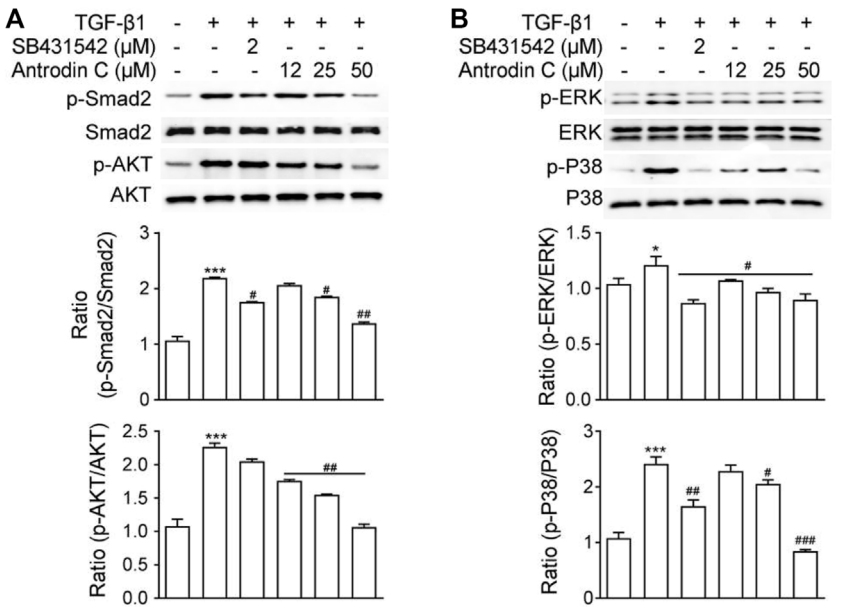

FIGURE 3 | Effects of Antrodin C on the TGF-β1-induced signaling pathway. **(A,B)** CFSC-8B cells were treated with Antrodin C (12–50 μM) for 2 h and then induced by TGF-β1 for 1 h, and total cellular extracts were prepared and subjected to Western blot analysis to measure the levels of phosphorylated Smad2, AKT, ERK, and P38. Total Smad, AKT, ERK, and P38 were used for normalization. Data represent mean ± SD (n = 3), *p < 0.05, ***p < 0.001 compared with control; #p < 0.05, ##p < 0.01, ###p < 0.001 compared with TGF-β1 treated only.

phospho-Smad2, P38, phospho-P38, ERK, phospho-ERK, AKT, phospho-AKT were purchased from Cell Signaling Technology (Danvers, MA, United States). The bands were visualized using ECL reagents (Pierce, Thermofisher Scientific, USA). Band intensity was quantified using Image lab software (Bio-Rad Laboratories, Inc. USA) and expressed as relative intensity compared with control. GAPDH level served as an internal control.

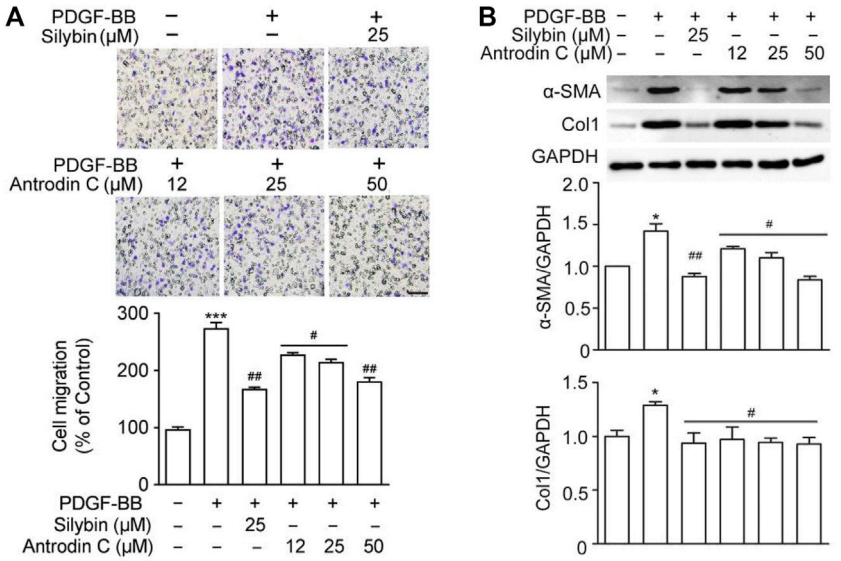

FIGURE 4 | Effects of Antrodin C on PDGF-BB induced cell migration, α-SMA and Col1 production in CFSC-8B cells. **(A)** Representative images of migrated CSFC-8B cells treated with or without Antrodin C (12–50 μM) and Silybin in the presence or absence of PDGF-BB. The data were normalized to % of migrated control cells. Scale bar, 100 μm. **(B)** Western blot analysis of α-SMA and Col1 expression. GAPDH was used as an internal control. Data represent mean ± SD (n = 3), ***p < 0.001 compared with control; #p < 0.05, ##p < 0.01, ###p < 0.001 compared with PDGF-BB treated only.

Statistical Analysis

Data are expressed as means ± SD. Differences in measured variables among groups were assessed by using One-way analysis of variance (ANOVA), and the Tukey test was used for determining the significance (Graphpad, San Diego, CA, United States). Results were considered statistically significant at $p < 0.05$.

RESULTS

Effect of Antrodin C on the Survival of CFSC-8B Cells

We examined the cytotoxic effects of Antrodin C (**Figure 1A**) on hepatic stellate CSFC-8B cells using an MTT assay. CFSC-8B cells were treated with 10–200 μM Antrodin C for 24 h (**Figure 1B**). When the concentration of Antrodin C was above 60 μM, the cell survival rate was less than 80%. Antrodin C at the concentration of 200 μM significantly inhibited CFSC-8B cell proliferation with 82% inhibition. The median inhibitory concentration (IC50) of Antrodin C for CFSC-8B cells was 147.91 μM. The data showed that Antrodin C is able to reduce the proliferation of HSCs, and because we found that the concentrations below 50 μM of Antrodin C do not have significant cytotoxic effects on CFSC-8B cells, we used these concentrations (12, 25, 50 μM) in the following experiments.

Antrodin C Inhibits TGF-β1 Induced Cell Migration in CFSC-8B Cells

A previous study suggested that the cell migration of aHSCs is involved in the initial pathological development of liver fibrosis (Selenina et al., 2019). As anticipated, TGF-β1 (10 ng/ml) up-regulated CFSC-8B cell migration, while TGF-β receptor inhibitor SB431542 (Geng et al., 2016) dramatically decreased TGF-β1 induced cell migration (**Figure 2A**). Antrodin C (12–50 μM) inhibited cell migration stimulated by TGF-β1 in a dose-dependent manner in CFSC-8B cells (**Figure 2A**). These results suggest that Antrodin C might play an inhibitory role in TGF-β1-mediated HSCs activation.

Antrodin C Reduces Activation and ECM Accumulation Induced by TGF-β1 in CFSC-8B Cells

To reveal the role of Antrodin C in HSCs activation, we assessed the effect of Antrodin C intervention on TGF-β1 induced expression of α-SMA and collagen I, that were the markers of HSCs activation (Tsuchida and Friedman, 2017). As shown in **Figure 2B**, TGF-β1 significantly increased a-SMA and Col1 expression in CFSC-8B cells. Antrodin C at a concentration of 50 μM suppressed a-SMA protein expression. The production of Col1 was also suppressed by the addition of Antrodin C (12–50 μM) in a dose-dependent manner (**Figure 2B**). Similar results were observed at the gene expression of a-SMA and Col1 by qRT-PCR analysis (**Supplementary Figure S5A**). Furthermore, Antrodin C (25–50 μM) inhibited TGF-β1 induced Col3 and Fibronectin (Fn) transcription in CFSC-8B cells (**Supplementary Figure S5A**). These data indicate that Antrodin C can inhibit the TGF-β1 induced HSCs activation and ECM production.

Antrodin C Suppresses TGF-β1-Stimulated Phosphorylation of Smad2, AKT, ERK, and P38 in CFSC-8B Cells

TGF-β1 is a well-known fibrogenic cytokine that activates HSCs and induces ECM production. Classical TGF-β1 signaling is

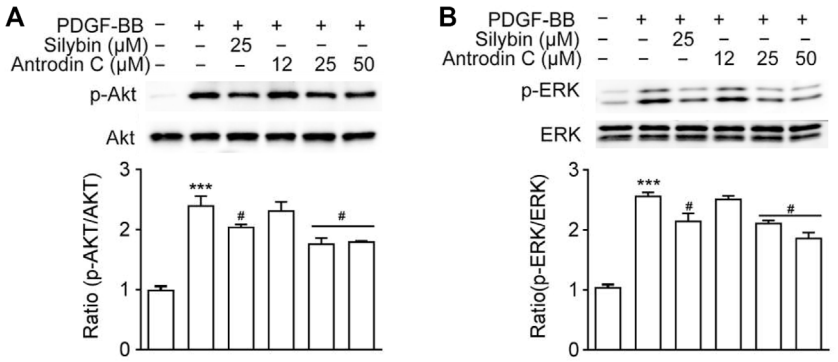

FIGURE 5 | Effects of Antrodin C on the PDGF-BB-induced signaling pathway. **(A,B)** CFSC-8B cells were treated with Antrodin C (12–50 μM) for 2 h and then induced by PDGF-BB for 1 h, and total cellular extracts were prepared and subjected to Western blot analysis to measure the levels of phosphorylated AKT and ERK. Total AKT and ERK were used for normalization. Data represent means ± SD (n = 3), ***p < 0.001 compared with control; #p < 0.05 compared with PDGF-BB treated only.

initiated with ligand-induced oligomerization of serine/threonine receptor kinases, then through phosphorylation of the cytoplasmic signaling molecules Smad2 and Smad3 (Zhao et al., 2020). As expected, TGF-β1 stimulated p-Smad2 expression in CFSC-8B cells, which was blocked by TGF-β1 receptor inhibitor SB431542 (**Figure 3A**). Within the safe doses (25–50 μM), treatment with Antrodin C reversed TGF-β1 induced p-Smad2 (**Figure 3**). TGF-β signaling can also modulate Smad-independent pathways, including PI3K/AKT, ERK, JNK, and p38 MAPK pathways (Suwanabol et al., 2012). We found that TGF-β1 significantly up regulated the phosphorylation of AKT, ERK and P38 in CFSC-8B cells (**Figure 3**). Antrodin C treatment dose dependently inhibit TGF-β1 induced phosphorylation of AKT, ERK, and P38 (**Figure 3**). These results suggest that Antrodin C not only inhibits the classical TGF-β1 pathway, but also suppresses non-classical TGF-β1 signaling in HSCs activation, which is characterized by decreased TGF-β1 induced phosphorylation level of Smad2, AKT, ERK, and P38.

Antrodin C Inhibits PDGF-BB-Induced Cell Migration in CFSC-8B Cells

The presence of PDGF-BB accelerated HSCs migration by chemoattractant mechanism (Ikeda et al., 2010). We found that PDGF-BB (10 ng/ml) induced cell migration (**Figure 4A**), while the positive control Silybin (25 μM) which is the major active constituent of hepatoprotective and anti-fibrotic drug, inhibited this effect (Brinda et al., 2012). Antrodin C (12–50 μM) suppressed the migration of CFSC-8B cells stimulated with PDGF-BB (10 ng/ml) in a dose-dependent manner (**Figure 4A**).

Antrodin C Reduces HSC Activation and ECM Accumulation Induced by PDGF-BB in CFSC-8B Cells

We then examined whether Antrodin C was able to inhibit the HSCs activation and ECM production induced by PDGF-BB at the molecular level. The remarkable makers of HSCs activation α-SMA and Col1 were both significantly induced by PDGF-BB treatment (**Figure 4B**). These inductions were suppressed by the addition of Silybin (25 μM) as well as Antrodin C (12–50 μM) (**Figure 4B**). Furthermore, α-SMA, Col1, Col3, and Fn transcription levels were significantly decreased in PDGF-BB stimulated CFSC-8B cells after 50 μM Antrodin C treatment (**Supplementary Figure S5B**). Thus, Antrodin C inhibits PDGF-BB induced HSCs activation and ECM production.

Antrodin C Treatment Downregulates PDGF-BB-Induced ERK and Akt Phosphorylation in CFSC-8B Cells

PDGF-BB is one of the most potent HSC mitogen, which binds to PDGFR-β, then sequentially activates Raf-1, MEK and extracellular-signal regulated kinase (ERK). PDGF also induces PI3K/Akt signaling pathway, which is necessary for both mitogenesis and chemotaxis and involved in activating the Ras-ERK pathway (Tricarico et al., 2002). As shown in **Figure 5A**, Antrodin C (25, 50 μM) decreased the phosphorylation of ERK compared to that of PDGF-BB-induced cells. Antrodin C (25, 50 μM) also significantly blocked PDGF-BB induced Akt phosphorylation (**Figure 5B**). These results demonstrate that the inhibitory effect of Antrodin C on liver fibrosis might be through inactivation of PDGF-BB induced p-ERK and p-Akt.

Antrodin C Protects CCl_4 Induced Liver Fibrosis in Mice

To determine the role of Antrodin C *in vivo*, we used the well-established model of CCl_4 induced liver fibrosis in mice. Histopathological analysis by H&E and Sirius-red staining showed a considerable increase in the extent of liver fibrosis after repeated injection of CCl_4 (**Figure 6A**). The oral administration of Antrodin C or positive control Silymarin reduced the degree of liver fibrosis as determined by histopathological analysis as well as the quantification of Sirus-red staining (**Figures 6A,B**). Hydroxyproline content further confirmed that Antrodin C inhibited CCl_4 induced collagen production in mice (**Figure 6C**). ALT (alanine transaminase) and AST (aspartate aminotransferase) have been recognized as indicators of liver function (Odiba et al., 2014). The elevated serum ALT and AST revealed that CCl_4 treatment

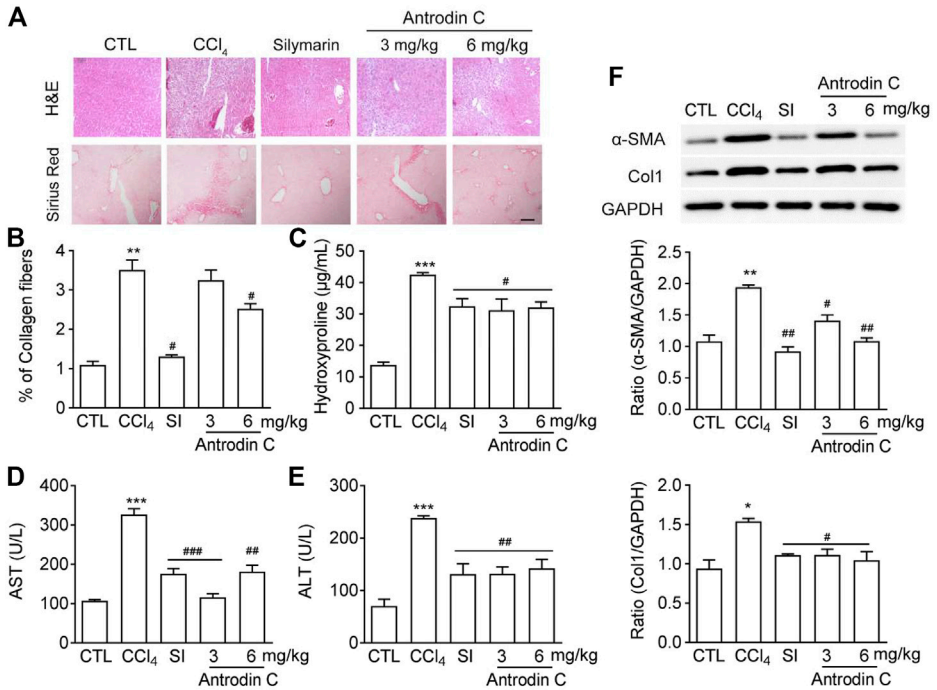

FIGURE 6 | Effects of Antrodin C on liver fibrosis induced by CCl_4 *in vivo*. **(A)** Representative images of H&E and Sirius Red staining of liver tissue sections from the different treatment groups. Scale bar, 100 μm. **(B)** The Sirius red staining was normalized to % of collagen fibers of the control group. **(C)** Hydroxyproline contents, **(D)** ALT and **(E)** AST activity in serum of CCl_4-induced mice or control mice. **(F)** Western blot analysis of α-SMA and Col1 expression in livers tissues. GAPDH was used as an internal control. Data represent means ± SD (n = 6), $^{*}p < 0.05$, $^{**}p < 0.01$, $^{***}p < 0.001$ compared with control group; $\#p < 0.05$, $\#\#p < 0.01$, $\#\#\#p < 0.001$ compared with CCl_4-treated group. CTL: the control group; CCl_4: the CCl_4 treated group; SI: the Silymarin treated group.

cause hepatotoxicity, while Antrodin C treatment dramatically inhibited this effect (**Figures 6D,E**). HSCs are mainly responsible in the progression of liver fibrosis which produces massive ECM including collagens, and α-SMA is a marker of the activated HSCs (Tsuchida and Friedman, 2017). Repeated CCl_4 injection resulted in the liver fibrosis with increased α-SMA and Col1 protein expression (**Figure 6F**). Immunoblotting analysis revealed that α-SMA and Col1 were less expressed in the liver tissues from the Antrodin C treated group than the CCl_4 group (**Figure 6F**). Therefore, Antrodin C showed a protective effect on liver injury and fibrosis.

Antrodin C Inhibits CCl_4 Induced Phosphorylation of Smad2, -Akt, -ERK and -P38 MAPK in Mice

To explore a potential signaling pathways affected by Antrodin C treatments, we determined the levels of p-Smad2, p-Akt, p-ERK, and p-P38 MAPK, which belong to the TGF-β1 or PDGF-BB mediated signaling pathways. The results showed that the p-Smad2, p-Akt, p-ERK, and p-P38 were increased in mice treated with CCl_4 compared with the control group (**Figures 7A,B**). Antrodin C treatment significantly inhibited the phosphorylation of Smad2, Akt, ERK, JNK and P38 (**Figures 7A,B**). These results demonstrate that Antrodin C offers a promising therapeutic strategy for patients with liver fibrosis through inhibiting p-Smad2, p-Akt, p-ERK, and p-P38.

DISCUSSION

Many bioactive components/compounds were identified in *A. camphorata*, including triterpenoids, polysaccharides, benzenoids, lignans, steroids, succinic, and maleic derivatives (Geethangili and Tzeng, 2010). However, little attention has been focused on why *A. camphorate* can inhibit liver fibrosis and what ingredients play a key role. In our study, we found that Antrodin C isolated from *A. camphorata* demonstrate significant anti-liver fibrosis properties. Antrodin C significantly inhibited cell migration, ECM production and HSCs activation induced by TGF-β1 or PDGF-BB in a dosage-dependent manner. In terms of mechanism, Antrodin C suppressed TGF-β1 induced p-Smad2, p-AKT, p-ERK, p-P38, as well as PDGF-BB induced p-AKT and p-ERK. We also showed that Antrodin C could attenuate CCl_4-induced liver fibrosis in mice through blocking phosphorylation of Smad2/Akt/ERK/P38.

HSCs are believed to be a key player of liver fibrosis. Growth factors (TGF-β and PDGF) can provoke the activation of the HSCs, and activated HSCs migrate to the sites of damaged tissue and contribute to the expansion of fibrotic lesions in liver. We used CFSC-8B cells which are an immortalized rat liver stellate cell line as an *in vitro* cell model of hepatic fibrosis (Greenwel et al., 1995). We observed that Antrodin C inhibited TGF-β1 or PDGF-BB stimulated CFSC-8B cell activation, migration and ECM production.

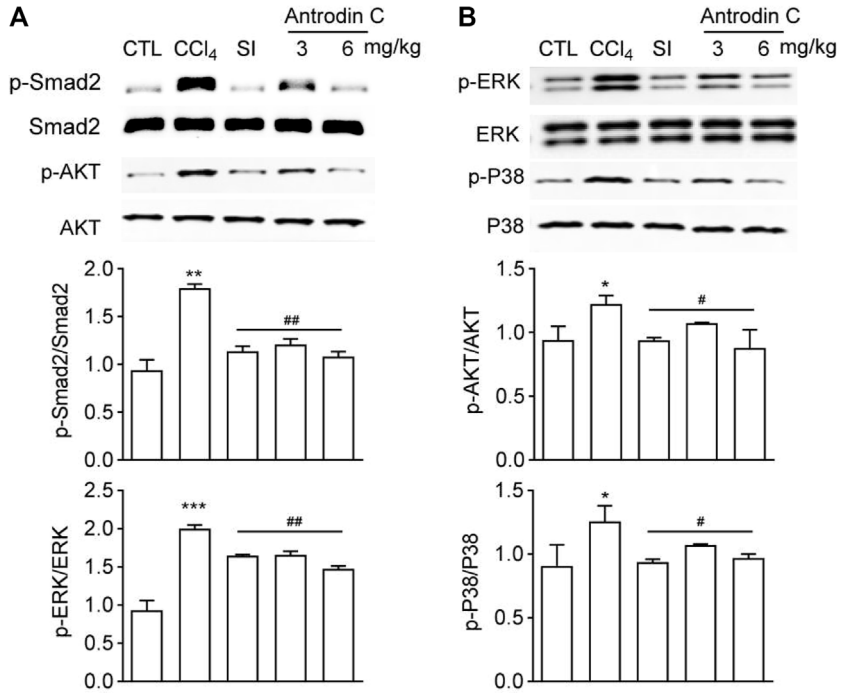

FIGURE 7 | Effects of Antrodin C on phosphorylation of Smad2, AKT, ERK, and P38 in the livers of CCl_4-treated mice. **(A,B)** Western blot analysis of phosphorylated and total Smad2, AKT, ERK, and P38 in livers tissues. Total Smad2, AKT, ERK, and P38 were used for normalization, respectively. Data represent mean ± SD ($n = 6$), $^*p < 0.05$, $^{**}p < 0.01$, $^{***}p < 0.001$ compared with control group; $\#p < 0.05$, $\#\#p < 0.01$ compared with CCl_4-treated group. CTL: the control group; CCl_4: the CCl_4-treated group; SI: the Silymarin treated group.

Current anti-fibrotic therapeutic strategies include inhibition of HSCs migration, TGF-β expression and activation, blocking TGF-β canonical or non-canonical signaling pathways (Rosenbloom et al., 2013). TGF-β signaling pathways are critical for the fibrotic response. The canonical TGF-β1 signaling is mediated through receptor binding, then through receptor activating Smads, Smad2, or Smad3 (Kastanis et al., 2011). In addition to the Smad dependent pathway, TGF-β1 also activate PI3K/AKT, ERK, JNK, and P38 MAPK signaling pathways, which play an important role in regulating HSC activation and ECM synthesis (Voloshenyuk et al., 2011). Our data showed that TGF-β1 stimulated the canonical or non-canonical signaling indicated by the up regulation of phosphorylation of Smad2, Akt, ERK, and p38 MAPK, which could be inhibited by Antrodin C.

PDGF signaling plays a critical role in various cellular responses including proliferation, chemotaxis and actin reorganization. PDGFs bind and activate tyrosine kinase receptors, PDGFRα and PDGFRβ, which leads to overlapping signaling, including Src family kinases, PI3K/AKT and Ras-MAPK. PDGF can affect the fibrotic progression of several organs, including liver, lung and kidney (Steiner and Higgins, 2018). Several reports have implicated that there was a crosstalk between TGF-β1 and PDGF signaling (Novosyadlyy et al., 2006). Our results demonstrated that Antrodin C might suppress the PDGF induced activation of HSCs through blocking phosphorylation of Akt and ERK.

CCl_4-induced hepatic fibrosis in mice is a well-known *in vivo* model for screening anti-fibrotic drugs (Kuwahata et al., 2012). The metabolites of CCl_4 cause the apoptosis of hepatocyte and liver injury. Repeated injection of CCl_4 causes chronic injury to the liver, eventually results in liver fibrosis. Hepatocyte integrity indicators ALT and AST were both up regulated after CCl_4 treatment. We found that the treatment with Antrodin C significantly diminished the liver fibrosis accompanied by the decreasing AST and ALT levels in blood circulation. Antrodin C also inhibited the activation of HSC *in vivo* revealed by the decreased expression level of α-SMA. In terms of mechanism, it was found that repeated CCl_4 injections could induce the phosphorylation of Smad2, Akt and MAPK in the mouse liver tissues (Yoshida et al., 2005), whereas the oral administration with Antrodin C suppressed the phosphorylation of Smad2, Akt, ERK and P38 in the fibrotic livers. Further studies are needed to identify the underlying receptor-dependent. Moreover, Antrodin C may inhibits liver fibrosis by other Signaling pathways like TNF-α-NF-κB, AMPK, and β-Catenin Signaling pathway (Yang et al., 2019).

In conclusion, Antrodin C suppresses HSC activation, migration and ECM production, partially through inhibition of PDGF and TGF-β1 signaling pathways, that are the two most potent stimuli of liver fibrosis. Our study provides new insights for the development of therapeutic drugs against liver fibrosis. However, further studies are needed to fully understand

the cellular and molecular mechanisms of Antrodin C in liver fibrosis.

DATA AVAILABILITY STATEMENT

The original contributions presented in the study are included in the article/**Supplementary Material**, further inquiries can be directed to the corresponding authors.

ETHICS STATEMENT

The animal study was reviewed and approved by the Experimental Animal ethics committee of jiangnan unversity.

AUTHOR CONTRIBUTIONS

X-YX and YG conceived and designed this research. X-YX and YR performed most of the experiments and analyzed data. YM and H-XX contributed to reagents and materials. X-YX and YG contributed to the manuscript editing. All authors contributed and reviewed the results and approved the final version of the manuscript.

FUNDING

This work was supported by the National Natural Science Foundation of China (Grant No. 31970746, 31771514, 31201020) and the Qing Lan Project in Jiangsu Province.

ACKNOWLEDGMENTS

We thank Xiao-Qian Xie and Qing Sun for their technical assistance.

SUPPLEMENTARY MATERIAL

The Supplementary Material for this article can be found online at: https://www.frontiersin.org/articles/10.3389/fmolb.2022.835508/full#supplementary-material

REFERENCES

Aydin, M. M., and Akcali, K. C. (2018). Liver Fibrosis. *Turk J. Gastroenterol.* 29 (1), 14–21. doi:10.5152/tjg.2018.17330

Brinda, B. J., Zhu, H.-J., and Markowitz, J. S. (2012). A Sensitive LC-MS/MS Assay for the Simultaneous Analysis of the Major Active Components of Silymarin in Human Plasma. *J. Chromatogr. B* 902, 1–9. doi:10.1016/j.jchromb.2012.06.003

Caligiuri, A., Gentilini, A., Pastore, M., Gitto, S., and Marra, F. (2021). Cellular and Molecular Mechanisms Underlying Liver Fibrosis Regression. *Cells* 10 (10). doi:10.3390/cells10102759

David, V., and George, J. (2008). Disease-Specific Mechanisms of Fibrosis: Hepatitis C Virus and Nonalcoholic Steatohepatitis. *Clin. Liver Dis.* 12 (4), 805–824.

Deng, X. X., Li, H., Zhang, Z. F., and Gu, Q. L. (2020). Research Progress of Liver Sinusoidal Endothelial Cells in the Regulation of Liver Microenvironment to Affect Liver Fibrosis. *Zhonghua Gan Zang Bing Za Zhi* 28 (4), 357–360. doi:10.3760/cma.j.cn501113-20190715-00247

Dhar, D., Baglieri, J., Kisseleva, T., and Brenner, D. A. (2020). Mechanisms of Liver Fibrosis and its Role in Liver Cancer. *Exp. Biol. Med. (Maywood)* 245 (2), 96–108. doi:10.1177/1535370219898141

Geethangili, M., and Tzeng, Y. M. (2010). Review of Pharmacological Effects of Antrodia Camphorata and its Bioactive Compounds. *Evid. Based Complement. Alternat Med.* 2011 (1741-427X), 212641. doi:10.1093/ecam/nep108

Geng, Y., Wang, J., Sun, Q., Xie, M., Lu, Z. M., Xu, H. Y., et al. (2016). Identification of Antrodin B from Antrodia Camphorata as a New Anti-hepatofibrotic Compound Using a Rapid Cell Screening Method and Biological Evaluation. *Hepatol. Res.* 46, E15–E25. doi:10.1111/hepr.12516

George, J., Tsuchishima, M., and Tsutsumi, M. (2019). Molecular Mechanisms in the Pathogenesis of N-Nitrosodimethylamine Induced Hepatic Fibrosis. *Cel Death Dis.* 10. doi:10.1038/s41419-018-1272-8

Goldstein, N. S., Hastah, F., Galan, M. V., and Gordon, S. C. (2005). Fibrosis Heterogeneity in Nonalcoholic Steatohepatitis and Hepatitis C Virus Needle Core Biopsy Specimens. *Am. J. Clin. Pathol.* 123 (3), 382–387. doi:10.1309/ey72f1en9xcb1kxx

Guerra, S., Mamede, A. C., Carvalho, M. J., Laranjo, M., Tralhão, J. G., Abrantes, A. M., et al. (2016). Liver Diseases: what Is Known So Far about the Therapy with Human Amniotic Membrane? *Cell Tissue Bank* 17 (4), 653–663. doi:10.1007/s10561-016-9579-0

Greenwel, P., Schwartz, M., Rosas, M., Peyrol, S., Grimaud, J. A., and Rojkind, M. (1991). . Characterization of Fat-Storing Cell Lines Derived From Normal and CCl4-Cirrhotic Livers. Differences in the Production of Interleukin-6. *Laboratory Investigation, 1991. 65(6): p. 644-653.* 65 (6), 644–653.

Huang, T. T., Lan, Y. W., Chen, C. M., Ko, Y. F., Ojcius, D. M., Martel, J., et al. (2019). Antrodia Cinnamomea Induces Anti-tumor Activity by Inhibiting the STAT3 Signaling Pathway in Lung Cancer Cells. *Sci. Rep.* 9, 5145. doi:10.1038/s41598-019-41653-9

Ikeda, K., Wakahara, T., Wang, Y. Q., Kadoya, H., Kawada, N., and Kaneda, K. (2010). *In Vitro* migratory Potential of Rat Quiescent Hepatic Stellate Cells and its Augmentation by Cell Activation. *Hepatology* 29 (6), 1760–1767. doi:10.1002/hep.510290640

Jin, C. H., Jang, J., and Min, K. T. (2020). The Role of Hepatic Stellate Cells in Fibrotic Liver Diseases. *J. Anim. Reproduciton Biotechnol.* 35 (2), 113–118.

Kang, K.-H., Qian, Z.-J., Ryu, B., Karadeniz, F., Kim, D., and Kim, S.-K. (2013). Hepatic Fibrosis Inhibitory Effect of Peptides Isolated from Navicula Incerta on TGF-β Induced Activation of LX-2 Human Hepatic Stellate Cells. *Jfn* 18 (2), 124–132. doi:10.3746/pnf.2013.18.2.124

Kastanis, G. J., Hernandez-Nazara, Z., Nieto, N., Rincón-Sanchez, A. R., Popratiloff, A., Dominguez-Rosales, J. A., et al. (2011). The Role of Dystroglycan in PDGF-BB-dependent Migration of Activated Hepatic Stellate Cells/myofibroblasts. *Am. J. Physiology-Gastrointestinal Liver Physiol.* 301 (3), G464–G474. doi:10.1152/ajpgi.00078.2011

Kumar, K. J. S., Vani, M. G., Chueh, P. J., Mau, J. L., and Wang, S. Y. (2015). Antrodin C Inhibits Epithelial-To-Mesenchymal Transition and Metastasis of Breast Cancer Cells via Suppression of Smad2/3 and Beta-Catenin Signaling Pathways. *Plos One* 10 (2). doi:10.1371/journal.pone.0117111

Kuwahata, M., Kubota, H., Kanouchi, H., Ito, S., Ogawa, A., Kobayashi, Y., et al. (2012). Supplementation with Branched-Chain Amino Acids Attenuates Hepatic Apoptosis in Rats with Chronic Liver Disease. *Nutr. Res.* 32 (7), 522–529. doi:10.1016/j.nutres.2012.06.007

Lee, A. S., Jung, Y. J., Kim, D., Nguyen-Thanh, T., Kang, K. P., Lee, S., et al. (2014). SIRT2 Ameliorates Lipopolysaccharide-Induced Inflammation in Macrophages. *Biochem. Biophysical Res. Commun.* 450 (4), 1363–1369. doi:10.1016/j.bbrc.2014.06.135

Nakamura, N., Hirakawa, A., Gao, J.-J., Kakuda, H., Shiro, M., Komatsu, Y., et al. (2004). Five New Maleic and Succinic Acid Derivatives from the Mycelium of Antrodia Camphorata and Their Cytotoxic Effects on LLC Tumor Cell Line. *J. Nat. Prod.* 67 (1), 46–48. doi:10.1021/np030293k

Novosyadlyy, R., Dudas, J., and Pannem, R. (2006). Crosstalk Between PDGF and IGF-I Receptors in Rat Liver Myofibroblasts: Implication for Liver Fibrogenesis. *Lab. Invest.* 86, 710–723.

Odiba, A. S., Ukegbu, C., Okechukwu, I., and Iruoghene, O. (2014). Transaminase [Alanine aminotransferase (ALT) and Aspartate aminotransferase (AST)] Activity of HIVFemale Patients on Drugs and Female Patients Not on Drugs. *IOSR J. Pharm. Biol. Sci.* 9 (7), 60–65.

Rosenbloom, J., Mendoza, F. A., and Jimenez, S. A. (2013). Strategies for Anti-fibrotic Therapies. *Biochim. Biophys. Acta* 1832 (7), 1088–1103. doi:10.1016/j.bbadis.2012.12.007

Schyman, P., Printz, R. L., Estes, S. K., O'Brien, T. P., Shiota, M., and Wallqvist, A. (2019). Assessing Chemical-Induced Liver Injury *In Vivo* from *In Vitro* Gene Expression Data in the Rat: The Case of Thioacetamide Toxicity. *Front. Genet.* 10, 1233. doi:10.3389/fgene.2019.01233

Selenina, A., Tomilin, A., and Tsimokha, A. (2019). Evidences against Vesicle-dependent Trafficking and Involvement of Extracellular Proteasomes into Cell-To-Cell Communications. *Biochem. Biophysical Res. Commun.* 508 (2), 368–373.

Steiner, C. A., and Higgins, P. (2018). *Anti-Fibrotic Therapies from Other Organs: What the Gut Can Learn from the Liver, Skin, Lung and HeartFibrostenotic Inflammatory Bowel Disease*.

Suwanabol, P. A., Seedial, S. M., Zhang, F., Shi, X., Si, Y., Liu, B., et al. (2012). TGF-β and Smad3 Modulate PI3K/Akt Signaling Pathway in Vascular Smooth Muscle Cells. *Am. J. Physiology-Heart Circulatory Physiol.* 302 (11), H2211–H2219. doi:10.1152/ajpheart.00966.2011

Tan, Z., Sun, H., Xue, T., Gan, C., Liu, H., Xie, Y., et al. (2021). Liver Fibrosis: Therapeutic Targets and Advances in Drug Therapy. *Front. Cel Developmental Biol.* 9, 730176. doi:10.3389/fcell.2021.730176

Tricarico, C., Pinzani, P., Bianchi, S., Paglierani, M., Distante, V., Pazzagli, M., et al. (2002). Quantitative Real-Time Reverse Transcription Polymerase Chain Reaction: Normalization to rRNA or Single Housekeeping Genes Is Inappropriate for Human Tissue Biopsies. *Anal. Biochem.* 309 (2), 293–300. doi:10.1016/s0003-2697(02)00311-1

Trivedi, P., Wang, S., and Friedman, S. L. (2021). The Power of Plasticity-Metabolic Regulation of Hepatic Stellate Cells. *Cel Metab.* 33 (2), 242–257. doi:10.1016/j.cmet.2020.10.026

Tsuchida, T., and Friedman, S. L. (2017). Mechanisms of Hepatic Stellate Cell Activation. *Nat. Rev. Gastroenterol. Hepatol.* 14 (7), 397–411. doi:10.1038/nrgastro.2017.38

Voloshenyuk, T. G., Landesman, E. S., Khoutorova, E., Hart, A. D., and Gardner, J. D. (2011). Induction of Cardiac Fibroblast Lysyl Oxidase by TGF-B1 Requires PI3K/Akt, Smad3, and MAPK Signaling. *Cytokine* 55 (1), 90–97. doi:10.1016/j.cyto.2011.03.024

Yang, H., Bai, X., Zhang, H., Zhang, J., Wu, Y., Tang, C., et al. (2019). Antrodin C, an NADPH Dependent Metabolism, Encourages Crosstalk between Autophagy and Apoptosis in Lung Carcinoma Cells by Use of an AMPK Inhibition-independent Blockade of the Akt/mTOR Pathway. *Molecules* 24 (5). doi:10.3390/molecules24050993

Yoon, Y.-C., Fang, Z., Lee, J. E., Park, J. H., Ryu, J.-K., Jung, K. H., et al. (2020). Selonsertib Inhibits Liver Fibrosis via Downregulation of ASK1/MAPK Pathway of Hepatic Stellate Cells. *Biomolecules Ther.* 28 (6), 527–536. doi:10.4062/biomolther.2020.016

Yoshida, K., Matsuzaki, K., Mori, S., Tahashi, Y., Yamagata, H., Furukawa, F., et al. (2005). Transforming Growth Factor-β and Platelet-Derived Growth Factor Signal via C-Jun N-Terminal Kinase-dependent Smad2/3 Phosphorylation in Rat Hepatic Stellate Cells after Acute Liver Injury. *Am. J. Pathol.* 166 (4), 1029–1039. doi:10.1016/s0002-9440(10)62324-3

Zhao, Z., He, D., Ling, F., Chu, T., Huang, D., Wu, H., et al. (2020). CD4+ T Cells and TGFβ1/MAPK Signal Pathway Involved in the Valvular Hyperblastosis and Fibrosis in Patients with Rheumatic Heart Disease. *Exp. Mol. Pathol.* 114, 104402. doi:10.1016/j.yexmp.2020.104402

Zhenwei, Y., Liu, X., Liang, L., Wang, G., Xiong, Z., Zhang, H., et al. (2021). Antrodin A from Antrodia Camphorata Modulates the Gut Microbiome and Liver Metabolome in Mice Exposed to Acute Alcohol Intake. *Food Funct.* 12 (7), 2925–2937.

Conflict of Interest: The authors declare that the research was conducted in the absence of any commercial or financial relationships that could be construed as a potential conflict of interest.

Publisher's Note: All claims expressed in this article are solely those of the authors and do not necessarily represent those of their affiliated organizations, or those of the publisher, the editors and the reviewers. Any product that may be evaluated in this article, or claim that may be made by its manufacturer, is not guaranteed or endorsed by the publisher.

frontiers in Molecular Biosciences

ORIGINAL RESEARCH
published: 22 February 2022
doi: 10.3389/fmolb.2022.853654

Blockage of ERCC6 Alleviates Spinal Cord Injury Through Weakening Apoptosis, Inflammation, Senescence, and Oxidative Stress

Peng Zou[1,2†], Xiaoping Zhang[1†], Rui Zhang[1†], Xin Chai[2], Yuanting Zhao[2], Erliang Li[1], Qian Zhang[1], Rongbao Yan[1], Junsong Yang[2] and Bo Liao[1]**

[1]Department of Spinal Surgery, Tangdu Hospital, Second Affiliated Hospital of Air Force Military Medical University, Xi'an, China, [2]Department of Spinal Surgery, Honghui Hospital, Xi'an Jiaotong University, Xi'an, China

OPEN ACCESS

Edited by:
Leming Sun,
Northwestern Polytechnical University, China

Reviewed by:
Qing Li,
Army Medical University, China
Xing Niu,
ShengJing Hospital of China Medical University, China

***Correspondence:**
Bo Liao
liao_b@hotmail.com
Junsong Yang
yangjunsong1988@sina.com

†These authors have contributed equally to this work and share first authorship

Specialty section:
This article was submitted to Molecular Diagnostics and Therapeutics, a section of the journal Frontiers in Molecular Biosciences

Received: 12 January 2022
Accepted: 21 February 2022
Published: 22 February 2022

Citation:
Zou P, Zhang X, Zhang R, Chai X, Zhao Y, Li E, Zhang Q, Yan R, Yang J and Liao B (2022) Blockage of ERCC6 Alleviates Spinal Cord Injury Through Weakening Apoptosis, Inflammation, Senescence, and Oxidative Stress. Front. Mol. Biosci. 9:853654. doi: 10.3389/fmolb.2022.853654

Objective: Spinal cord injury (SCI) is a devastating disease resulting in lifelong disability, but the molecular mechanism remains unclear. Our study was designed to observe the role of excision repair cross-complementing group 6 (ERCC6) following SCI and to determine the underlying mechanism.

Methods: SCI mouse models and LPS-induced microglia cell models were established. ERCC6 expression was blocked by ERCC6-siRNA-carrying lentivirus. Nissl staining was utilized for detecting neuronal damage, and apoptosis was analyzed with TUNEL and Western blotting (apoptotic markers). Immunofluorescence was used for measuring macrophage markers (CD68 and F4/80) and astrocyte and microglia markers (GFAP and Iba-1). Pro-inflammatory cytokines (TNF-α, IL-1β, and IL-6) were measured *via* ELISA. Senescent cells were estimated *via* SA-β-Gal staining as well as Western blot (senescent markers p21 and p27). Oxidative stress was investigated by detecting the expression of 4-HNE, Nrf2, and Keap1, and intracellular ROS levels.

Results: ERCC6 expression was remarkably upregulated both in the spinal cord of SCI mice and LPS-induced microglia cells. ERCC6 deficiency alleviated neuronal damage and apoptosis. Macrophage infiltration and inflammatory response were suppressed by si-ERCC6 treatment. Moreover, ERCC6 blockage ameliorated astrocyte and microglia activation and cell senescence in the damaged spinal cord. Excessive oxidative stress was significantly decreased by ERCC6 knockdown in SCI.

Conclusion: Collectively, ERCC6 exerts crucial functions in mediating physiological processes (apoptosis, inflammation, senescence, and oxidative stress), implying that ERCC6 might act as a prospective therapeutic target against SCI.

Keywords: spinal cord injury, ERCC6, apoptosis, inflammation, senescence, oxidative stress

Abbreviations: SCI, spinal cord injury; ERCC6, excision repair cross-complementing group 6; LPS, lipopolysaccharide; siRNAs, small interfering RNAs; RT-qPCR, real-time quantitative PCR; TUNEL, terminal-deoxynucleoitidyl transferase mediated nick end labeling; ELISA, enzyme-linked immunosorbent assay; IL-1β, interleukin-1β; TNF-α, tumor necrosis factor-α; SA-β-Gal, senescence-associated β-galactosidase; ROS, reactive oxygen species; DCFH-DA, dichloro-dihydro-fluorescein diacetate.

INTRODUCTION

Spinal cord injury (SCI), a highly disabling neurological disorder, usually leads to permanent motor and sensory dysfunctions, affecting approximately 250,000–500,000 individuals each year (Zhou et al., 2020). SCI is characterized by the lesion cores or fibrotic scars without viable neural tissues, the scars of astrocytes around the lesion cores, and the area of surviving neural tissues with limited functions and functional plasticity (Zou, 2021). Despite the structural support provided by the lesion scars, there is a suppressive environment for the regeneration of severed axons, thereby suppressing the re-debilitation of the original target (Kuboyama et al., 2021). SCI is also characterized by astrocyte and infiltrating macrophage activation in the spinal cord (Van Broeckhoven et al., 2021). Following damage, the blood–spinal cord barrier is destroyed. Despite gradual recovery, it will be damaged for a long time, promoting immune cell extravasation as well as chronic inflammation (Zrzavy et al., 2021). Due to complex pathophysiology (apoptosis, inflammation, senescence, oxidative stress, etc.), the therapeutic options of SCI are limited (Xue Wang et al., 2021). At present, several therapeutic interventions have been applied for SCI, such as high-dose methylprednisolone, ganglioside, and immunoglobulin G, which show favorable clinical benefits for a subset of patients (Wu et al., 2021). Nevertheless, these drugs cannot improve recovery after SCI to a large extent.

SCI involves primary and secondary damage (Hough et al., 2021). Primary injury is usually triggered by mechanical damage of the spinal cord, while secondary injury can be caused by the delayed sequences of complex biochemical as well as cell processes (Feng et al., 2021). Altogether, primary and secondary injuries result in irreversible neuronal injury, eventually culminating in unfavorable functional recovery after SCI (Zhang et al., 2021). Hence, to prevent irreversible injury by targeting specific molecules is a feasible therapeutic regimen against SCI. Excision repair cross-complementing group 6 (ERCC6, as shown as CSB), a DNA-binding protein, is of importance for transcription-coupled excision repair as well as DNA repair processes (Takahashi et al., 2019). This protein possesses ATP-stimulated ATPase activity as well as interacts with transcription and excision repair proteins, thereby promoting the formation of complexes at DNA repair sites (Takahashi et al., 2019). ERCC6 expression is frequently upregulated in cancer cells, favoring cancer cell proliferation while suppressing apoptosis, which has been recognized as a promising actionable target for cancer treatment (Proietti-De-Santis et al., 2018). Moreover, ERCC6 is involved in the pathogenesis of age-related diseases. For instance, ERCC6 may disrupt autophagic flux in age-related cataract *via* binding to VCP (Cao et al., 2021). Ultraviolet-B-induced ERCC6 inhibition contributes to age-related nuclear cataract (Wang et al., 2016). However, the role of ERCC6 in SCI remains unknown. Herein, we investigated whether ERCC6 was highly expressed following SCI and targeting ERCC6 alleviated apoptosis, inflammation, senescence, and oxidative stress both in the SCI mouse and cellular models. Hence, ERCC6 might become a therapeutic target against SCI.

MATERIALS AND METHODS

Animals and Groups

All experimental protocols gained the approval of the Animal Research Committee of Tangdu Hospital, Second Affiliated Hospital of Air Force Military Medical University (KY-2020015). C57BL/6 mice (8–12 weeks old; 20–25 g) purchased from Changzhou Cavans Experimental Animal Co., Ltd. (China) were cared for strictly following the ethical guidelines on animal experimentation of Laboratory Animals of China National Institutes of Health. All mice were housed in a well-ventilated environment with a 12-h light–dark cycle, at 23 ± 2°C and 70 ± 10% humidity, with free food and water. They were randomized into control group, sham group, SCI-Day 3 group (SCI on day 3), SCI-Day 7 group (SCI on day 7), SCI-Day 14 group (SCI on day 14), and SCI-Day 28 group (SCI on day 28), with eight mice in each group. Abovementioned mice did not receive any medication. Other mice were randomly separated into control group, sham group, SCI + si-NC group, and SCI + si-ERCC6 group, with eight mice in each group.

Establishment of SCI Mouse Models and Treatment

C57BL/6 mice were anesthetized by intraperitoneally injecting sodium pentobarbital (30 mg/kg). The limbs were fixed and the chest was raised with cotton pads. All animals were placed on a constant heating pad for maintaining at 37°C throughout the operation. The dorsal skin tissues were opened along the spinal column, and the muscles were peeled off layer by layer, and the T9 and T10 segments of the spine were located. Under an operating microscope, laminectomy was carried out at the T9 and T10 levels for exposing the surface of the dorsal cord without damaging the dura mater. For the SCI group, a 10 g weight was dropped from 1.5 cm to the exposed spinal cord for inducing a SCI contusion and for keeping the dura mater unbroken. Thereafter, the muscle as well as skin was sutured layer by layer utilizing 4–0 silks and needles. Following SCI, the mice were free to drink and eat, and the breeding environment was kept at a constant temperature of 22°C and a constant humidity of 30–50%. The criteria for successful modeling were as follows: spinal cord tissues of mice presented swelling, edema, and bleeding; hind limbs were paralyzed; and the mice were unable to urinate or defecate spontaneously. Manual bladder emptying was conducted 3 times each day until the voluntary urination was restored. The mice were given intraperitoneal injection of penicillin (0.2 ml/kg) for three consecutive days to prevent infection. The control group did not undergo any treatment. For the sham group, only after the spinal cord was exposed, the incision was closed layer by layer in mice. On 3, 7, 14, 21, and 28 days following SCI, animals were euthanized and spinal cord tissues were collected.

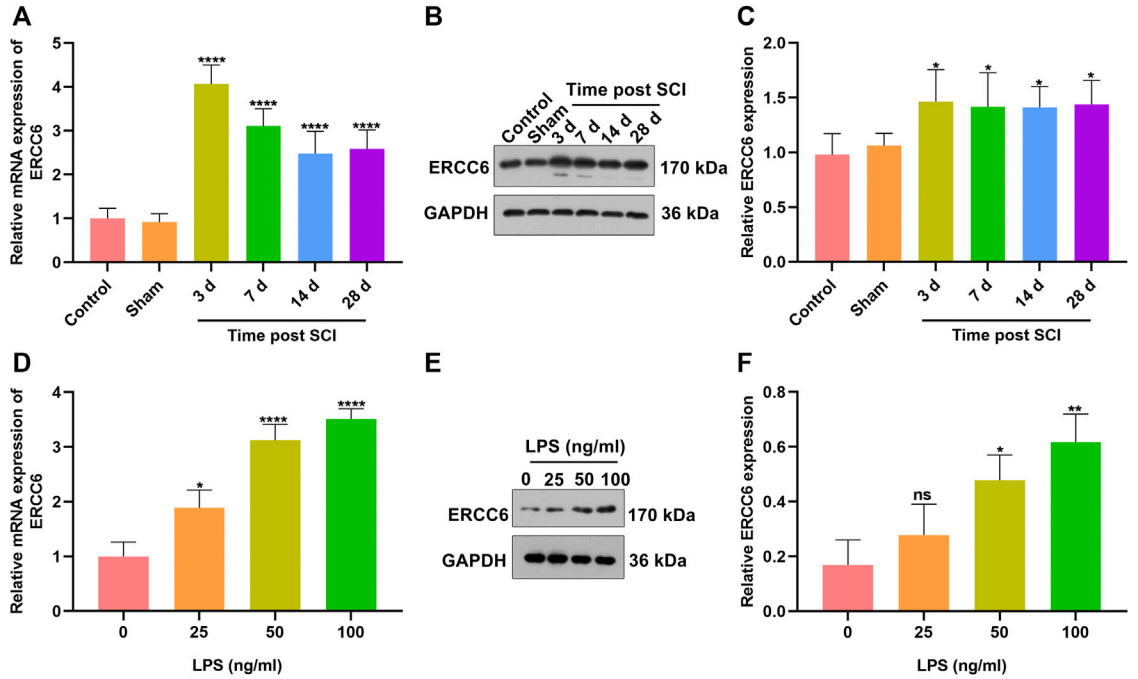

FIGURE 1 | ERCC6 is highly expressed in SCI mice and LPS-induced mouse microglia cells. **(A)** RT-qPCR analysis of ERCC6 expression in the damaged spinal cord of mouse models on days 3, 7, 14, and 18 following ICI operations as well as control and sham operation mice (N = 8 mice in each group). **(B,C)** Western blotting analysis of ERCC6 expression in the damaged spinal cord of mouse models on days 3, 7, 14, and 18 following ICI operations as well as control and sham operation mice (N = 8 mice in each group). **(D)** RT-qPCR analysis of ERCC6 expression in BV2 mouse microglia cells exposed to distinct concentrations of LPS (N = 3 mice in each group). **(E,F)** Western blotting analysis of ERCC6 expression in BV2 mouse microglia cells under exposure to distinct concentrations of LPS (N = 3 mice in each group). *p*-values were calculated with the ANOVA test. Ns: no significance; **p*-value < 0.05; ***p*-value < 0.01; *****p*-value < 0.0001.

Animal Treatment

For the evaluation of the functions of ERCC6 during spinal cord damage, siRNAs against ERCC6 (si-ERCC6) were cloned into LV-3 lentivirus vectors. The LV-3 vectors inserted with non-specific siRNAs were utilized as negative control (si-NC). In the SCI + si-NC group and SCI + si-ERCC6 group, the mice received SCI treatment, and were injected with si-NC or si-ERCC6 (10^5 plaque-forming units) in the intrathecal space utilizing glass micropipettes following SCI. Following 28 days, mice were euthanized by intraperitoneally injecting pentobarbital sodium (200 mg / kg). Euthanasia was judged by complete cessation of heartbeat, breathing, and loss of reflexes. Then, spinal cord tissues were collected.

Cell Culture

The murine BV2 microglial cell line (ATCC, United States) was grown in DMEM plus 10% FBS and 1% penicillin/streptomycin in a 5% CO_2 incubator at 37°C. Until the confluence reached about 80%, the cells were digested by trypsin and passaged for subsequent experiments. Lipopolysaccharide (LPS) was obtained from Sigma-Aldrich (United States). BV2 cells were exposed to LPS (0, 25, 50, and 100 ng/ml) lasting 24 h.

Transfection of Small Interfering RNAs

SiRNAs against ERCC6 (si-ERCC6) and negative control (si-NC) were designed and synthesized by Generay Biotech (Shanghai, China). After treatment with LPS for 24 h, transfection of siRNAs was implemented in accordance with the manufacturer's instructions. In brief, the Lipofectamine 3,000 transfection reagent (Beyotime, China) and siRNAs were mixed together in Opti-MEM. Thereafter, the cell culture medium was exchanged with Opti-MEM lasting 6 h. The cells were exchanged with the normal medium and continued to culture, lasting 48 h.

Real-Time Quantitative PCR

Total RNA extracts were conducted utilizing TRIzol reagent. 5 μg RNA was utilized for synthesizing cDNA. RT-qPCR was implemented on SYBR Green (Sigma-Aldrich, United States). cDNA was amplified on the 7,500 fast RT-PCR system (ABI, United States). The relative mRNA expression was normalized to the housekeeping gene GAPDH with $2^{-\Delta\Delta CT}$ approach. The oligonucleotide primers were as follows: ERCC6, 5′-ATGTTC CACGAGGAAGTTCCC-3' (forward) and 5′-GCCCAACTG GCATGTCTTTG-3' (reverse), and GAPDH, 5′-AGGTCGGTG TGAACGGATTTG-3' (forward) and 5′-GGGGTCGTTGAT GGCAACA-3' (reverse).

Western Blotting

Extraction of total protein was conducted utilizing QIAzol™ lysis reagent (Qiagen, CA). 40 μg protein was subjected to SDS–PAGE as well as transferred onto PVDF membranes (Millipore, MA). Thereafter, the blots were blocked with 5% blotting grade milk

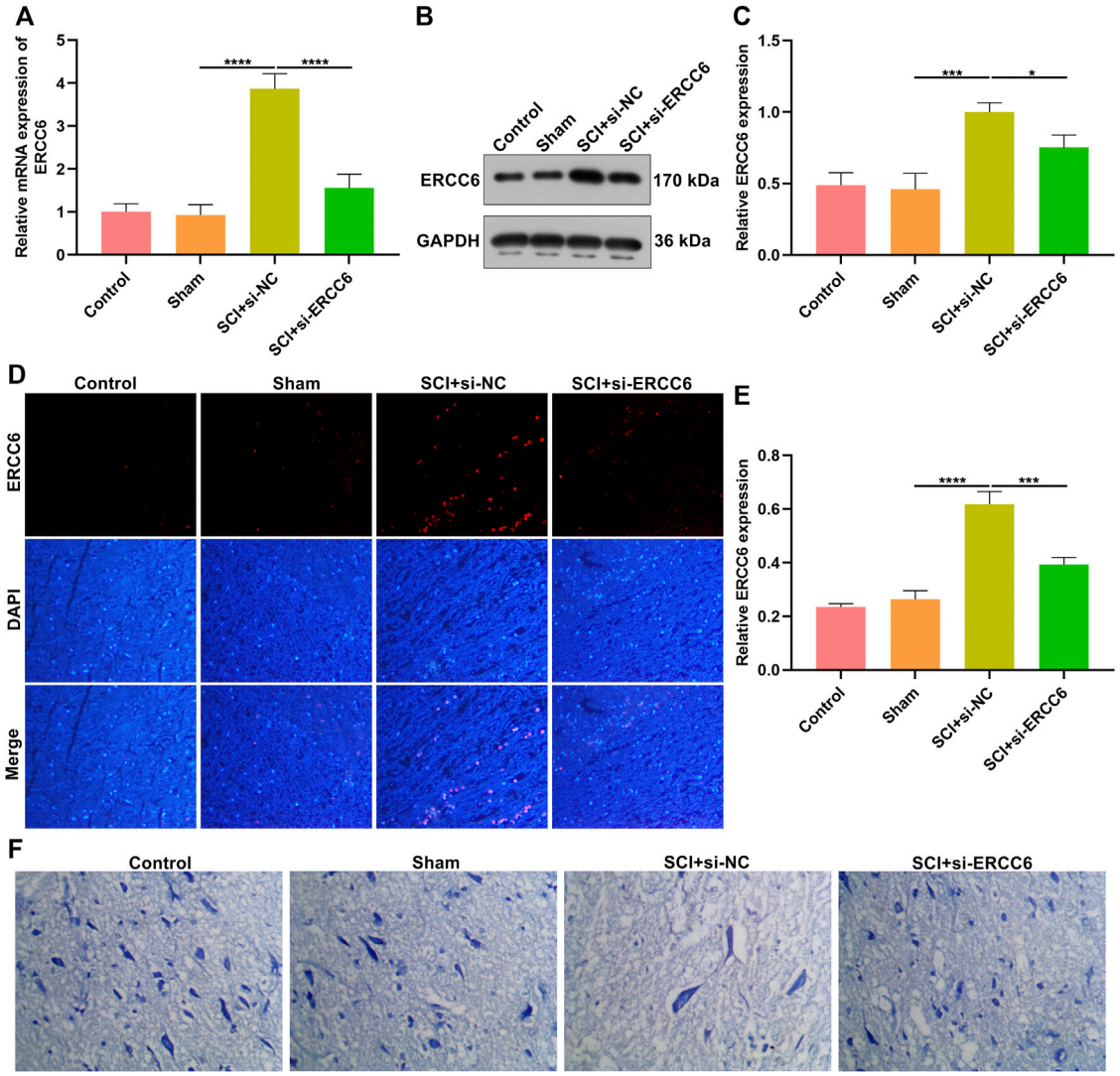

FIGURE 2 | ERCC6 knockdown alleviates neuronal damage in the ICI mice. **(A)** RT-qPCR analysis of ERCC6 expression in the spinal cord of SCI mice injected with si-ERCC6 or si-NC as well as control and sham operation mice. **(B,C)** Western blotting analysis of ERCC6 expression in the damaged spinal cord of mouse models injected by si-ERCC6 or si-NC as well as control and sham operation mice. **(D,E)** Immunofluorescence staining of ERCC6 expression in the damaged spinal cord of mouse models injected by si-ERCC6 or si-NC as well as control and sham operation mice (scale bar, 50 μm). **(F)** Nissl staining of spinal cord sections of SCI mice injected with si-ERCC6 or si-NC as well as control and sham operation mice (scale bar, 50 μm; N = 8 mice in each group). *p*-values were calculated with the ANOVA test. **p*-value < 0.05; ****p*-value < 0.001; *****p*-value < 0.0001.

lasting 1 h and were incubated with a primary antibody against ERCC6 (#24291-1-AP; 1:500; Proteintech, Wuhan, China), GAPDH (#10494-1-AP; 1:10000; Proteintech), Bax (#60267-1-Ig; 1:5000; Proteintech), cleaved caspase-3 (#19677-1-AP; 1:500; Proteintech), Bcl-2 (#26593-1-AP; 1:1000; Proteintech), p21 (#10355-1-AP; 1:1000; Proteintech), p27 (#25614-1-AP; 1:1000; Proteintech), 4-HNE (#ab46545; 1:3000; Abcam, United States), and Nrf2 (#16396-1-AP; 1:500; Proteintech) or Keap1 (#10503-2-AP; 1:2000; Proteintech) overnight at 4°C. The following day, the blots were incubated in horseradish peroxidase-conjugated goat anti-rabbit (#ab7090; 1:5000; Abcam) or anti-mouse secondary antibody (#ab7063; 1:5000; Abcam) lasting 1 h at room temperature. Thereafter, the blots were developed with enhanced chemiluminescence. The gray value was quantified *via* ImageJ software.

Immunofluorescence Staining

The spinal cord close to the lesion epicenter was fixed by 4% paraformaldehyde, embedded in paraffin, and cut into 4-μm-thick sections. The spinal cord sections were permeabilized and sealed utilizing PBST with 1% BSA lasting 1 h at room temperature. Thereafter, the sections were incubated with the primary antibody against ERCC6 (#24291-1-AP; 1:100; Proteintech), CD68 (#CL594-25747; 1:100; Proteintech), or F4/80 (#ab6640; 1:100; Abcam) overnight at 4°C. After rinsing with PBS, the slices were incubated by the secondary antibody lasting 1 h at room temperature. The nuclei

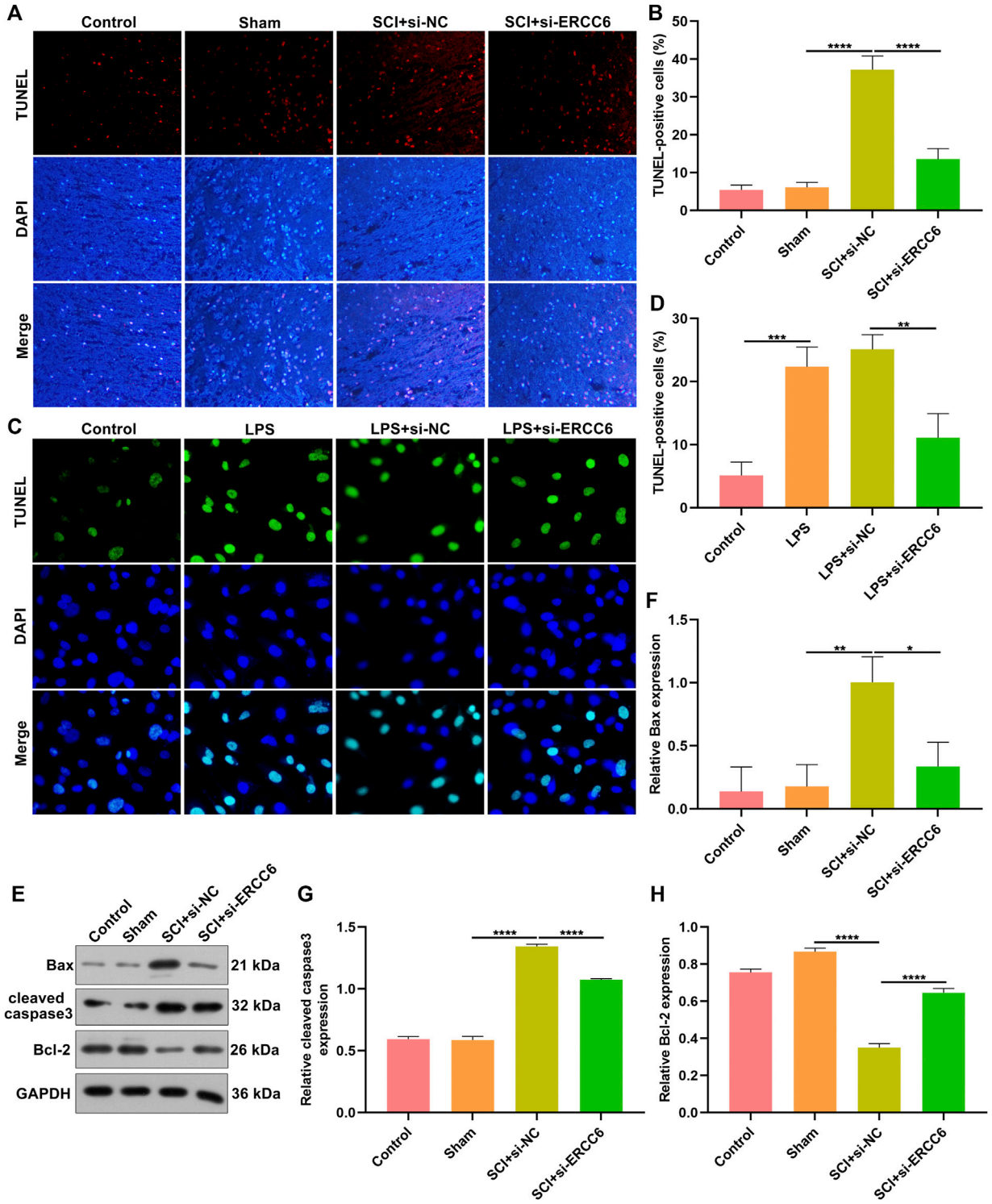

FIGURE 3 | ERCC6 knockdown decreases apoptosis in the spinal cord of ICI mice and LPS-induced mouse microglia cells. **(A,B)** TUNEL staining of apoptotic levels in the damaged spinal cord of mouse models injected with si-ERCC6 or si-NC as well as control and sham operation mice (scale bar, 50 μm; N = 8 mice in each group). **(C,D)** TUNEL staining of apoptotic levels in LPS-exposed BV2 mouse microglia cells treated with si-ERCC6 or si-NC (scale bar, 50 μm; N = 3 mice in each group). **(E–H)** Western blotting analysis for Bax, cleaved caspase-3 as well as Bcl-2 in the spinal cord tissues of SCI mice injected with si-ERCC6 or si-NC as well as control and sham operation mice (N = 8 mice in each group). *p*-values were calculated with ANOVA test. **p*-value < 0.05; ***p*-value < 0.01; ****p*-value < 0.001; *****p*-value < 0.0001.

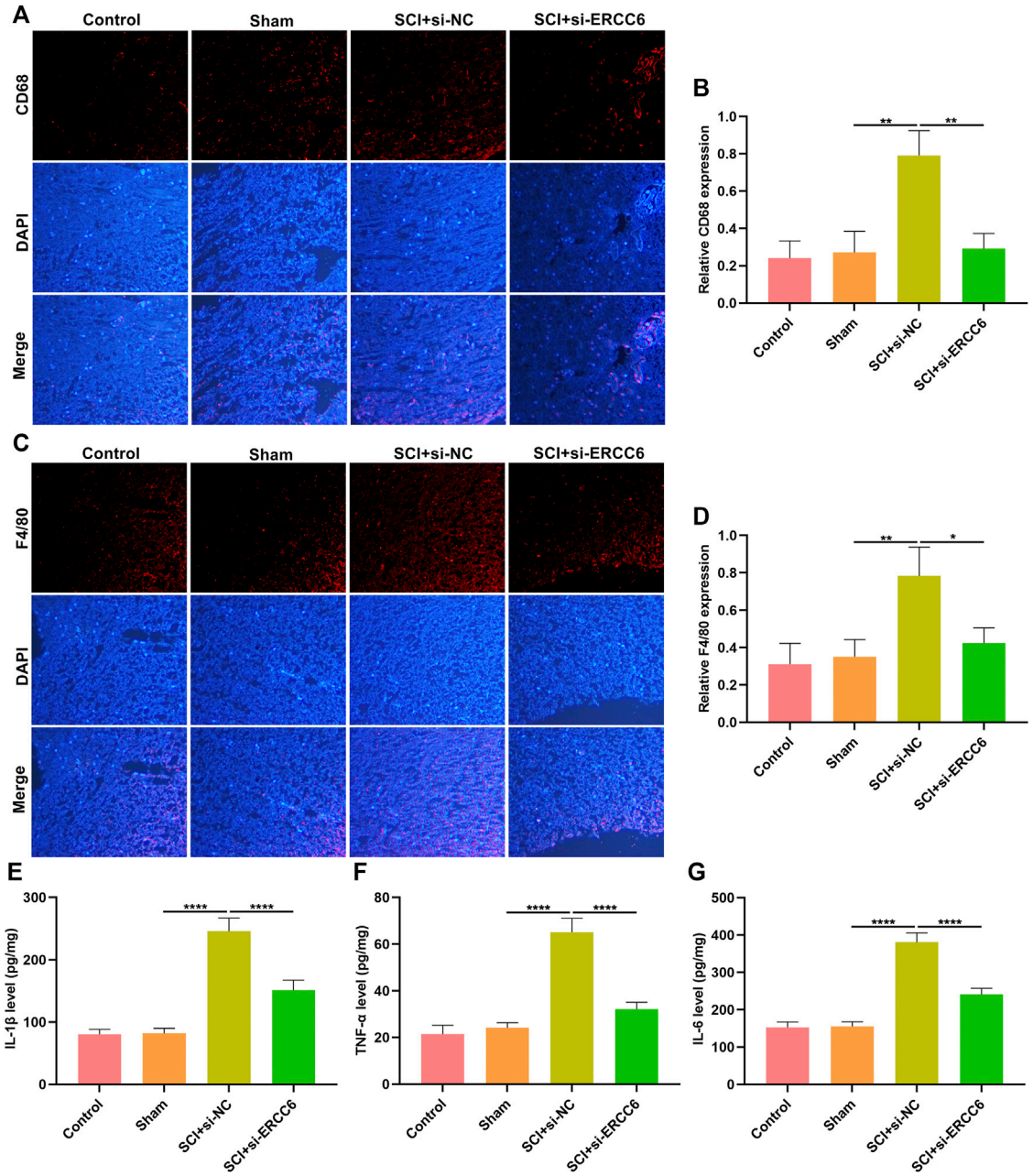

FIGURE 4 | ERCC6 knockdown alleviates inflammation in the spinal cord of ICI mice. **(A,B)** Immunofluorescence staining of CD68 expression in the damaged spinal cord of mouse models injected by si-ERCC6 or si-NC as well as control and sham operation mice (scale bar, 50 μm). **(C,D)** Immunofluorescence staining of F4/80 expression in the spinal cord of mouse models injected by si-ERCC6 or si-NC as well as control and sham operation mice (scale bar, 50 μm). **(E–G)** ELISA analysis of the levels of inflammatory factors containing **(E)** IL-1β, **(F)** TNF-α as well as **(G)** IL-6 in spinal cord of mouse models injected with si-ERCC6 or si-NC as well as control and sham operation mice (N = 8 mice in each group). *p*-values were calculated with the ANOVA test. **p*-value < 0.05; ***p*-value < 0.01; *****p*-value < 0.0001.

were stained utilizing DAPI, and the slices were photographed under a fluorescence microscope (Olympus, Japan).

Nissl Staining

Nissl staining (Solarbio, China) was conducted for detecting neuronal damage. The spinal cord sections were rinsed with PBS, and were maintained at 55 °C lasting 3 hours. Thereafter, the slices were placed into 0.9% crystal violet lasting 2 h at 37°C. Thereafter, slice dehydration was achieved in 70, 80, 90, and 100% ethanol lasting 5 minutes, followed by mounting utilizing neutral balsam. Investigation of images was implemented under a fluorescence microscope.

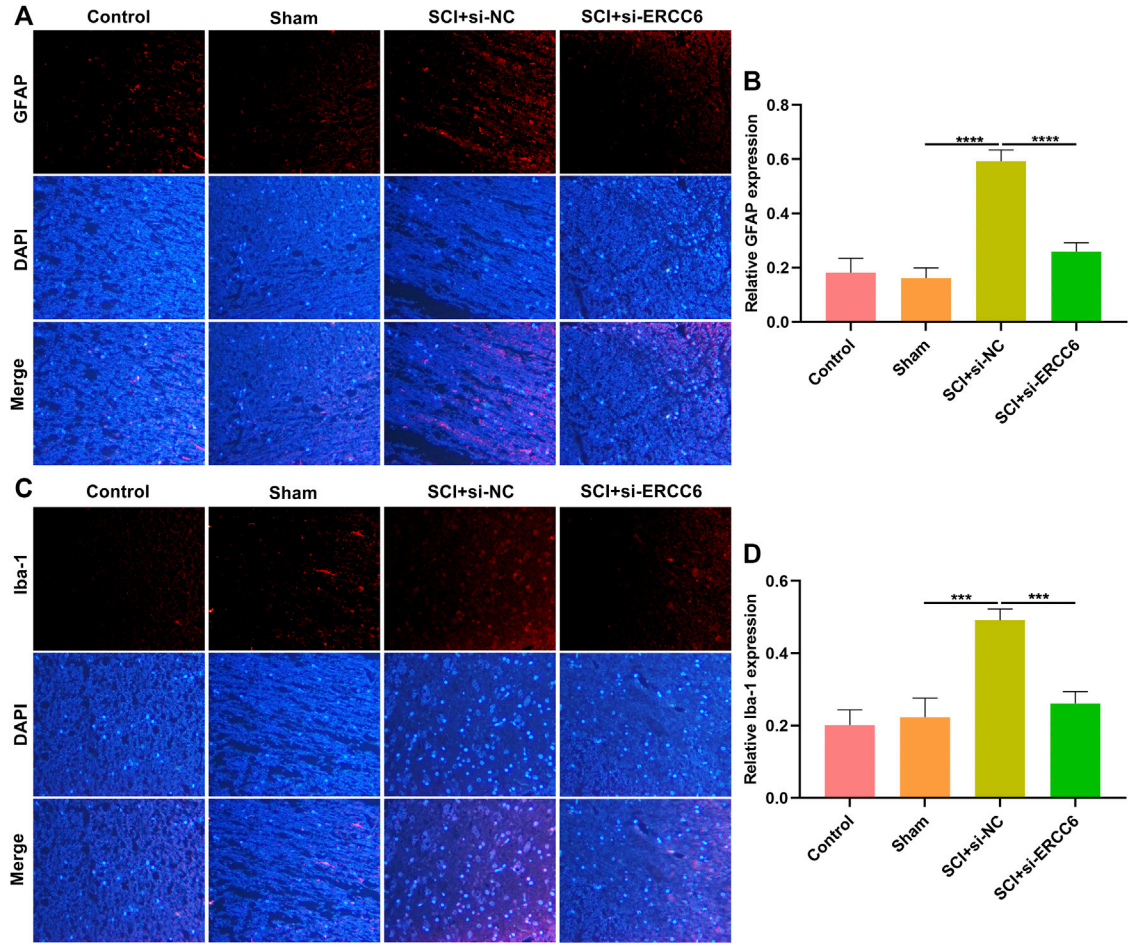

FIGURE 5 | ERCC6 ablation alleviates astrocyte and microglia activation in the spinal cord of SCI mice. **(A,B)** Immunofluorescence staining of GFAP expression in the spinal cord tissues of SCI mice injected with si-ERCC6 or si-NC as well as control and sham operation mice (scale bar, 50 μm). **(C,D)** Immunofluorescence staining of Iba-1 expression in the spinal cord of mouse models injected by si-ERCC6 or si-NC as well as control and sham operation mice (scale bar, 50 μm; N = 8 mice in each group). *p*-values were calculated with the ANOVA test. ***p-value < 0.001; ****p-value < 0.0001.

Terminal-Deoxynucleoitidyl Transferase Mediated Nick End Labeling Staining

Apoptosis was measured utilizing the TUNEL kit (Solarbio, China). BV2 cells were planted onto glass coverslips in a 24 well-plate. These cells were fixed by 4% paraformaldehyde lasting 20 min at 37°C. Following permeabilization by 0.1% Triton X-100/PBS lasting 15 min, the cells were sealed by PBS with 5% BSA at room temperature for 1 hour. Thereafter, incubation of the spinal cord slices or cells with TUNEL solution was implemented at 4°C overnight. TUNEL-positive cells under five random fields of view were estimated using ImageJ software.

Enzyme-Linked Immunosorbent Assays

100 mg of the spinal cord was used for homogenate. Following centrifugation at 1,500 g lasting 15 min 4°C, the supernatant was harvested, and the levels of interleukin (IL)-1β (#SEKM-0002) and IL-6 (#SEKM-0007), and tumor necrosis factor-α (TNF-α; # SEKM-0034) in spinal cord tissues were measured *via* ELISA kits (Solarbio, China). The detection process was conducted in strict accordance with the corresponding kit instructions. The microplate reader was utilized for detecting the absorbance at 450 nm.

Senescence-Associated β-Galactosidase Staining

SA-β-Gal staining (#C0602; Beyotime, China) was conducted in accordance with the manufacturer's instruction. In brief, spinal cord tissues were washed with PBS as well as fixed lasting 15 min at room temperature. Thereafter, the tissues were incubated in the SA-β-gal staining solution overnight at 37°C and photographed under a light microscope (Olympus, Japan).

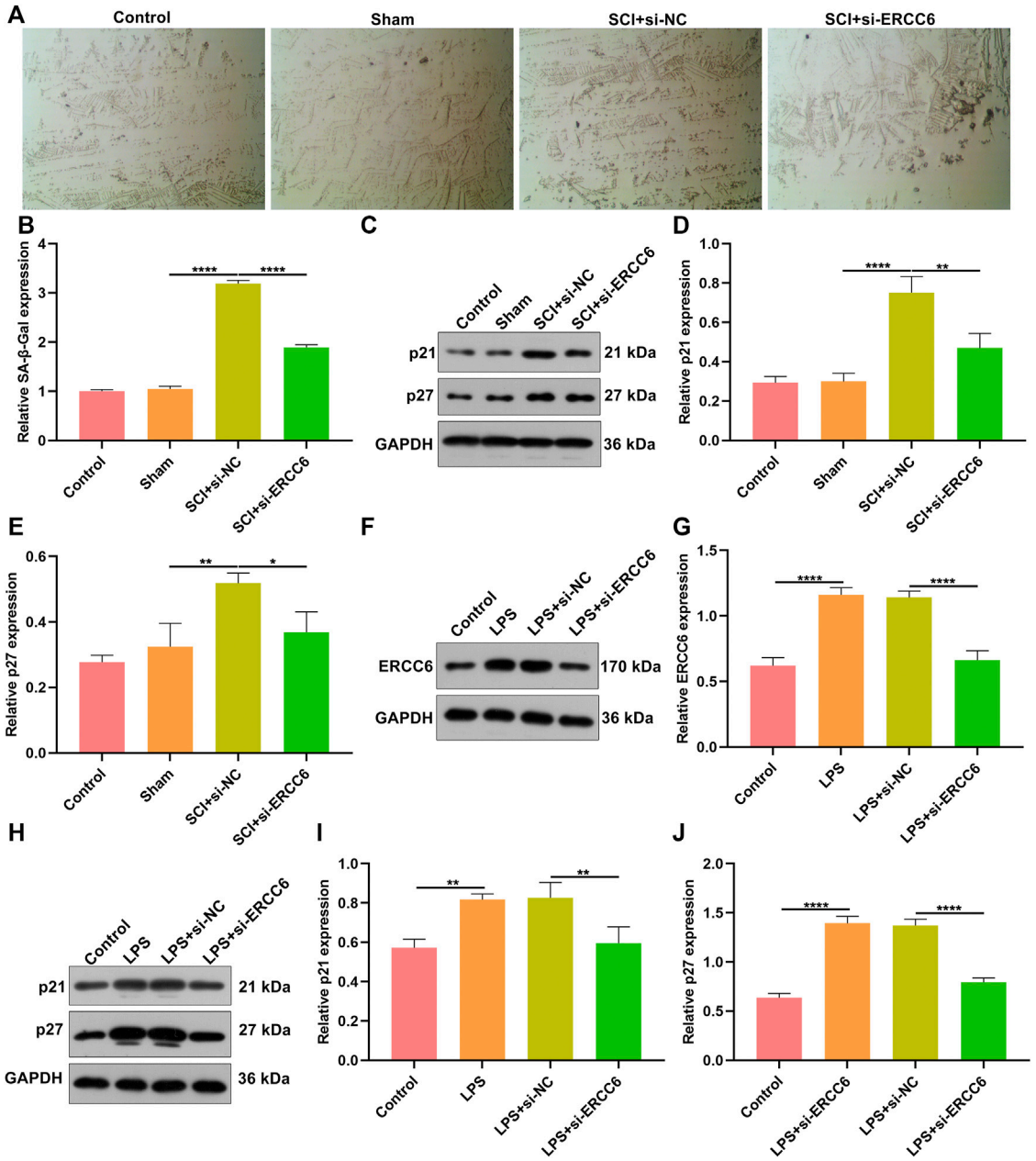

FIGURE 6 | ERCC6 ablation ameliorates cell senescence in the spinal cord of SCI mice and LPS-induced mouse microglia cells. **(A,B)** SA-β-Gal staining of the spinal cord of mouse models injected by si-ERCC6 or si-NC as well as control and sham operation mice (scale bar, 50 μm; N = 8 mice in each group). **(C–E)** Western blotting for senescent markers p21 as well as p27 in the spinal cord tissues of SCI mice injected with si-ERCC6 or si-NC as well as control and sham operation mice (N = 8 mice in each group). **(F,G)** Western blotting analysis of ERCC6 expression in LPS-exposed BV2 mouse microglia cells treated with si-ERCC6 or si-NC (N = 3 mice in each group). **(H–J)** Western blotting analysis of the expression of senescent markers p21 and p27 in LPS-exposed BV2 mouse microglia cells treated with si-ERCC6 or si-NC (N = 3 mice in each group). *p*-values were calculated with the ANOVA test. **p*-value < 0.05; ***p*-value < 0.01; *****p*-value < 0.0001.

Intracellular Reactive Oxygen Species Evaluation

The intracellular ROS was quantified utilizing ROS assay kits utilizing dichloro-dihydro-fluorescein diacetate (DCFH-DA; #287810; Sigma-Aldrich, United States) oxidized to fluorescent probes. BV2 cell line was stained by DCFH-DA following the manufacturer's specifications. The intracellular ROS levels were determined in accordance with 488 nm excitation wavelength as well as 525 nm emission wavelength.

Statistical Analysis

All analyses were implemented utilizing GraphPad Prism 8 software. One-way analysis of variance (ANOVA) was

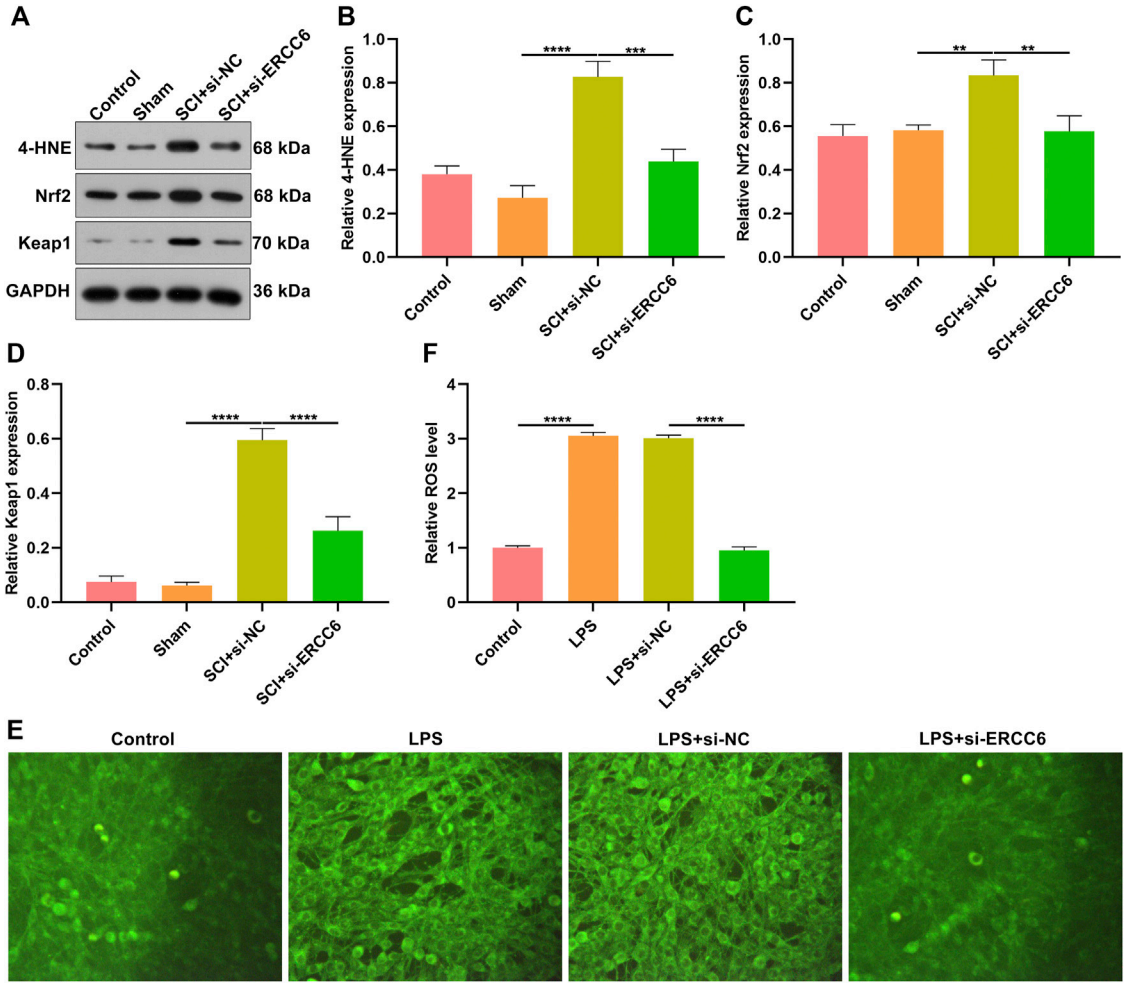

FIGURE 7 | ERCC6 ablation alleviates oxidative stress in the spinal cord of SCI mice. **(A–D)** Western blotting analysis of the expression of oxidative stress markers 4-HNE, Nrf2, and Keap1 in the spinal cord of mouse models injected by si-ERCC6 or si-NC as well as control and sham operation mice (N = 8 mice in each group). **(E,F)** The levels of ROS fluorescence in LPS-exposed BV2 mouse microglia cells treated with si-ERCC6 or si-NC (scale bar, 50 μm; N = 3 mice in each group). *p*-values were calculated with the ANOVA test. ***p*-value < 0.01; ****p*-value < 0.001; *****p*-value < 0.0001.

applied for comparisons among groups, with Tukey's *post hoc* testing. Results were considered significant when *p*-value < 0.05. All quantitative data are displayed as mean ± standard deviation.

RESULTS

ERCC6 Is Highly Expressed in SCI Mice and LPS-Induced Mouse Microglia Cells

To investigate the role of ERCC6 during SCI, we established SCI mouse models and measured the ERCC6 expression alterations. In **Figure 1A**, ERCC6 presented significantly higher mRNA expression in damaged spinal cord on Days 3, 7, 14, and 18 following operations than sham operation mice. Similarly, ERCC6 protein expression was significantly higher in the spinal cord tissues of SCI mice on Days 3, 7, 14, and 18 after operations (**Figures 1B,C**). We also constructed LPS-induced BV2 mouse microglia cell models to simulate SCI. As LPS concentration increased, ERCC6 expression was significantly elevated in BV2 cells (**Figures 1D–F**). *In vitro* and *in vivo* evidence suggested that ERCC6 upregulation might enable to participate in SCI progression.

ERCC6 Knockdown Alleviates Neuronal Damage in ICI Mice

We investigated whether ERCC6 deficiency enabled to alleviate SCI. Following injection with si-ERCC6 for 3 days, ERCC6 expression was measured in the spinal cord of SCI mice. As expected, ERCC6 expression was remarkably decreased in damaged spinal cord with si-ERCC6 treatment relative to those with si-NC treatment (**Figures**

2A–E). Nissl staining was conducted for detecting neuronal damage. In comparison with sham operation mice, the number of Nissl bodies in damaged spinal cord was significantly reduced (**Figure 2F**). Si-ERCC6 treatment remarkably increased the number of Nissl bodies in the spinal cord tissues of SCI mice. Hence, ERCC6 deficiency enabled to alleviate neuronal damage in ICI mice.

ERCC6 Knockdown Decreases Apoptosis in Spinal Cord of ICI Mice and LPS-Induced Mouse Microglia Cells

TUNEL staining was conducted for investigating the apoptosis alterations in spinal cord tissues. As illustrated in **Figures 3A,B**, the apoptotic level was remarkedly elevated in the damaged spinal cord relative to sham operation mice. Additionally, si-ERCC6 injection significantly decreased the apoptotic levels in the damaged spinal cord. This study also investigated the significantly enhanced apoptosis in LPS-exposed BV2 cells (**Figures 3C,D**). Nevertheless, si-ERCC6 treatment markedly alleviated apoptotic levels in LPS-exposed BV2 cells. The apoptotic proteins were further measured in spinal cord tissues. We noted that Bax and cleaved caspase-3 expression were markedly elevated as well as Bcl-2 was lowly expressed in the damaged spinal cord relative to sham operation mice (**Figures 3E–H**). As expected, si-ERCC6 administration remarkably reduced the expression of Bax and cleaved caspase-3 expression as well as enhanced the expression of Bcl-2 in the damaged spinal cord. Altogether, ERCC6 deficiency decreased apoptosis both in the damaged spinal cord and LPS-exposed mouse microglia cells.

ERCC6 Knockdown Alleviates Inflammation in the Spinal Cord of ICI Mice

Excessive inflammatory response participates in SCI pathogenesis (Rong et al., 2019; Liu et al., 2020). Herein, we investigated whether ERCC6 modulated inflammatory response during SCI. Immunofluorescence staining showed that macrophage markers CD68 as well as F4/80 were remarkably highly expressed in the spinal cord tissues of ICI mice relative to sham operation mice (**Figures 4A–D**). Nevertheless, si-ERCC6 administration significantly decreased the expression of CD68 and F4/80 in the spinal cord tissues of ICI mice. The levels of inflammatory factors containing IL-1β, TNF-α, and IL-6 were significantly higher in the spinal cord of ICI mice relative to sham operation mice (**Figures 4E–G**). By contrast, ERCC6 knockdown remarkably decreased the levels of IL-1β, TNF-α, and IL-6 in the spinal cord of ICI mice. Collectively, the abovementioned data indicated that ERCC6 deficiency alleviated excessive inflammatory responses in the damaged spinal cord.

ERCC6 Ablation Alleviates Astrocyte and Microglia Activation in the Damaged Spinal Cord

Astrocyte and microglia activation were separately assessed through GFAP and Iba-1 immunofluorescence. As illustrated in **Figures 5A,B**, GFAP presented markedly higher expression in the damaged spinal cord relative to sham operation mice. Nevertheless, si-ERCC6 administration remarkably decreased GFAP expression in the damaged spinal cord, indicating that ERCC6 deficiency alleviated astrocyte activation in the damaged spinal cord. We also noted the significantly enhanced expression of Iba-1 in damaged spinal cord tissues, but si-ERCC6 administration decreased its expression (**Figures 5C,D**). This indicated that ERCC6 deficiency decreased microglia activation in the spinal cord of SCI mice.

ERCC6 Ablation Ameliorates Cell Senescence in Damaged Spinal Cord and LPS-Induced Mouse Microglia Cells

Further analysis was conducted for investigating the role of ERCC6 on neural senescence during SCI. Compared with sham operation mice, senescent cells were remarkably elevated in damaged spinal cord tissues (**Figures 6A,B**). However, si-ERCC6 treatment markedly decreased senescent cells in the damaged spinal cord. The expression of senescent markers p21 and p27 was also measured. Higher expression of p21 and p27 was found in spinal cord tissues of SCI mice relative to sham operation mice (**Figures 6C–E**). The expression of both was markedly reduced by si-ERCC6 administration in SCI mice. We also observed the role of ERCC6 on microglia senescence. First, our data affirmed that ERCC6 expression was remarkably enhanced in BV2 cells by LPS (**Figures 6F,G**). However, its expression was prominently decreased by si-ERCC6. As expected, there was a markedly increased expression of p21 and p27 in the LPS-exposed BV2 cells (**Figures 6H–J**). Their expression was alleviated by si-ERCC6 administration. Altogether, ERCC6 ablation enabled to ameliorate cell senescence both in the damaged spinal cord and LPS-induced microglia cells.

ERCC6 Ablation Alleviates Oxidative Stress in the Spinal Cord of SCI Mice and LPS-Induced Microglia Cells

Oxidative stress results in microglial and astrocyte activation, and promotes the release of inflammatory factors. Thus, the influence of ERCC6 on oxidative stress following SCI was further investigated. In comparison with sham operation mice, the expression of oxidative stress markers 4-HNE, Nrf2, and Keap1 was remarkably elevated in the damaged spinal cord (**Figures 7A–D**). However, si-ERCC6 administration markedly lowered the expression of 4-HNE, Nrf2, and Keap1 in the spinal cord of SCI mouse models. As illustrated in **Figures 7E,F**, there were significantly higher ROS levels in the LPS-induced BV2 cells relative to controls. Nevertheless, si-ERCC6 administration markedly lowered ROS accumulation in the LPS-induced BV2 cells. Hence, ERCC6 ablation alleviated oxidative stress in the spinal cord of SCI mice as well as LPS-induced BV2 cells.

DISCUSSION

SCI represents a severe neurological disease inducing neurological dysfunction and permanent injury (Wang et al., 2020). Hence, it is urgently required to develop novel effective therapeutic regimens against SCI-triggered neurological disorders and tissue damage. In the present study, ERCC6 blockage remarkably alleviated spinal cord damage by weakening apoptosis, inflammation, senescence, and oxidative stress both in the SCI mouse models and LPS-induced microglia cells. Thus, our findings provided a basis for future research on the targeted therapy following SCI regarding to ERCC6.

This research was the first evidence to demonstrate that ERCC6 expression was remarkably upregulated both in the damaged spinal cord of mouse models and LPS-induced microglia cells. Previously, ERCC6 upregulation was linked with aging-related diseases (age-related macular degeneration, *etc.*) (Baas et al., 2010). Following injection with ERCC6-siRNA-carrying lentivirus, neuronal damage of SCI mice was remarkably ameliorated. When the spinal cord is damaged, neuronal cellular deaths are key pathological events resulting in neurological deficiency (Wang et al., 2019; Abbaszadeh et al., 2020; Fang Wang et al., 2021). Meanwhile, apoptosis is a vital cell death process in SCI. ERCC6 blockage alleviated apoptotic levels in the damaged spinal cord of mouse models and LPS-induced microglia cells. The Bcl family is categorized as pro-apoptotic proteins (Bax, etc.) as well as anti-apoptotic proteins (Bcl-2, etc.). ERCC6 blockage upregulated Bax and cleaved caspase-3 as well as downregulated Bcl-2 in the spinal cord of SCI mouse models. Hence, ERCC6 blockage enabled to ameliorate the apoptotic process in the damaged spinal cord.

Neuroinflammation is a critical event during SCI and involves multiple cell types (Rong et al., 2019; Liu et al., 2020). Microglia cells are the main resident immune populations within the central nervous system (CNS), which can respond to stimuli in several minutes as well as colonize the damaged sites, thereby resulting in peripheral immune cell infiltrations (especially macrophages) (Lin et al., 2021). Excessive inflammation can promote secondary injury after SCI, accompanied by cascade excitement of cytokines (Lin et al., 2021). Our data demonstrated that ERCC6 blockage decreased the expression of macrophage markers CD68 as well as F4/80 in the damaged spinal cord. Moreover, its knockdown reduced the levels of IL-1β, TNF-α, and IL-6 in the damaged spinal cord of mouse models. The activation of GFAP-expressing astrocytes and Iba-1-expressing microglial cells are also key effectors of neuroinflammation (Bellver-Landete et al., 2019; Li et al., 2021). The expression of both was downregulated in the damaged spinal cord through blocking ERCC6. Thus, ERCC6 deficiency alleviated excessive inflammation in the damaged spinal cord.

Persistent senescent cells act as a determinant of the organ repair process (Wyss–Coray, 2016). In a previous study, cell senescence was induced in SCI-regenerating zebrafish and SCI-scarred mice (Paramos-de-Carvalho et al., 2021). Although the senescent cells induced in zebrafish were gradually eliminated, they were accumulated in mouse models over time. Using distinct aging agents, senescent cells in SCI mice were removed and the functions were recovered. The functional recovery was linked with the inhibition of fibrotic scars and inflammatory response (Paramos-de-Carvalho et al., 2021). Consistently, senescent cells were accumulated in the spinal cord of SCI mice. Thus, alleviating senescent cells is a prospective treatment regimen for SCI. Replicative senescence induced by replication-mediated DNA damage or shortened telomeres determines persistent DNA damage response as well as leads to the stabilization of transcription factor p53 and the expression of cyclin-dependent kinase inhibitor p21 (Xu et al., 2021). Higher expression of p21 and p27 was found in the spinal cord of SCI mice as well as LPS-induced microglia cells, indicating replicative senescence accumulation during SCI. ERCC6 promoter downregulation through histone H3 hypoacetylation blocks p21-independent replicative senescence (Crochemore et al., 2019). Herein, we noted that ERCC6 deficiency alleviated senescent cells as well as decreased the expression of p21 and p27 in the spinal cord of SCI mice and LPS-induced microglia cells. Hence, targeting ERCC6 might enable to ameliorate cell senescence in SCI.

Oxidative stress plays a destructive role during SCI, which generates ROS in the spinal cord to destroy protein, lipid, or DNA (Li et al., 2019). ROS accumulation enhances the demand for ascorbic acid as well as changes the capacity of antioxidant enzymes (Liu et al., 2020). Alleviating excessive oxidative stress can improve the locomotor functional recovery following SCI (Qian et al., 2019; Ungerer et al., 2020). Evidence suggests that ERCC6 enables to trigger oxidative DNA damage through recruiting XRCC1 (Menoni et al., 2018). Moreover, it mediates the chromatin structure as well as coordinates gene expression in response to oxidative stress (Lake et al., 2016). The Nrf2 signaling pathway represents the major reason why cells resist oxidative stress (Rao et al., 2019). In SCI mice, ERCC6 blockage downregulated the expression of oxidative stress markers 4-HNE, Nrf2, and Keap1 as well as excessive ROS accumulation in the LPS-induced BV2 cells. Hence, ERCC6 ablation ameliorated oxidative stress in the damaged spinal cord. However, several limitations should be pointed out. First, more experiments should be carried out to investigate the roles of ERCC6 on the recovery of motor function after SCI. Second, the molecular mechanisms involving ERCC6 in SCI should be further validated through *in vitro* and *in vivo* experiments.

CONCLUSION

Altogether, ERCC6 expression presented remarkable upregulation both in damaged spinal cord of mouse models and LPS-induced microglia cell models. Its deficiency enabled to alleviate diverse physiological processes (apoptosis, inflammation, senescence, oxidative stress, etc.). Our findings implied that ERCC6 acted as a prospective therapeutic target against SCI.

DATA AVAILABILITY STATEMENT

The original contributions presented in the study are included in the article/Supplementary Material, further inquiries can be directed to the corresponding authors.

ETHICS STATEMENT

The animal study was reviewed and approved by the Animal Care and Use Committee of Tangdu Hospital, Second Affiliated Hospital of Air Force Military Medical University (KY-2020015).

AUTHOR CONTRIBUTIONS

BL, JY conceived and designed the study. PZ, XZ, RZ, and XC conducted most of the experiments and data analysis and wrote the manuscript. YZ, EL, QZ, and RY participated in collecting data and helped to draft the manuscript. All authors reviewed and approved the manuscript.

FUNDING

This work was funded by National Natural Science Foundation of China (81830077).

REFERENCES

Abbaszadeh, F., Fakhri, S., and Khan, H. (2020). Targeting Apoptosis and Autophagy Following Spinal Cord Injury: Therapeutic Approaches to Polyphenols and Candidate Phytochemicals. *Pharmacol. Res.* 160, 105069. doi:10.1016/j.phrs.2020.105069

Baas, D. C., Despriet, D. D., Gorgels, T. G. M. F., Bergeron-Sawitzke, J., Uitterlinden, A. G., Hofman, A., et al. (2010). The ERCC6 Gene and Age-Related Macular Degeneration. *PLoS One* 5 (11), e13786. doi:10.1371/journal.pone.0013786

Bellver-Landete, V., Bretheau, F., Mailhot, B., Vallières, N., Lessard, M., Janelle, M.-E., et al. (2019). Microglia Are an Essential Component of the Neuroprotective Scar that Forms after Spinal Cord Injury. *Nat. Commun.* 10 (1), 518. doi:10.1038/s41467-019-08446-0

Cao, Y., Li, P., Zhang, G., Kang, L., Zhou, T., Wu, J., et al. (2021). MicroRNA Let-7c-5p-Mediated Regulation of ERCC6 Disrupts Autophagic Flux in Age-Related Cataract via the Binding to VCP. *Curr. Eye Res.* 46 (9), 1353–1362. doi:10.1080/02713683.2021.1900273

Crochemore, C., Fernández-Molina, C., Montagne, B., Salles, A., and Ricchetti, M. (2019). CSB Promoter Downregulation via Histone H3 Hypoacetylation Is an Early Determinant of Replicative Senescence. *Nat. Commun.* 10 (1), 5576. doi:10.1038/s41467-019-13314-y

Fang Wang, F., Chang, S., Li, J., Wang, D., Li, H., and He, X. (2021). Lithium Alleviated Spinal Cord Injury (SCI)-induced Apoptosis and Inflammation in Rats via BDNF-AS/miR-9-5p axis. *Cell Tissue Res* 384 (2), 301–312. doi:10.1007/s00441-020-03298-3

Feng, Z., Min, L., Chen, H., Deng, W., Tan, M., Liu, H., et al. (2021). Iron Overload in the Motor Cortex Induces Neuronal Ferroptosis Following Spinal Cord Injury. *Redox Biol.* 43, 101984. doi:10.1016/j.redox.2021.101984

Hough, R. A., Pale, T., Benes, J. A., and McClellan, A. D. (2021). Spinal Cord Injury Significantly Alters the Properties of Reticulospinal Neurons: I. Biophysical Properties, Firing Patterns, Excitability, and Synaptic Inputs. *Cells* 10 (8), 1921. doi:10.3390/cells10081921

Kuboyama, T., Kominato, S., Nagumo, M., and Tohda, C. (2021). Recovery from Spinal Cord Injury via M2 Microglial Polarization Induced by Polygalae Radix. *Phytomedicine* 82, 153452. doi:10.1016/j.phymed.2020.153452

Lake, R. J., Boetefuer, E. L., Won, K.-J., and Fan, H.-Y. (2016). The CSB Chromatin Remodeler and CTCF Architectural Protein Cooperate in Response to Oxidative Stress. *Nucleic Acids Res.* 44 (5), 2125–2135. doi:10.1093/nar/gkv1219

Li, Z., Wu, F., Xu, D., Zhi, Z., and Xu, G. (2019). Inhibition of TREM1 Reduces Inflammation and Oxidative Stress after Spinal Cord Injury (SCI) Associated with HO-1 Expressions. *Biomed. Pharmacother.* 109, 2014–2021. doi:10.1016/j.biopha.2018.08.159

Li, L., Acioglu, C., Heary, R. F., and Elkabes, S. (2021). Role of Astroglial Toll-like Receptors (TLRs) in central Nervous System Infections, Injury and Neurodegenerative Diseases. *Brain Behav. Immun.* 91, 740–755. doi:10.1016/j.bbi.2020.10.007

Lin, S., Zhou, Z., Zhao, H., Xu, C., Guo, Y., Gao, S., et al. (2021). TNF Promotes M1 Polarization through Mitochondrial Metabolism in Injured Spinal Cord. *Free Radic. Biol. Med.* 172, 622–632. doi:10.1016/j.freeradbiomed.2021.07.014

Liu, Z., Yao, X., Jiang, W., Li, W., Zhu, S., Liao, C., et al. (2020). Advanced Oxidation Protein Products Induce Microglia-Mediated Neuroinflammation via MAPKs-NF-Kb Signaling Pathway and Pyroptosis after Secondary Spinal Cord Injury. *J. Neuroinflammation* 17 (1), 90. doi:10.1186/s12974-020-01751-2

Menoni, H., Wienholz, F., Theil, A. F., Janssens, R. C., Lans, H., Campalans, A., et al. (2018). The Transcription-Coupled DNA Repair-Initiating Protein CSB Promotes XRCC1 Recruitment to Oxidative DNA Damage. *Nucleic Acids Res.* 46 (15), 7747–7756. doi:10.1093/nar/gky579

Paramos-de-Carvalho, D., Martins, I., Cristóvão, A. M., Dias, A. F., Neves-Silva, D., Pereira, T., et al. (2021). Targeting Senescent Cells Improves Functional Recovery after Spinal Cord Injury. *Cel Rep.* 36 (1), 109334. doi:10.1016/j.celrep.2021.109334

Proietti-De-Santis, L., Balzerano, A., and Prantera, G. (2018). CSB: An Emerging Actionable Target for Cancer Therapy. *Trends Cancer* 4 (3), 172–175. doi:10.1016/j.trecan.2018.01.005

Qian, D., Li, L., Rong, Y., Liu, W., Wang, Q., Zhou, Z., et al. (2019). Blocking Notch Signal Pathway Suppresses the Activation of Neurotoxic A1 Astrocytes after Spinal Cord Injury. *Cell Cycle* 18 (21), 3010–3029. doi:10.1080/15384101.2019.1667189

Rao, S., Lin, Y., Du, Y., He, L., Huang, G., Chen, B., et al. (2019). Designing Multifunctionalized Selenium Nanoparticles to Reverse Oxidative Stress-Induced Spinal Cord Injury by Attenuating ROS Overproduction and Mitochondria Dysfunction. *J. Mater. Chem. B* 7 (16), 2648–2656. doi:10.1039/c8tb02520g

Rong, Y., Liu, W., Wang, J., Fan, J., Luo, Y., Li, L., et al. (2019). Neural Stem Cell-Derived Small Extracellular Vesicles Attenuate Apoptosis and Neuroinflammation after Traumatic Spinal Cord Injury by Activating Autophagy. *Cell Death Dis* 10 (5), 340. doi:10.1038/s41419-019-1571-8

Takahashi, T. S., Sato, Y., Yamagata, A., Goto-Ito, S., Saijo, M., and Fukai, S. (2019). Structural Basis of Ubiquitin Recognition by the Winged-helix Domain of Cockayne Syndrome Group B Protein. *Nucleic Acids Res.* 47 (7), 3784–3794. doi:10.1093/nar/gkz081

Ungerer, G., Cui, J., Ndam, T., Bekemeier, M., Song, H., Li, R., et al. (2020). Harpagophytum Procumbens Extract Ameliorates Allodynia and Modulates Oxidative and Antioxidant Stress Pathways in a Rat Model of Spinal Cord Injury. *Neuromol Med.* 22 (2), 278–292. doi:10.1007/s12017-019-08585-z

Van Broeckhoven, J., Sommer, D., Dooley, D., Hendrix, S., and Franssen, A. J. P. M. (2021). Macrophage Phagocytosis after Spinal Cord Injury: when Friends Become Foes. *Brain* 144 (10), 2933–2945. doi:10.1093/brain/awab250

Wang, Y., Li, F., Zhang, G., Kang, L., and Guan, H. (2016). Ultraviolet-B Induces ERCC6 Repression in Lens Epithelium Cells of Age-Related Nuclear Cataract through Coordinated DNA Hypermethylation and Histone Deacetylation. *Clin. Epigenet* 8, 62. doi:10.1186/s13148-016-0229-y

Wang, C., Zhang, L., Ndong, J. D. L. C., Hettinghouse, A., Sun, G., Chen, C., et al. (2019). Progranulin Deficiency Exacerbates Spinal Cord Injury by Promoting Neuroinflammation and Cell Apoptosis in Mice. *J. Neuroinflammation* 16 (1), 238. doi:10.1186/s12974-019-1630-1

Wang, H., Zheng, Z., Han, W., Yuan, Y., Li, Y., Zhou, K., et al. (2020). Metformin Promotes Axon Regeneration after Spinal Cord Injury through Inhibiting Oxidative Stress and Stabilizing Microtubule. *Oxidative Med. Cell Longevity* 2020, 1–20. doi:10.1155/2020/9741369

Wu, C., Chen, H., Zhuang, R., Zhang, H., Wang, Y., Hu, X., et al. (2021). Betulinic Acid Inhibits Pyroptosis in Spinal Cord Injury by Augmenting Autophagy via

the AMPK-mTOR-TFEB Signaling Pathway. *Int. J. Biol. Sci.* 17 (4), 1138–1152. doi:10.7150/ijbs.57825

Wyss-Coray, T. (2016). Ageing, Neurodegeneration and Brain Rejuvenation. *Nature* 539 (7628), 180–186. doi:10.1038/nature20411

Xu, C., Shen, W.-B., Reece, E. A., Hasuwa, H., Harman, C., Kaushal, S., et al. (2021). Maternal Diabetes Induces Senescence and Neural Tube Defects Sensitive to the Senomorphic Rapamycin. *Sci. Adv.* 7 (27), eabf5089. doi:10.1126/sciadv.abf5089

Xue Wang, X., Wu, J., Liu, X., Tang, K., Cheng, L., Li, J., et al. (2021). Engineered Liposomes Targeting the Gut-CNS Axis for Comprehensive Therapy of Spinal Cord Injury. *J. Controlled Release* 331, 390–403. doi:10.1016/j.jconrel.2021.01.032

Zhang, C., Yan, Z., Maknojia, A., Riquelme, M. A., Gu, S., Booher, G., et al. (2021). Inhibition of Astrocyte Hemichannel Improves Recovery from Spinal Cord Injury. *JCI Insight* 6 (5), e134611. doi:10.1172/jci.insight.134611

Zhou, K., Zheng, Z., Li, Y., Han, W., Zhang, J., Mao, Y., et al. (2020). TFE3, a Potential Therapeutic Target for Spinal Cord Injury via Augmenting Autophagy Flux and Alleviating ER Stress. *Theranostics* 10 (20), 9280–9302. doi:10.7150/thno.46566

Zou, Y. (2021). Targeting Axon Guidance Cues for Neural Circuit Repair after Spinal Cord Injury. *J. Cereb. Blood Flow Metab.* 41 (2), 197–205. doi:10.1177/0271678x20961852

Zrzavy, T., Schwaiger, C., Wimmer, I., Berger, T., Bauer, J., Butovsky, O., et al. (2021). Acute and Non-resolving Inflammation Associate with Oxidative Injury after Human Spinal Cord Injury. *Brain* 144 (1), 144–161. doi:10.1093/brain/awaa360

Conflict of Interest: The authors declare that the research was conducted in the absence of any commercial or financial relationships that could be construed as a potential conflict of interest.

Publisher's Note: All claims expressed in this article are solely those of the authors and do not necessarily represent those of their affiliated organizations, or those of the publisher, the editors and the reviewers. Any product that may be evaluated in this article, or claim that may be made by its manufacturer, is not guaranteed or endorsed by the publisher.

frontiers | Frontiers in Molecular Biosciences

ORIGINAL RESEARCH
published: 11 April 2022
doi: 10.3389/fmolb.2022.848463

Identification of Novel Immune Cell-Relevant Therapeutic Targets and Validation of Roles of TK1 in BMSCs of Systemic Lupus Erythematosus

Fangru Chen[1], *Jian Meng*[1], *Wenjie Yan*[1], *Mengjiao Wang*[1], *Yunfei Jiang*[1] *and Jintao Gao*[2]*

[1]Department of Dermatology, Affiliated Hospital of Guilin Medical University, Guilin, China, [2]College of Biotechnology, Guilin Medical University, Guilin, China

Objective: Systemic lupus erythematosus (SLE) displays the characteristics of abnormal activity of the immune system, contributing to diverse clinical symptoms. Herein, this study was conducted for discovering novel immune cell-relevant therapeutic targets.

Methods: The abundance of diverse immune cells was estimated in PBMCs of SLE and healthy controls from the GSE50772 dataset with CIBERSORT approach. Immune cell-relevant co-expression modules were screened with WGCNA and relevant characteristic genes were determined with LASSO algorithm. Inflammatory chemokines were measured in serum of twenty SLE patients and twenty controls through ELISA. Bone marrow mesenchymal stem cells (BMSCs) were isolated and TK1 expression was measured in BMSCs through RT-qPCR and western blotting. TK1-overexpressed and TK-1-silenced BMSCs of SLE were conducted and apoptosis and cell cycle were measured with flow cytometry. Apoptosis-, cell cycle- and senescence-relevant proteins were tested with western blotting.

Results: We determined three co-expression modules strongly linked to immune cells. Five characteristic genes (CXCL1, CXCL2, CXCL8, CXCR1 and TK1) were screened and ROC curves proved the excellent diagnostic performance of this LASSO model. Inflammatory chemokines presented widespread up-regulations in serum of Systemic lupus erythematosus patients, demonstrating the activation of inflammatory response. TK1 expression was remarkably elevated in SLE BMSCs than controls. TK1 overexpression enhanced IL-1β expression, apoptosis, cell cycle arrest, and senescent phenotypes of SLE BMSCs and the opposite results were proved in TK1-silenced SLE BMSCs.

Conclusion: Collectively, our findings demonstrate that silencing TK1 alleviates inflammation, growth arrest and senescence in BMSCs of SLE, which highlights TK1 as a promising therapeutic target against SLE.

Keywords: systemic lupus erythematosus, TK1, immune cells, bone marrow mesenchymal stem cells, apoptosis, cell cycle, senescence

OPEN ACCESS

Edited by:
Leming Sun,
Northwestern Polytechnical University, China

Reviewed by:
Saeed Mohammadi,
Golestan University of Medical Sciences, Iran
Shangxue Yan,
Anhui Medical University, China

***Correspondence:**
Jintao Gao
jintao_gao@glmc.edu.cn

Specialty section:
This article was submitted to Molecular Diagnostics and Therapeutics, a section of the journal Frontiers in Molecular Biosciences

Received: *04 January 2022*
Accepted: *11 February 2022*
Published: *11 April 2022*

Citation:
Chen F, Meng J, Yan W, Wang M, Jiang Y and Gao J (2022) Identification of Novel Immune Cell-Relevant Therapeutic Targets and Validation of Roles of TK1 in BMSCs of Systemic Lupus Erythematosus. Front. Mol. Biosci. 9:848463. doi: 10.3389/fmolb.2022.848463

INTRODUCTION

Systemic lupus erythematosus (SLE) represents an autoimmune disease with the characteristics of loss of self-tolerance and formation of nuclear autoantigen and immune complex, contributing to inflammatory response in multiple organs (Durcan et al., 2019; Kiriakidou and Ching 2020). It is prevalent among females and those with non-white races (Durcan et al., 2019; Kiriakidou and Ching 2020). SLE patients present the wide heterogeneity in clinical manifestation like rash, arthritis, and nephritis, involving one or more organs (Furie et al., 2019). Genomic analyses have enhanced our comprehending of SLE through offering crucial insights into the molecular heterogeneity of SLE. Variable genetic, hormonal, immunologic, and environmental factors result in SLE pathogenesis. However, advances in therapeutic approaches are of difficulty due to distinct biological basis as well as phenotypic presentation (Mathias and Stohl 2020). Treatment modalities like antimalarial, corticosteroid, and immunosuppressive agent remain partially effective as well as present widespread toxicity (Furie et al., 2019). Hence, it is urgently required for developing novel therapeutic agents.

SLE progression is highly complex, involving diverse cell types as well as immune and non-immune mechanisms (Furie et al., 2019). Evidences suggest the significance of innate and adaptive immune cells and inflammatory mediators in triggering and potentiating SLE (Hanaoka et al., 2020). For instance, specific regulatory T cells characterized by dichotomic immunoregulatory and T helper 17 phenotypes show elevated expression in SLE patients' serum specimens, involving the pathogenic process of SLE (Hanaoka et al., 2020). Silencing Kv1.3 channel within T lymphocytes alleviates the clinical manifestation of SLE (Khodoun et al., 2020). To alleviate the immune imbalance of Th17 with regulatory T cell populations has become a treatment strategy against SLE (Yang et al., 2011). Despite this, SLE progression remains poorly understood. SLE bone marrow mesenchymal stem cells (BMSCs) display defects like growth arrest, senescent phenotype, secretion of cytokines as well as immunomodulation (Yuan et al., 2019). Several molecules have been found to regulate the capacity of immune modulation of SLE BMSCs. For instance, Let-7f-5p alleviates inflammation through targeting NLRP3 in BMSCs in patients with SLE (Tan et al., 2019). Moreover, silencing Let-7f in BMSCs may trigger Treg/Th17 imbalance in SLE (Geng et al., 2020). MicroRNA-663 can induce immune dysregulation via suppressing TGF-β1 production in BMSCs in patients with SLE (Geng et al., 2019). Hence, manipulating BMSCs is in favor of improving the immune response among SLE patients. Based on accumulated evidences, this study firstly characterized the landscape of immune cells among SLE with CIBERSORT algorithm. Through combining WGCNA and LASSO approaches, immune-relevant hub genes were determined and their diagnostic value was evaluated. Due to defects in immunomodulation of SLE BMSCs, we verified the expression of immune-relevant hub gene TK1 in SLE BMSCs, and investigated the effects of TK1 on BMSC growth, senescence and inflammatory response. Overall, our findings proposed the potential of TK1 as a diagnostic biomarker of SLE as well as a therapeutic target for assisting mesenchymal stem cell therapy.

MATERIALS AND METHODS

Retrieval of gene Expression Profiling

Gene expression profiling of SLE was retrospectively gathered from the Gene Expression Omnibus (GEO) repository (https://www.ncbi.nlm.nih.gov/gds/). Two available datasets (GSE50772 and GSE81622) were finally included in our study. Microarray expression profiling of peripheral blood mononuclear cells (PBMCs) from 61 SLE patients and 20 normal donor controls was curated from the GSE50772 dataset on the Affymetrix platform (Kennedy et al., 2015). Additionally, we harvested the expression profiles of PBMCs from 15 SLE patients and 25 normal controls in the GSE81622 dataset on the Illumina platform (Zhu et al., 2016). The raw microarray data were normalized through robust multi array averaging approach. Here, GSE50772 served as the training set while GSE81622 was utilized as the testing set.

Estimation of the Abundance of Immune Cell Populations

The cell-type identification by estimating relative subsets of RNA transcript (CIBERSORT) deconvolution algorithm (Newman et al., 2015) was adopted for computing the enrichment of infiltrating immune cell populations following the gene sets of diverse immune cell types. The degree of immune cell infiltrations was inferred utilizing the CIBERSORT package with LM22 the reference set. This analysis was implemented with 1,000 simulations as well as the results were filtered with $p < 0.05$.

Weighted gene Co-expression Analyses

A co-expression network was established utilizing the WGCNA package (Langfelder and Horvath 2008). The RNA expression profiles and immune cell features were converted into the available format. The first 25% of genes with the highest expression variance were identified for construction of the co-expression network. Through Pearson's correlation, the correlation coefficients between genes were computed as well as a correlation matrix was produced. Thereafter, the soft thresholding power (β value) was determined in accordance with the scale-free topological fit index along with mean connectivity. The optimal β value was confirmed through scale-free fit index = 0.9 and the largest mean connectivity through presenting gradient tests (ranging 1–20). The topological overlap matrices (TOM) were conducted through computing the topological overlapping with paired genes. Utilizing the TOM matrix, hierarchical clustering, followed by dynamic tree cut, was conducted for detecting gene modules. The smallest module size was set as 100 as well as similar modules were merged on the basis of the threshold of 0.25. For excavating the co-expression modules that presented

high associations with the immune cells, correlation analyses of modules with immune cells were carried out through computing Spearman's correlation coefficients between module eigengenes (MEs) and immune cell characteristics. The ME represents the main components of RNA expression profiles in a specific module. Modules that displayed significant interactions with immune cells were determined. Thereafter, gene significance (GS) as well as module membership (MM) were separately computed for intramodular analyses. GS represents the interaction of RNA expression with immune cell feature. Additionally, MM indicates the correlation of RNA expression profiling with ME of a specified module. The module comprising of genes with remarkable associations between GS and MM was regarded meaningful.

Functional Enrichment Analyses

Gene ontology (GO) analyses were adopted for classifying the genes into three categories in accordance with the bio-function, comprised of biological processes (BPs), cellular components (CCs), and molecular functions (MFs). Additionally, Kyoto encyclopedia of genes and genomes (KEGG) pathway enrichment analyses were conducted for exploring the biological features. GO and KEGG pathway analyses were both implemented with the clusterProfiler package (Yu et al., 2012). Adjusted p-value<0.05 was regarded as significant enrichment, which was computed with the Benjamini and Hochberg approach.

Determination of Hub Genes

Through the online database Search Tool for Retrieval of Interacting Genes/Proteins (STRING; http://string-db.org), the protein-protein interaction (PPI) network was conducted (Szklarczyk et al., 2017). The Molecular Complex Detection (MCODE) approach (Doncheva et al., 2019) was adopted for screening modules of the PPI network in accordance with node score cut-off = 0.2, degree cut-off = 2, k-core = 2 and max depth = 100.

Least Absolute Shrinkage and Selection Operator Analyses

LASSO approach was adopted to reduce complexity as well as prevent overfitting of the model according to the optimal value of lambda based on the expression profiles of hub genes utilizing the glmnet package (Engebretsen and Bohlin 2019). The diagnostic model was conducted through combining the optimal characteristic gene expression with the regression coefficient weight computed from the multivariate model.

Receiver Operator Characteristic Curve Analyses

The multivariate model with integrated characteristic genes were adopted for determining the high sensitivity and specificity for diagnosing SLE. The ROCs were drawn both in the GSE50772 and GSE81622 datasets as well as area under curves (AUCs) were computed to evaluate the performance of the model utilizing the pROC package (Robin et al., 2011).

Gene Set Enrichment Analyses

GSEA was employed to investigate whether certain sets of genes displayed significant difference between two groups (Subramanian et al., 2005). The "c2. cp.kegg.v7.1. symbols" gene set from the Molecular Signatures Database (https://www.gsea-msigdb.org/gsea/msigdb) (Liberzon et al., 2015) was utilized as the reference gene set. The default settings were set with 10,000 gene set permutations and terms with nominal $p < 0.05$ were regarded as significant enrichment.

Patients

Twenty SLE patients and twenty healthy volunteers were recruited in this project. SLE patients were diagnosed at Affiliated Hospital of Guilin Medical University in accordance with American College of Rheumatology. The inclusion criteria were as follows: 1) all patients were diagnosed as SLE; 2) the participants had a complete understanding of the content of this study; 3) the participants' information was complete. The exclusion criteria were as follows: 1) patients with rheumatoid arthritis, cardiovascular and cerebrovascular diseases, liver and kidney failure, diabetes, mental illness, etc.; 2) females who were breastfeeding or pregnant; 3) patients who recently took drugs that had an effect on this study. Each participator provided written informed consent as well as this project was approved by the Ethical Committee of Affiliated Hospital of Guilin Medical University (YXLL-2016-WJWZC-14).

Enzyme-Linked Immunosorbent Assay

ELISA kits of interferon-γ (IFN-γ; H025), interleukin-12 (IL-12; H010), interleukin-6 (IL-6; H007-1-1), interleukin-13 (IL-13; H011), interleukin-18 (IL-18; H015), and interleukin-1β (IL-1β; H002) were purchased from Nanjing Jiancheng Bioengineering Institute (China). Their serum levels were measured in accordance with the manufacturer's instructions.

Bone Marrow Mesenchymal Stem Cell Isolation and Culture

Bone marrow was harvested from iliac crest from five SLE and five controls. Thereafter, bone marrow mononuclear cells were extracted utilizing Ficoll separation medium (TBD, China), followed by resuspending in low glucose DMEM (Gibco, United States) plus 10% FBS and 1% antibiotic-antimycotic solution. All cells were maintained in an atmosphere with 5% CO_2 at 37°C. Following 2 days, medium including non-adherent cells was exchanged every 3 days. When the confluence reached 90%, cells were digested through 0.25% trypsin-ethylenediaminetetraacetic acid. At passage four, BMSCs were collected for subsequent assays.

Real-Time Quantitative Polymerase Chain Reaction

Total RNA was extracted from BMSCs utilizing TRIzol (Invitrogen, United States). The cDNA was retrieved through PrimeScript™ RT reagent kit with gDNA Eraser. Thereafter, RT-qPCR was conducted through SYBR® Premix Ex Taq™ II and Bulk kit (Takara, China). The RT-qPCR condition was one cycle of denaturation at 95°C lasting 30 s as well as forty cycles of

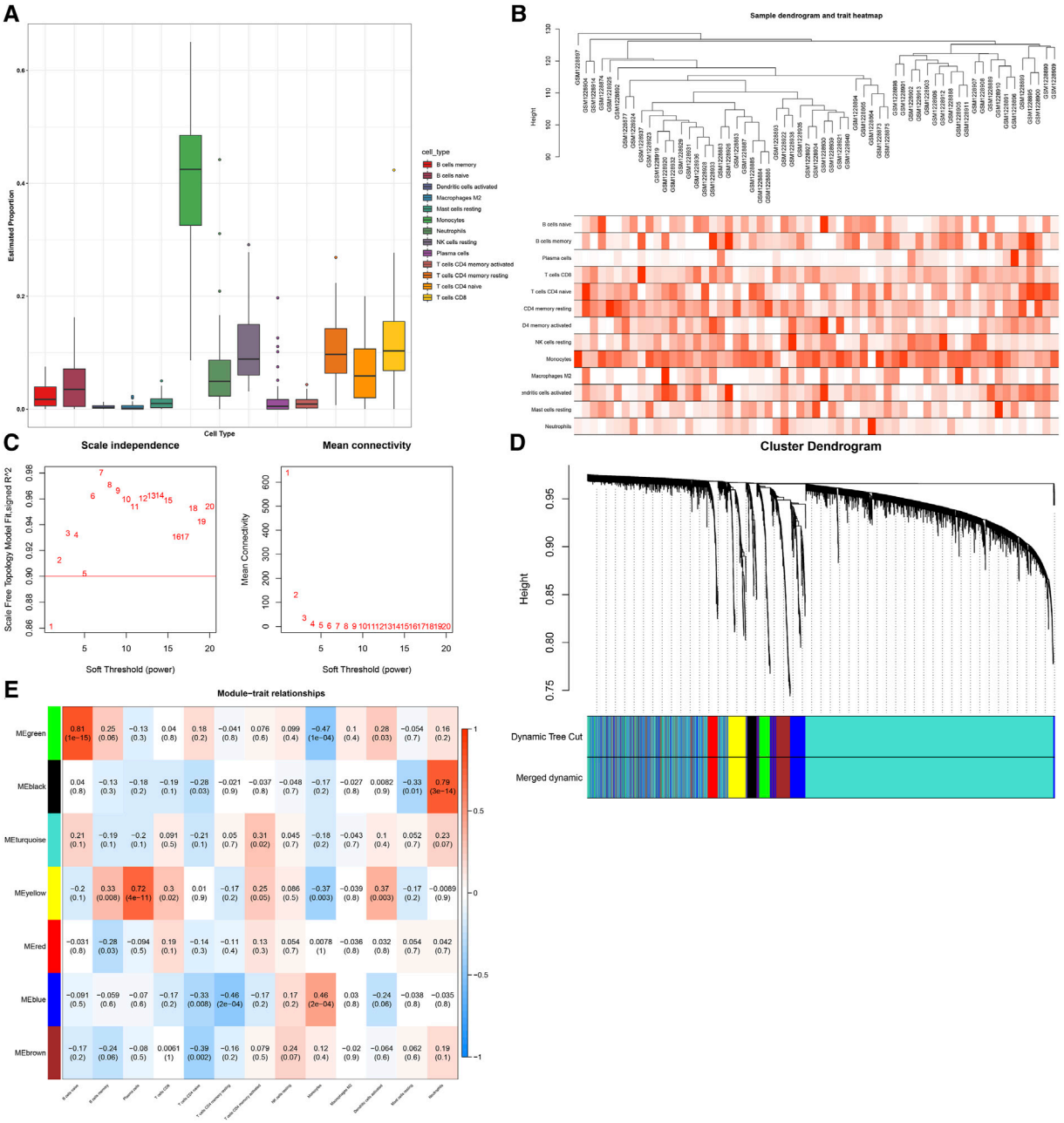

FIGURE 1 | Establishment of immune cell-relevant co-expression modules with WGCNA approach. **(A)** Quantification of the abundance of diverse immune cells in SLE specimens through the CIBERSORT approach. **(B)** Sample clustering for detecting outliers. **(C)** Determining soft-thresholding power (*β*) through analyses of (left) scale-free fit index and (right) mean connectivity. **(D)** Dendrogram of consensus module eigengenes. Gene dendrogram is generated following clustering the dissimilarity. **(E)** Heatmap of the association between diverse immune cells and module eigengenes. Each row and column separately indicate a consensus module and immune cells. The cells are colored in line with the correlation (red: positive correlation; blue, negative correlation). The intensity of the color reflects the strength of the correlation.

denaturation at 95°C lasting 5 s and annealing at 60°C lasting 34 s. GAPDH was adopted as an internal reference. The primer sequences were as follows: TK1, 5′-GGGCAGATCCAGGTG ATTCTC-3’ (forward), 5′-TGTAGCGAGTGTCTTTGGCATA-3’ (reverse); GAPDH, 5′-ACAACTTTGGTATCGTGGAAGG-3’ (forward), 5′-GCCATCACGCCACAGTTTC-3’ (reverse). The $2^{-\Delta\Delta Cq}$ approach was adopted for quantification.

Western Blotting

BMSCs were lysed through protein extraction reagent (Thermo Scientific, United States) and protease inhibitors. The protein was collected under centrifugation of 12,000 g lasting 15 min at 4°C. Protein concentration was measured utilizing NanoDrop 2000 spectrophotometer. 20 μl protein was separated through 12% SDS-PAGE as well as transferred onto polyvinylidene fluoride

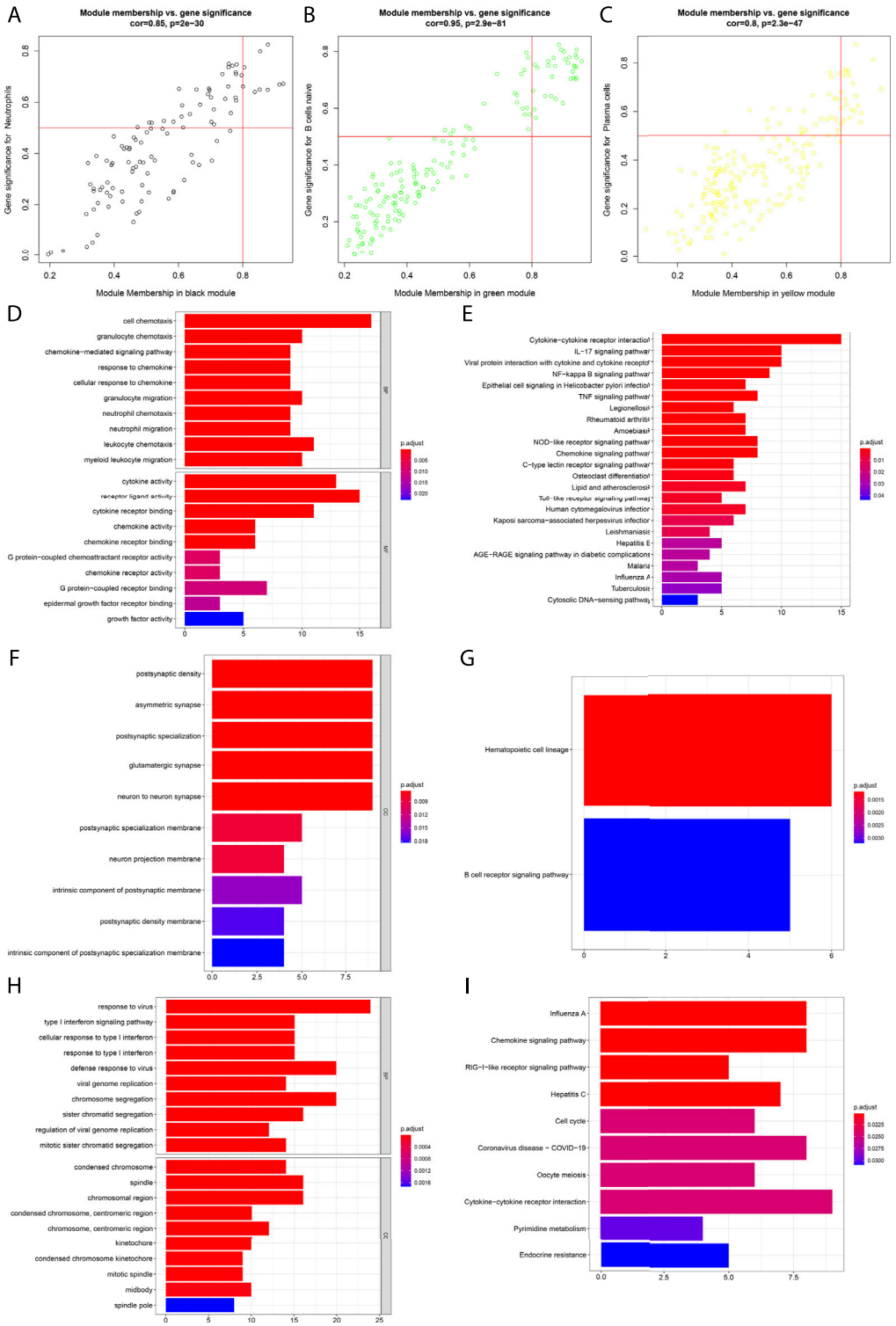

FIGURE 2 | Analyses of immune cell-infiltration-relevant genes and their biological significance. **(A)** Scatter plots depict the interactions of module membership with gene significance for neutrophils in the black module. **(B)** Scatter plots show the interactions of module membership with gene significance for B cells naïve in the green module. **(C)** Scatter plots present the interactions of module membership with gene significance for plasma cells in the yellow module. **(D,E)** GO and KEGG enrichment results of genes in the black module. **(F,G)** GO and KEGG enrichment results of genes in the green module. **(H,I)** GO and KEGG enrichment results of genes in the yellow module.

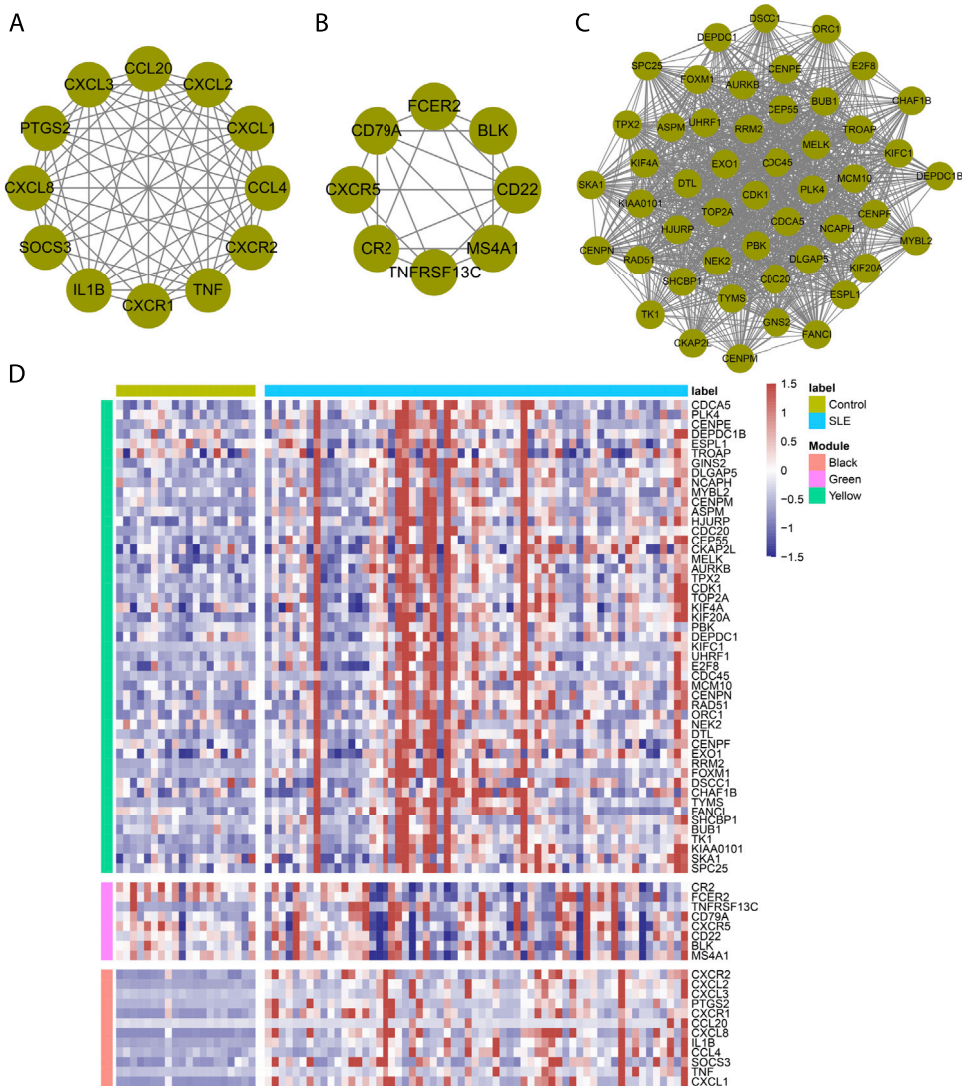

FIGURE 3 | Determination of immune cell-relevant hub genes. **(A–C)** Hub gene clusters in the **(A)** black, **(B)** green, and **(C)** yellow modules through MCODE approach. **(D)** Heatmap depicts the expression of hub genes in SLE and normal PBMCs in the GSE50772 dataset.

membrane. The membrane was sealed through 5% non-fat dry milk, followed by incubation overnight at 4°C with primary antibodies targeting TK1 (1:1,000; ab239509; Abcam, United States), GAPDH (1:1,000; ab181602; Abcam, United States), Cleaved caspase-3 (1:500; ab2302; Abcam, United States), Bax (1:500; ab53154; Abcam, United States), Bcl-2 (1:1,000; ab196495; Abcam, United States), CyclinD1 (1: 10,000; ab134175; Abcam, United States), p53 (1:10,000; ab32389; Abcam, United States), p21 (1:1,000; ab188224; Abcam, United States), and p27 (1:1,000; ab190851; Abcam, United States). Thereafter, the membrane was incubated by secondary antibody (1:2,000; ab7090; Abcam, United States) lasting 2 hours at room temperature. The immunoreactive protein was visualized through a chemiluminescence kit (Beyotime, China) as well as band density analyses were conducted utilizing ImageJ software.

Transfection

For generating TK1-overexpressing BMSCs, the cDNA of TK1 was PCR-amplified as well as cloned into the EcoRI and XbaI sites of the LV-003 lentivirus vectors (GenePharma, China). The lentivirus vectors were co-transfected by packaging vectors into 293T cells for producing recombinant lentivirus. Thereafter, BMSCs were co-cultured with recombinant lentivirus in the culture medium containing 2 μg/ml puromycin for generation of TK1-overexpressing BMSCs as well as empty vector BMSCs. Si-TK1 was acquired from GenePharma company (China). BMSCs were planted onto a 6-well plate. Following 12 h, 100 nM siRNA was transfected into BMSCs utilizing Lipofectamine 2000 (Invitrogen, United States) in accordance with the manufacturer's protocol. At 48 h post-transfection, BMSC expression was measured with RT-qPCR and western blotting.

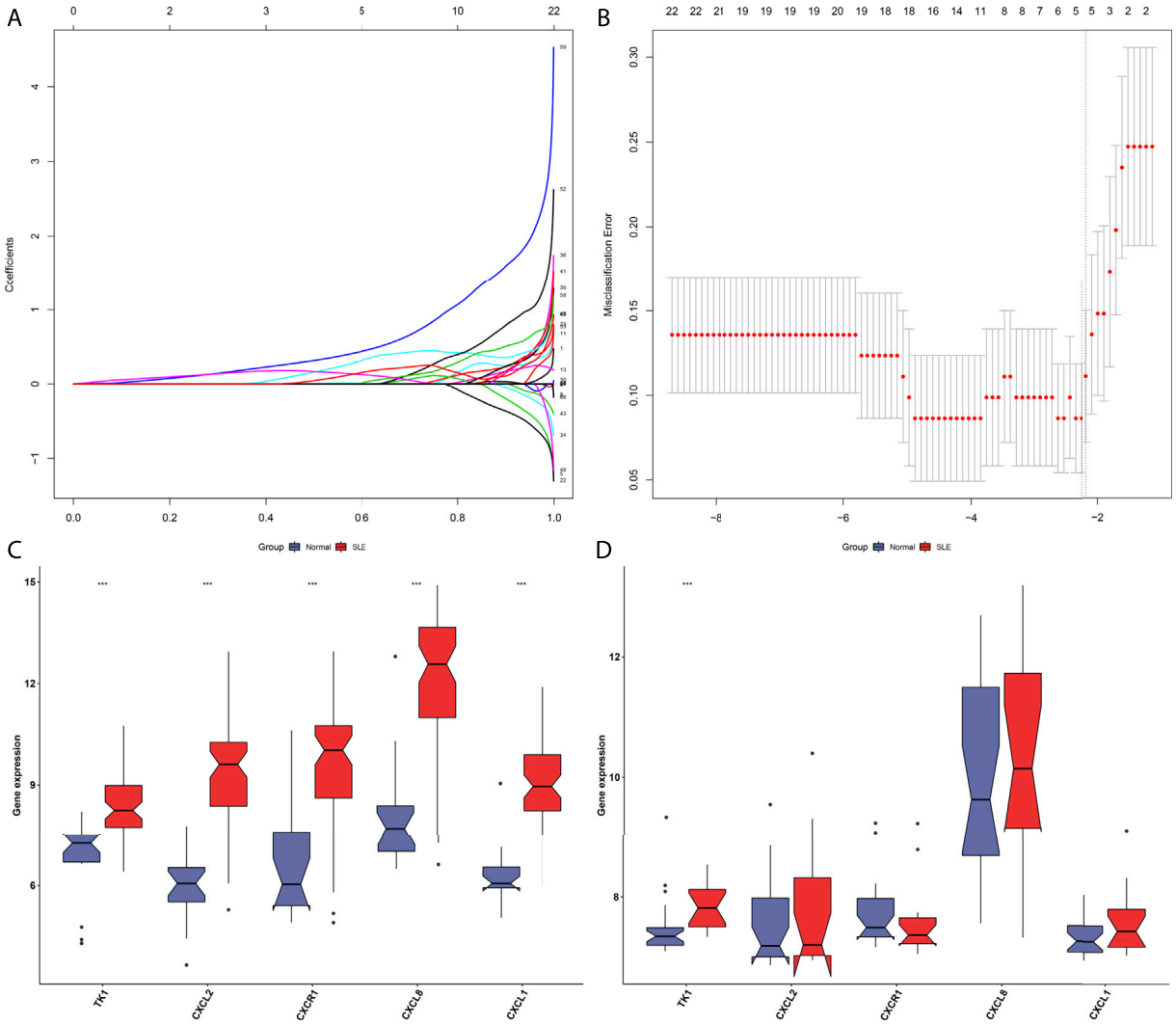

FIGURE 4 | Establishment of a LASSO model for distinguishing SLE from normal controls. **(A)** Ten-fold cross-verification of turning parameter selection in the LASSO model. **(B)** LASSO coefficient profiling of the hub genes. **(C)** Box plots show the expression of characteristic genes in SLE and normal PBMCs in the GSE50772 dataset. **(D)** Verification of the expression of characteristic genes in SLE and normal PBMCs in the GSE81622 dataset. ***$p < 0.001$.

Flow Cytometry Analyses

Apoptosis and cell cycle of BMSCs were measured with flow cytometry analyses. Following trypsinization and rinsing by PBS, BMSCs were fixed with 70% ethanol as well as incubated on the ice lasting 15 min. Thereafter, BMSCs were labeled by propidium iodide (PI)/RNase staining solution (Beyotime, China), followed by incubation at room temperature lasting 15 min. Apoptosis and cell cycle were analyzed utilizing BD FACSAria™ (BD, United States). Data analyses were conducted with FlowJo software.

Statistical Analyses

Student's *t* test was adopted for determining the difference between two groups. Meanwhile, one-way analyses of variance followed by post hoc Bonferroni correction were conducted for comparing multiple groups. Data are presented as mean ± SD. All statistical analyses were implemented with R software and GraphPad Prism software. The difference was regarded significant at a $p < 0.05$.

RESULTS

Establishment of Immune Cell-Relevant Co-expression Modules

With the CIBERSORT approach, we quantified the infiltration levels of diverse immune cells of SLE in the GSE50772 dataset, as depicted in **Figure 1A**. For discovering immune cell -relevant co-expression modules, we carried out WGCNA in SLE. In **Figure 1B**, all specimens were in the clusters and pass the cutoff thresholds. To guarantee a scale-free co-expression network, the optimal soft-

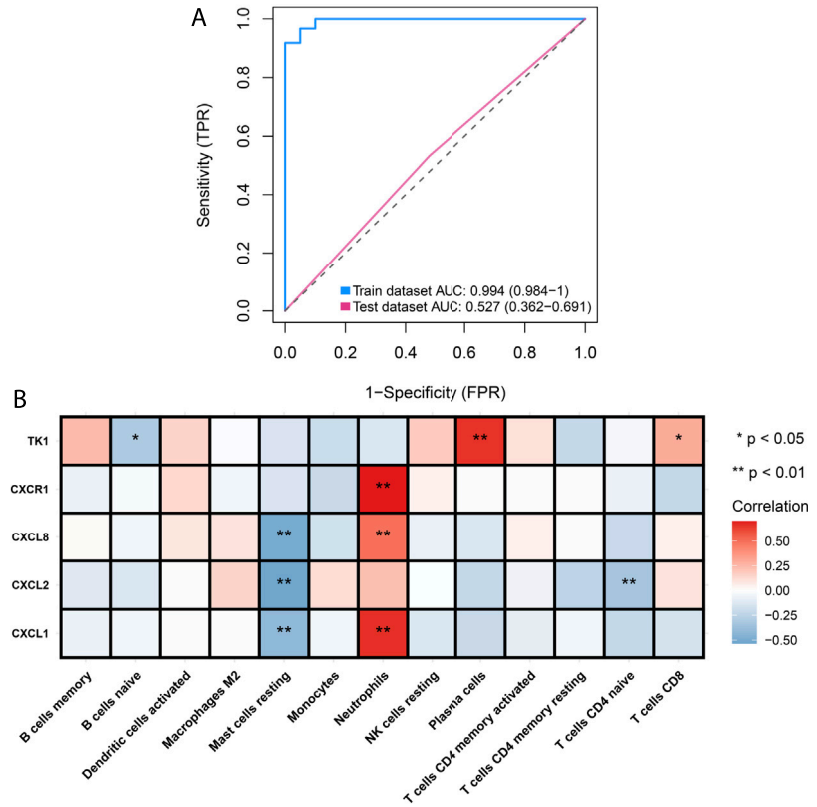

FIGURE 5 | Analyses of diagnostic efficacy of the LASSO model and associations of characteristic genes with infiltrating immune cells. **(A)** ROCs for evaluating the diagnostic efficacy of the LASSO model both in the GSE50772 and GSE81622 datasets. **(B)** Heatmap depicts the associations of characteristic genes (CXCL1, CXCL2, CXCL8, CXCR1 and TK1) with infiltrating immune cells in the GSE50772 dataset. *$p < 0.05$; **$p < 0.01$.

thresholding β value was determined when scale-free fit index = 0.9 (**Figure 1C**). Following dynamic tree cut approach, seven co-expression modules were finally clustered (**Figure 1D**). Analyses of module-trait relationships demonstrated that black module displayed a strong correlation to neutrophils ($r = 0.79$; $p = 3e\text{-}14$); green module showed a strong interaction with B cells naïve ($r = 0.81$; $p = 1e\text{-}15$); and yellow module was strongly linked to plasma cells ($r = 0.72$; $p = 4e\text{-}11$), as depicted in **Figure 1E**. Above modules were regarded as immune cell-relevant co-expression modules.

Analyses of Immune Cell-Infiltration-Relevant Genes and Their Biological Significance

Scatter analyses demonstrated the remarkable interactions of module membership with gene significance for neutrophils in the black module (**Figure 2A**). In **Figure 2B**, there was a prominent correlation between module membership and gene significance for B cells naïve in the green module. Additionally, we noted the significant interactions of module membership with gene significance for plasma cells in the yellow module (**Figure 2C**). Above data uncovered that the genes in the black, green, and yellow modules presented remarkable correlations to immune cells. Their biological significance was further investigated. It was proven that the genes in the black module were significantly linked to neutrophil chemotaxis and inflammation like cytokine-cytokine receptor interaction, IL-17 and TNF signaling pathways (**Figures 2D,E**). The genes in the green module presented prominent interactions with hematopoietic cell lineage and B cell receptor signaling pathway (**Figures 2F,G**). Additionally, the genes in the yellow module were prominently linked to viral infection (**Figures 2H,I**).

Determination of Immune Cell-Relevant Hub Genes

With the MCODE approach, hub genes in the immune cell-relevant models were further determined. As a result, there were twelve hub genes (CXCR2, CXCL2, CXCL3, PTGS2, CXCR1, CCL20, CXCL8, IL1B, CCL4, SOCS3, TNF, and CXCL1) in the black model (**Figure 3A**). **Figure 3B** depicted eight hub genes (CR2, FCER2, TNFRSF13C, CD79A, CXCR5, CD22, BLK, and MS4A1) in the green model. Additionally, we determined 49 hub genes in the yellow module, containing CDCA5, PLK4, CENPE, DEPDC1B, ESPL1, TROAP, GINS2, DLGAP5, NCAPH, MYBL2, CENPM, ASPM,

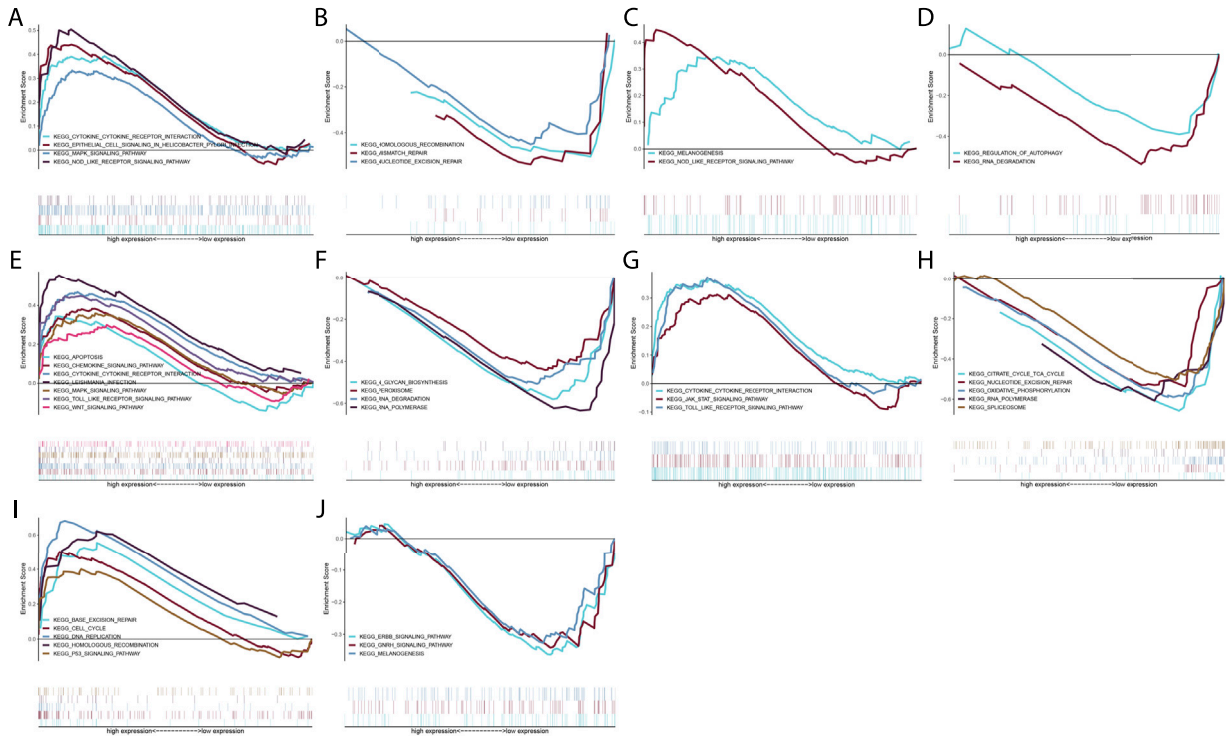

FIGURE 6 | Signaling pathways involving characteristic genes. **(A–J)** GSEA enrichment analyses of high and low expression of characteristic genes: **(A,B)** CXCL1, **(C,D)** CXCL2, **(E,F)** CXCL8, **(G,H)** CXCR1 and **(I,J)** TK1 in the GSE50772 dataset.

HJURP, CDC20, CEP55, CKAP2L, MELK, AURKB, TPX2, CDK1, TOP2A, KIF4A, KIF20A, PBK, DEPDC1, KIFC1, UHRF1, E2F8, CDC45, MCM10, CENPN, RAD51, ORC1, NEK2, DTL, CENPF, EXO1, RRM2, FOXM1, DSCC1, CHAF1B, TYMS, FANCI, SHCBP1, BUB1, TK1, KIAA0101, SKA1, and SPC25 (**Figure 3C**). **Figure 3D** presented the remarkable discrepancy in hub gene expression between SLE and normal PBMCs in the GSE50772 dataset.

Establishment of a Least Absolute Shrinkage and Selection Operator Model for Diagnosing Systemic Lupus Erythematosus

Hub genes in the black, green, and yellow modules were integrated for LASSO analyses. Under ten-fold cross-verification, five characteristic genes (CXCL1, CXCL2, CXCL8, CXCR1 and TK1) were determined and the LASSO model was constructed for SLE (**Figures 4A,B**). All of them presented remarkable up-regulations in SLE compared with normal PBMCs in the GSE50772 dataset (**Figure 4C**). Their expressions were verified in the GSE81622 dataset. It was proven that TK1 displayed prominent up-regulation in SLE (**Figure 4D**). ROCs were conducted for estimating the diagnostic potency of this LASSO model. AUC reached 0.994 in the GSE50772 dataset, proving the favorable diagnostic efficacy of this model (**Figure 5A**). The diagnostic performance was confirmed in the GSE81622 dataset.

Associations of Characteristic Genes With Infiltrating Immune Cells in Systemic Lupus Erythematosus

Further Spearman correlation analyses were conducted for unraveling the interactions of characteristic genes with infiltrating immune cells. In **Figure 5B**, CXCL1 and CXCL8 were negatively linked to mast cells resting but were positively correlated with neutrophils. CXCL2 displayed negative interactions with mast cells resting and T cells CD4 naïve. There was a positive interaction of CXCR1 with neutrophils. Additionally, we noted that TK1 showed the negative association with B cells naïve while displayed the positive associations with plasma cells and T cells CD8. These data indicated the tight interactions of characteristic genes with infiltrating immune cells in SLE.

Signaling Pathways Involving Characteristic Genes

GSEA was conducted through comparing high and low expression groups of characteristic genes in the GSE50772 dataset. Our results demonstrated that cytokine-cytokine receptor interaction, epithelial cell signaling in *helicobacter pylori* infection, MAPK signaling pathway and NOD-like receptor signaling pathway were remarkably activated in high CXCL1 expression group (**Figure 6A**) while homologous recombination, mismatch repair and nucleotide excision repair were prominently activated in low CXCL1 expression group (**Figure 6B**).

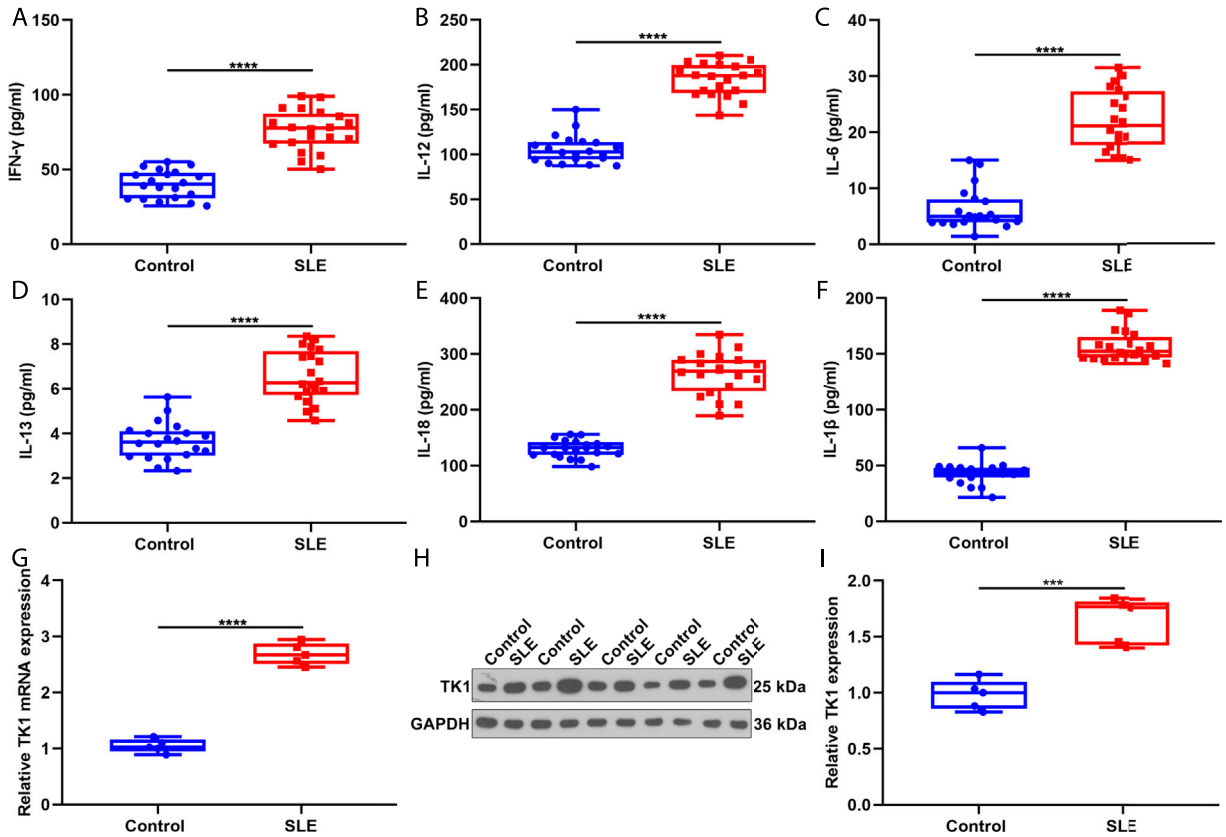

FIGURE 7 | Activation of inflammatory response in SLE and up-regulation of TK1 in SLE BMSCs. **(A–F)** Serum levels of **(A)** IFN-γ, **(B)** IL-12, **(C)** IL-6, **(D)** IL-13, **(E)** IL-18 as well as **(F)** IL-1β were measured in twenty SLE patients and twenty controls through ELISA. **(G–I)** TK1 mRNA expression was tested in BMSCs from five SLE patients and five controls through **(G)** RT-qPCR and **(H,I)** western blotting. ***$p < 0.001$; ****$p < 0.0001$.

CXCL2 presented positive interactions with melanogenesis and NOD-like receptor pathway (**Figure 6C**) while was negatively linked to regulation of autophagy and RNA degradation (**Figure 6D**). In **Figure 6E**, high CXCL8 expression group showed the remarkable activation of apoptosis, chemokine signaling pathway, cytokine-cytokine receptor interaction, leishmania infection, MAPK signaling pathway, TOLL-like receptor signaling pathway and Wnt signaling pathway. But low CXCL8 expression group presented the prominent activation of n-glycan biosynthesis, peroxisome, RNA degradation and RNA polymerase (**Figure 6F**). We also noted that cytokine-cytokine receptor interaction, JAK-STAT signaling pathway and Toll-like receptor signaling pathway were significantly activated in high CXCR1 expression group (**Figure 6G**) while citrate cycle TCA cycle, nucleotide excision repair, oxidative phosphorylation, RNA polymerase and spliceosome were remarkably activated in low CXCR1 expression group (**Figure 6H**). Additionally, base excision repair, cell cycle, DNA replication, homologous recombination as well as p53 pathway presented prominent activation in high TK1 expression group (**Figure 6I**) while ERBB signaling pathway, GNRH signaling pathway and melanogenesis showed significant activation in low TK1 expression group (**Figure 6J**). Overall, above data were indicative of the molecular mechanisms underlying characteristic genes.

Activation of Inflammatory Response in Systemic Lupus Erythematosus Patients

This study recruited twenty SLE patients and twenty controls and measured the serum levels of inflammatory factors through ELISA. Consequently, IFN-γ, IL-12, IL-6, IL-13, IL-18 and IL-1β presented remarkable up-regulations in serum of SLE patients in comparison to healthy controls (**Figures 7A–F**). These data proved that inflammatory response was prominently activated in SLE.

Verification of Up-Regulation of TK1 in Systemic Lupus Erythematosus Bone Marrow Mesenchymal Stem Cells

We isolated BMSCs from five SLE patients and five controls and verified the expression of TK1 in SLE. As expected, our data proved that TK1 mRNA displayed remarkable up-regulation in SLE compared with control BMSCs (**Figure 7G**). Consistently, TK1 protein was markedly overexpressed in SLE than control BMSCs (**Figures 7H,I**). Overall, our data proved the up-regulation of TK1 in SLE BMSCs.

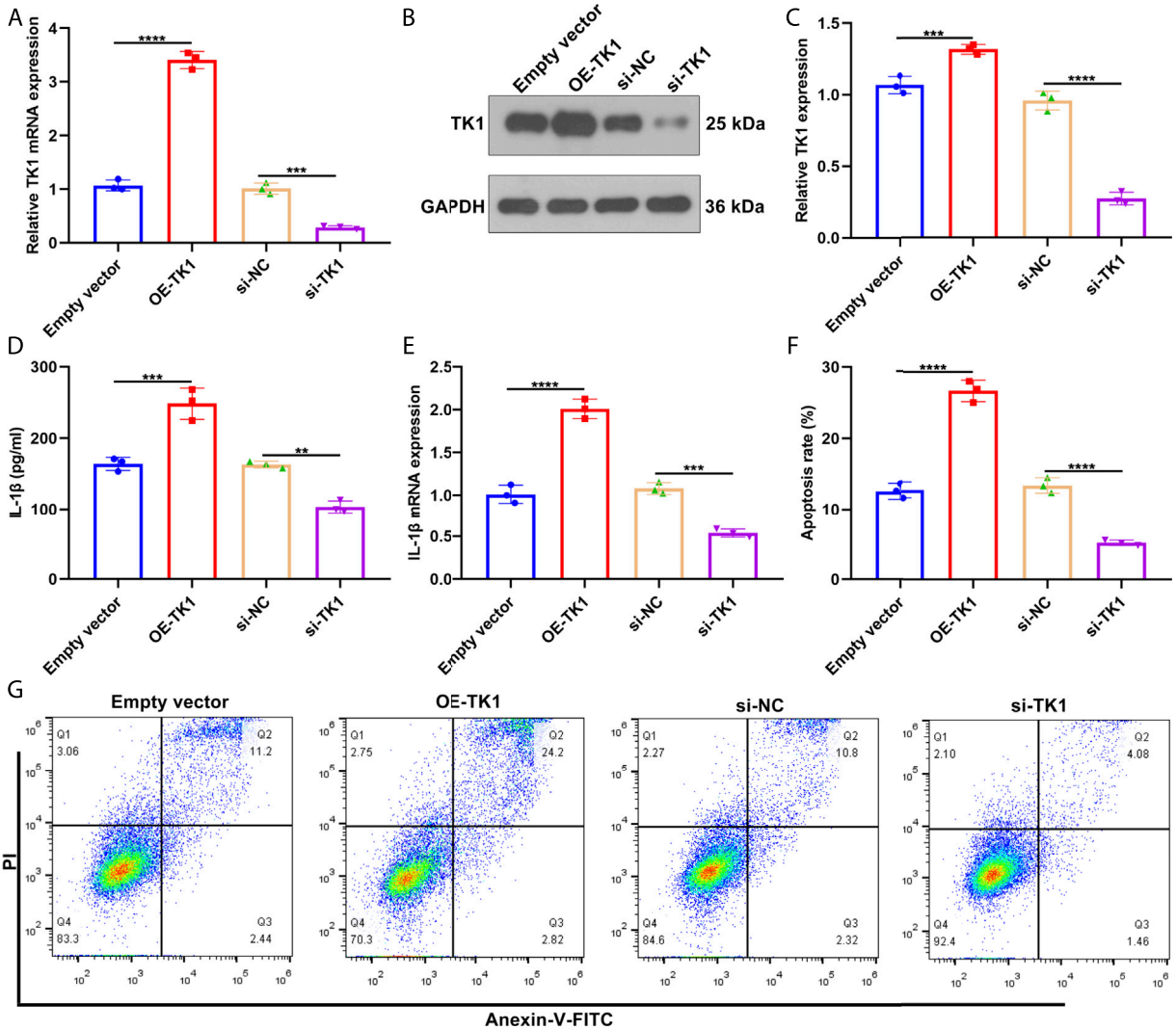

FIGURE 8 | Silencing TK1 relieves inflammatory response and apoptosis in SLE BMSCs. **(A)** TK1 mRNA expression was measured in SLE BMSCs with TK1 overexpression or TK1 knockdown through RT-qPCR. **(B,C)** TK1 protein expression was tested in SLE BMSCs with TK1 overexpression or TK1 knockdown via western blotting. **(D)** IL-1β levels were quantified in the supernatant of specified SLE BMSCs through ELISA. **(E)** RT-qPCR was adopted to measure the mRNA expression of IL-1β in specified SLE BMSCs. **(F,G)** Flow cytometry analyses were conducted to test the apoptosis levels of specified SLE BMSCs. $^{**}p < 0.01$; $^{***}p < 0.001$; $^{****}p < 0.0001$.

Silencing TK1 Relieves Inflammatory Response and Apoptosis in Systemic Lupus Erythematosus Bone Marrow Mesenchymal Stem Cells

To investigate the function of TK1 in SLE pathogenesis, TK1 expression was remarkably overexpressed as well as weakened in SLE BMSCs (**Figures 8A–C**). In **Figure 8D**, TK1-overexpressed SLE BMSCs presented prominently up-regulated IL-1β levels in the supernatant. Also, decreased IL-1β levels were tested in the supernatant of TK1-silenced SLE BMSCs. We also investigated that TK1 up-regulation elevated IL-1β expression in SLE BMSCs (**Figure 8E**). Oppositely, IL-1β expression was weakened by TK1 knockdown in SLE BMSCs. Moreover, remarkably enhanced apoptosis levels were noted in TK1-overexpressed SLE BMSCs while the opposite results were investigated in TK1-silenced SLE BMSCs (**Figures 8F,G**). Overall, targeting TK1 relieved inflammatory response and apoptosis in SLE BMSCs.

TK1 Knockdown Relieves Apoptosis, Cell Cycle Arrest and Senescence in Systemic Lupus Erythematosus Bone Marrow Mesenchymal Stem Cells

Further, we measured the influence of TK1 on the expression of cell cycle- and apoptosis-relevant proteins in SLE BMSCs via western blotting (**Figure 9A**). As a result, TK1 up-regulation

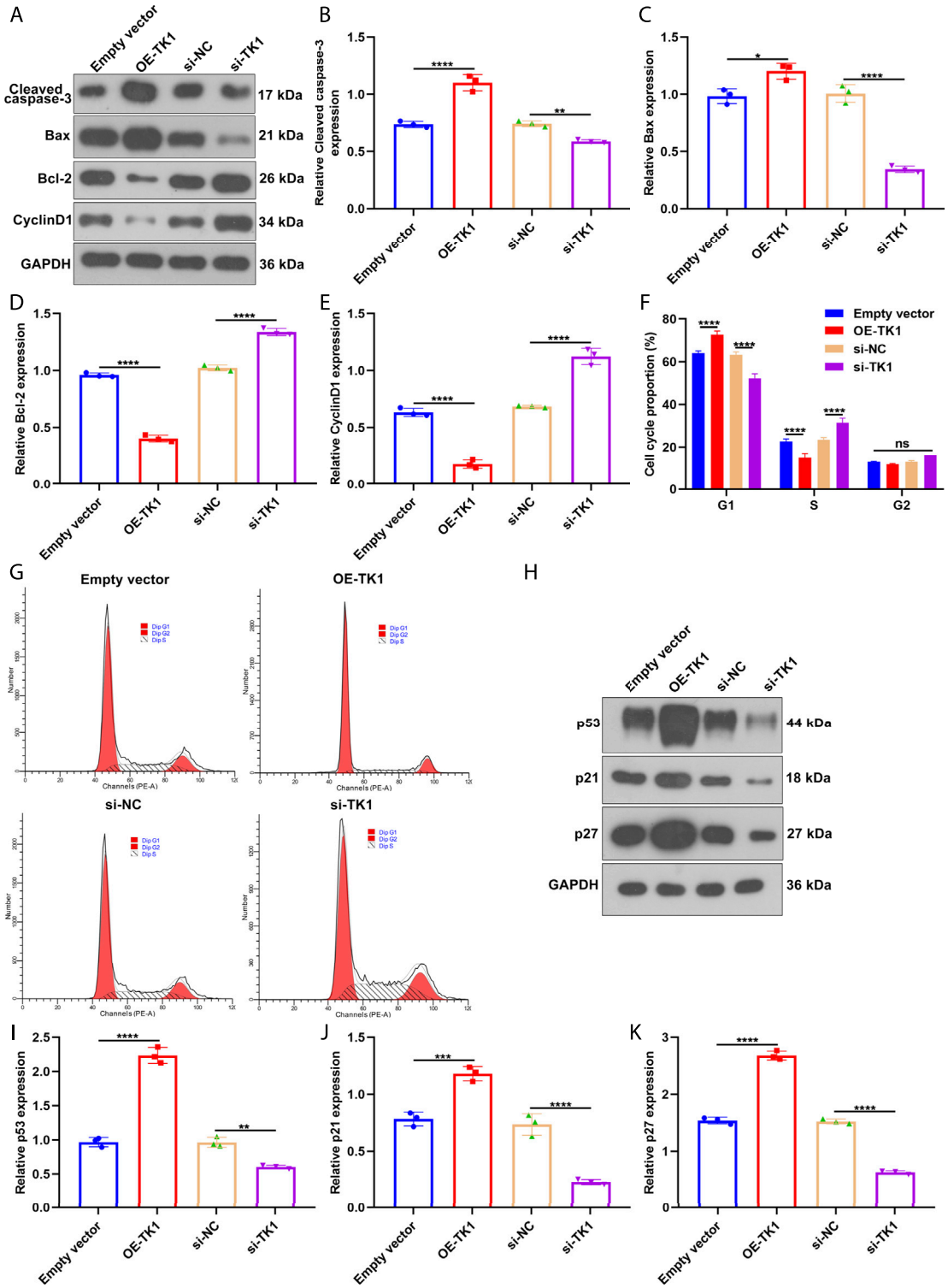

FIGURE 9 | TK1 knockdown relieves apoptosis, cell cycle arrest and senescence in SLE BMSCs. **(A–E)** The expression of cell cycle- and apoptosis-relevant proteins was measured in SLE BMSCs with TK1 overexpression or TK1 knockdown through western blotting, containing **(B)** Cleaved caspase-3, **(C)** Bax, **(D)** Bcl-2 as well as **(E)** CyclinD1. **(F,G)** Cell cycle proportions were tested in specified SLE BMSCs via flow cytometry analyses. **(H–K)** The expression of senescence-relevant proteins was measured in specified SLE BMSCs. Ns: not significant; *$p < 0.05$; **$p < 0.01$; ***$p < 0.001$; ****$p < 0.0001$.

facilitated Cleaved caspase-3 (**Figure 9B**) and Bax (**Figure 9C**) expressions but weakened the expression of Bcl-2 (**Figure 9D**) in SLE BMSCs. Also, the expression of Cleaved caspase-3 an Bax was reduced as well as the expression of Bcl-2 was enhanced in TK1-silenced SLE BMSCs. Hence, silencing TK1 relieved apoptosis of SLE BMSCs. Also, cell cycle-relevant protein CyclinD1 expression was remarkably reduced in TK1-overexpressed SLE BMSCs as well as it was enhanced in TK1-silenced SLE BMSCs (**Figure 9E**). In **Figures 9F,G**, G1 arrest was investigated in TK1-overexpressed SLE BMSCs. Oppositely, G1 phase was remarkably shortened by TK1 knockdown in SLE BMSCs. The influence of TK1 on senescence was further investigated in SLE BMSCs. Consequently, there was prominently enhanced expression of senescence-relevant proteins containing p53, p21 and p27 in TK1-overexpressed SLE BMSCs (**Figures 9H–K**). Also, their expression was weakened in TK1-silenced SLE BMSCs. Overall, TK1 knockdown relieved apoptosis, cell cycle arrest and senescence in SLE BMSCs.

DISCUSSION

SLE represents a chronic autoimmune rheumatic disease with high heterogeneity in clinical presentations, treatment responses and clinical outcomes (Arnaud and Tektonidou 2020). Due to the highly complicated pathogenesis of SLE, to comprehend pathophysiology provides an in-depth understanding of the molecular mechanisms (Arnaud and Tektonidou 2020). The activity of SLE severely depends on evaluating inflammation in multiple organs (Fousert et al., 2020; Wei et al., 2020). Computational and biological, advances in bioinformatics accelerate the capacity of predicting alterations in SLE activity as well as optimizing treatment modalities (Banchereau et al., 2016; Yang et al., 2020; Zhao et al., 2021).

SLE is characterized by autoimmune, and inflammatory processes (Zhao et al., 2021). Our CIBERSORT results demonstrated the widespread infiltration of diverse immune cell populations in SLE, consistent with previous research (Zhao et al., 2021). The experimental evidences showed the remarkable up-regulations of serum levels of inflammatory chemokines containing IFN-γ, IL-12, IL-6, IL-13, IL-18 and IL-1β in SLE patients than controls, proving the activation of inflammatory response in SLE. With WGCNA approach, we determined three immune cell-relevant co-expression modules that displayed strong correlations to neutrophils, B cells naïve, and plasma cells. Further functional enrichment analyses proved the crucial roles of genes in the three modules in modulating neutrophils, B cells naïve, and plasma cells. Thus, above genes could be utilized as immune cell-relevant genes. With MCODE approach, immune cell-relevant hub genes were determined. Among them, five characteristic genes were screened (containing CXCL1, CXCL2, CXCL8, CXCR1 and TK1) with LASSO approach. These characteristic genes displayed remarkable up-regulations in SLE in comparison to controls. The AUC of ROCs was 0.994 in the GSE50772 dataset, proving the favorable diagnostic efficacy of this multivariate model. Further analyses were indicative of the interactions of five characteristic genes with diverse immune cells in SLE. Additionally, GSEA results demonstrated that five characteristic genes exerted crucial roles in modulating distinct pathways. Chemokines exert remarkable functions in the pathogenesis of SLE, not only inducing autoimmune response in multiple organs, but also amplifying the induced inflammatory response (Ghafouri-Fard et al., 2021). For instance, decreasing CXCL2 facilitates innate immune activation and neutrophil extracellular trap formation (Yang et al., 2021). Nevertheless, the roles of TK1 in SLE progression remain indistinct.

BMSCs have been proposed as promising and alternative cells for treatment of SLE due to the self-renewal, pluripotent differentiation capacity and reduced immunogenicity (Gao et al., 2020). Previous research indicated allogenic BMSC transplantation as a safe and effective treatment against refractory SLE (Sun et al., 2009). Unfortunately, in-depth research proved that syngeneic BMSC transplantation is not effective (Gu et al., 2012). Recent evidences suggest that SLE BMSCs characterized by apoptosis, cell cycle arrest, and senescent phenotype could result in SLE progression (Ji et al., 2019). Here, we isolated BMSCs from five SLE patients and five controls. TK1 expression was proved to be up-regulated in BMSCs of SLE. TK1-overexpressed BMSCs of SLE presented enhanced IL-1β expression, apoptosis, G1 arrest and senescent phenotype as well as the opposite results were proved in TK1-silenced BMSCs of SLE. Hence, our findings might offer a novel therapeutic agent against SLE. Despite this, there are several limitations in our study. Firstly, the number of SLE patients is limited, and more patients should be included to validate the expression of TK1 in BMSCs of SLE patients. Secondly, *in vivo* experiments are required to verify the roles of TK1 in BMSCs of SLE. Thirdly, the molecular mechanisms of TK1 in modulating BMSCs of SLE should be further explored.

CONCLUSION

Collectively, our study demonstrated that TK1 triggered inflammatory response, apoptosis, cell cycle arrest and senescence in BMSCs of SLE and suppressing TK1 remarkably alleviated inflammation, growth arrest and senescent phenotype of SLE BMSCs. Hence, TK1 blockade might become a potential therapeutic target against SLE. In our future studies, we will validate the therapeutic roles of TK1-silenced BMSCs against SLE through *in vivo* experiments.

DATA AVAILABILITY STATEMENT

The original contributions presented in the study are included in the article/supplementary material, further inquiries can be directed to the corresponding author.

ETHICS STATEMENT

The studies involving human participants were reviewed and approved by Affiliated Hospital of Guilin Medical University

(YXLL-2016-WJWZC-14). The patients/participants provided their written informed consent to participate in this study.

AUTHOR CONTRIBUTIONS

JG conceived and designed the study. FC, JM and WY conducted most of the experiments and data analysis and wrote the manuscript. MW, YJ participated in collecting data and helped to draft the manuscript. All authors reviewed and approved the manuscript.

FUNDING

This work was funded by National Natural Science Foundation of China (81760562); Guangxi Zhuang Autonomous Region Health and Family Planning Commission Planning Project (Z2016383).

REFERENCES

Arnaud, L., and Tektonidou, M. G. (2020). Long-term Outcomes in Systemic Lupus Erythematosus: Trends over Time and Major Contributors. *Rheumatology (Oxford)* 59 (Suppl. 5), v29–v38. doi:10.1093/rheumatology/keaa382

Banchereau, R., Hong, S., Cantarel, B., Baldwin, N., Baisch, J., Edens, M., et al. (2016). Personalized Immunomonitoring Uncovers Molecular Networks that Stratify Lupus Patients. *Cell* 165 (3), 551–565. doi:10.1016/j.cell.2016.03.008

Doncheva, N. T., Morris, J. H., Gorodkin, J., and Jensen, L. J. (2019). Cytoscape StringApp: Network Analysis and Visualization of Proteomics Data. *J. Proteome Res.* 18 (2), 623–632. doi:10.1021/acs.jproteome.8b00702

Durcan, L., O'Dwyer, T., and Petri, M. (2019). Management Strategies and Future Directions for Systemic Lupus Erythematosus in Adults. *The Lancet* 393 (10188), 2332–2343. doi:10.1016/s0140-6736(19)30237-5

Engebretsen, S., and Bohlin, J. (2019). Statistical Predictions with Glmnet. *Clin. Epigenet* 11 (1), 123. doi:10.1186/s13148-019-0730-1

Fousert, E., Toes, R., and Desai, J. (2020). Neutrophil Extracellular Traps (NETs) Take the Central Stage in Driving Autoimmune Responses. *Cells* 9 (4), 915. doi:10.3390/cells9040915

Furie, R., Werth, V. P., Merola, J. F., Stevenson, L., Reynolds, T. L., Naik, H., et al. (2019). Monoclonal Antibody Targeting BDCA2 Ameliorates Skin Lesions in Systemic Lupus Erythematosus. *J. Clin. Invest.* 129 (3), 1359–1371. doi:10.1172/jci124466

Gao, L., OConnell, M., Liesveld, J., McDavid, A., Anolik, J. H., and Looney, R. J. (2020). Bone Marrow Mesenchymal Stem Cells from Patients with SLE Maintain an Interferon Signature during *In Vitro* Culture. *Cytokine* 132, 154725. doi:10.1016/j.cyto.2019.05.012

Geng, L., Tang, X., Wang, S., Sun, Y., Wang, D., Tsao, B. P., et al. (2020). Reduced Let-7f in Bone Marrow-Derived Mesenchymal Stem Cells Triggers Treg/Th17 Imbalance in Patients with Systemic Lupus Erythematosus. *Front. Immunol.* 11, 233. doi:10.3389/fimmu.2020.00233

Geng, L., Tang, X., Zhou, K., Wang, D., Wang, S., Yao, G., et al. (2019). MicroRNA-663 Induces Immune Dysregulation by Inhibiting TGF-B1 Production in Bone Marrow-Derived Mesenchymal Stem Cells in Patients with Systemic Lupus Erythematosus. *Cell Mol Immunol* 16 (3), 260–274. doi:10.1038/cmi.2018.1

Ghafouri-Fard, S., Shahir, M., Taheri, M., and Salimi, A. (2021). A Review on the Role of Chemokines in the Pathogenesis of Systemic Lupus Erythematosus. *Cytokine* 146, 155640. doi:10.1016/j.cyto.2021.155640

Gu, F., Molano, I., Ruiz, P., Sun, L., and Gilkeson, G. S. (2012). Differential Effect of Allogeneic versus Syngeneic Mesenchymal Stem Cell Transplantation in MRL/lpr and (NZB/NZW)F1 Mice. *Clin. Immunol.* 145 (2), 142–152. doi:10.1016/j.clim.2012.08.012

Hanaoka, H., Nishimoto, T., Okazaki, Y., Takeuchi, T., and Kuwana, M. (2020). A Unique Thymus-Derived Regulatory T Cell Subset Associated with Systemic Lupus Erythematosus. *Arthritis Res. Ther.* 22 (1), 88. doi:10.1186/s13075-020-02183-2

Ji, J., Fu, T., Dong, C., Zhu, W., Yang, J., Kong, X., et al. (2019). Targeting HMGB1 by Ethyl Pyruvate Ameliorates Systemic Lupus Erythematosus and Reverses the Senescent Phenotype of Bone Marrow-Mesenchymal Stem Cells. *Aging* 11 (13), 4338–4353. doi:10.18632/aging.102052

Kennedy, W. P., Maciuca, R., Wolslegel, K., Tew, W., Abbas, A. R., Chaivorapol, C., et al. (2015). Association of the Interferon Signature Metric with Serological Disease Manifestations but Not Global Activity Scores in Multiple Cohorts of Patients with SLE. *Lupus Sci. Med.* 2 (1), e000080. doi:10.1136/lupus-2014-000080

Khodoun, M., Chimote, A. A., Ilyas, F. Z., Duncan, H. J., Moncrieffe, H., Kant, K. S., et al. (2020). Targeted Knockdown of Kv1.3 Channels in T Lymphocytes Corrects the Disease Manifestations Associated with Systemic Lupus Erythematosus. *Sci. Adv.* 6 (47), eabd1471. doi:10.1126/sciadv.abd1471

Kiriakidou, M., and Ching, C. L. (2020). Systemic Lupus Erythematosus. *Ann. Intern. Med.* 172 (11), Itc81–itc96. doi:10.7326/aitc202006020

Langfelder, P., and Horvath, S. (2008). WGCNA: an R Package for Weighted Correlation Network Analysis. *BMC Bioinformatics* 9, 559. doi:10.1186/1471-2105-9-559

Liberzon, A., Birger, C., Thorvaldsdóttir, H., Ghandi, M., Mesirov, J. P., and Tamayo, P. (2015). The Molecular Signatures Database Hallmark Gene Set Collection. *Cel Syst.* 1 (6), 417–425. doi:10.1016/j.cels.2015.12.004

Mathias, L. M., and Stohl, W. (2020). Systemic Lupus Erythematosus (SLE): Emerging Therapeutic Targets. *Expert Opin. Ther. Targets* 24 (12), 1283–1302. doi:10.1080/14728222.2020.1832464

Newman, A. M., Liu, C. L., Green, M. R., Gentles, A. J., Feng, W., Xu, Y., et al. (2015). Robust Enumeration of Cell Subsets from Tissue Expression Profiles. *Nat. Methods* 12 (5), 453–457. doi:10.1038/nmeth.3337

Robin, X., Turck, N., Hainard, A., Tiberti, N., Lisacek, F., Sanchez, J.-C., et al. (2011). pROC: an Open-Source Package for R and S+ to Analyze and Compare ROC Curves. *BMC Bioinformatics* 12, 77. doi:10.1186/1471-2105-12-77

Subramanian, A., Tamayo, P., Mootha, V. K., Mukherjee, S., Ebert, B. L., Gillette, M. A., et al. (2005). Gene Set Enrichment Analysis: a Knowledge-Based Approach for Interpreting Genome-wide Expression Profiles. *Proc. Natl. Acad. Sci.* 102 (43), 15545–15550. doi:10.1073/pnas.0506580102

Sun, L., Akiyama, K., Zhang, H., Yamaza, T., Hou, Y., Zhao, S., et al. (2009). Mesenchymal Stem Cell Transplantation Reverses Multiorgan Dysfunction in Systemic Lupus Erythematosus Mice and Humans. *Stem Cells* 27 (6), 1421–1432. doi:10.1002/stem.68

Szklarczyk, D., Morris, J. H., Cook, H., Kuhn, M., Wyder, S., Simonovic, M., et al. (2017). The STRING Database in 2017: Quality-Controlled Protein-Protein Association Networks, Made Broadly Accessible. *Nucleic Acids Res.* 45 (D1), D362–d368. doi:10.1093/nar/gkw937

Tan, W., Gu, Z., Leng, J., Zou, X., Chen, H., Min, F., et al. (2019). Let-7f-5p Ameliorates Inflammation by Targeting NLRP3 in Bone Marrow-Derived Mesenchymal Stem Cells in Patients with Systemic Lupus Erythematosus. *Biomed. Pharmacother.* 118, 109313. doi:10.1016/j.biopha.2019.109313

Wei, K., Korsunsky, I., Korsunsky, I., Marshall, J. L., Gao, A., Watts, G. F. M., et al. (2020). Notch Signalling Drives Synovial Fibroblast Identity and Arthritis Pathology. *Nature* 582 (7811), 259–264. doi:10.1038/s41586-020-2222-z

Yang, B., Huang, X., Xu, S., Li, L., Wu, W., Dai, Y., et al. (2021). Decreased miR-4512 Levels in Monocytes and Macrophages of Individuals with Systemic Lupus Erythematosus Contribute to Innate Immune Activation and Neutrsophil NETosis by Targeting TLR4 and CXCL2. *Front. Immunol.* 12, 756825. doi:10.3389/fimmu.2021.756825

Yang, F., Zhai, Z., Luo, X., Luo, G., Zhuang, L., Zhang, Y., et al. (2020). Bioinformatics Identification of Key Candidate Genes and Pathways Associated with Systemic Lupus Erythematosus. *Clin. Rheumatol.* 39 (2), 425–434. doi:10.1007/s10067-019-04751-7

Yang, J., Yang, X., Zou, H., Chu, Y., and Li, M. (2011). Recovery of the Immune Balance between Th17 and Regulatory T Cells as a Treatment for Systemic Lupus Erythematosus. *Rheumatology* 50 (8), 1366–1372. doi:10.1093/rheumatology/ker116

Yu, G., Wang, L.-G., Han, Y., and He, Q.-Y. (2012). clusterProfiler: an R Package for Comparing Biological Themes Among Gene Clusters. *OMICS: A J. Integr. Biol.* 16 (5), 284–287. doi:10.1089/omi.2011.0118

Yuan, X., Qin, X., Wang, D., Zhang, Z., Tang, X., Gao, X., et al. (2019). Mesenchymal Stem Cell Therapy Induces FLT3L and CD1c+ Dendritic Cells in Systemic Lupus Erythematosus Patients. *Nat. Commun.* 10 (1), 2498. doi:10.1038/s41467-019-10491-8

Zhao, X., Zhang, L., Wang, J., Zhang, M., Song, Z., Ni, B., et al. (2021). Identification of Key Biomarkers and Immune Infiltration in Systemic Lupus Erythematosus by Integrated Bioinformatics Analysis. *J. Transl Med.* 19 (1), 35. doi:10.1186/s12967-020-02698-x

Zhu, H., Mi, W., Luo, H., Chen, T., Liu, S., Raman, I., et al. (2016). Whole-genome Transcription and DNA Methylation Analysis of Peripheral Blood Mononuclear Cells Identified Aberrant Gene Regulation Pathways in Systemic Lupus Erythematosus. *Arthritis Res. Ther.* 18, 162. doi:10.1186/s13075-016-1050-x

Conflict of Interest: The authors declare that the research was conducted in the absence of any commercial or financial relationships that could be construed as a potential conflict of interest.

Publisher's Note: All claims expressed in this article are solely those of the authors and do not necessarily represent those of their affiliated organizations, or those of the publisher, the editors and the reviewers. Any product that may be evaluated in this article, or claim that may be made by its manufacturer, is not guaranteed or endorsed by the publisher.

GLOSSARY

AUC area under curve

BMSCs bone marrow mesenchymal stem cells

CIBERSORT cell-type identification by estimating relative subsets of RNA transcript

ELISA Enzyme-linked immunosorbent assay

GEO Gene Expression Omnibus

GO Gene ontology

GS gene significance

GSEA Gene set enrichment analyses

IFN-γ interferon-γ

IL-12 interleukin-12

IL-13 interleukin-13

IL-18 interleukin-18

IL-1β interleukin-1β

IL-6 interleukin-6

KEGG Kyoto encyclopedia of genes and genomes

LASSO Least absolute shrinkage and selection operator

MCODE Molecular Complex Detection

MEs module eigengenes

MM module membership

PBMCs peripheral blood mononuclear cells

PPI protein-protein interaction

ROC receiver operator characteristic curve

RT-qPCR real-time quantitative polymerase chain reaction

SLE systemic lupus erythematosus

STRING Search Tool for Retrieval of Interacting Genes/Proteins

TOM topological overlap matrix

WGCNA weighted gene co-expression analyses

frontiers | Frontiers in Molecular Biosciences

REVIEW
published: 25 May 2022
doi: 10.3389/fmolb.2022.909151

Triglyceride and Triglyceride-Rich Lipoproteins in Atherosclerosis

Bai-Hui Zhang, Fan Yin, Ya-Nan Qiao and Shou-Dong Guo**

Institute of Lipid Metabolism and Atherosclerosis, Innovative Drug Research Centre, School of Pharmacy, Weifang Medical University, Weifang, China

Cardiovascular disease (CVD) is still the leading cause of death globally, and atherosclerosis is the main pathological basis of CVDs. Low-density lipoprotein cholesterol (LDL-C) is a strong causal factor of atherosclerosis. However, the first-line lipid-lowering drugs, statins, only reduce approximately 30% of the CVD risk. Of note, atherosclerotic CVD (ASCVD) cannot be eliminated in a great number of patients even their LDL-C levels meet the recommended clinical goals. Previously, whether the elevated plasma level of triglyceride is causally associated with ASCVD has been controversial. Recent genetic and epidemiological studies have demonstrated that triglyceride and triglyceride-rich lipoprotein (TGRL) are the main causal risk factors of the residual ASCVD. TGRLs and their metabolites can promote atherosclerosis via modulating inflammation, oxidative stress, and formation of foam cells. In this article, we will make a short review of TG and TGRL metabolism, display evidence of association between TG and ASCVD, summarize the atherogenic factors of TGRLs and their metabolites, and discuss the current findings and advances in TG-lowering therapies. This review provides information useful for the researchers in the field of CVD as well as for pharmacologists and clinicians.

Keywords: hypertriglyceridemia, cardiovascular disease, triglyceride-rich lipoprotein, residual risk, lipid-lowering

OPEN ACCESS

Edited by:
Leming Sun,
Northwestern Polytechnical University, China

Reviewed by:
Guojun Zhao,
The Sixth Affiliated Hospital of Guangzhou Medical University, China
Jian Tu,
Guilin Medical University, China

****Correspondence:***
Ya-Nan Qiao
18253164654@163.com
Shou-Dong Guo
SD-GUO@hotmail.com

Specialty section:
This article was submitted to Molecular Diagnostics and Therapeutics, a section of the journal Frontiers in Molecular Biosciences

Received: *31 March 2022*
Accepted: *06 May 2022*
Published: *25 May 2022*

Citation:
Zhang B-H Yin F, Qiao Y-N and Guo S-D (2022) Triglyceride and Triglyceride-Rich Lipoproteins in Atherosclerosis. Front. Mol. Biosci. 9:909151. doi: 10.3389/fmolb.2022.909151

INTRODUCTION

According to the WHO report in 2021, cardiovascular disease (CVD) is still the leading cause of death worldwide, and atherosclerotic CVD (ASCVD) is the most representative and dangerous one (Lin et al., 2021; WHO, 2021). Cholesterol carried by lipoproteins in blood is the major inducer of ASCVD. Among the lipoproteins, low-density lipoprotein (LDL) carries approximately 75% of total cholesterol (TC) that is carried by non-high density lipoprotein (HDL) particles (Jacobson et al., 2015). People with low LDL cholesterol (LDL-C) levels are less likely to develop CVD compared with those having average or high levels of LDL-C (Cohen et al., 2006; Ference et al., 2012). For instance, a long-term exposure to lower LDL-C is associated with a 54.5% reduction in the risk of coronary heart disease (CHD) for each mmol/L (38.7 mg/dl) reduction of LDL-C (Ference et al., 2012). The first line lipid-lowering drug, statins, can significantly reduce LDL-C levels, leading to a reduction in CVD events by 25%–40% (Michos et al., 2012; Silverman et al., 2016; Toth et al., 2019a). Moreover, the antibodies or siRNA of proprotein convertase subtilisin/kexin-type 9 (PCSK9) can further decrease LDL-C level as an add-on-statin therapy. However, patients-treated with statins in combination with PCSK9 inhibitors still experience ASCVD events even their LDL-C levels meet the clinical goals (Sampson et al., 2012; Nishikido and Ray, 2021; Su et al., 2021). Therefore, researchers are impelled to find novel strategies for treatment of residual ASCVD.

Given a low HDL cholesterol (HDL-C) level is a strong and independent risk factor associated with CVD events, enhancing HDL-C level has ever been expected to prevent and/or recover CVD (Catapano et al., 2016; Mach et al., 2020). Cholesteryl ester transport protein (CETP) inhibitors can significantly improve HDL-C levels and reverse cholesterol transport. However, these inhibitors are found to be useless in prevention of CVD events (Liu N et al., 2021). HDL dysfunction in patients with CVD may partially explain the failure of these CETP inhibitors (Sandesara et al., 2019). Recent studies suggested that although HDL-C is a useful risk biomarker, accumulating evidence from Mendelian randomization studies and other research have demonstrated that HDL-C is not a causal risk factor for ASCVD (Nordestgaard, 2016; Lincoff et al., 2017; Barter and Genest, 2019; Goyal et al., 2021). Therefore, researchers turn their attention to other targets for treatment of ASCVD.

Previously, whether the elevated plasma triglyceride (TG) levels are causally associated with ASCVD has been controversial. Genetic and epidemiological studies have demonstrated that TG and TG-rich lipoprotein (TGRL) are main causes of residual ASCVD (Do et al., 2013; Jørgensen et al., 2013; Thomsen et al., 2014; Nordestgaard, 2016; Generoso et al., 2019; Laufs et al., 2019; Matsunage et al., 2020; Farnier et al., 2021; Nordestgaard et al., 2021). For instance, approximately 26% adults in United State, including one-third of statin users, have a TG ≥ 150 mg/dl, and approximately 40% adults with diabetes have a TG ≥ 150 mg/dl despite statin use. These elevated TGs are associated with CVD risk even in patients with low LDL-C levels (Hoogeveen and Ballantyne, 2020; Toth et al., 2020). In the genome-wide association studies, the susceptibility sites for CHD are associated with genes involved in TG metabolism (Teslovich et al., 2010; Schunkert et al., 2011). Mendelian randomization studies also indicate that there is a causal relationship between TG metabolism and the risk of atherosclerosis (Johansen and Hegele, 2013; Jørgensen et al., 2013; Varbo et al., 2013; Thomsen et al., 2014; Si et al., 2021). The atherogenic effects of TG, TGRL, and TGRL metabolites are dependent on their roles in endothelial function, inflammation, oxidative stress, and formation of foam cells. In this review, we will make a short review of TG and TGRL metabolism, discuss the association between TG and ASCVD, summarize the atherogenic factors of TGRL, and outline the current advances in TG-lowering therapies and the targets with potential applications in TG modulation.

A SHORT REVIEW OF TG AND TGRL

TG is the major storage form of fatty acid (FA) within cells and in circulation (Alves-Bezerra and Cohen, 2017; Duran and Pradhan, 2021). Liver is the central organ for metabolism of FAs that are originated from the plasma and/or hepatocellular *de novo* biosynthesis. FA synthesis is precisely controlled by a series of enzymes including sterol regulatory element binding protein (SREBP) 1c. When glucose is abundant, plasma insulin activates the endoplasmic reticulum (ER) membrane-bound transcription factor SREBP-1c, which can upregulate genes related to FA biosynthesis (Alves-Bezerra and Cohen, 2017). Within hepatocytes, FA is esterified to glycerol-3-phosphate (G3P) to generate TG. It is estimated that more than 90% of the total TG is synthesized by the G3P pathway in most mammalians (Alves-Bezerra and Cohen, 2017; Lee and Ridgway, 2020). The acylation of G3P is a rate-limiting step because G3P acyltransferase (GPAT) family members have the lowest specific activity within the enzymes involved in TG synthesis. GPAT1 is highly expressed in the liver, and deficiency of GPAT1 can reduce the plasma level of TG and secretion rate of VLDL (Hammond et al., 2005; Neschen et al., 2005). TG synthesis pathways and its metabolism in liver have been well-documented in the literature (Alves-Bezerra and Cohen, 2017; Lee and Ridgway, 2020; Castillo-Núñez et al., 2022). The assembly of TG is the primary way for the liver to store and export FA. However, only a small amount of FA is stored in the form of TG as lipid droplet because most of the FAs are either oxidized in the mitochondrion or packaged in the core of very low-density lipoprotein (VLDL) as TG and secreted into the blood.

As TG is a kind of nonpolar and hydrophobic molecule, it must be combined with related proteins and lipids to form lipoprotein particles during transportation in blood (Do et al., 2013; Castillo-Núñez et al., 2022). In the liver, a large amount of TGs are assembled with cholesterol, phospholipids, and apolipoprotein (apo) B100 (apoB100) into VLDL. In the small intestine, dietary TG is decomposed into FA and monoglyceride or diglyceride before being absorbed by enterocytes. These decomposition products are reassembled into CM with cholesterol, phospholipids, and apoB48 (Julve et al., 2016; Santos-Baez and Ginsberg, 2020). Next, CMs are released into the lymphatic system and enter the circulation, where they obtain other apolipoproteins including apoCII, apoCIII, and apoE (Rosenson et al., 2014; Nakajima and Tanaka, 2018a). Of importance, microsomal triglyceride transfer protein (MTP) plays a key role in the assembly of VLDL and CM via transporting the related lipids to apoB particles (Iqbal et al., 2020). Furthermore, recent studies have demonstrated that CETP increases the production of VLDL-TG in response to estrogen treatment via enhancing the expression of nuclear receptor and small heterodimer partner in female CETP transgenic mice (Palmisano et al., 2016; Palmisano et al., 2021). Therefore, some endogenous molecules, such as estrogen, mediate sex-specific modulation of TG metabolism. The secreted VLDL and CM particles transport FAs to muscle and adipose tissue for energy usage and/or storage via the blood flow (Duran and Pradhan, 2021; Castillo-Núñez et al., 2022).

In circulation, lipoprotein lipase (LPL) located at the surface of capillary lumen hydrolyzes TGs that are encapsulated in the core of CM and VLDL into FAs. LPL binds to its endothelial coenzyme, glycosylphosphatidylinositol-anchored HDL binding protein 1 (GPIHBP1), to provide a platform for

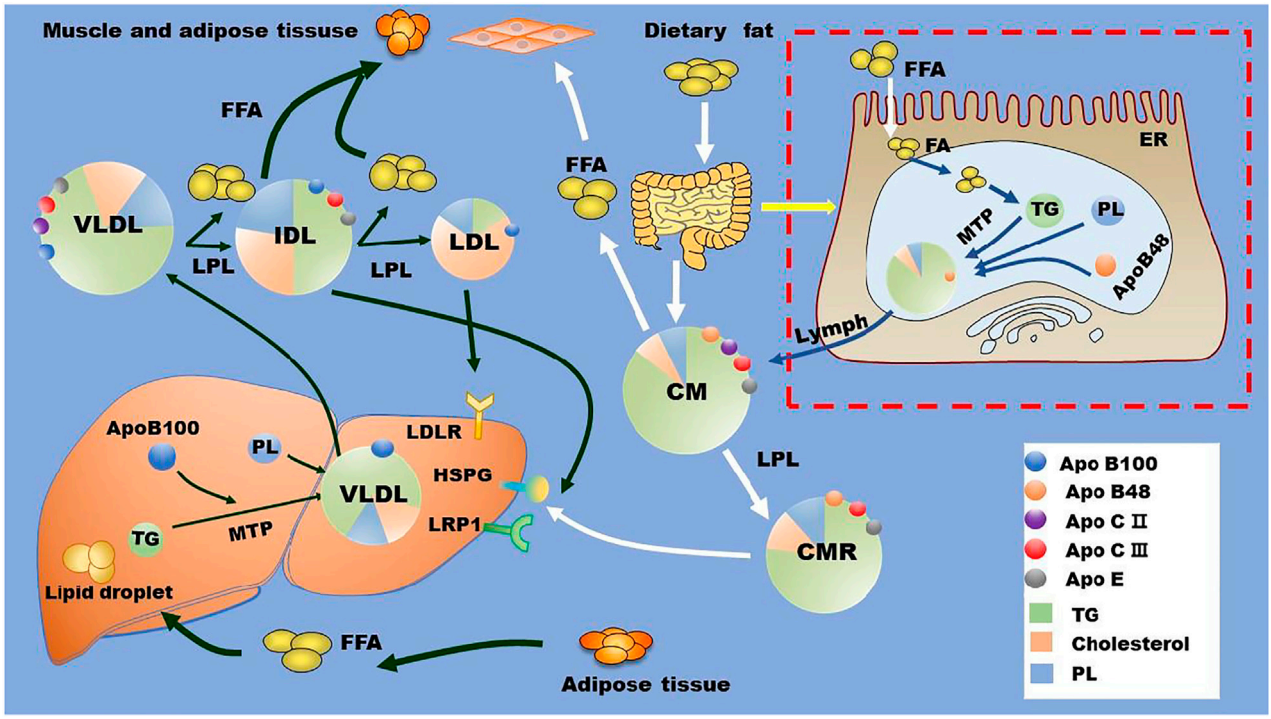

FIGURE 1 | TG and TGRL metabolism. Dietary fat is metabolized by intestinal cells into FAs, which are reassembled with cholesterol, phospholipids, and apoB48 to form CMs. These CMs are released into blood *via* lymph. In the liver, exogenous and *de novo* synthesized FAs are assembled with cholesterol, phospholipids, and apoB100 to form VLDL with the assistant of MTP. In the circulation, LPL located at the surface of the capillary lumen hydrolyzes the TG in the core of TGRL (CM and VLDL) and promotes the production of TGRL remnants and free FAs. TGRL remnants are cleared by liver through receptors including HSPG, LDLR, LRP1, and other potentially unidentified receptors. Apo, apolipoprotein; CM, chylomicron; CMR, chylomicron residual; ER, endoplasmic reticulum; FA, fatty acid; FFA, free fatty acid; HSPG, heparan sulfate proteoglycan; IDL, intermediate density lipoprotein; LDL, low-density lipoprotein; LDLR, low-density lipoprotein receptor; LPL, lipoprotein lipase; LRP1, LDLR-related protein 1; MTP, microsomal triglyceride transfer protein; PL, phospholipids; TG, triglycerides; VLDL, very low-density lipoproteins.

lipolysis of apoB-containing lipoproteins on the surface of vascular endothelium (Davies et al., 2010; Young et al., 2019; Basu and Goldberg, 2020). Of note, the activity of LPL is highly regulated by several proteins, such as apoCII, apoCIII, apoE, and angiopoietin-like protein (ANGPTL)3, ANGPTL4, and ANGPTL8 (Rosenson et al., 2014; Wu et al., 2021). Along with TG hydrolysis, CM gradually turns into smaller and cholesterol-rich CM remnant (CMR), and VLDL becomes intermediate density lipoprotein (IDL), which is further catabolized to be LDL via hepatic TG lipase (HTGL) on the surface of hepatic sinusoidal endothelial cell cavity (Young and Zechner, 2013). TGRL remnants in circulation are cleared by liver receptors including LDL receptor (LDLR), LDLR-related protein (LRP)-1, scavenger receptor B type 1 (SR-B1), and heparan sulfate proteoglycan (HSPG) (Toth, 2016; Kockx and Kritharides, 2018; Christopoulou et al., 2019). For instance, small particles, such as LDL, are cleared through the binding of apoE and/or apoB to LDLR, while larger particles, such as CMR, are eliminated by the binding of apoE to HSPG and other potentially undefined hepatic receptors (Kockx and Kritharides, 2018; Christopoulou et al., 2019). The metabolism of TG and TGRL is summarized in **Figure 1**.

HYPERTRIGLYCERIDEMIA AND ATHEROSCLEROSIS

Generally, lipid analysis (such as TC and TG levels) is performed using overnight fasted blood samples. However, recent studies have demonstrated that non-fasting and fasting plasma samples show similar lipid profiles, and all these data can be used for prediction of CVD risk (Bansal et al., 2007; Nordestgaard et al., 2007; Jørgensen et al., 2013; Thomsen et al., 2014). On average, non-fasting plasma TG levels are approximately 0.3 mmol/L (27 mg/dl) higher than the corresponding fasting samples (Catapano et al., 2016; Mach et al., 2020). TG levels reach peak at 4–6 h after food intake. Therefore, people are in a state of non-fasting at most of the times within a day, and non-fasting lipid levels are more representative than those of fasting lipid profiles. Presently, the standard measurement of plasma TG is still performed under fasting conditions. Generally, the fasting TG concentration <1.7 mmol/L (150 mg/dl) is defined as normal, 1.7–11.4 mmol/L (150–1000 mg/dl) is defined as moderate HTG, and >11.4 mmol/L (1000 mg/dl) is defined as severe HTG (Parhofer and Laufs, 2019). Extreme HTG is

rare and is defined as fasting TG concentration >20 mmol/L (~1750 mg/dl) (Parhofer and Laufs, 2019; Mach et al., 2020). Of note, severe HTG is generally associated with pancreatitis (Laufs et al., 2019; Parhofer and Laufs, 2019). Although the threshold TG level of 1.7 mmol/L is accepted by all medical societies, moderate and severe HTG are differently defined by distinct medical societies. Such as, severe HTG is also defined as TG level >10 mmol/L (850 mg/dl) (Laufs et al., 2019).

Genetic studies indicate that HTG can be caused by both single gene and multiple gene variants (Dron and Hegele, 2020; Matsunage et al., 2020; Ginsberg et al., 2021; Tokgözoğlu and Libby, 2022). For instance, homozygous or biallelic variants in LPL, apoCII, apoCIII, apoAV, lipase maturation factor 1, GPIHBP1, and ANGPTLs are demonstrated to be correlated with HTG (Jørgensen et al., 2013; Rosenson et al., 2014; Dron and Hegele, 2020; Gill et al., 2021). TGRL is consisted of a TG, cholesterol ester, and cholesterol core that is surrounded by phospholipids and apolipoproteins. These apolipoproteins play important roles in CM assembly and degradation. Carriers of the rare non-synonymous mutation of apoAV have higher levels of plasma TG compared with those of non-carriers (Do et al., 2015). An E40K loss-of-function variant in the gene encoding ANGPTL4 is associated with substantially reduced plasma levels of TG in white persons (Folsom et al., 2008). Furthermore, GPIHBP1 deficiency develops severe plasma CM in mouse even on a low-fat diet (Beigneux et al., 2007). In apoA-IV knockout mice, larger CM particles are formed and the clearance of these larger CMs is significantly delayed in circulation compared with those of wild-type mice (Kohan et al., 2012). Mechanistically, apoA-IV may influence particle assembly and/or lipidation in the ER, thereby modulating CM size and secretion (Black, 2007). Furthermore, obese adolescents show higher levels of ANGPTL3 and apoCIII, which potentially inhibit LPL activity, leading to increased TGRL levels and residual atherosclerosis risk (Rodríguez-Mortera et al., 2020).

HTG is reported to affect 15–20% of the adult population and is associated with overweight, metabolic syndrome, and diabetes mellitus (Parhofer and Laufs, 2019). Of note, approximately 50% of patients with type 2 diabetes are accompanied with HTG (Parhofer and Laufs, 2019). Patients with mild to moderate HTG have a higher risk of atherosclerosis than people with normal TG (Crea, 2021; Nordestgaard et al., 2021; Tokgözoğlu and Libby, 2022). One study indicates that TG ≥ 150 and TG ≥ 200–499 mg/dl may enhance CVD risk by 25.0% and 34.9%, respectively (Toth et al., 2021). In patients with severe HTG, individuals with CMRs that are rich in TG also have an increased risk of atherosclerosis (Dron and Hegele, 2020). Accumulating epidemiological studies have indicated that plasma level of TG (both fasting and non-fasting) has a strong correlation with atherosclerosis, and elevated TG levels are an independent risk factor for ASCVD (Nordestgaard et al., 2007; Pirillo et al., 2014; Werner et al., 2014; Kockx and Kritharides, 2018; Shahid et al., 2018; Laufs et al., 2019). Some research support that non-fasting TG levels are more closely associated with incident CVD events than fasting TG levels (Bansal et al., 2007; Adiels et al., 2012). Of importance, each reduction of 88.5 mg/dl of TG level is associated with approximately 50% reduction in CVD risk (Jun et al., 2010). Therefore, lowering TG treatment can reduce the risk of ASCVD as that of lowering LDL-C (Ference et al., 2019). In 2019, European Society of Cardiology and European Atherosclerosis Society has clearly pointed out that TG ≥ 175 mg/dl is a risk factor of ASCVD events and TG-lowering therapy is recommended for residual ASCVD therapy (Mach et al., 2020).

TGRL AND ATHEROSCLEROSIS

TG is the main component of TGRL (CM and VLDL), and their remnants CMR and IDL (Duran and Pradhan, 2021; Castillo-Núñez et al., 2022). Therefore, plasma TG concentration is a biomarker for TGRL and their remnants in circulation. The methods used for isolation and quantification of TGRL remnants have been recently reviewed by distinct groups (Hoogeveen and Ballantyne, 2020; Duran and Pradhan, 2021). After meals, TGs are transported from the small intestine to bloodstream by CM particles, where they are converted to atherogenic CMRs by LPL in tissues (Ginsberg et al., 2021). Similarly, liver secreted VLDL particles are converted to IDL and then LDL by LPL and HTGL in circulation. TGRL and the hydrolyzed residuals including free FAs bind to leukocytes and endothelial cells in circulation, leading to a state of acute activation that is characterized by expression of integrins, generation of ROS, production of cytokines as well as a complement activation (DeVries et al., 2014). Recent studies have demonstrated that TGRL and their remnants are positively associated with atherosclerosis by up-regulating inflammation, oxidative stress, and foam cell formation as shown in **Figure 2**.

TGRLs Activate Inflammation

Atherosclerosis is characterized as a chronic inflammatory disease. Of note, each mmol/L (39 mg/dl) increase of TGRL cholesterol is associated with a 37% increase of C-reactive protein level, suggesting TGRL cholesterol increases inflammatory response (Varbo et al., 2013). Furthermore, plasma levels of interleukin (IL)-6 and tumor necrosis factor-alpha (TNFα) are significantly higher in postprandial subjects than those in fasting state, suggesting that elevated levels of postprandial TGRL cholesterol are associated with inflammatory response, causing increased susceptibility for premature atherosclerosis (Twickler et al., 2003). TGRLs with high TG content up-regulate the level of TNF-α, thereby inducing the expression of vascular cell adhesion molecule (VCAM)-1 in human aortic endothelial cells and monocyte adhesion. On the contrary, TGRLs with low TG content have an atheroprotective effect by reducing VCAM-1 expression and monocyte recruitment (Gower et al., 2011; Wang et al., 2011; Sun et al., 2012). Postprandially released VLDL particles have an increased level of apoCIII (Wang et al., 2011; Sun et al., 2012), and these particles activate inflammation in endothelial cells by enhancing the protein kinase C (PKC)/NF-κB signaling pathway (Libby,

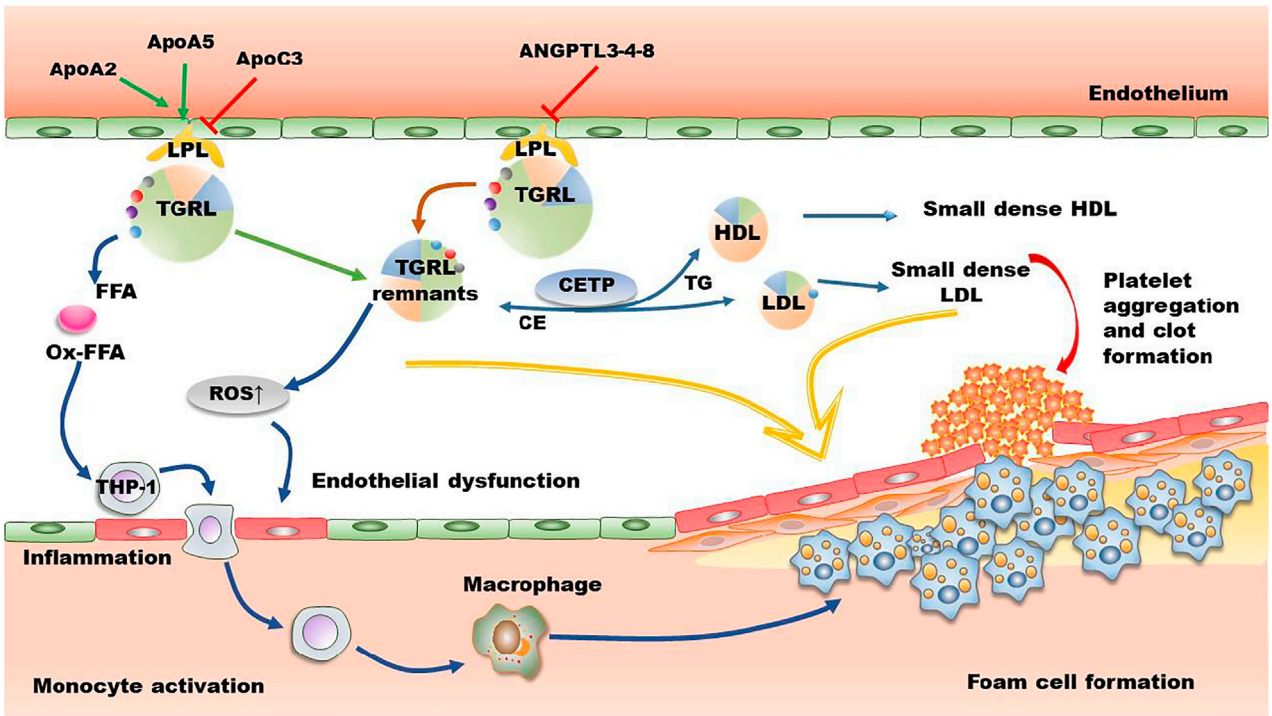

FIGURE 2 | The mechanisms of TGRL on promoting atherosclerosis. In circulation, apoAII and apoAV enhance the activity of LPL, while apoAIII and ANGPTL3-4-8 suppress LPL-induced TGRL lipolysis. However, several studies demonstrate that apoAIII has no effect on the activity of LPL. The released FFA and the lipolysis process promote the production of ROS and secretion of inflammatory factors, leading to endothelial dysfunction and formation of foam cells. CETP-mediated lipid exchange between TGRL and HDL/LDL increases the production of small dense LDL and small dense HDL, further promoting deterioration of atherosclerosis. Furthermore, lipolytic products activate platelet and induce clot formation. ANGPTL, angiopoietin-like protein; Apo, apolipoprotein; CE, cholesteryl ester; CETP, cholesteryl ester transport protein; FFA, free fatty acid; HDL, high density lipoprotein; LDL, low-density lipoprotein; LPL, lipoprotein lipase; Ox-FFA, oxidized FFA; ROS, reactive oxygen species; TG, triglycerides; TGRL, triglyceride-rich lipoprotein.

2007). Similarly, VLDL particles promote inflammation by activating the NF-κB signaling pathway in endothelial cells (Dichtl et al., 1999; den Hartigh et al., 2014). However, ApoCIII A allele at rs2070667 shows an inhibitory effect on polyunsaturated fatty acids (PUFA)-containing TGs and hepatic inflammation in nonalcoholic fatty liver disease (Xu et al., 2020).

Macrophage is a central link between lipid metabolism and inflammatory response. TG synthesis (lipid droplet formation) enhances macrophage inflammation (Castoldi et al., 2020). *In vitro*, VLDL enhances the expression of TNF-α, IL-1β, monocyte chemoattractant protein 1 (MCP-1), intercellular adhesion molecule-1 (ICAM-1), matrix metalloproteinase 3, and macrophage inflammatory protein 1-α. Mechanistically, VLDL activates mitogen-activated protein kinase (MAPK) signaling cascades including the phosphorylation of extracellular signal-regulated kinase (ERK) 1/2, c-Jun NH2-terminal kinase (JNK), and p38 MAPK (Jinno et al., 2011). VLDL particles further enhance the expression of TNF-α in macrophages that are induced by LPS *via* activating ERK1/2, MAPK kinase (MEK)1/2, and the transcription factor AP-1 rather than nuclear factor-κB (NF-κB) or peroxisome proliferator activated receptor (PPAR) γ (Stollenwerk et al., 2004). TGRL also induces inflammation by activating the inflammasome nucleotide binding domain like receptor family pyrrole domain containing protein 1 (NLRP1) (Bleda et al., 2016; Bleda et al., 2017). Furthermore, VLDL intensifies its pro-inflammatory effects by binding to LRP and activating the downstream p38 MAPK/NF-κB signaling pathway (Libby, 2007). Of note, ER stress and the unfolded protein response are also involved in TGRL-induced inflammation (Ozcan et al., 2004; Civelek et al., 2009; Wang et al., 2013). In addition, CMRs stimulate the expression of IL-1β via activating caspase-1 and NF-κB in THP-1 cells (Okumura et al., 2006). CMRs also activate human monocytes and enhance their migration *in vitro*, contributing to an inflammatory environment in the early stage of atherosclerosis (Bentley et al., 2011). The inflammation-associated hormone, growth and differentiation factor 15, is also involved in TGRL-mediated inflammation (Luan et al., 2019).

Accumulating evidence have demonstrated that TGRLs and their remnants increase endothelial inflammation and facilitate monocytes infiltration of the arterial wall. A previous study demonstrated that TGRL induces monocyte adhesion to vascular endothelial cells by sequentially activating the expression of PKC, RhoA, focal adhesion kinase, and integrins *in vitro*, suggesting a mechanism of TGRL remnants-mediated vascular inflammation during atherogenesis (Kawakami et al., 2002). TGRL remnants also induce the expression of TNF-α, VCAM-1, ICAM-1, E-selectin, and MCP-1 through modulation

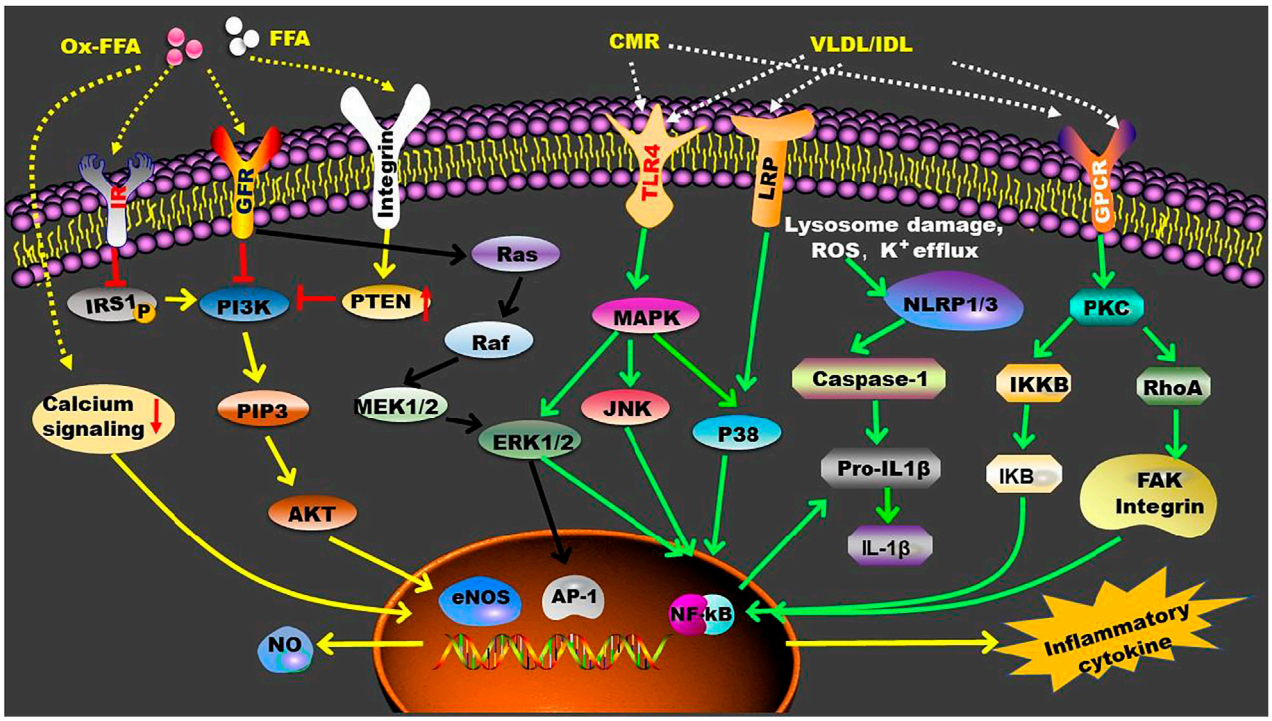

FIGURE 3 | TGRL and TGRL metabolites-mediated inflammatory signaling pathways. In circulation, LPL converts TGRL to TGRL remnants, such as CMR and IDL, and promotes the production of FFA. These TGRL metabolites enhance inflammation by activating multiple receptors that located on the cell membrane. Furthermore, FFA can penetrate cell membrane and exert their functions intracellularly. AP-1, activating protein-1; eNOS, endothelial nitric oxide synthase; ERK1/2, extracellular signal-regulated kinase 1/2; FAK, focal adhesion kinase; FFA, free fatty acid; GFR, growth factor receptor; GPCR, G protein-coupled receptor; IKB, nuclear factor-kappa B inhibitor; IKKB, Inhibitor of kappa B kinase; IL-1β, interleukin-1β; IR, insulin receptor; IRS1, insulin receptor substrate 1; JNK, c-Jun NH2-terminal kinase; LRP, LDL receptor-related protein; MAPK, mitogen-activated protein kinase; MEK1/2, mitogen-activated protein kinase kinases 1/2; NF-kB, nuclear factor-kappa B; NLRP, nucleotide binding domain like receptor family pyrrole domain containing protein; NO, Nitric oxide; P38, P38 mitogen-activated protein kinase; PI3K, phosphoinositide 3-kinase; PIP3, phosphatidylinositol 3,4,5-trisphosphate; PKC, protein kinase C; PTEN, phosphatase and tensin homolog; RhoA, Ras homolog family member A; TRL-4, Toll-like receptor 4.

of lectin-like receptor for oxidized LDL (LOX-1) receptor and NF-κB-dependent nuclear transcription (Park et al., 2005). Furthermore, JNK and activating transcription factor 3 (ATF3) are involved in TGRL lipolysis products-induced vascular inflammation via upregulating the levels of IL-8 and E-selectin (Aung et al., 2013). Postprandial TGRL also stimulate inflammation via interferon regulatory factor-1, especially under shear stress in cultured endothelium (Sherrod DeVerse, et al., 2013). Oxylipids in TGRLs are found to promote endothelial inflammation following a high fat meal (Rajamani et al., 2019). Of importance, TGRL hydrolysis and the accumulation of intracellular TGs and free FAs, especially oxidized free FAs, play key roles in TGRL-mediated inflammation. Reductions in susceptibility of VLDL to LPL can attenuate the above inflammatory reactions (Saraswathi and Hasty, 2006; Jinno et al., 2011; Castillo-Núñez et al., 2022). FAs are transported into cells passively or actively by transporters including plasma membrane fatty acid-binding protein, fatty acid transport proteins, and cluster of differentiation 36 (Mallick and Duttaroy, 2022). Neutral and oxidized free FAs released during TGRL hydrolysis are found to induce endothelial inflammation and vascular apoptosis (Wang et al., 2009). The relationship between free FAs and inflammation has been reviewed recently by distinct groups (Mallick and Duttaroy, 2022; Panda et al., 2022; Ren et al., 2022). Some presently known inflammatory signaling pathways that are modulated by TGRL, TGRL remnants, and free FAs are summarized in **Figure 3**.

TGRLs Induce Oxidative Stress and Endothelial Cell Dysfunction

Oxidative stress plays an important role in the progression of atherosclerosis by interacting with inflammation, foam cell formation, and endothelial dysfunction. TGRL remnant cholesterol stimulates NAD(P)H oxidase–dependent superoxide formation and cytokine secretion in human umbilical vein endothelial cells by activation of LOX-1, leading to reduction in cell viability (Shin et al., 2004). Furthermore, TGRL remnant cholesterol upregulates endothelial expression of ICAM-1, VCAM-1, and tissue factor through a redox-sensitive mechanism, thus affecting the progression of atherosclerosis (Doi et al., 2000). CMRs also cause rapid and prolonged generation of ROS in monocytes, thereby influencing monocyte activation and

migration (Bentley et al., 2011). Exposure of J774 macrophages to a pro-oxidizing state further promotes CMR-induced accumulation of intracellular lipids (Napolitano et al., 2001).

Endothelial dysfunction is one of the early pathological mechanisms of atherosclerosis. Free FAs released during lipolysis of TGRL can activate NADPH oxidase- and cytochrome P450-mediated ROS production within endothelial cells, causing oxidative stress and dysfunction of endothelial barrier (Wang et al., 2009). The mechanisms of action of FAs on modulation of endothelium function have been reviewed recently by Mallick and Duttaroy (2022). Furthermore, high levels of TGRL remnant cholesterol and TG have a strong correlation with endothelial vasomotor dysfunction. These TGRL remnants increase the susceptibility of coronary endothelium to oxidative stress, leading to inhibition of nitric oxide-mediated vascular dilation (Nakamura et al., 2005). Of note, postprandial elevated TGRL remnant cholesterol is associated with atherosclerotic progression even in normolipidemic subjects by affecting endothelial dysfunction, such as endothelium-dependent vasorelaxation (Inoue et al., 1998; Funada et al., 2002). TGRL lipolysis induces ROS production and alterations of lipid raft in morphology and protein components, such as LRP, nitric oxide synthase, and caveolin-1, leading to endothelial dysfunction (Wang et al., 2008). Furthermore, TGRL and their lipolytic products activate platelet aggregation and clot formation by suppressing fibrinolysis and promoting the assembly of prothombinase complex, the expression of plasminogen activator inhibitor-1 and its antigen, and the endothelial expression of tissue factor (Gianturco and Bradley, 1999; Toth, 2016; Reiner, 2017). Furthermore, TGs are found to increase the risk of atherosclerosis by increasing plasma viscosity, leading to impaired microcirculatory flow and enhanced interactions between atherogenic lipoproteins and endothelium (Rosenson et al., 2001).

TGRLs Promote Foam Cell Formation

Lipid accumulation in the subcutaneous space of endothelium is a key characteristic of atherosclerosis (Lin et al., 2021). Reductions in plasma TG levels are associated with reduced all-cause mortality in CVD patients potentially due to the low cholesterol content in TGRL and TGRL remnant particles. Indeed, TGRL remnant cholesterol is an independent risk factor for menopausal women with CHD (Feng X. et al., 2020). Another study indicates that the cholesterol levels of TGRL are a residual risk of future CVDs in patients with stable CHD and even in those with LDL-C < 70 mg/dl after statin therapy (Fujihara et al., 2019). Of note, the elevated postprandial VLDL residues are the main cause of the occurrence and development of atherosclerosis (Nakajima and Tanaka, 2018b). Furthermore, the reduced TGRL removal efficacy maybe a causal factor of the increased atherosclerosis in elderly people (Maranhão et al., 2020).

TGRLs carry approximately 25% of the TC carried by non-HDL particles. Due to the big size, the cholesterol content carried by each TGRL particle is approximately 5–20 times higher than that carried by each LDL particle (Toth, 2016; Ginsberg et al., 2021). Except for CM particles, TGRL and TGRL remnant particles, can penetrate blood vessel and be recognized and directly ingested by macrophages through the ligand apoE located at the surface of TGRL (Ohmura, 2019; Ginsberg et al., 2021). As is known, only modified LDL (such as oxidation) particles are ingested by macrophages. TGRLs are the only natural, unmodified lipoproteins that can cause rapid lipid accumulation in macrophages as revealed *in vitro* (Gianturco and Bradley, 1999; Peng and Wu, 2022). First, TGRLs are trapped in artery walls through the interaction between positively charged residues on apoB with negatively charged groups of proteoglycans located at the endothelium lining (Sandesara et al., 2019). In the subcutaneous space, TGRL particles are internalized by macrophages and smooth muscle cells, contributing to plaque formation and development (Padro et al., 2021). Therefore, TGRL is more pathogenic than LDL in causing atherosclerosis.

Indeed, both apoB48 and apoB100 are found in human aortic atherosclerotic plaques, indicating that TGRLs are involved in the formation of atherosclerotic plaque (Nakano et al., 2008; Behbodikhah et al., 2021). Furthermore, the majority of apoB proteins isolated from human atherosclerotic plaques are derived from VLDL and IDL, but not LDL, suggesting that VLDL and IDL play a key atherosclerotic role in the intima of the arteries (Rapp et al., 1994; Proctor and Mamo, 1998; Castillo-Núñez et al., 2022). Furthermore, a proportion of arterial plaque cholesterol is derived from VLDL and its residue IDL in patients with mild-to-moderate HTG (Gill et al., 2021). Of note, plasma VLDL cholesterol (VLDL-C) is an increased risk factor for major adverse CVD events, independent of the established risk factors such as LDL-C (Heidemann et al., 2021). It seems that the remnant cholesterol, but not TG, in TGRL particles is a causal factor of atherosclerosis (Jørgensen et al., 2013; Varbo and Nordestgaard, 2016; Dron and Hegele, 2020). However, TGs in TGRL particles assist the ingestion process of the cells, such as macrophages, involved in plaque foam cell formation. Unlike VLDL particles isolated from people with normal TG levels, VLDL particles obtained from patients with HTG have a high affinity for scavenger receptors, such as LDLR and VLDLR, that are specifically expressed by monocytes, macrophages, and endothelial cells (Gianturco et al., 1982; Takahashi, 2017).

CMRs also contribute to lipid accumulation in the atherosclerotic plaques. Unlike LDL particles, CMRs carrying dietary lipids induce the formation of foam cells without the oxidation process in circulation, and the uptake of CMRs by macrophages can induce intracellular accumulation of both TG and cholesterol. The rate of uptake and lipid accumulation is affected by the type of dietary fat in the granules (Botham et al., 2007; Morita, 2016). In the absence of LDLR or its ligand apoE, CMRs still contribute to lipid accumulation during atherosclerotic plaque formation (Fujioka et al., 1998; Bravo and Napolitano, 2007). For instance, apoB48 receptor is involved in CMR uptake and foam cell formation independent of the apoE-mediated pathway. Of note, apoB48 receptor can be used for further uptake of TGRL particles even when macrophages are accumulated with a large amount of lipids (Kawakami et al., 2005; Bermudez et al., 2012). In

macrophages, CMR internalization results in rapid accumulation of cholesterol in lysosomes and cell death due to lysosomal instability, thereby promoting atherosclerosis deterioration (Wakita et al., 2015). Additionally, TG contained in TGRL particles can activate CETP, which promotes the exchange of core lipids between major lipoproteins, promoting the accumulation of residual cholesterol in TGRL remnants, thereby aggravating atherosclerosis (Brinton, 2015). For instance, CETP mediates the exchange of TG in TGRL with cholesterol in LDL, thereby promoting the production of small, dense LDL particles that are more atherosclerotic than LDL particles (Gianturco et al., 1982; Merkel, 2009). Similarly, TGRL promotes HDL remodeling and the formation of smaller, low-cholesterol HDL particles that are lack of atherosclerotic protection (Feng M. et al., 2020).

STRATEGIES FOR TREATMENT OF HYPERTRIGLYCERIDEMIA

Except for statins, clinical drugs that can be used to treat HTG are fibrates, niacin, and omega-3 fatty acids (Preston Mason, 2019). Several previous reviews have summarized the effects of these clinically used drugs for TG-lowering (Sando and Knight, 2015; Simons, 2018; Feingold, 2021). Furthermore, our team demonstrated that exogenous supplement of N-acetylneuraminic acid can reduce TG by more than 60% in apoE$^{(-/-)}$ mice (Guo et al., 2016; Hou et al., 2019). Here, we make a short review about these clinically used drugs, and then focus on some targets with potential applications for TG-lowering.

Clinical Drugs

Statins

Statins are the standard therapy for many types of dyslipidemias because they can effectively decrease the endogenous biosynthesis of cholesterol via inhibiting 3-hydroxy-3-methyl glutaryl coenzyme A reductase and enhance the hepatic uptake of LDL particles by up-regulating LDLR through SREBP-2. In individuals with normal TG levels, statins have little effects on plasma VLDL. However, statins decrease VLDL and CM and their remnants via improving hepatic clearance in patients with HTG (Caslake and Packard, 2004). A previous study demonstrates that statin treatment decreases not only fasting TG but also postprandial TGs (Mora-Rodriguez et al., 2020). However, a survey in United State adults (9593 participants) indicates that the prevalence of TG < 150, 150–199, and ≥200 mg/dl is 75.3%, 12.8%, and 11.9% in adults without statin treatment; among statin users, the ratios are 68.4%, 16.2%, and 15.4%, respectively. Furthermore, the estimated mean 10-years ASCVD risk from TG < 150 to ≥500 mg/dl, ranges from 11.3% to 19.1% in statin users and 6.0%–15.6% in nonusers. These data suggest that statin treatment moderately elevates TG levels as well as ASCVD risk in patients with TG > 150 mg/dl (Fan et al., 2019). Another meta-analysis of randomized-controlled trials demonstrates that statins only reduce plasma TG by 8.4% in children and adolescents with familial hypercholesterolaemia (Anagnostis et al., 2020). Patients with increased CVD risk generally display high levels of plasma TGs and low levels of HDL-C, even after statin therapy (Larsson et al., 2014). Of importance, statin-treated patients with TG levels ≥ 150 mg/dl have even worse CVD risk than those with TG < 150 mg/dl (Toth et al., 2019a; Toth et al., 2019b). Collectively, statins show limited effects on TG-lowering in patients with dyslipidemia.

Fibrates

Mechanistically, fibrates exert their bioactivity primarily by activating PPARα (Chapman et al., 2010). Fibrate treatment reduces plasma TG levels by approximately 20%–70% (Katsiki et al., 2013; Wang et al., 2015). Compared with placebo, gemfibrozil (1.2 g/d) reduces TG level by 31% and increases HDL-C by 6% along with a reduction in the risk of CVD events by 4.4% in CHD patients (Rubins et al., 1999). Oral bezafibrate treatment (400 mg/d, twice) leads to a significant reduction in serum TG level (42.7%) as well as increases in HDL2-C, HDL3-C, and plasma content and activity of LPL. Bezafibrate may increase HDL3-C and HDL2-C by promoting TGRL catabolism and the conversion of HDL3 to HDL2, respectively (Sakuma et al., 2003). Fenofibrate or fenofibric acid can significantly reduce TG level in combination with statin (Huang et al., 2009; Ouwens et al., 2015). A meta-analysis demonstrates that fibrate reduces TG level by 46.5% in combination with statin. However, this combination increases risk of side effects (Choi et al., 2014). Pemafibrate (k-877), a selective PPARα modulator, is found to be superior to fenofibrate (106.6 mg/d) in TG lowering in patients with high TG (≥1.7 mmol/L and <5.7 mmol/L) and relatively low HDL-C levels at the dosage of 0.2–0.4 mg/d (Ishibashi et al., 2018). However, a meta-analysis suggests that pemafibrate reduces plasma TG levels and increases HDL-C similar as that of fenofibrate (Ida et al., 2019). In a multicenter, randomized, double-blind, phase IV study, fenofibrate significantly decreases TG levels from 269.8 to 145.5 mg/dl as an add-on-statin therapy, while statin monotherapy has no effect on TG levels (Park et al., 2021). A recent retrospective longitudinal study indicates that pemafibrate significantly reduces plasma TG by 43.8% and increases HDL-C by 10.8% in patients with dyslipidemia after 3 months treatment. Furthermore, this molecule improves liver function and serum levels of uric acid and hemoglobin A1c (Yanai et al., 2022).

Niacin

Niacin (nicotinic acid) decreases TG levels by up to 30%, and reduces LDL-C and lipoprotein (α)) levels to the greatest extent by 15% and 30%, respectively (Chapman et al., 2010). It inhibits the lipolysis of adipose tissue and reduces the flow of free FAs to the liver, leading to a reduction in hepatic synthesis of VLDL (Khetarpal et al., 2016). This molecule can successfully reduce TGs in patients with familial CM syndrome potentially by reducing the production of apoB48 and CM (Pang et al., 2016). Furthermore, niacin mimics the role of the physiological ligand β-hydroxybutyrate by interacting with the type 3 hydroxycarboxylic acid receptor (Chaudhry et al., 2018). In a clinical follow-up study, niacin treatment decreases TG level from 164 mg/dl to 122 mg/dl, reduces LDL-C from 74 mg/dl to

62 mg/dl, and increases HDL-C level from 35 mg/dl to 42 mg/dl. However, there is no incremental clinical benefit from the addition of niacin (1.5–2 g/d) to statin treatment (40–80 mg/d) during the 3 years of follow-up period in patients with ASCVD (Boden et al., 2011). A large randomized trial demonstrates that although the extended-release niacin treatment reduces TG levels by 33 mg/dl on average compared with placebo, the addition of niacin to statin therapy has no effect on reducing the risk of major vascular events. On the contrary, niacin is found to increase the risk of myopathy, especially in patient after simvastatin treatment (HPS2-THRIVE Collaborative Group, 2013). Therefore, the use of niacin in clinical practice is limited due to its useless for reducing CVD events and the high incidence of adverse reactions.

Omega-3 Fatty Acid

The beneficial roles and metabolism of PUFA have been recently review by several groups (Chen et al., 2022; Mallick and Duttaroy, 2022; Ren et al., 2022). Omega 3 FAs belong to the family of PUFA and play an important role in the formation and stability of cell membranes as well as cell physiology (Ganda et al., 2018). Omega-3 FAs, such as eicosapentaenoic acid (EPA) and docosahexaenoic acid (DHA), can reduce TG levels, improve blood vessel function, and suppress inflammation, platelet aggregation, liver steatosis, and insulin resistance (Mozaffarian and Wu, 2011; Shahidi and Ambigaipalan, 2018). A previous review indicates that DHA and EPA treatment is associated with a net decrease in TG by 22.4% and 15.6%, respectively. Furthermore, DHA supplement is associated with more significant increases in LDL-C and HDL-C compared to that of EPA (Jacobson et al., 2012; Kotwal et al., 2012). These Omega 3 FAs affect lipid raft organization by disrupting acyl chain packing and molecular order within lipid rafts, thereby modulating protein lateral distribution and signaling (Shaikh, 2012). Of note, EPA and DHA have different effects on membrane bilayer width, membrane fluidity, and cholesterol crystalline domain formation, suggesting omegar-3 FAs with different structural characteristics may show distinct effects (Preston Mason et al., 2016). The TG-lowering mechanisms of action of these compounds are associated with increased FA degradation through peroxisome β-oxidation, reduced hepatic fat production, and enhanced TG clearance in circulation (Harris et al., 2008).

In a 12-weeks clinical trial, the EPA ethyl ester, AMR101, reduces TG level by 10.1% and 21.5% at the dosage of 2 and 4 g/d, respectively, in high-risk statin-treated patients with residually high TG (>200 and <500 mg/dl) (Ballantyne et al., 2012). In patients with fasting TG levels of 1.52–5.63 mmol/L and LDL-C levels of 1.06–2.59 mmol/L, 2 g/d of EPA ethyl (twice daily) significantly reduces the relative risk of ischemic events by 25% compared with the placebo group (Bhatt et al., 2019). Of note, EPA (1.8 g/d) combined with pitavastatin (4 mg/d) is found to reduce coronary plaque volume and reinforce plaque stabilization compared to pitavastatin monotherapy (Watanabe et al., 2017). Another study in Japan demonstrates that EPA (1.8 g/d) reduces CVD events by 19% in patients receiving statin therapy and decreases CVD events by 53% in patients with TG ≥ 150 mg/dl and HDL-C < 40 mg/dl, suggesting EPA is more effective in patient with abnormal TG and HDL-C levels (Saito et al., 2008). Icosapent ethyl is recommended for treatment of ASCVD patients with fasting TG between 139 and 499 mg/dl in combination with statin therapy (Orringer et al., 2019). However, omega-3 FA supplementation has no protective effects in patients with diabetes without evidence of CVD (Bowman et al., 2018). A meta-analysis involving 77917 high-risk individuals suggests that omegar-3 FAs have no significant association with fatal and nonfatal CHD or any major vascular events (Aung et al., 2018). Epanova, a mix of omega-3 free FAs, lowers plasma TG level by up to 31%. In 2018, the STRENGTH study was designed to check whether 4 g/day of epanova can reduce the incidence of CVD events in patients with HTG and low levels of HDL-C (Nicholls et al., 2018). This STRENGTH study terminated on 8 January 2020 demonstrates that there is no significant difference between omega-3 FA treatment and corn oil intervention (Nicholls et al., 2020; Nissen et al., 2021; Reyes-Soffer, 2021). Therefore, omega-3 FAs mix may also have limited application in clinical therapy for HTG.

EMERGING TARGETS FOR LOWERING TRIGLYCERIDE

Mendelian randomization and genetic studies provide evidence of potential therapeutic targets for reducing TG and the risk of ASCVD. These potential targets include LPL and LPL-related proteins, such as apoCIII, apoCII, apoAV, ANGPTL4, and GPIHBP1, which cause alterations in TG levels and are related to the development of ASCVD. For instance, in a systematic review and meta-analysis, apoCIII is found to cause HTG and atherosclerosis (Wyler von Ballmoos et al., 2015; Rocha et al., 2017). The proatherosclerotic effects of GPIHBP1 deficiency are probably caused by the markedly elevated levels of CM/VLDL, which exacerbate atherosclerosis through increasing the formation of TGRL remnants and generation of proatherogenic lipid products (Vallerie and Bornfeldt, 2015). Furthermore, accumulating evidence have demonstrated that gut microbiota is also associated with TG metabolism.

Targeting LPL

LPL maintains TG homeostasis in blood and is the rate-limiting enzyme for the hydrolysis of TGs that are encapsulated in the core of TGRL particles (Wang and Eckel, 2009; Tada et al., 2018; Kumari et al., 2021). It has been reported that gain-of-function and loss-of-function gene mutations of LPL lead to the imbalance of plasma TG levels, thereby influencing CVD events (Rip et al., 2006; Wang and Eckel, 2009; Burnett et al., 2019). LPL S447X is a naturally occurring gain-of-function mutation (Rip et al., 2006). In 2012, alipogene tiparvovec (AAV1-LPL^{S447X}) was approved in Europe for treatment of severe HTG and recurrent pancreatitis in patients with complete loss-of-function of LPL. This highly active recombinant LPL with S447X variant reduces the fasting TG level by >40% in half of the patients between 3 and 12 weeks (Gaudet et al., 2013). Furthermore, several interesting compounds are found to increase the activity of LPL. Among these agonists, 50F10 is found to stabilize LPL *in vitro* and successfully reduce

postprandial HTG in apoAV$^{(-/-)}$ mice (Larsson et al., 2014). The agonist NO-1886 (ibrolipim) mainly increases the mRNA level of LPL, while the compound C10d primarily affects the hydrolysis activity of LPL (Larsson et al., 2014). Although a long-term administration of NO-1886 significantly inhibits the development of coronary atherosclerosis, this compound shows severe side effects. Except for lowering TG, the agonist C10d lowers TC, body fat, and fatty liver, suggesting its potential application in HTG treatment (Geldenhuys et al., 2017).

Targeting ApoCIII

ApoCIII is synthesized in the liver and intestine, and it is distributed in TGRL and HDL particles (Borén et al., 2020). This apolipoprotein is previously demonstrated to be an effective inhibitor of LPL (Christopoulou et al., 2019). However, several studies have shown that apoCIII has pleiotropic effects in regulating the metabolism of TGRL without affecting LPL (Gordts et al., 2016; Kovrov et al., 2022). ApoCIII mainly suppresses the hepatic clearance of TGRLs and their remnants through LDLR and LRP-1, thereby inducing HTG (Gordts et al., 2016; Christopoulou et al., 2019; Kegulian et al., 2019; Reyes-Soffer and Ginsberg, 2019). People with apoCIII loss-of-function mutations are associated with approximately 40% reductions in plasma TG and the risk of CVD (Pollin et al., 2008; Crosby et al., 2014; Jørgensen et al., 2014). Therefore, apoCIII is a therapeutic target for patients with severe HTG. Volanesorsen is an antisense oligonucleotide targeting apoCIII mRNA, and it is developed for treatment of familial CM syndrome (FCS), HTG, and familial partial lipodystrophy (Gouni-Berthold, 2017; Paik and Duggan, 2019). Based on the beneficial effects observed in the phase III study, volanesorsen was approved in the European Union for treatment of adult FCS patients in May 2019 (Hegele et al., 2018; Corbin et al., 2020; Gouni-Berthold et al., 2021; Lazarte and Hegele, 2021). The average TG level in FCS patients decreases by 77% after treatment using volanesorsen (300 mg) once a week for 3 months (Witztum et al., 2019). Subcutaneous injection of volanesorsen (300 mg) once a week for 3 months reduces the average TG level by 71.2% in patients that have applied conventional TG-lowering therapy but have a fasting TG > 500 mg/dl (Gouni-Berthold et al., 2021). However, this compound may cause side effects such as thrombocytopenia (Witztum et al., 2019).

Targeting ApoCII

ApoCII is a key cofactor for activation of LPL. A complete deficiency of apoCII causes the same phenotype, severe HTG, as LPL deficiency (Hegele et al., 2020). The apoCII mimetic peptide (C-II-a, 30 mg/kg) is found to reduce plasma TG level by 85% in apoE$^{(-/-)}$ mice (Amar et al., 2015). Intravenous injection of this short peptide (0.2–5 μmol/L) reverses HTG in apoCII$^{(-/-)}$ mice in a dose-dependent manner (Sakurai et al., 2016). C-II-a peptide is found to promote plasma clearance of TG-rich lipid emulsions and improve the following incorporation of FAs from these TG emulsions into specific peripheral tissues (Komatsu et al., 2019). However, this mimic peptide only acutely activates LPL due to its short half-life (1.33 h) (Sakurai et al., 2016). Recent studies have shown that apoCII mimic peptide D6PV is a novel compound for the treatment of HTG and apoCII deficiency (Wolska et al., 2020a; Wolska et al., 2020b). In apoCII$^{(-/-)}$ mice and human apoCIII-transgenic mice, this peptide consisted of 40-amino acid causes a rapid decrease in plasma TG and apoB by approximately 80% and 65%, respectively. Furthermore, it also works independent of LPL (Wolska et al., 2020a). Of importance, D6PV displays good TG-lowering bioactivity in nonhuman primates and shows an extended terminal half-life of 42–50 h (Wolska et al., 2020a). These data suggest that apoCII mimetic peptides have an attractive future for treatment of HTG.

Targeting ApoAV

Genetic association studies have established a clear link between apoAV variation and TG metabolism (Nilsson et al., 2011; Flores-Viveros et al., 2019). ApoAV variants affect not only TG concentration but also the distribution of lipoprotein subclasses, shifting them to atherogenic particles in high-risk subjects (Guardiola et al., 2015; Guardiola and Ribalta, 2017). A previous study demonstrates that three mutations including p.(Ser232_Leu235)del, p.Leu253Pro, and p.Asp332ValfsX4 are the direct cause of HTG by apoAV (Mendoza-Barberá et al., 2013). Furthermore, there is a significant association between c.56C > G (rs3135506) apoAV gene polymorphism and coronary artery disease in the Moroccan population (Morjane et al., 2020). Liver-derived apoAV facilitates LPL-mediated TG hydrolysis in circulation. Furthermore, apoAV is co-localized with perilipin through binding LRP-1, and it reduces intracellular TG concentration by suppressing adipogenesis-related factors in adipocytes (Su et al., 2020; Xu et al., 2020). ApoAV shows a protective effect against atherosclerosis in apoE2 gene knock-in and human apoAV transgenic mice via reducing TG and the residual particles rich in cholesterol esters, such as LDL and VLDL (Mansouri et al., 2008). Intravenous injection of wild-type apoAV reconstituted HDL significantly reduces TG by 60% in apoAV$^{(-/-)}$ mice, and this effect requires the functional GPIHBP1-LPL-apoAV axis (Shu et al., 2010). Furthermore, adenovirus overexpression of human apoAV reduces serum levels of TG and cholesterol in mice (Van der Vliet et al., 2002). However, apoAV is involved in fructose-induced metabolic dysregulation and is associated with hepatic steatosis. Furthermore, there is a significantly lower levels of hepatic TG in apoAV$^{(-/-)}$ mice compared with the control (Ress et al., 2020). Therefore, the working mechanisms of action of apoAV and the actual application for treatment of HTG by targeting apoAV need to be clarified in future.

Targeting ANGPTL

ANGPTL is a family of secreted glycoproteins consisting of eight members (ANGPTL1-8). These proteins, especially ANGPTL3, ANGPTL4, and ANGPTL8 are found to regulate the activity of LPL (Li et al., 2020; Kumari et al., 2021). In the following, we mainly describe several intensively studied ANGPTL members that have potential applications for treatment of HTG.

ANGPTL3

ANGPTL3 is a secreted protein mostly expressed in the liver. This protein increases the plasma levels of TG and LDL-C. However, loss-of-function variants in ANGPTL3 are associated with decreased plasma levels of TG, LDL-C, and HDL-C, as well as reduced ASCVD risk (Musunuru et al., 2012; Dewey et al., 2017). In mice, lack of ANGPTL3 reduces the plasma levels of TG, TC, and free FA, and increases the activity of LPL (Koishi et al., 2002; Fujimoto et al., 2006). In humans, evinacumab, an ANGPTL3 antibody, reduces fasting TG and LDL-C levels by approximately 76% and 23%, respectively, without affecting LDLR (Dewey et al., 2017). In an open-label study, 4 weeks evinacumab treatment reduces the plasma levels of TG, LDL-C, apoB, non-HDL-C, and HDL-C by 47%, 49%, 46%, 49%, and 36%, respectively, in patients with homozygous familial hypercholesterolemia (Gaudet et al., 2017). Evinacumab increases the fractional catabolic rate of IDL apoB and LDL apoB, suggesting this molecule may improve hepatic clearance of TGRL remnants (Reeskamp et al., 2021). The fully human monoclonal antibody (REGN1500) has a high affinity with ANGPTL3, and its effectiveness in reducing the plasma TG and LDL-C levels has been confirmed in monkeys and mice (Gusarova et al., 2015). Targeting ANGPTL3 mRNA by the antisense oligonucleotide, named as ANGPTL3-L_{Rx}, causes reductions in the levels of ANGPTL3 protein by 46.6%–84.5%, TG by 33.2%–63.1%, LDL-Cs by 1.3%–32.9%, VLDL-C by 27.9%–60.0%, non-HDL-C by10.0%–36.6%, apoB by 3.4%–25.7%, and apoCIII by18.9%–58.8% in mice (Graham et al., 2017). Gene editing through CRISPR-Cas9 technology has been established as a potential strategy for treatment of patients with atherosclerotic dyslipidemia. For instance, injection of BE3-ANGPTL3 causes reductions in TG, TC, and ANGPTL3 by 49%, 51%, and 19%, respectively, in $LDLR^{(-/-)}$ mice (Chadwick et al., 2018). Furthermore, a lipid nanoparticle delivery platform has recently been developed for targeted-delivery of CRISPR-Cas9-based genome editing of ANGPTL3. In this study, the reductions in ANGPTL3 mRNA and plasma TG level are stable for at least 100 days after a single administration (Qiu et al., 2021).

ANGPTL4

ANGPTL4 is mainly expressed in liver, adipose tissue, kidney, intestine, and heart. This protein plays an important role in lipid metabolism, especially in TG metabolism (Aryal et al., 2019). It mediates fasting-induced repression of LPL activity by promoting LPL unfolding, thereby enhancing degradation of LPL. However, this protein may show distinct bioactivity in distinct organs or cells. The biological functions of ANGPTL4 have been previously reviewed by Aryal et al. (2019) and Kersten (2021). ANGPTL4 derived from liver and adipose tissue primarily acts as an endocrine factor that regulates systemic lipid metabolism, while ANGPTL4 in macrophages reduces the formation of foam cells (Yang et al., 2020). Like ANGPTL3, loss-of-function mutations in ANGPTL4 are associated with low TG levels and reduced CVD risk (Dewey et al., 2016). ANGPTL4 monoclonal antibody (REGN1001) inhibits ANGPTL4 and reduces plasma levels of TG in mice and non-human primates (Dewey et al., 2016). Compared to wild-type mice, $ANGPTL4^{(-/-)}$ mice have lower levels of TG and TC due to the enhanced VLDL clearance and decreased VLDL production. Of note, the anti-ANGPTL4 monoclonal antibody, 14D12, is found to reduce TG by 50% in C57BL/6J mice. This antibody also reduces plasma levels of TG in $LDLR^{(-/-)}$, $apoE^{(-/-)}$, and db/db mice (Desai et al., 2007). Adipocyte-derived ANGPTL4 plays a key role in regulation of plasma TG in mice fed a regular chow diet, but this effect is diminished after a chronic high-fat diet feeding (Spitler et al., 2021). Of importance, clinical trials are needed for determining the actual effects of inhibiting ANGPTL4 on TG-lowering.

ANGPTL 8

ANGPTL8, also known as adipin/betatrophin, regulates LPL activity in the heart and skeletal muscle. This protein is also expressed in liver and adipose tissue (Zhang, 2016). Although ANGPTL8 has a functional LPL inhibitory motif, it only inhibits LPL and increases plasma TG levels in the presence of ANGPTL3 or possibly other ANGPTL family members in mice (Haller et al., 2017). Therefore, ANGPTL8 seems to increase plasma TG level by interacting with ANGPTL3. The fully human monoclonal antibody, REGN3776, can bind monkey and human ANGPTL8 with a high affinity, and reduces plasma TG by up-regulating LPL activity in humanized ANGPTL8 mice. In addition, blocking ANGPTL8 by this antibody reduces serum TG and increases serum HDL-C in cynomolgus monkeys with spontaneous HTG (Gusarova et al., 2017). An ANGPTL3-4-8 model has been provided for explaining the mechanisms of action of ANGPTLs in regulation of TG metabolism (Zhang, 2016). In brief, food intake induces the expression of ANGPTL8 in the liver and white adipose tissue. In the liver, ANGPTL8 activates ANGPTL3 and promotes the formation of ANGPTL3-8 complexes, which finally suppress the activity of LPL in circulation. In the white adipose tissue, ANGPTL8 promotes the formation of ANGPTL4-8 complexes, which enhance the activity of LPL locally. On the contrary, fasting inactivates the expression of ANGPTL8, thereby modulating LPL by an inverse way (Zhang and Zhang, 2022).

Other ANGPTLs

ANGPTL5 is primarily expressed in adipose tissue and heart. This protein is positively associated with obesity, type 2 diabetes, oxidized LDL, and especially glucose metabolism disorders, suggesting ANGPTL5 is involved in modulation of TG and glucose homeostasis (Alghanim et al., 2019; Hammad et al., 2020; Liu Y. Z et al., 2021). The plasma level of ANGPTL7 is also elevated in obese subjects and is positively associated with TG level, suggesting ANGPTL7 may be explored as a therapeutic target for modulating TG metabolism (Abu-Farha et al., 2017; Liu Y. Z et al., 2021). As reviewed previously, ANGPTL2 primarily derived from visceral fat is positively associated with inflammation and insulin resistance, while ANGPTL6 expressed in the liver is found to counteract obesity and insulin resistance by suppressing gluconeogenesis and enhancing energy expenditure (Kadomatsu et al., 2011). A recent study demonstrates that serum ANGPTL6 levels are a valuable predictor of metabolic syndrome (Namkung et al., 2019). Furthermore, ANGPTL6 is suggested to primarily maintain glucose homeostasis in response to hyperglycemia (Fan et al.,

2020). Among the 8 ANGPTL members, ANGPTL1 shows a limited correlation with TG metabolism (Carbone et al., 2018). Although ANGPTL5-7 are associated with TG metabolism, the underlying mechanisms of action of these three ANGPTLs are still far from clear.

Targeting Gut Microbiota

In recent years, the relationship between gut microbiota and lipid metabolism has been paid more and more attentions. Cotillard et al. point out that reductions of microbial abundance in obese patients are related to the elevated levels of serum TC and TG (Cotillard et al., 2013). Similarly, another study suggests that individuals with low microbial gene counts have higher TG levels than individuals with high microbial gene counts (Le Chatelier et al., 2013). Compared with healthy volunteers, the phylum *Bacteroides* is decreased and the order *Lactobacillus* is increased in patients with coronary artery disease (Emoto et al., 2016). In apoE$^{(-/-)}$ mice, the relative abundances of *Verrucomicrobia*, *Bacteroidaceae*, *Bacteroides*, and *Akkermansia* are positively correlated with serum levels of TC, TG, HDL-C, and LDL-C. In addition, the relative abundance of Ruminococcaceae is positively correlated with HDL-C level, and the abundance of Rikenellaceae is negatively correlated with TG and LDL-C levels (Liu et al., 2020a).

Probiotics are live bacteria that colonize the gastrointestinal tract and endow beneficial effects for health. Some probiotics alleviate fat by modulating gut microbiota-short chain FA-hormone axis (Yadav et al., 2013). Of note, supplementation of *Lactobacillus plantarum* FRT10 is found to reduce the body weight, fat weight, and hepatic TG via upregulating the mRNA expression of PPARα and carnitine palmitoyltransferase-1α and down-regulating the mRNA expression of SREBP-1 and TG synthase diacylglycerol acyltransferase 1 in the liver of mice fed a high-fat diet (Cai et al., 2020). Furthermore, *Lactobacillus plantarum* FRT10 intervention is found to increase the abundance of *Lactobacillus*, *Bifidobacterium*, and *Akkermansia*, which could improve the imbalance of gut flora caused by a high-fat diet (Cai et al., 2020). Liraglutide is a glucagon-like peptide-1 (GLP-1) analog. This molecule significantly reduces hepatic TG content, insulin resistance, and serum LDL-C in db/db mice. Mechanistically, liraglutide significantly increases the abundance of *Akkermansia*, *Romboutsia*, and *norank_f_Bacteroidales_S24-7_group*, and decreases the abundance of *Klebsiella*, *Anaerotruncus*, *Bacteroides*, *Lachnospiraceae_UCG-001*, *Lachnospiraceae_NK4A136_group*, *Ruminiclostridium*, and *Desulfovibrio* (Liu et al., 2020b). Furthermore, oligofructose promotes satiety and reduces plasma TG in rats fed a high-fat diet by up-regulating the level of GLP-1 in the gut (Cani et al., 2005). Another study demonstrates that oligofructose increases the abundance of *Bifidobacteria* and *lactobacilli* in the gut of obese rats (Bomhof et al., 2014). Some polysaccharides may also exert their TG-lowering effects by regulating the gut microbiota (Yin et al., 2021; Li et al., 2022).

FUTURE DIRECTIONS

Statins only provide 25%–40% reductions in CVD risk, and high TG levels are closely associated with residual CVD risk. Cholesterol carried by TGRLs and their remnants is a causal factor of ASCVD except for LDL-C. The structural characteristics of TGRLs and their remnants, such as lipid content, apolipoprotein components, particle size, and retention time in circulation, determine the burden of atherosclerosis (Aguilar Salinas and John Chapman, 2020; Packard et al., 2020; Duran and Pradhan, 2021). Although there are several available methods for quantification of TGRLs and their remnants, more specific methods are needed to accurately determine and quantify the subclasses of these particles that are derived from different metabolic pathways. The recently developed omics technologies may assist the clarification of the component of these particles. These data will clarify what kinds of TGRLs and their remnants primarily determine the progression of atherosclerosis. Furthermore, the underlying mechanisms of action of the recently identified therapeutic targets, such as ANGPTLs, on modulating TG metabolism and even their own metabolism or interactions between each other are still far from clear.

Of importance, the presently used clinical TG-lowering drugs, such as fibrate, omega-3 FAs, and niacin, show equivocal effects or even futile in reduction of CVD risk by monotherapy or in combination with statin. The reasons need to be clarified in future. Although several novel compounds exhibit good TG-lowering and/or even CVD protective effects in animal models and/or clinical trials, their actual functions need to be verified in practice. Furthermore, pill burden of the patients with dyslipidemia is another question need to be resolved (Bittner, 2019; Toth et al., 2019b). Last but not the least, lifestyle changes, including reductions in carbohydrate (such as glucose, sucrose, and starch) intake, alcohol intake, smoking, and body weight, are the main measures to control HTG.

AUTHOR CONTRIBUTIONS

B-HZ and FY performed reference collection and prepared the manuscript; Y-NQ and S-DG: Funding acquisition and editing.

FUNDING

This work was supported by the National Natural Science Foundation of China (82070469 and 81770463).

REFERENCES

Abu-Farha, M., Cherian, P., Al-Khairi, I., Madhu, D., Tiss, A., Warsam, S., et al. (2017). Plasma and Adipose Tissue Level of Angiopoietin-like 7 (ANGPTL7) Are Increased in Obesity and Reduced after Physical Exercise. *PLoS. One.* 12 (3), e0173024. doi:10.1371/journal.pone.0173024

Adiels, M., Matikainen, N., Westerbacka, J., Söderlund, S., Larsson, T., Olofsson, S.-O., et al. (2012). Postprandial Accumulation of Chylomicrons and Chylomicron Remnants Is Determined by the

Clearance Capacity. *Atherosclerosis* 222 (1), 222–228. doi:10.1016/j.atherosclerosis.2012.02.001

Alghanim, G., Qaddoumi, M. G., Alhasawi, N., Cherian, P., Al-Khairi, I., Nizam, R., et al. (2019). Higher Levels of ANGPTL5 in the Circulation of Subjects with Obesity and Type 2 Diabetes Are Associated with Insulin Resistance. *Front. Endocrinol.* 10, 495. doi:10.3389/fendo.2019.00495

Alves-Bezerra, M., and Cohen, D. E. (2017). Triglyceride Metabolism in the Liver. *Compr. Physiol.* 8 (1), 1–22. doi:10.1002/cphy.c170012

Amar, M. J. A., Sakurai, T., Sakurai-Ikuta, A., Sviridov, D., Freeman, L., Ahsan, L., et al. (2015). A Novel Apolipoprotein C-II Mimetic Peptide that Activates Lipoprotein Lipase and Decreases Serum Triglycerides in Apolipoprotein E-Knockout Mice. *J. Pharmacol. Exp. Ther.* 352 (2), 227–235. doi:10.1124/jpet.114.220418

Anagnostis, P., Vaitsi, K., Kleitsioti, P., Mantsiou, C., Pavlogiannis, K., Athyros, V. G., et al. (2020). Efficacy and Safety of Statin Use in Children and Adolescents with Familial Hypercholesterolaemia: a Systematic Review and Meta-Analysis of Randomized-Controlled Trials. *Endocrine* 69 (2), 249–261. doi:10.1007/s12020-020-02302-8

Aryal, B., Price, N. L., Suarez, Y., and Fernández-Hernando, C. (2019). ANGPTL4 in Metabolic and Cardiovascular Disease. *Trends Mol. Med.* 25 (8), 723–734. doi:10.1016/j.molmed.2019.05.010

Aung, H. H., Lame, M. W., Gohil, K., An, C.-I., Wilson, D. W., and Rutledge, J. C. (2013). Induction of ATF3 Gene Network by Triglyceride-Rich Lipoprotein Lipolysis Products Increases Vascular Apoptosis and Inflammation. *Atvb* 33 (9), 2088–2096. doi:10.1161/ATVBAHA.113.301375

Aung, T., Halsey, J., Kromhout, D., Gerstein, H. C., Marchioli, R., Tavazzi, L., et al. (2018). Associations of Omega-3 Fatty Acid Supplement Use with Cardiovascular Disease Risks. *JAMA Cardiol.* 3 (3), 225–234. doi:10.1001/jamacardio.2017.5205

Ballantyne, C. M., Bays, H. E., Kastelein, J. J., Stein, E., Isaacsohn, J. L., Braeckman, R. A., et al. (2012). Efficacy and Safety of Eicosapentaenoic Acid Ethyl Ester (AMR101) Therapy in Statin-Treated Patients with Persistent High Triglycerides (From the ANCHOR Study). *Am. J. Cardiol.* 110 (7), 984–992. doi:10.1016/j.amjcard.2012.05.031

Bansal, S., Buring, J. E., Rifai, N., Mora, S., Sacks, F. M., and Ridker, P. M. (2007). Fasting Compared with Nonfasting Triglycerides and Risk of Cardiovascular Events in Women. *JAMA* 298 (3), 309–316. doi:10.1001/jama.298.3.309

Barter, P., and Genest, J. (2019). HDL Cholesterol and ASCVD Risk Stratification: A Debate. *Atherosclerosis* 283, 7–12. doi:10.1016/j.atherosclerosis.2019.01.001

Basu, D., and Goldberg, I. J. (2020). Regulation of Lipoprotein Lipase-Mediated Lipolysis of Triglycerides. *Curr. Opin. Lipidol.* 31 (3), 154–160. doi:10.1097/MOL.0000000000000676

Behbodikhah, J., Ahmed, S., Elyasi, A., Kasselman, L. J., De Leon, J., Glass, A. D., et al. (2021). Apolipoprotein B and Cardiovascular Disease: Biomarker and Potential Therapeutic Target. *Metabolites* 11 (10), 690. doi:10.3390/metabo11100690

Beigneux, A. P., Davies, B. S. J., Gin, P., Weinstein, M. M., Farber, E., Qiao, X., et al. (2007). Glycosylphosphatidylinositol-anchored High-Density Lipoprotein-Binding Protein 1 Plays a Critical Role in the Lipolytic Processing of Chylomicrons. *Cell Metab.* 5 (4), 279–291. doi:10.1016/j.cmet.2007.02.002

Bentley, C., Hathaway, N., Widdows, J., Bejta, F., De Pascale, C., Avella, M., et al. (2011). Influence of Chylomicron Remnants on Human Monocyte Activation *In Vitro*. *Nutr. Metabolism Cardiovasc. Dis.* 21 (11), 871–878. doi:10.1016/j.numecd.2010.02.019

Bermudez, B., Lopez, S., Varela, L. M., Ortega, A., Pacheco, Y. M., Moreda, W., et al. (2012). Triglyceride-rich Lipoprotein Regulates APOB48 Receptor Gene Expression in Human THP-1 Monocytes and Macrophages. *J. Nutr.* 142 (2), 227–232. doi:10.3945/jn.111.149963

Bhatt, D. L., Steg, P. G., Miller, M., Brinton, E. A., Jacobson, T. A., Ketchum, S. B., et al. (2019). Cardiovascular Risk Reduction with Icosapent Ethyl for Hypertriglyceridemia. *N. Engl. J. Med.* 380 (1), 11–22. doi:10.1056/NEJMoa1812792

Bittner, V. (2019). Implications for REDUCE IT in Clinical Practice. *Prog. Cardiovasc. Dis.* 62 (5), 395–400. doi:10.1016/j.pcad.2019.11.003

Black, D. D. (2007). Development and Physiological Regulation of Intestinal Lipid Absorption. I. Development of Intestinal Lipid Absorption: Cellular Events in Chylomicron Assembly and Secretion. *Am. J. Physiology-Gastrointestinal Liver Physiology* 293 (3), G519–G524. doi:10.1152/ajpgi.00189.2007

Bleda, S., de Haro, J., and Acin, F. (2017). Nuclear Factor-Kappa B Role in NLRP1 Inflammasome Activation by Triglycerides and VLDL Cholesterol in Endothelial Cells. *Int. J. Cardiol.* 234, 104. doi:10.1016/j.ijcard.2016.12.161

Bleda, S., de Haro, J., Varela, C., Ferruelo, A., and Acin, F. (2016). Elevated Levels of Triglycerides and Vldl-Cholesterol Provoke Activation of Nlrp1 Inflammasome in Endothelial Cells. *Int. J. Cardiol.* 220, 52–55. doi:10.1016/j.ijcard.2016.06.193

Boden, W. E., Boden, W. E., Probstfield, J. L., Anderson, T., Chaitman, B. R., Desvignes-Nickens, P., et al. (2011). Niacin in Patients with Low HDL Cholesterol Levels Receiving Intensive Statin Therapy. *N. Engl. J. Med.* 365 (24), 2255–2267. doi:10.1056/NEJMoa1107579

Bomhof, M. R., Saha, D. C., Reid, D. T., Paul, H. A., and Reimer, R. A. (2014). Combined Effects of Oligofructose andBifidobacterium Animalison Gut Microbiota and Glycemia in Obese Rats. *Obesity* 22 (3), 763–771. doi:10.1002/oby.20632

Borén, J., Packard, C. J., and Taskinen, M.-R. (2020). The Roles of ApoC-III on the Metabolism of Triglyceride-Rich Lipoproteins in Humans. *Front. Endocrinol.* 11, 474. doi:10.3389/fendo.2020.00474

Botham, K. M., Moore, E. H., Pascale, C. D., and Bejta, F. (2007). The Induction of Macrophage Foam Cell Formation by Chylomicron Remnants. *Biochem. Soc. Trans.* 35 (Pt3), 454–458. doi:10.1042/BST0350454

Bowman, L., Mafham, M., Wallendszus, K., Stevens, W., Buck, G., Barton, J., et al. (2018). Effects of N−3 Fatty Acid Supplements in Diabetes Mellitus. *N. Engl. J. Med.* 379 (16), 1540–1550. doi:10.1056/NEJMoa1804989

Bravo, E., and Napolitano, M. (2007). Mechanisms Involved in Chylomicron Remnant Lipid Uptake by Macrophages. *Biochem. Soc. Trans.* 35 (Pt3), 459–463. doi:10.1042/BST0350459

Brinton, E. A. (2015). Management of Hypertriglyceridemia for Prevention of Atherosclerotic Cardiovascular Disease. *Cardiol. Clin.* 33 (2), 309–323. doi:10.1016/j.ccl.2015.02.007

Burnett, J. R., Hooper, A. J., and Hegele, R. A. (2019). Lipids and Cardiovascular Disease. *Pathology* 51 (2), 129–130. doi:10.1016/j.pathol.2018.12.001

Cai, H., Wen, Z., Li, X., Meng, K., and Yang, P. (2020). Lactobacillus Plantarum FRT10 Alleviated High-Fat Diet-Induced Obesity in Mice through Regulating the PPARα Signal Pathway and Gut Microbiota. *Appl. Microbiol. Biotechnol.* 104 (13), 5959–5972. doi:10.1007/s00253-020-10620-0

Cani, P. D., Neyrinck, A. M., Maton, N., and Delzenne, N. M. (2005). Oligofructose Promotes Satiety in Rats Fed a High-Fat Diet: Involvement of Glucagon-like Peptide-1. *Obes. Res.* 13 (6), 1000–1007. doi:10.1038/oby.2005.117

Carbone, C., Piro, G., Merz, V., Simionato, F., Santoro, R., Zecchetto, C., et al. (2018). Angiopoietin-like Proteins in Angiogenesis, Inflammation and Cancer. *Ijms* 19 (2), 431. doi:10.3390/ijms19020431

Caslake, M. J., and Packard, C. J. (2004). Phenotypes, Genotypes and Response to Statin Therapy. *Curr. Opin. Lipidol.* 15, 387–392. doi:10.1097/01.mol.0000137225.46654.4d

Castillo-Núñez, Y., Morales-Villegas, E., and Aguilar-Salinas, C. A. (2022). Triglyceride-rich Lipoproteins: Their Role in Atherosclerosis. *Ric* 74 (2), 61–70. doi:10.24875/RIC.21000416

Castoldi, A., Monteiro, L. B., van Teijlingen Bakker, N., Sanin, D. E., Rana, N., Corrado, M., et al. (2020). Triacylglycerol Synthesis Enhances Macrophage Inflammatory Function. *Nat. Commun.* 11 (1), 4107. doi:10.1038/s41467-020-17881-3

Catapano, A. L., Graham, I., De Backer, G., Wiklund, O., Chapman, M. J., Drexel, H., et al. (2016). 2016 ESC/EAS Guidelines for the Management of Dyslipidaemias. *Eur. Heart J.* 37 (39), 2999–3058. doi:10.1093/eurheartj/ehw272

Chadwick, A. C., Evitt, N. H., Lv, W., and Musunuru, K. (2018). Reduced Blood Lipid Levels with *In Vivo* CRISPR-Cas9 Base Editing of ANGPTL3. *Circulation* 137 (9), 975–977. doi:10.1161/CIRCULATIONAHA.117.031335

Chapman, M. J., Redfern, J. S., McGovern, M. E., and Giral, P. (2010). Niacin and Fibrates in Atherogenic Dyslipidemia: Pharmacotherapy to Reduce Cardiovascular Risk. *Pharmacol. Ther.* 126 (3), 314–345. doi:10.1016/j.pharmthera.2010.01.008

Chaudhry, R., Viljoen, A., and Wierzbicki, A. S. (2018). Pharmacological Treatment Options for Severe Hypertriglyceridemia and Familial Chylomicronemia Syndrome. *Expert Rev. Clin. Pharmacol.* 11 (6), 589–598. doi:10.1080/17512433.2018.1480368

Chen, J., Jayachandran, M., Bai, W., and Xu, B. (2022). A Critical Review on the Health Benefits of Fish Consumption and its Bioactive Constituents. *Food Chem.* 369, 130874. doi:10.1016/j.foodchem.2021.130874

Choi, H. D., Shin, W. G., Lee, J.-Y., and Kang, B. C. (2015). Safety and Efficacy of Fibrate-Statin Combination Therapy Compared to Fibrate Monotherapy in Patients with Dyslipidemia: A Meta-Analysis. *Vasc. Pharmacol.* 65-66, 23–30. doi:10.1016/j.vph.2014.11.002

Christopoulou, E., Tsimihodimos, V., Filippatos, T., and Elisaf, M. (2019). Apolipoprotein CIII and Diabetes. Is There a Link? *Diabetes. Metab. Res. Rev.* 35 (3), e3118. doi:10.1002/dmrr.3118

Civelek, M., Manduchi, E., Riley, R. J., Stoeckert, C. J., Jr, and Davies, P. F. (2009). Chronic Endoplasmic Reticulum Stress Activates Unfolded Protein Response in Arterial Endothelium in Regions of Susceptibility to Atherosclerosis. *Circulation Res.* 105 (5), 453–461. doi:10.1161/CIRCRESAHA.109.203711

Cohen, J. C., Boerwinkle, E., Mosley, T. H., Jr, and Hobbs, H. H. (2006). Sequence Variations inPCSK9,Low LDL, and Protection against Coronary Heart Disease. *N. Engl. J. Med.* 354 (12), 1264–1272. doi:10.1056/NEJMoa054013

Corbin, L. J., Hughes, D. A., Chetwynd, A. J., Taylor, A. E., Southam, A. D., Jankevics, A., et al. (2020). Metabolic Characterisation of Disturbances in the APOC3/triglyceride-Rich Lipoprotein Pathway through Sample-Based Recall by Genotype. *Metabolomics* 16 (6), 69. doi:10.1007/s11306-020-01689-9

Cotillard, A., Kennedy, S. P., Kong, L. C., Prifti, E., Pons, N., Le Chatelier, E., et al. (2013). Dietary Intervention Impact on Gut Microbial Gene Richness. *Nature* 500 (7464), 585–588. doi:10.1038/nature12480

Crea, F. (2021). An Update on Triglyceride-Rich Lipoproteins and Their Remnants in Atherosclerotic Cardiovascular Disease. *Eur. Heart J.* 42 (47), 4777–4780. doi:10.1093/eurheartj/ehab844

Crosby, J., Peloso, G. M., Auer, P. L., Crosslin, D. R., Stitziel, N. O., Lange, L. A., et al. (2014). Loss-of-Function Mutations inAPOC3,Triglycerides, and Coronary Disease. *N. Engl. J. Med.* 371 (1), 22–31. doi:10.1056/NEJMoa1307095

Davies, B. S. J., Beigneux, A. P., Barnes, R. H., 2nd, Tu, Y., Gin, P., Weinstein, M. M., et al. (2010). GPIHBP1 Is Responsible for the Entry of Lipoprotein Lipase into Capillaries. *Cell Metab.* 12 (1), 42–52. doi:10.1016/j.cmet.2010.04.016

de Vries, M. A., Klop, B., Janssen, H. W., Njo, T. L., Westerman, E. M., and Castro Cabezas, M. (2014). Postprandial Inflammation: Targeting Glucose and Lipids. *Adv. Exp. Med. Biol.* 824, 161–170. doi:10.1007/978-3-319-07320-0_12

den Hartigh, L. J., Altman, R., Norman, J. E., and Rutledge, J. C. (2014). Postprandial VLDL Lipolysis Products Increase Monocyte Adhesion and Lipid Droplet Formation via Activation of ERK2 and NFκB. *Am. J. Physiology-Heart Circulatory Physiology* 306 (1), H109–H120. doi:10.1152/ajpheart.00137.2013

Desai, U., Lee, E.-C., Chung, K., Gao, C., Gay, J., Key, B., et al. (2007). Lipid-lowering Effects of Anti-angiopoietin-like 4 Antibody Recapitulate the Lipid Phenotype Found in Angiopoietin-like 4 Knockout Mice. *Proc. Natl. Acad. Sci. U.S.A.* 104 (28), 11766–11771. doi:10.1073/pnas.0705041104

DeVerse, J. S., Sandhu, A. S., Mendoza, N., Edwards, C. M., Sun, C., Simon, S. I., et al. (2013). Shear Stress Modulates VCAM-1 Expression in Response to TNF-α and Dietary Lipids via Interferon Regulatory Factor-1 in Cultured Endothelium. *Am. J. Physiology-Heart Circulatory Physiology* 305 (8), H1149–H1157. doi:10.1152/ajpheart.00311.2013

Dewey, F. E., Gusarova, V., Dunbar, R. L., O'Dushlaine, C., Schurmann, C., Gottesman, O., et al. (2017). Genetic and Pharmacologic Inactivation of ANGPTL3 and Cardiovascular Disease. *N. Engl. J. Med.* 377 (3), 211–221. doi:10.1056/NEJMoa1612790

Dewey, F. E., Gusarova, V., O'Dushlaine, C., Gottesman, O., Trejos, J., Hunt, C., et al. (2016). Inactivating Variants in ANGPTL4 and Risk of Coronary Artery Disease. *N. Engl. J. Med.* 374 (12), 1123–1133. doi:10.1056/NEJMoa1510926

Dichtl, W., Nilsson, L., Goncalves, I., Ares, M. P. S., Banfi, C., Calara, F., et al. (1999). Very Low-Density Lipoprotein Activates Nuclear Factor-Kb in Endothelial Cells. *Circulation Res.* 84 (9), 1085–1094. doi:10.1161/01.res.84.9.1085

Do, R., Willer, C. J., Schmidt, E. M., Sengupta, S., Gao, C., Peloso, G. M., et al. (2013). Common Variants Associated with Plasma Triglycerides and Risk for Coronary Artery Disease. *Nat. Genet.* 45 (11), 1345–1352. doi:10.1038/ng.2795

Do, R., Stitziel, N. O., Stitziel, N. O., Won, H.-H., Jørgensen, A. B., Duga, S., et al. (2015). Exome Sequencing Identifies Rare LDLR and APOA5 Alleles Conferring Risk for Myocardial Infarction. *Nature* 518 (7537), 102–106. doi:10.1038/nature13917

Doi, H., Kugiyama, K., Ohgushi, M., Sugiyama, S., Matsumura, T., Ohta, Y., et al. (1998). Remnants of Chylomicron and Very Low Density Lipoprotein Impair Endothelium-dependent Vasorelaxation. *Atherosclerosis* 137 (2), 341–349. doi:10.1016/s0021-9150(97)00291-8

Doi, H., Kugiyama, K., Oka, H., Sugiyama, S., Ogata, N., Koide, S.-i., et al. (2000). Remnant Lipoproteins Induce Proatherothrombogenic Molecules in Endothelial Cells through a Redox-Sensitive Mechanism. *Circulation* 102 (6), 670–676. doi:10.1161/01.cir.102.6.670

Dron, J. S., and Hegele, R. A. (2020). Genetics of Hypertriglyceridemia. *Front. Endocrinol.* 11, 455. doi:10.3389/fendo.2020.00455

Duran, E. K., and Pradhan, A. D. (2021). Triglyceride-rich Lipoprotein Remnants and Cardiovascular Disease. *Clin. Chem.* 67 (1), 183–196. doi:10.1093/clinchem/hvaa296

Emoto, T., Yamashita, T., Sasaki, N., Hirota, Y., Hayashi, T., So, A., et al. (2016). Analysis of Gut Microbiota in Coronary Artery Disease Patients: A Possible Link between Gut Microbiota and Coronary Artery Disease. *Jat* 23 (8), 908–921. doi:10.5551/jat.32672

Fan, K.-C., Wu, H.-T., Wei, J.-N., Chuang, L.-M., Hsu, C.-Y., Yen, I.-W., et al. (2020). Serum Angiopoietin-like Protein 6, Risk of Type 2 Diabetes, and Response to Hyperglycemia: A Prospective Cohort Study. *J. Clin. Endocrinol. Metab.* 105 (5), e1949–e1957. doi:10.1210/clinem/dgaa103

Fan, W., Philip, S., Granowitz, C., Toth, P. P., and Wong, N. D. (2019). Hypertriglyceridemia in Statin-Treated US Adults: The National Health and Nutrition Examination Survey. *J. Clin. Lipidol.* 13 (1), 100–108. doi:10.1016/j.jacl.2018.11.008

Farnier, M., Zeller, M., Masson, D., and Cottin, Y. (2021). Triglycerides and Risk of Atherosclerotic Cardiovascular Disease: An Update. *Archives Cardiovasc. Dis.* 114 (2), 132–139. doi:10.1016/j.acvd.2020.11.006

Feingold, K. R. (2021). "Triglyceride Lowering Drugs," in *Endotext [Internet]* (South Dartmouth (MA): MDText.com, Inc.).

Feng, M., Darabi, M., Tubeuf, E., Canicio, A., Lhomme, M., Frisdal, E., et al. (2020a). Free Cholesterol Transfer to High-Density Lipoprotein (HDL) upon Triglyceride Lipolysis Underlies the U-Shape Relationship between HDL-Cholesterol and Cardiovascular Disease. *Eur. J. Prev. Cardiol.* 27 (15), 1606–1616. doi:10.1177/2047487319894114

Feng, X., Guo, Q., Zhou, S., Sun, T., Liu, Y., Zhou, Z., et al. (2020b). Could Remnant-like Particle Cholesterol Become a Risk Factor in Diabetic Menopausal Women with Coronary Artery Disease? A Cross-Sectional Study of Single Academic Center in China. *Lipids Health. Dis.* 19 (1), 44. doi:10.1186/s12944-020-01224-8

Ference, B. A., Kastelein, J. J. P., Ray, K. K., Ginsberg, H. N., Chapman, M. J., Packard, C. J., et al. (2019). Association of Triglyceride-Lowering LPL Variants and LDL-C-Lowering LDLR Variants with Risk of Coronary Heart Disease. *JAMA* 321, 364–373. doi:10.1001/jama.2018.20045

Ference, B. A., Yoo, W., Alesh, I., Mahajan, N., Mirowska, K. K., Mewada, A., et al. (2012). Effect of Long-Term Exposure to Lower Low-Density Lipoprotein Cholesterol Beginning Early in Life on the Risk of Coronary Heart Disease. *J. Am. Coll. Cardiol.* 60 (25), 2631–2639. doi:10.1016/j.jacc.2012.09.017

Flores-Viveros, K. L., Aguilar-Galarza, B. A., Ordóñez-Sánchez, M. L., Anaya-Loyola, M. A., Moreno-Celis, U., Vázquez-Cárdenas, P., et al. (2019). Contribution of Genetic, Biochemical and Environmental Factors on Insulin Resistance and Obesity in Mexican Young Adults. *Obes. Res. Clin. Pract.* 13 (6), 533–540. doi:10.1016/j.orcp.2019.10.012

Folsom, A. R., Peacock, J. M., Demerath, E., and Boerwinkle, E. (2008). Variation in ANGPTL4 and Risk of Coronary Heart Disease: the Atherosclerosis Risk in Communities Study. *Metabolism* 57 (11), 1591–1596. doi:10.1016/j.metabol.2008.06.016

Fujihara, Y., Nakamura, T., Horikoshi, T., Obata, J.-e., Fujioka, D., Watanabe, Y., et al. (2019). Remnant Lipoproteins Are Residual Risk Factor for Future Cardiovascular Events in Patients with Stable Coronary Artery Disease and On-Statin Low-Density Lipoprotein Cholesterol Levels <70 mg/dL. *Circ. J.* 83 (6), 1302–1308. doi:10.1253/circj.CJ-19-0047

Fujimoto, K., Koishi, R., Shimizugawa, T., and Ando, Y. (2006). Angptl3-null Mice Show Low Plasma Lipid Concentrations by Enhanced Lipoprotein Lipase Activity. *Exp. Anim.* 55 (1), 27–34. doi:10.1538/expanim.55.27

Fujioka, Y., Cooper, A. D., and Fong, L. G. (1998). Multiple Processes Are Involved in the Uptake of Chylomicron Remnants by Mouse Peritoneal Macrophages. *J. Lipid Res.* 39 (12), 2339–2349. doi:10.1016/s0022-2275(20)33313-7

Funada, J.-i., Sekiya, M., Hamada, M., and Hiwada, K. (2002). Postprandial Elevation of Remnant Lipoprotein Leads to Endothelial Dysfunction. *Circ. J.* 66 (2), 127–132. doi:10.1253/circj.66.127

Ganda, O. P., Bhatt, D. L., Mason, R. P., Miller, M., and Boden, W. E. (2018). Unmet Need for Adjunctive Dyslipidemia Therapy in Hypertriglyceridemia Management. *J. Am. Coll. Cardiol.* 72 (3), 330–343. doi:10.1016/j.jacc.2018.04.061

Gaudet, D., Gipe, D. A., Pordy, R., Ahmad, Z., Cuchel, M., Shah, P. K., et al. (2017). ANGPTL3 Inhibition in Homozygous Familial Hypercholesterolemia. *N. Engl. J. Med.* 377 (3), 296–297. doi:10.1056/NEJMc1705994

Gaudet, D., Méthot, J., Déry, S., Brisson, D., Essiembre, C., Tremblay, G., et al. (2013). Efficacy and Long-Term Safety of Alipogene Tiparvovec (AAV1-Lpls447x) Gene Therapy for Lipoprotein Lipase Deficiency: An Open-Label Trial. *Gene Ther.* 20 (4), 361–369. doi:10.1038/gt.2012.43

Geldenhuys, W. J., Caporoso, J., Leeper, T. C., Lee, Y.-K., Lin, L., Darvesh, A. S., et al. (2017). Structure-activity and *In Vivo* Evaluation of a Novel Lipoprotein Lipase (LPL) Activator. *Bioorg. Med. Chem. Lett.* 27 (2), 303–308. doi:10.1016/j.bmcl.2016.11.053

Generoso, G., Janovsky, C. C. P. S., and Bittencourt, M. S. (2019). Triglycerides and Triglyceride-Rich Lipoproteins in the Development and Progression of Atherosclerosis. *Curr. Opin. Endocrinol. Diabetes Obes.* 26 (2), 109–116. doi:10.1097/MED.0000000000000468

Gianturco, S. H., and Bradley, W. A. (1999). Pathophysiology of Triglyceride-Rich Lipoproteins in Atherothrombosis: Cellular Aspects. *Clin. Cardiol.* 22 (6 Suppl. l), II–7. doi:10.1002/clc.4960221403

Gianturco, S. H., Brown, F. B., Gotto, A. M., Jr, and Bradley, W. A. (1982). Receptor-mediated Uptake of Hypertriglyceridemic Very Low Density Lipoproteins by Normal Human Fibroblasts. *J. Lipid Res.* 23 (7), 984–993. doi:10.1016/s0022-2275(20)38070-6

Gill, P. K., Dron, J. S., and Hegele, R. A. (2021). Genetics of Hypertriglyceridemia and Atherosclerosis. *Curr. Opin. Cardiol.* 36 (3), 264–271. doi:10.1097/HCO.0000000000000839

Ginsberg, H. N., Packard, C. J., Chapman, M. J., Borén, J., Aguilar-Salinas, C. A., Averna, M., et al. (2021). Triglyceride-rich Lipoproteins and Their Remnants: Metabolic Insights, Role in Atherosclerotic Cardiovascular Disease, and Emerging Therapeutic Strategies-A Consensus Statement from the European Atherosclerosis Society. *Eur. Heart J.* 42 (47), 4791–4806. doi:10.1093/eurheartj/ehab551

Gordts, P. L. S. M., Nock, R., Son, N.-H., Ramms, B., Lew, I., Gonzales, J. C., et al. (2016). ApoC-III Inhibits Clearance of Triglyceride-Rich Lipoproteins through LDL Family Receptors. *J. Clin. Invest.* 126 (8), 2855–2866. doi:10.1172/JCI86610

Gouni-Berthold, I., Alexander, V. J., Yang, Q., Hurh, E., Steinhagen-Thiessen, E., Moriarty, P. M., et al. (2021). Efficacy and Safety of Volanesorsen in Patients with Multifactorial Chylomicronaemia (COMPASS): a Multicentre, Double-Blind, Randomised, Placebo-Controlled, Phase 3 Trial. *Lancet Diabetes & Endocrinol.* 9 (5), 264–275. doi:10.1016/S2213-8587(21)00046-2

Gouni-Berthold, I. (2017). The Role of Antisense Oligonucleotide Therapy against Apolipoprotein-CIII in Hypertriglyceridemia. *Atheroscler. Suppl.* 30, 19–27. doi:10.1016/j.atherosclerosissup.2017.05.003

Gower, R. M., Wu, H., Foster, G. A., Devaraj, S., Jialal, I., Ballantyne, C. M., et al. (2011). CD11c/CD18 Expression Is Upregulated on Blood Monocytes during Hypertriglyceridemia and Enhances Adhesion to Vascular Cell Adhesion Molecule-1. *Atvb* 31, 160–166. doi:10.1161/atvbaha.110.215434

Goyal, S., Tanigawa, Y., Zhang, W., Chai, J.-F., Almeida, M., Sim, X., et al. (2021). APOC3 Genetic Variation, Serum Triglycerides, and Risk of Coronary Artery Disease in Asian Indians, Europeans, and Other Ethnic Groups. *Lipids Health Dis.* 20 (1), 113. doi:10.1186/s12944-021-01531-8

Graham, M. J., Lee, R. G., Brandt, T. A., Tai, L.-J., Fu, W., Peralta, R., et al. (2017). Cardiovascular and Metabolic Effects of ANGPTL3 Antisense Oligonucleotides. *N. Engl. J. Med.* 377 (3), 222–232. doi:10.1056/NEJMoa1701329

Guardiola, M., Cofán, M., de Castro-Oros, I., Cenarro, A., Plana, N., Talmud, P. J., et al. (2015). APOA5 Variants Predispose Hyperlipidemic Patients to Atherogenic Dyslipidemia and Subclinical Atherosclerosis. *Atherosclerosis* 240 (1), 98–104. doi:10.1016/j.atherosclerosis.2015.03.008

Guardiola, M., and Ribalta, J. (2017). Update on APOA5 Genetics: toward a Better Understanding of its Physiological Impact. *Curr. Atheroscler. Rep.* 19 (7), 30. doi:10.1007/s11883-017-0665-y

Guo, S., Tian, H., Dong, R., Yang, N., Zhang, Y., Yao, S., et al. (2016). Exogenous Supplement of N-Acetylneuraminic Acid Ameliorates Atherosclerosis in Apolipoprotein E-Deficient Mice. *Atherosclerosis* 251, 183–191. doi:10.1016/j.atherosclerosis

Gusarova, V., Alexa, C. A., Wang, Y., Rafique, A., Kim, J. H., Buckler, D., et al. (2015). ANGPTL3 Blockade with a Human Monoclonal Antibody Reduces Plasma Lipids in Dyslipidemic Mice and Monkeys. *J. Lipid Res.* 56 (7), 1308–1317. doi:10.1194/jlr.M054890

Gusarova, V., Banfi, S., Alexa-Braun, C. A., Shihanian, L. M., Mintah, I. J., Lee, J. S., et al. (2017). ANGPTL8 Blockade with a Monoclonal Antibody Promotes Triglyceride Clearance, Energy Expenditure, and Weight Loss in Mice. *Endocrinology* 158 (5), 1252–1259. doi:10.1210/en.2016-1894

Haller, J. F., Mintah, I. J., Shihanian, L. M., Stevis, P., Buckler, D., Alexa-Braun, C. A., et al. (2017). ANGPTL8 Requires ANGPTL3 to Inhibit Lipoprotein Lipase and Plasma Triglyceride Clearance. *J. Lipid Res.* 58 (6), 1166–1173. doi:10.1194/jlr.M075689

Hammad, M. M., Abu-Farha, M., Al-Taiar, A., Alam-Eldin, N., Al-Sabah, R., Shaban, L., et al. (2020). Correlation of Circulating ANGPTL5 Levels with Obesity, High Sensitivity C-Reactive Protein and Oxidized Low-Density Lipoprotein in Adolescents. *Sci. Rep.* 10 (1), 6330. doi:10.1038/s41598-020-63076-7

Hammond, L. E., Neschen, S., Romanelli, A. J., Cline, G. W., Ilkayeva, O. R., Shulman, G. I., et al. (2005). Mitochondrial Glycerol-3-Phosphate Acyltransferase-1 Is Essential inLiver for the Metabolism of ExcessAcyl-CoAs. *J. Biol. Chem.* 280 (27), 25629–25636. doi:10.1074/jbc.M503181200

Harris, W. S., Miller, M., Tighe, A. P., Davidson, M. H., and Schaefer, E. J. (2008). Omega-3 Fatty Acids and Coronary Heart Disease Risk: Clinical and Mechanistic Perspectives. *Atherosclerosis* 197, 12–24. doi:10.1016/j.atherosclerosis.2007.11.008

Hegele, R. A., Berberich, A. J., Ban, M. R., Wang, J., Digenio, A., Alexander, V. J., et al. (2018). Clinical and Biochemical Features of Different Molecular Etiologies of Familial Chylomicronemia. *J. Clin. Lipidol.* 12 (4), 920–927. doi:10.1016/j.jacl.2018.03.093

Hegele, R. A., Borén, J., Ginsberg, H. N., Arca, M., Averna, M., Binder, C. J., et al. (2020). Rare Dyslipidaemias, from Phenotype to Genotype to Management: a European Atherosclerosis Society Task Force Consensus Statement. *Lancet Diabetes & Endocrinol.* 8 (1), 50–67. doi:10.1016/S2213-8587(19)30264-5

Heidemann, B. E., Koopal, C., Bots, M. L., Asselbergs, F. W., Westerink, J., and Visseren, F. L. J. (2021). The Relation between VLDL-Cholesterol and Risk of Cardiovascular Events in Patients with Manifest Cardiovascular Disease. *Int. J. Cardiol.* 322, 251–257. doi:10.1016/j.ijcard.2020.08.030

Hoogeveen, R. C., and Ballantyne, C. M. (2020). Residual Cardiovascular Risk at Low LDL: Remnants, Lipoprotein(a), and Inflammation. *Clin. Chem.* 67 (1), 143–153. doi:10.1093/clinchem/hvaa252

Hou, P., Hu, S., Wang, J., Yang, Z., Yin, J., Zhou, G., et al. (2019). Exogenous Supplement of N-Acetylneuraminic Acid Improves Macrophage Reverse Cholesterol Transport in Apolipoprotein E-Deficient Mice. *Lipids Health Dis.* 18 (1), 24. doi:10.1186/s12944-019-0971-1

HPS2-THRIVE Collaborative Group (2013). HPS2-THRIVE Randomized Placebo-Controlled Trial in 25 673 High-Risk Patients of ER Niacin/laropiprant: Trial Design, Pre-specified Muscle and Liver Outcomes, and Reasons for Stopping Study Treatment. *Eur. Heart. J.* 34 (17), 1279–1291. doi:10.1093/eurheartj/eht055

Huang, X.-s., Zhao, S.-p., Bai, L., Hu, M., Zhao, W., and Zhang, Q. (2009). Atorvastatin and Fenofibrate Increase Apolipoprotein AV and Decrease Triglycerides by Up-Regulating Peroxisome Proliferator-Activated Receptor-α. *Brit. J. Pharmacol.* 158, 706–712. doi:10.1111/j.1476-5381.2009.00350.x

Ida, S., Kaneko, R., and Murata, K. (2019). Efficacy and Safety of Pemafibrate Administration in Patients with Dyslipidemia: a Systematic Review and Meta-Analysis. *Cardiovasc. Diabetol.* 18 (1), 38. doi:10.1186/s12933-019-0845-x

Inoue, T., Saniabadi, A. R., Matsunaga, R., Hoshi, K., Yaguchi, I., and Morooka, S. (1998). Impaired Endothelium-dependent Acetylcholine-Induced Coronary Artery Relaxation in Patients with High Serum Remnant Lipoprotein Particles. *Atherosclerosis* 139 (2), 363–367. doi:10.1016/s0021-9150(98)00098-7

Iqbal, J., Jahangir, Z., and Al-Qarni, A. A. (2020). Microsomal Triglyceride Transfer Protein: From Lipid Metabolism to Metabolic Diseases. *Adv. Exp. Med. Biol.* 1276, 37–52. doi:10.1007/978-981-15-6082-8_4

Ishibashi, S., Arai, H., Yokote, K., Araki, E., Suganami, H., and Yamashita, S. (2018). Efficacy and Safety of Pemafibrate (K-877), a Selective Peroxisome Proliferator-Activated Receptor α Modulator, in Patients with Dyslipidemia: Results from a 24-week, Randomized, Double Blind, Active-Controlled, Phase 3 Trial. *J. Clin. Lipidol.* 12 (1), 173–184. doi:10.1016/j.jacl.2017.10.006

Jacobson, T. A., Glickstein, S. B., Rowe, J. D., and Soni, P. N. (2012). Effects of Eicosapentaenoic Acid and Docosahexaenoic Acid on Low-Density Lipoprotein Cholesterol and Other Lipids: A Review. *J. Clin. Lipidol.* 6 (1), 5–18. doi:10.1016/j.jacl.2011.10.018

Jacobson, T. A., Ito, M. K., Maki, K. C., Orringer, C. E., Bays, H. E., Jones, P. H., et al. (2015). National Lipid Association Recommendations for Patient-Centered Management of Dyslipidemia: Part 1-Full Report. *J. Clin. Lipidol.* 9 (2), 129–169. doi:10.1016/j.jacl.2015.02.003

Jinno, Y., Nakakuki, M., Kawano, H., Notsu, T., Mizuguchi, K., and Imada, K. (2011). Eicosapentaenoic Acid Administration Attenuates the Pro-inflammatory Properties of VLDL by Decreasing its Susceptibility to Lipoprotein Lipase in Macrophages. *Atherosclerosis* 219 (2), 566–572. doi:10.1016/j.atherosclerosis.2011.09.046

Johansen, C. T., and Hegele, R. A. (2013). Using Mendelian Randomization to Determine Causative Factors in Cardiovascular Disease. *J. Intern. Med.* 273 (1), 44–47. doi:10.1111/j.1365-2796.2012.02586.x

Jørgensen, A. B., Frikke-Schmidt, R., Nordestgaard, B. G., and Tybjærg-Hansen, A. (2014). Loss-of-Function Mutations inAPOC3and Risk of Ischemic Vascular Disease. *N. Engl. J. Med.* 371 (1), 32–41. doi:10.1056/NEJMoa1308027

Jørgensen, A. B., Frikke-Schmidt, R., West, A. S., Grande, P., Nordestgaard, B. G., and Tybjærg-Hansen, A. (2013). Genetically Elevated Non-fasting Triglycerides and Calculated Remnant Cholesterol as Causal Risk Factors for Myocardial Infarction. *Eur. Heart. J.* 34 (24), 1826–1833. doi:10.1093/eurheartj/ehs431

Julve, J., Martín-Campos, J. M., Escolà-Gil, J. C., and Blanco-Vaca, F. (2016). Chylomicrons: Advances in Biology, Pathology, Laboratory Testing, and Therapeutics. *Clin. Chim. Acta* 455, 134–148. doi:10.1016/j.cca.2016.02.004

Jun, M., Foote, C., Lv, J., Neal, B., Patel, A., Nicholls, S. J., et al. (2010). Effects of Fibrates on Cardiovascular Outcomes: A Systematic Review and Meta-Analysis. *Lancet* 375, 1875–1884. doi:10.1016/S0140-6736(10)60656-3

Kadomatsu, T., Tabata, M., and Oike, Y. (2011). Angiopoietin-like Proteins: Emerging Targets for Treatment of Obesity and Related Metabolic Diseases. *FEBS J.* 278 (4), 559–564. doi:10.1111/j.1742-4658.2010.07979.x

Katsiki, N., Nikolic, D., Montalto, G., Banach, M., Mikhailidis, D. P., and Rizzo, M. (2013). The Role of Fibrate Treatment in Dyslipidemia: An Overview. *Cpd* 19 (17), 3124–3131. doi:10.2174/1381612811319170020

Kawakami, A., Tanaka, A., Nakajima, K., Shimokado, K., and Yoshida, M. (2002). Atorvastatin Attenuates Remnant Lipoprotein-Induced Monocyte Adhesion to Vascular Endothelium under Flow Conditions. *Circulation Res.* 91 (3), 263–271. doi:10.1161/01.res.0000028454.42385.8b

Kawakami, A., Tani, M., Chiba, T., Yui, K., Shinozaki, S., Nakajima, K., et al. (2005). Pitavastatin Inhibits Remnant Lipoprotein-Induced Macrophage Foam Cell Formation through ApoB48 Receptor-dependent Mechanism. *Atvb* 25 (2), 424–429. doi:10.1161/01.ATV.0000152632.48937.2d

Kegulian, N. C., Ramms, B., Horton, S., Trenchevska, O., Nedelkov, D., Graham, M. J., et al. (2019). ApoC-III Glycoforms Are Differentially Cleared by Hepatic TRL (Triglyceride-Rich Lipoprotein) Receptors. *Atvb* 39 (10), 2145–2156. doi:10.1161/ATVBAHA.119.312723

Kersten, S. (2021). Role and Mechanism of the Action of Angiopoietin-like Protein ANGPTL4 in Plasma Lipid Metabolism. *J. Lipid Res.* 62, 100150. doi:10.1016/j.jlr.2021.100150

Khetarpal, S. A., Qamar, A., Millar, J. S., and Rader, D. J. (2016). Targeting ApoC-III to Reduce Coronary Disease Risk. *Curr. Atheroscler. Rep.* 18 (9), 54. doi:10.1007/s11883-016-0609-y

Kockx, M., and Kritharides, L. (2018). Triglyceride-rich Lipoproteins. *Cardiol. Clin.* 36 (2), 265–275. doi:10.1016/j.ccl.2017.12.008

Kohan, A. B., Wang, F., Li, X., Bradshaw, S., Yang, Q., Caldwell, J. L., et al. (2012). Apolipoprotein A-IV Regulates Chylomicron Metabolism-Mechanism and Function. *Am. J. Physiology-Gastrointestinal Liver Physiology* 302 (6), G628–G636. doi:10.1152/ajpgi.00225.2011

Koishi, R., Ando, Y., Ono, M., Shimamura, M., Yasumo, H., Fujiwara, T., et al. (2002). Angptl3 Regulates Lipid Metabolism in Mice. *Nat. Genet.* 30 (2), 151–157. doi:10.1038/ng814

Komatsu, T., Sakurai, T., Wolska, A., Amar, M. J., Sakurai, A., Vaisman, B. L., et al. (2019). Apolipoprotein C-II Mimetic Peptide Promotes the Plasma Clearance of Triglyceride-Rich Lipid Emulsion and the Incorporation of Fatty Acids into Peripheral Tissues of Mice. *J. Nutr. Metabolism* 2019, 1–9. doi:10.1155/2019/7078241

Kotwal, S., Jun, M., Sullivan, D., Perkovic, V., and Neal, B. (2012). Omega 3 Fatty Acids and Cardiovascular Outcomes. *Circ Cardiovasc. Qual. Outcomes* 5 (6), 808–818. doi:10.1161/CIRCOUTCOMES.112.966168

Kovrov, O., Landfors, F., Saar-Kovrov, V., Näslund, U., and Olivecrona, G. (2022). Lipoprotein Size Is a Main Determinant for the Rate of Hydrolysis by Exogenous LPL in Human Plasma. *J. Lipid Res.* 63 (1), 100144. doi:10.1016/j.jlr.2021.100144

Kumari, A., Kristensen, K. K., Ploug, M., and Winther, A.-M. L. (2021). The Importance of Lipoprotein Lipase Regulation in Atherosclerosis. *Biomedicines* 9 (7), 782. doi:10.3390/biomedicines9070782

Larsson, M., Caraballo, R., Ericsson, M., Lookene, A., Enquist, P.-A., Elofsson, M., et al. (2014). Identification of a Small Molecule that Stabilizes Lipoprotein Lipase *In Vitro* and Lowers Triglycerides *In Vivo*. *Biochem. Biophysical Res. Commun.* 450 (2), 1063–1069. doi:10.1016/j.bbrc.2014.06.114

Laufs, U., Parhofer, K. G., Ginsberg, H. N., and Hegele, R. A. (2019). Clinical Review on Triglycerides. *Eur. Heart. J.* 41 (1), 99–109c. doi:10.1093/eurheartj/ehz785

Lazarte, J., and Hegele, R. A. (2021). Volanesorsen for Treatment of Familial Chylomicronemia Syndrome. *Expert Rev. Cardiovasc. Ther.* 19 (8), 685–693. doi:10.1080/14779072.2021.1955348

Le Chatelier., E., Nielsen, T., Qin, J., Prifti, E., Hildebrand, F., Falony, G., et al. (2013). Richness of Human Gut Microbiome Correlates with Metabolic Markers. *Nature* 500 (7464), 541–546. doi:10.1038/nature12506

Lee, J., and Ridgway, N. D. (2020). Substrate Channeling in the Glycerol-3-Phosphate Pathway Regulates the Synthesis, Storage and Secretion of Glycerolipids. *Biochimica Biophysica Acta (BBA) - Mol. Cell Biol. Lipids* 1865 (1), 158438. doi:10.1016/j.bbalip.2019.03.010

Prospective Studies CollaborationLewington, S., Whitlock, G., Clarke, R., Sherliker, P., Emberson, J., Halsey, J., et al. (2007). Blood Cholesterol and Vascular Mortality by Age, Sex, and Blood Pressure: A Meta-Analysis of Individual Data from 61 Prospective Studies with 55,000 Vascular Deaths. *Lancet* 370 (9602), 1829–1839. doi:10.1016/S0140-6736(07)61778-4

Li, J., Li, L., Guo, D., Li, S., Zeng, Y., Liu, C., et al. (2020). Triglyceride Metabolism and Angiopoietin-like Proteins in Lipoprotein Lipase Regulation. *Clin. Chim. Acta* 503, 19–34. doi:10.1016/j.cca.2019.12.029

Li, Y., Miao, M., Yin, F., Shen, N., Yu, W.-Q., and Guo, S.-D. (2022). The Polysaccharide-Peptide Complex from Mushroom *Cordyceps Militaris* Ameliorates Atherosclerosis by Modulating the lncRNA-miRNA-mRNA axis. *Food Funct.* 13 (6), 3185–3197. doi:10.1039/d1fOo03285b10.1039/d1fo03285b

Libby, P. (2007). Fat Fuels the Flame. *Circulation Res.* 100 (3), 299–301. doi:10.1161/01.RES.0000259393.89870.58

Lin, P., Ji, H.-H., Li, Y.-J., and Guo, S.-D. (2021). Macrophage Plasticity and Atherosclerosis Therapy. *Front. Mol. Biosci.* 8, 679797. doi:10.3389/fmolb.2021.679797

Lincoff, A. M., Nicholls, S. J., Riesmeyer, J. S., Barter, P. J., Brewer, H. B., Fox, K. A. A., et al. (2017). Evacetrapib and Cardiovascular Outcomes in High-Risk Vascular Disease. *N. Engl. J. Med.* 376 (20), 1933–1942. doi:10.1056/NEJMoa1609581

Liu, N., Si, Y., Zhang, Y., Guo, S., and Qin, S. (2021). Human Cholesteryl Ester Transport Protein Transgene Promotes Macrophage Reverse Cholesterol Transport in C57BL/6 Mice and Phospholipid Transfer Protein Gene Knockout Mice. *J. Physiol. Biochem.* 77 (4), 683–694. doi:10.1007/s13105-021-00834-9

Liu, Q., Cai, B.-y., Zhu, L.-x., Xin, X., Wang, X., An, Z.-m., et al. (2020b). Liraglutide Modulates Gut Microbiome and Attenuates Nonalcoholic Fatty Liver in Db/db Mice. *Life Sci.* 261, 118457. doi:10.1016/j.lfs.2020.118457

Liu, Q., Li, Y., Song, X., Wang, J., He, Z., Zhu, J., et al. (2020a). Both gut Microbiota and Cytokines Act to Atherosclerosis in ApoE−/− Mice. *Microb. Pathog.* 138, 103827. doi:10.1016/j.micpath.2019.103827

Liu, Y.-Z., Zhang, C., Jiang, J.-F., Cheng, Z.-B., Zhou, Z.-Y., Tang, M.-Y., et al. (2021). Angiopoietin-like Proteins in Atherosclerosis. *Clin. Chim. Acta* 521, 19–24. doi:10.1016/j.cca.2021.06.024

Luan, H. H., Wang, A., Hilliard, B. K., Carvalho, F., Rosen, C. E., Ahasic, A. M., et al. (2019). GDF15 Is an Inflammation-Induced Central Mediator of Tissue Tolerance. *Cell* 178 (5), 1231–1244. doi:10.1016/j.cell.2019.07.033

Mach, F., Baigent, C., Catapano, A. L., Koskinas, K. C., Casula, M., Badimon, L., et al. (2020). 2019 ESC/EAS Guidelines for the Management of Dyslipidaemias: Lipid Modification to Reduce Cardiovascular Risk. *Eur. Heart J.* 41, 111–188. doi:10.1093/eurheartj/ehz455

Mallick, R., and Duttaroy, A. K. (2022). Modulation of Endothelium Function by Fatty Acids. *Mol. Cell. Biochem.* 477 (1), 15–38. doi:10.1007/s11010-021-04260-9

Mansouri, R. M., Bauge´, E., Gervois, P., Fruchart-Najib, J., Fie´vet, C., Staels, B., et al. (2008). Atheroprotective Effect of Human Apolipoprotein A5 in a Mouse Model of Mixed Dyslipidemia. *Circulation Res.* 103 (5), 450–453. doi:10.1161/CIRCRESAHA.108.179861

Maranhão, R. C., Pala, D., and Freitas, F. R. (2020). Lipoprotein Removal Mechanisms and Aging: Implications for the Cardiovascular Health of the Elderly. *Curr. Opin. Endocrinol. Diabetes. Obes.* 27 (2), 104–109. doi:10.1097/MED.0000000000000529

Mason, R. P., Jacob, R. F., Shrivastava, S., Sherratt, S. C. R., and Chattopadhyay, A. (2016). Eicosapentaenoic Acid Reduces Membrane Fluidity, Inhibits Cholesterol Domain Formation, and Normalizes Bilayer Width in Atherosclerotic-like Model Membranes. *Biochimica Biophysica Acta (BBA) - Biomembr.* 1858 (12), 3131–3140. doi:10.1016/j.bbamem.2016.10.002

Matsunaga, A., Nagashima, M., Yamagishi, H., and Saku, K. (2020). Variants of Lipid-Related Genes in Adult Japanese Patients with Severe Hypertriglyceridemia. *Jat* 27 (12), 1264–1277. doi:10.5551/jat.51540

Mendoza-Barberá, E., Julve, J., Nilsson, S. K., Lookene, A., Martín-Campos, J. M., Roig, R., et al. (2013). Structural and Functional Analysis of APOA5 Mutations Identified in Patients with Severe Hypertriglyceridemia. *J. Lipid Res.* 54 (3), 649–661. doi:10.1194/jlr.M031195

Merkel, M. (2009). Diabetische Dyslipoproteinämie: jenseits von LDL. *Dtsch. Med. Wochenschr.* 134 (20), 1067–1073. doi:10.1055/s-0029-1222571

Michos, E. D., Sibley, C. T., Baer, J. T., Blaha, M. J., and Blumenthal, R. S. (2012). Niacin and Statin Combination Therapy for Atherosclerosis Regression and Prevention of Cardiovascular Disease Events. *J. Am. Coll. Cardiol.* 59 (23), 2058–2064. doi:10.1016/j.jacc.2012.01.045

Mora-Rodriguez, R., Ortega, J. F., Morales-Palomo, F., Ramirez-Jimenez, M., and Moreno-Cabañas, A. (2020). Effects of Statin Therapy and Exercise on Postprandial Triglycerides in Overweight Individuals with Hypercholesterolaemia. *Br. J. Clin. Pharmacol.* 86 (6), 1089–1099. doi:10.1111/bcp.14217

Morita, S.-y. (2016). Metabolism and Modification of Apolipoprotein B-Containing Lipoproteins Involved in Dyslipidemia and Atherosclerosis. *Biol. Pharm. Bull.* 39 (1), 1–24. doi:10.1248/bpb.b15-00716

Morjane, I., Charoute, H., Ouatou, S., Elkhattabi, L., Benrahma, H., Saile, R., et al. (2020). Association of c.56C > G (Rs3135506) Apolipoprotein A5 Gene Polymorphism with Coronary Artery Disease in Moroccan Subjects: A Case-Control Study and an Updated Meta-Analysis. *Cardiol. Res. Pract.* 2020, 1–8. doi:10.1155/2020/5981971

Mozaffarian, D., and Wu, J. H. Y. (2011). Omega-3 Fatty Acids and Cardiovascular Disease. *J. Am. Coll. Cardiol.* 58 (20), 2047–2067. doi:10.1016/j.jacc.2011.06.063

Musunuru, K., Pirruccello, J. P., Do, R., Peloso, G. M., Guiducci, C., Sougnez, C., et al. (2010). Exome Sequencing,ANGPTL3Mutations, and Familial Combined Hypolipidemia. *N. Engl. J. Med.* 363 (23), 2220–2227. doi:10.1056/NEJMoa1002926

Nakajima, K., and Tanaka, A. (2018b). Atherogenic Postprandial Remnant Lipoproteins; VLDL Remnants as a Causal Factor in Atherosclerosis. *Clin. Chim. Acta* 478, 200–215. doi:10.1016/j.cca.2017.12.039

Nakajima, K., and Tanaka, A. (2018a). Postprandial Remnant Lipoproteins as Targets for the Prevention of Atherosclerosis. *Curr. Opin. Endocrinol. Diabetes Obes.* 25 (2), 108–117. doi:10.1097/MED.0000000000000393

Nakamura, T., Takano, H., Umetani, K., Kawabata, K.-i., Obata, J.-e., Kitta, Y., et al. (2005). Remnant Lipoproteinemia Is a Risk Factor for Endothelial Vasomotor Dysfunction and Coronary Artery Disease in Metabolic Syndrome. *Atherosclerosis* 181 (2), 321–327. doi:10.1016/j.atherosclerosis.2005.01.012

Nakano, T., Nakajima, K., Niimi, M., Fujita, M. Q., Nakajima, Y., Takeichi, S., et al. (2008). Detection of Apolipoproteins B-48 and B-100 Carrying Particles in Lipoprotein Fractions Extracted from Human Aortic Atherosclerotic Plaques in Sudden Cardiac Death Cases. *Clin. Chim. Acta* 390 (1-2), 38–43. doi:10.1016/j.cca.2007.12.012

Namkung, J., Sohn, J. H., Chang, J. S., Park, S.-W., Kim, J.-Y., Koh, S.-B., et al. (2019). Increased Serum Angiopoietin-like 6 Ahead of Metabolic Syndrome in a Prospective Cohort Study. *Diabetes. Metab. J.* 43 (4), 521–529. doi:10.4093/dmj.2018.0080

Napolitano, M., Rivabene, R., Avella, M., Botham, K. M., and Bravo, E. (2001). The Internal Redox Balance of the Cells Influences the Metabolism of Lipids of Dietary Origin by J774 Macrophages: Implications for Foam Cell Formation. *J. Vasc. Res.* 38 (4), 350–360. doi:10.1159/000051066

Neschen, S., Morino, K., Hammond, L. E., Zhang, D., Liu, Z.-X., Romanelli, A. J., et al. (2005). Prevention of Hepatic Steatosis and Hepatic Insulin Resistance in Mitochondrial Acyl-CoA:glycerol-Sn-3-Phosphate Acyltransferase 1 Knockout Mice. *Cell Metab.* 2 (1), 55–65. doi:10.1016/j.cmet.2005.06.006

Nicholls, S. J., Lincoff, A. M., Bash, D., Ballantyne, C. M., Barter, P. J., Davidson, M. H., et al. (2018). Assessment of Omega-3 Carboxylic Acids in Statin-Treated Patients with High Levels of Triglycerides and Low Levels of High-Density Lipoprotein Cholesterol: Rationale and Design of the STRENGTH Trial. *Clin. Cardiol.* 41 (10), 1281–1288. doi:10.1002/clc.23055

Nicholls, S. J., Lincoff, A. M., Garcia, M., Bash, D., Ballantyne, C. M., Barter, P. J., et al. (2020). Effect of High-Dose Omega-3 Fatty Acids vs Corn Oil on Major Adverse Cardiovascular Events in Patients at High Cardiovascular Risk. *JAMA* 324 (22), 2268–2280. doi:10.1001/jama.2020.22258

Nilsson, S. K., Heeren, J., Olivecrona, G., and Merkel, M. (2011). Apolipoprotein A-V; a Potent Triglyceride Reducer. *Atherosclerosis* 219 (1), 15–21. doi:10.1016/j.atherosclerosis.2011.07.019

Nishikido, T., and Ray, K. K. (2021). Targeting the Peptidase PCSK9 to Reduce Cardiovascular Risk: Implications for Basic Science and Upcoming Challenges. *Br. J. Pharmacol.* 178 (11), 2168–2185. doi:10.1111/bph.14851

Nissen, S. E., Lincoff, A. M., Wolski, K., Ballantyne, C. M., Kastelein, J. J. P., Ridker, P. M., et al. (2021). Association between Achieved ω-3 Fatty Acid Levels and Major Adverse Cardiovascular Outcomes in Patients with High Cardiovascular Risk. *JAMA Cardiol.* 6 (8), 910–918. doi:10.1001/jamacardio.2021.1157

Nordestgaard, B. G., Benn, M., Schnohr, P., and Tybjærg-Hansen, A. (2007). Nonfasting Triglycerides and Risk of Myocardial Infarction, Ischemic Heart Disease, and Death in Men and Women. *JAMA* 298 (3), 299–308. doi:10.1001/jama.298.3.299

Nordestgaard, B. G. (2016). Triglyceride-Rich Lipoproteins and Atherosclerotic Cardiovascular Disease. *Circ. Res.* 118 (4), 547–563. doi:10.1161/CIRCRESAHA.115.306249

Nordestgaard, L. T., Christoffersen, M., Afzal, S., Nordestgaard, B. G., Tybjærg-Hansen, A., and Frikke-Schmidt, R. (2021). Triglycerides as a Shared Risk Factor between Dementia and Atherosclerotic Cardiovascular Disease: A Study of 125 727 Individuals. *Clin. Chem.* 67 (1), 245–255. doi:10.1093/clinchem/hvaa269

Ohmura, H. (2019). Triglycerides as Residual Risk for Atherosclerotic Cardiovascular Disease. *Circ. J.* 83 (5), 969–970. doi:10.1253/circj.CJ-19-0239

Okumura, T., Fujioka, Y., Morimoto, S., Masai, M., Sakoda, T., Tsujino, T., et al. (2006). Chylomicron Remnants Stimulate Release of Interleukin-1.BETA. By THP-1 Cells. *Jat* 13 (1), 38–45. doi:10.5551/jat.13.38

Orringer, C. E., Jacobson, T. A., and Maki, K. C. (2019). National Lipid Association Scientific Statement on the Use of Icosapent Ethyl in Statin-Treated Patients with Elevated Triglycerides and High or Very-High ASCVD Risk. *J. Clin. Lipidol.* 13 (6), 860–872. doi:10.1016/j.jacl.2019.10.014

Ouwens, M. J. N. M., Nauta, J., Ansquer, J.-C., and Driessen, S. (2015). Systematic Literature Review and Meta-Analysis of Dual Therapy with Fenofibrate or Fenofibric Acid and a Statin versus a Double or Equivalent Dose of Statin Monotherapy. *Curr. Med. Res. Opin.* 31 (12), 2273–2285. doi:10.1185/03007995.2015.1098597

O'zcan, U., Cao, Q., Yilmaz, E., Lee, A.-H., Iwakoshi, N. N., O'zdelen, E., et al. (2004). Endoplasmic Reticulum Stress Links Obesity, Insulin Action, and Type 2 Diabetes. *Science* 306 (5695), 457–461. doi:10.1126/science.1103160

Packard, C. J., Boren, J., and Taskinen, M.-R. (2020). Causes and Consequences of Hypertriglyceridemia. *Front. Endocrinol.* 11, 252. doi:10.3389/fendo.2020.00252

Padro, T., Muñoz-Garcia, N., and Badimon, L. (2021). The Role of Triglycerides in the Origin and Progression of Atherosclerosis. *Clínica Investig. Arterioscler.* 33, 20–28. doi:10.1016/j.arteri.2021.02.007

Paik, J., and Duggan, S. (2019). Volanesorsen: First Global Approval. *Drugs* 79 (12), 1349–1354. doi:10.1007/s40265-019-01168-z

Palmisano, B. T., Le, T. D., Zhu, L., Lee, Y. K., and Stafford, J. M. (2016). Cholesteryl Ester Transfer Protein Alters Liver and Plasma Triglyceride Metabolism through Two Liver Networks in Female Mice. *J. Lipid Res.* 57 (8), 1541–1551. doi:10.1194/jlr.M069013

Palmisano, B. T., Zhu, L., Litts, B., Burman, A., Yu, S., Neuman, J. C., et al. (2021). Hepatocyte Small Heterodimer Partner Mediates Sex-specific Effects on Triglyceride Metabolism via Androgen Receptor in Male Mice. *Metabolites* 11 (5), 330. doi:10.3390/metabo11050330

Panda, C., Varadharaj, S., and Voruganti, V. S. (2022). PUFA, Genotypes and Risk for Cardiovascular Disease. *Prostagl. Leukot. Essent. Fat. Acids* 176, 102377. doi:10.1016/j.plefa.2021.102377

Pang, J., Chan, D. C., Hamilton, S. J., Tenneti, V. S., Watts, G. F., and Barrett, P. H. R. (2016). Effect of Niacin on Triglyceride-Rich Lipoprotein Apolipoprotein B-48 Kinetics in Statin-Treated Patients with Type 2 Diabetes. *Diabetes. Obes. Metab.* 18 (4), 384–391. doi:10.1111/dom.12622

Parhofer, K. G., and Laufs, U. (2019). The Diagnosis and Treatment of Hypertriglyceridemia. *Dtsch. Arztebl. Int.* 116 (49), 825–832. doi:10.3238/arztebl.2019.0825

Park, M. S., Youn, J.-C., Kim, E. J., Han, K. H., Lee, S. H., Kim, S. H., et al. (2021). Efficacy and Safety of Fenofibrate-Statin Combination Therapy in Patients with Inadequately Controlled Triglyceride Levels Despite Previous Statin Monotherapy: A Multicenter, Randomized, Double-Blind, Phase IV Study. *Clin. Ther.* 43, 1735–1747. doi:10.1016/j.clinthera.2021.08.005

Park, S. Y., Lee, J. H., Kim, Y. K., Kim, C. D., Rhim, B. Y., Lee, W. S., et al. (2005). Cilostazol Prevents Remnant Lipoprotein Particle-Induced Monocyte Adhesion to Endothelial Cells by Suppression of Adhesion Molecules and Monocyte Chemoattractant Protein-1 Expression via Lectin-like Receptor for Oxidized Low-Density Lipoprotein Receptor Activation. *J. Pharmacol. Exp. Ther.* 312 (3), 1241–1248. doi:10.1124/jpet.104.077826

Peng, X., and Wu, H. (2022). Inflammatory Links between Hypertriglyceridemia and Atherogenesis. *Curr. Atheroscler. Rep.* 24 (5), 297–306. doi:10.1007/s11883-022-01006-w

Pirillo, A., Norata, G. D., and Catapano, A. L. (2014). Postprandial Lipemia as a Cardiometabolic Risk Factor. *Curr. Med. Res. Opin.* 30 (8), 1489–1503. doi:10.1185/03007995.2014.909394

Pollin, T. I., Damcott, C. M., Shen, H., Ott, S. H., Shelton, J., Horenstein, R. B., et al. (2008). A Null Mutation in Human APOC3 Confers a Favorable Plasma Lipid Profile and Apparent Cardioprotection. *Science* 322 (5908), 1702–1705. doi:10.1126/science.1161524

Preston Mason, R. (2019). New Insights into Mechanisms of Action for Omega-3 Fatty Acids in Atherothrombotic Cardiovascular Disease. *Curr. Atheroscler. Rep.* 21 (1), 2. doi:10.1007/s11883-019-0762-1

Proctor, S. D., and L. Mamo, J. C. (1998). Retention of Fluorescent-Labelled Chylomicron Remnants within the Intima of the Arterial Wall - Evidence that Plaque Cholesterol May Be Derived from Post-prandial Lipoproteins. *Eur. J. Clin. Investigation* 28 (6), 497–503. doi:10.1046/j.1365-2362.1998.00317.x

Qiu, M., Glass, Z., Chen, J., Haas, M., Jin, X., Zhao, X., et al. (2021). Lipid Nanoparticle-Mediated Codelivery of Cas9 mRNA and Single-Guide RNA Achieves Liver-specific *In Vivo* Genome Editing of Angptl3. *Proc. Natl. Acad. Sci. U.S.A.* 118 (10), e2020401118. doi:10.1073/pnas.2020401118

Rajamani, A., Borkowski, K., Akre, S., Fernandez, A., Newman, J. W., Simon, S. I., et al. (2019). Oxylipins in Triglyceride-Rich Lipoproteins of Dyslipidemic Subjects Promote Endothelial Inflammation Following a High Fat Meal. *Sci. Rep.* 9 (1), 8655. doi:10.1038/s41598-019-45005-5

Rapp, J. H., Lespine, A., Hamilton, R. L., Colyvas, N., Chaumeton, A. H., Tweedie-Hardman, J., et al. (1994). Triglyceride-rich Lipoproteins Isolated by Selected-Affinity Anti-apolipoprotein B Immunosorption from Human Atherosclerotic Plaque. *Arterioscler. Thromb.* 14 (11), 1767–1774. doi:10.1161/01.atv.14.11.1767

Reeskamp, L. F., Millar, J. S., Wu, L., Jansen, H., van Harskamp, D., Schierbeek, H., et al. (2021). ANGPTL3 Inhibition with Evinacumab Results in Faster Clearance of IDL and LDL apoB in Patients with Homozygous Familial Hypercholesterolemia-Brief Report. *Atvb* 41 (5), 1753–1759. doi:10.1161/ATVBAHA.120.315204

Reiner, Ž. (2017). Hypertriglyceridaemia and Risk of Coronary Artery Disease. *Nat. Rev. Cardiol.* 14 (7), 401–411. doi:10.1038/nrcardio.2017.31

Ren, J., Ren, A., Deng, X., Huang, Z., Jiang, Z., Li, Z., et al. (2022). Long-chain Polyunsaturated Fatty Acids and Their Metabolites Regulate Inflammation in Age-Related Macular Degeneration. *Jir* 15, 865–880. doi:10.2147/JIR.S347231

Ress, C., Dobner, J., Rufinatscha, K., Staels, B., Hofer, M., Folie, S., et al. (2021). Apolipoprotein A5 Controls Fructose-Induced Metabolic Dysregulation in Mice. *Nutr. Metabolism Cardiovasc. Dis.* 31 (3), 972–978. doi:10.1016/j.numecd.2020.11.008

Reyes-Soffer, G., and Ginsberg, H. N. (2019). Life Is Complicated: So Is apoCIII. *J. Lipid Res.* 60 (8), 1347–1349. doi:10.1194/jlr.C119000214

Reyes-Soffer, G. (2021). Triglyceride-rich Lipoproteins and Atherosclerotic Cardiovascular Disease Risk: Current Status and Treatments. *Curr. Opin. Endocrinol. Diatetes. Obes.* 28 (2), 85–89. doi:10.1097/MED.0000000000000619

Rip, J., Nierman, M. C., Ross, C. J., Jukema, J. W., Hayden, M. R., Kastelein, J. J. P., et al. (2006). Lipoprotein Lipase S447X. *Atvb* 26 (6), 1236–1245. doi:10.1161/01.ATV.0000219283.10832.43

Rocha, N. A., East, C., Zhang, J., and McCullough, P. A. (2017). ApoCIII as a Cardiovascular Risk Factor and Modulation by the Novel Lipid-Lowering Agent Volanesorsen. *Curr. Atheroscler. Rep.* 19 (12), 62. doi:10.1007/s11883-017-0697-3

Rodríguez-Mortera, R., Caccavello, R., Garay-Sevilla, M. E., and Gugliucci, A. (2020). Higher ANGPTL3, apoC-III, and apoB48 Dyslipidemia, and Lower Lipoprotein Lipase Concentrations Are Associated with Dysfunctional Visceral Fat in Adolescents with Obesity. *Clin. Chim. Acta* 508, 61–68. doi:10.1016/j.cca.2020.05.014

Rosenson, R. S., Davidson, M. H., Hirsh, B. J., Kathiresan, S., and Gaudet, D. (2014). Genetics and Causality of Triglyceride-Rich Lipoproteins in Atherosclerotic Cardiovascular Disease. *J. Am. Coll. Cardiol.* 64 (23), 2525–2540. doi:10.1016/j.jacc.2014.09.042

Rosenson, R. S., Shott, S., Lu, L., and Tangney, C. C. (2001). Hypertriglyceridemia and Other Factors Associated with Plasma Viscosity. *Am. J. Med.* 110 (6), 488–492. doi:10.1016/s0002-9343(01)00643-x

Rubins, H. B., Robins, S. J., Collins, D., Fye, C. L., Anderson, J. W., Elam, M. B., et al. (1999). Gemfibrozil for the Secondary Prevention of Coronary Heart Disease in Men with Low Levels of High-Density Lipoprotein Cholesterol. *N. Engl. J. Med.* 341 (6), 410–418. doi:10.1056/NEJM199908053410604

Saito, Y., Yokoyama, M., Origasa, H., Matsuzaki, M., Matsuzawa, Y., Ishikawa, Y., et al. (2008). Effects of EPA on Coronary Artery Disease in Hypercholesterolemic Patients with Multiple Risk Factors: Sub-analysis of Primary Prevention Cases from the Japan EPA Lipid Intervention Study (JELIS). *Atherosclerosis* 200 (1), 135–140. doi:10.1016/j.atherosclerosis.2008.06.003

Sakuma, N., Ikeuchi, R., Hibino, T., Yoshida, T., Mukai, S., Akita, S., et al. (2003). Increased Serum Triglyceride Clearance and Elevated High-Density Lipoprotein 2 and 3 Cholesterol during Treatment of Primary Hypertriglyceridemia with Bezafibrate. *Curr. Ther. Res.* 64 (9), 697–706. doi:10.1016/j.curtheres.2003.10.002

Sakurai, T., Sakurai, A., Vaisman, B. L., Amar, M. J., Liu, C., Gordon, S. M., et al. (2016). Creation of Apolipoprotein C-II (ApoC-II) Mutant Mice and Correction of Their Hypertriglyceridemia with an ApoC-II Mimetic Peptide. *J. Pharmacol. Exp. Ther.* 356 (2), 341–353. doi:10.1124/jpet.115.229740

Salinas, C. A. A., and Chapman, M. J. (2020). Remnant Lipoproteins. *Curr. Opin. Lipidol.* 31 (3), 132–139. doi:10.1097/MOL.0000000000000682

Sampson, U. K., Fazio, S., and Linton, M. F. (2012). Residual Cardiovascular Risk Despite Optimal LDL Cholesterol Reduction with Statins: The Evidence, Etiology, and Therapeutic Challenges. *Curr. Atheroscler. Rep.* 14 (1), 1–10. doi:10.1007/s11883-011-0219-7

Sandesara, P. B., Virani, S. S., Fazio, S., and Shapiro, M. D. (2019). The Forgotten Lipids: Triglycerides, Remnant Cholesterol, and Atherosclerotic Cardiovascular Disease Risk. *Endocr. Rev.* 40 (2), 537–557. doi:10.1210/er.2018-00184

Sando, K. R., and Knight, M. (2015). Nonstatin Therapies for Management of Dyslipidemia: A Review. *Clin. Ther.* 37 (10), 2153–2179. doi:10.1016/j.clinthera.2015.09.001

Santos-Baez, L. S., and Ginsberg, H. N. (2020). Hypertriglyceridemia-causes, Significance, and Approaches to Therapy. *Front. Endocrinol.* 11, 616. doi:10.3389/fendo.2020.00616

Saraswathi, V., and Hasty, A. H. (2006). The Role of Lipolysis in Mediating the Proinflammatory Effects of Very Low Density Lipoproteins in Mouse Peritoneal Macrophages. *J. Lipid Res.* 47 (7), 1406–1415. doi:10.1194/jlr.M600159-JLR200

Schunkert, H., König, I. R., Kathiresan, S., Reilly, M. P., Assimes, T. L., Holm, H., et al. (2011). Large-scale Association Analysis Identifies 13 New Susceptibility Loci for Coronary Artery Disease. *Nat. Genet.* 43 (4), 333–338. doi:10.1038/ng.784

Shahid, S. U., Shabana, N. A., Rehman, A., and Humphries, S. (2018). GWAS Implicated Risk Variants in Different Genes Contribute Additively to Increase the Risk of Coronary Artery Disease (CAD) in the Pakistani Subjects. *Lipids. Health. Dis.* 17 (1), 89. doi:10.1186/s12944-018-0736-2

Shahidi, F., and Ambigaipalan, P. (2018). Omega-3 Polyunsaturated Fatty Acids and Their Health Benefits. *Annu. Rev. Food Sci. Technol.* 9, 345–381. doi:10.1146/annurev-food-111317-095850

Shaikh, S. R. (2012). Biophysical and Biochemical Mechanisms by Which Dietary N-3 Polyunsaturated Fatty Acids from Fish Oil Disrupt Membrane Lipid Rafts. *J. Nutr. Biochem.* 23 (2), 101–105. doi:10.1016/j.jnutbio.2011.07.001

Shin, H. K., Kim, Y. K., Kim, K. Y., Lee, J. H., and Hong, K. W. (2004). Remnant Lipoprotein Particles Induce Apoptosis in Endothelial Cells by NAD(P)H Oxidase-Mediated Production of Superoxide and Cytokines via Lectin-like Oxidized Low-Density Lipoprotein Receptor-1 Activation. *Circulation* 109 (8), 1022–1028. doi:10.1161/01.CIR.0000117403.64398.53

Shu, X., Nelbach, L., Weinstein, M. M., Burgess, B. L., Beckstead, J. A., Young, S. G., et al. (2010). Intravenous Injection of Apolipoprotein A-V Reconstituted High-Density Lipoprotein Decreases Hypertriglyceridemia in Apoav −/− Mice and Requires Glycosylphosphatidylinositol-Anchored High-Density Lipoprotein-Binding Protein 1. *Atvb* 30 (12), 2504–2509. doi:10.1161/ATVBAHA.110.210815

Si, S., Hou, L., Chen, X., Li, W., Liu, X., Liu, C., et al. (2022). Exploring the Causal Roles of Circulating Remnant Lipid Profile on Cardiovascular and Cerebrovascular Diseases: Mendelian Randomization Study. *J. Epidemiol.* 32, 205–214. doi:10.2188/jea.JE20200305

Silverman, M. G., Ference, B. A., Im, K., Wiviott, S. D., Giugliano, R. P., Grundy, S. M., et al. (2016). Association between Lowering LDL-C and Cardiovascular Risk Reduction Among Different Therapeutic Interventions. *JAMA* 316 (12), 1289–1297. doi:10.1001/jama.2016.13985

Simons, L. A. (2019). An Updated Review of Lipid-modifying Therapy. *Med. J. Aust.* 211 (2), 87–92. doi:10.5694/mja2.50142

Spitler, K. M., Shetty, S. K., Cushing, E. M., Sylvers-Davie, K. L., and Davies, B. S. J. (2021). Regulation of Plasma Triglyceride Partitioning by Adipose-Derived ANGPTL4 in Mice. *Sci. Rep.* 11 (1), 7873. doi:10.1038/s41598-021-87020-5

Stollenwerk, M. M., Schiopu, A., Fredrikson, G. N., Dichtl, W., Nilsson, J., and Ares, M. P. S. (2005). Very Low Density Lipoprotein Potentiates Tumor Necrosis Factor-α Expression in Macrophages. *Atherosclerosis* 179 (2), 247–254. doi:10.1016/j.atherosclerosis.2004.12.002

Su, X., Cheng, Y., and Chang, D. (2021). Lipid-lowering Therapy: Guidelines to Precision Medicine. *Clin. Chim. Acta* 514, 66–73. doi:10.1016/j.cca.2020.12.019

Su, X., and Peng, D. (2020). The Exchangeable Apolipoproteins in Lipid Metabolism and Obesity. *Clin. Chim. Acta* 503, 128–135. doi:10.1016/j.cca.2020.01.015

Su, X., Weng, S., and Peng, D. (2020). New Insights into Apolipoprotein A5 and the Modulation of Human Adipose-Derived Mesenchymal Stem Cells Adipogenesis. *Cmm* 20 (2), 144–156. doi:10.2174/1566524019666190927155702

Sun, C., Alkhoury, K., Wang, Y. I., Foster, G. A., Radecke, C. E., Tam, K., et al. (2012). IRF-1 and miRNA126 Modulate VCAM-1 Expression in Response to a High-Fat Meal. *Circ. Res.* 111 (8), 1054–1064. doi:10.1161/CIRCRESAHA.112.270314

Tada, H., Nohara, A., and Kawashiri, M.-a. (2018). Serum Triglycerides and Atherosclerotic Cardiovascular Disease: Insights from Clinical and Genetic Studies. *Nutrients* 10 (11), 1789. doi:10.3390/nu10111789

Takahashi, S. (2017). Triglyceride Rich Lipoprotein -LPL-VLDL Receptor and Lp(a)-VLDL Receptor Pathways for Macrophage Foam Cell Formation. *Jat* 24 (6), 552–559. doi:10.5551/jat.RV17004

Teslovich, T. M., Musunuru, K., Smith, A. V., Edmondson, A. C., Stylianou, I. M., Koseki, M., et al. (2010). Biological, Clinical and Population Relevance of 95 Loci for Blood Lipids. *Nature* 466 (7307), 707–713. doi:10.1038/nature09270

Thomsen, M., Varbo, A., Tybjærg-Hansen, A., and Nordestgaard, B. G. (2014). Low Nonfasting Triglycerides and Reduced All-Cause Mortality: A Mendelian Randomization Study. *Clin. Chem.* 60 (5), 737–746. doi:10.1373/clinchem.2013.219881

Tokgözoğlu, L., and Libby, P. (2022). The Dawn of a New Era of Targeted Lipid-Lowering Therapies. *Eur. Heart J.* 00, 1–13. doi:10.1093/eurheartj/ehab841

Toth, P. P., Fazio, S., Wong, N. D., Hull, M., and Nichols, G. A. (2020). Risk of Cardiovascular Events in Patients with Hypertriglyceridaemia: A Review of Real-world Evidence. *Diabetes. Obes. Metab.* 22 (3), 279–289. doi:10.1111/dom.13921

Toth, P. P., Hull, M., Granowitz, C., and Philip, S. (2021). Real-world Analyses of Patients with Elevated Atherosclerotic Cardiovascular Disease Risk from the Optum Research Database. *Future Cardiol.* 17 (4), 743–755. doi:10.2217/fca-2020-0123

Toth, P. P., Philip, S., Hull, M., and Granowitz, C. (2019b). Association of Elevated Triglycerides with Increased Cardiovascular Risk and Direct Costs in Statin-Treated Patients. *Mayo Clin. Proc.* 94 (9), 1670–1680. doi:10.1016/j.mayocp.2019.03.028

Toth, P. P., Philip, S., Hull, M., and Granowitz, C. (2019a). Elevated Triglycerides (≥150 mg/dL) and High Triglycerides (200-499 mg/dL) Are Significant Predictors of New Heart Failure Diagnosis: A Real-World Analysis of High-Risk Statin-Treated Patients. *Vhrm* 15, 533–538. doi:10.2147/VHRM.S221289

Toth, P. (2016). Triglyceride-rich Lipoproteins as a Causal Factor for Cardiovascular Disease. *Vhrm* 12, 171–183. doi:10.2147/VHRM.S104369

Twickler, T. B., Dallinga-Thie, G. M., Visseren, F. L. J., de Vries., W. R., Erkelens, D. W., and Koppeschaar, H. P. F. (2003). Induction of Postprandial Inflammatory Response in Adult Onset Growth Hormone Deficiency Is Related to Plasma Remnant-like Particle-Cholesterol Concentration. *J. Clin. Endocrinol. Metabolism* 88 (3), 1228–1233. doi:10.1210/jc.2002-020470

Vallerie, S. N., and Bornfeldt, K. E. (2015). Gpihbp1. *Circ. Res.* 116 (4), 560–562. doi:10.1161/CIRCRESAHA.115.305819

Van der Vliet, H. N., Schaap, F. G., Levels, J. H. M., Ottenhoff, R., Looije, N., Wesseling, J. G., et al. (2002). Adenoviral Overexpression of Apolipoprotein A-V Reduces Serum Levels of Triglycerides and Cholesterol in Mice. *Biochem. Biophysical Res. Commun.* 295 (5), 1156–1159. doi:10.1016/s0006-291x(02)00808-2

Varbo, A., Benn, M., Tybjærg-Hansen, A., and Nordestgaard, B. G. (2013). Elevated Remnant Cholesterol Causes Both Low-Grade Inflammation and Ischemic Heart Disease, whereas Elevated Low-Density Lipoprotein Cholesterol Causes Ischemic Heart Disease without Inflammation. *Circulation* 128 (12), 1298–1309. doi:10.1161/CIRCULATIONAHA.113.003008

Varbo, A., and Nordestgaard, B. G. (2016). Remnant Cholesterol and Triglyceride-Rich Lipoproteins in Atherosclerosis Progression and Cardiovascular Disease. *Atvb* 36 (11), 2133–2135. doi:10.1161/ATVBAHA.116.308305

Wakita, K., Morita, S.-y., Okamoto, N., Takata, E., Handa, T., and Nakano, M. (2015). Chylomicron Remnant Model Emulsions Induce Intracellular Cholesterol Accumulation and Cell Death Due to Lysosomal Destabilization. *Biochimica Biophysica Acta (BBA) - Mol. Cell Biol. Lipids* 1851 (5), 598–604. doi:10.1016/j.bbalip.2015.01.015

Wang, D., Liu, B., Tao, W., Hao, Z., and Liu, M. (2015). Fibrates for Secondary Prevention of Cardiovascular Disease and Stroke. *Cochrane Database Syst. Rev.* 2018 (10), CD009580. doi:10.1002/14651858.CD009580.pub2

Wang, H., and Eckel, R. H. (2009). Lipoprotein Lipase: from Gene to Obesity. *Am. J. Physiology-Endocrinology Metabolism* 297 (2), E271–E288. doi:10.1152/ajpendo.90920.2008

Wang, L., Gill, R., Pedersen, T. L., Higgins, L. J., Newman, J. W., and Rutledge, J. C. (2009). Triglyceride-rich Lipoprotein Lipolysis Releases Neutral and Oxidized FFAs that Induce Endothelial Cell Inflammation. *J. Lipid Res.* 50 (2), 204–213. doi:10.1194/jlr.M700505-JLR200

Wang, L., Sapuri-Butti, A. R., Aung, H. H., Parikh, A. N., and Rutledge, J. C. (2008). Triglyceride-rich Lipoprotein Lipolysis Increases Aggregation of Endothelial Cell Membrane Microdomains and Produces Reactive Oxygen Species. *Am. J. Physiology-Heart Circulatory Physiology* 295 (1), H237–H244. doi:10.1152/ajpheart.01366.2007

Wang, Y. I., Bettaieb, A., Sun, C., DeVerse, J. S., Radecke, C. E., Mathew, S., et al. (2013). Triglyceride-rich Lipoprotein Modulates Endothelial Vascular Cell Adhesion Molecule (VCAM)-1 Expression via Differential Regulation of Endoplasmic Reticulum Stress. *PLoS. One.* 8 (10), e78322. doi:10.1371/journal.pone.0078322

Wang, Y. I., Schulze, J., Raymond, N., Tomita, T., Tam, K., Simon, S. I., et al. (2011). Endothelial Inflammation Correlates with Subject Triglycerides and Waist Size after a High-Fat Meal. *Am. J. Physiology-Heart Circulatory Physiology* 300 (3), H784–H791. doi:10.1152/ajpheart.01036.2010

Watanabe, T., Ando, K., Daidoji, H., Otaki, Y., Sugawara, S., Matsui, M., et al. (2017). A Randomized Controlled Trial of Eicosapentaenoic Acid in Patients with Coronary Heart Disease on Statins. *J. Cardiol.* 70 (6), 537–544. doi:10.1016/j.jjcc.2017.07.007

Werner, C., Filmer, A., Fritsch, M., Groenewold, S., Gräber, S., Böhm, M., et al. (2014). Risk Prediction with Triglycerides in Patients with Stable Coronary Disease on Statin Treatment. *Clin. Res. Cardiol.* 103, 984–997. doi:10.1007/s00392-014-0740-0

WHO (2021). Cardiovascular Diseases (CVDs). Available at: https://www.who.int/news-room/fact-sheets/detail/cardiovascular-diseases-(cvds (accessed sept 20, 2021).

Witztum, J. L., Gaudet, D., Freedman, S. D., Alexander, V. J., Digenio, A., Williams, K. R., et al. (2019). Volanesorsen and Triglyceride Levels in Familial Chylomicronemia Syndrome. *N. Engl. J. Med.* 381 (6), 531–542. doi:10.1056/NEJMoa1715944

Wolska, A., Lo, L., Sviridov, D. O., Pourmousa, M., Pryor, M., Ghosh, S. S., et al. (2020a). A Dual Apolipoprotein C-II Mimetic-Apolipoprotein C-III Antagonist Peptide Lowers Plasma Triglycerides. *Sci. Transl. Med.* 12 (528), eaaw7905. doi:10.1126/scitranslmed.aaw7905

Wolska, A., Reimund, M., and Remaley, A. T. (2020b). Apolipoprotein C-II. *Curr. Opin. Lipidol.* 31 (3), 147–153. doi:10.1097/MOL.0000000000000680

Wu, S. A., Kersten, S., and Qi, L. (2021). Lipoprotein Lipase and its Regulators: An Unfolding Story. *Trends Endocrinol. Metabolism* 32 (1), 48–61. doi:10.1016/j.tem.2020.11.005

Wyler von Ballmoos, M. C., Haring, B., and Sacks, F. M. (2015). The Risk of Cardiovascular Events with Increased Apolipoprotein CIII: A Systematic Review and Meta-Analysis. *J. Clin. Lipidol.* 9 (4), 498–510. doi:10.1016/j.jacl.2015.05.002

Xu, Q.-Y., Li, H., Cao, H.-X., Pan, Q., and Fan, J.-G. (2020). ApoC3 Rs2070667 Associates with Serum Triglyceride Profile and Hepatic Inflammation in Nonalcoholic Fatty Liver Disease. *BioMed Res. Int.* 2020, 1–9. doi:10.1155/2020/8869674

Yadav, H., Lee, J.-H., Lloyd, J., Walter, P., and Rane, S. G. (2013). Beneficial Metabolic Effects of a Probiotic via Butyrate-Induced GLP-1 Hormone Secretion. *J. Biol. Chem.* 288 (35), 25088–25097. doi:10.1074/jbc.M113.452516

Yanai, H., Katsuyama, H., and Hakoshima, M. (2022). Effects of a Novel Selective Peroxisome Proliferator-Activated Receptor α Modulator, Pemafibrate, on Metabolic Parameters: A Retrospective Longitudinal Study. *Biomedicines* 10, 401. doi:10.3390/biomedicines10020401

Yang, J., Li, X., and Xu, D. (2020). Research Progress on the Involvement of ANGPTL4 and Loss-Of-Function Variants in Lipid Metabolism and Coronary Heart Disease: Is the "Prime Time" of ANGPTL4-Targeted Therapy for Coronary Heart Disease Approaching? *Cardiovasc. Drugs Ther.* 35 (3), 467–477. doi:10.1007/s10557-020-07001-0

Yin, F., Lin, P., Yu, W.-Q., Shen, N., Li, Y., and Guo, S.-D. (2021). The Cordyceps Militaris-Derived Polysaccharide CM1 Alleviates Atherosclerosis in LDLR(-/-) Mice by Improving Hyperlipidemia. *Front. Mol. Biosci.* 8, 783807. doi:10.3389/fmolb.2021.783807

Young, S. G., Fong, L. G., Beigneux, A. P., Allan, C. M., He, C., Jiang, H., et al. (2019). GPIHBP1 and Lipoprotein Lipase, Partners in Plasma Triglyceride Metabolism. *Cell Metab.* 30 (1), 51–65. doi:10.1016/j.cmet.2019.05.023

Young, S. G., and Zechner, R. (2013). Biochemistry and Pathophysiology of Intravascular and Intracellular Lipolysis. *Genes Dev.* 27 (5), 459–484. doi:10.1101/gad.209296.112

Zhang, R. (2016). The ANGPTL3-4-8 Model, a Molecular Mechanism for Triglyceride Trafficking. *Open Biol.* 6 (4), 150272. doi:10.1098/rsob.150272

Zhang, R., and Zhang, K. (2022). An Updated ANGPTL3-4-8 Model as a Mechanism of Triglyceride Partitioning between Fat and Oxidative Tissues. *Prog. Lipid Res.* 85, 101140. doi:10.1016/j.plipres.2021.101140

Conflict of Interest: The authors declare that the research was conducted in the absence of any commercial or financial relationships that could be construed as a potential conflict of interest.

Publisher's Note: All claims expressed in this article are solely those of the authors and do not necessarily represent those of their affiliated organizations, or those of the publisher, the editors and the reviewers. Any product that may be evaluated in this article, or claim that may be made by its manufacturer, is not guaranteed or endorsed by the publisher.

GLOSSARY

ANGPTL Angiopoietin-like protein
apo Apolipoprotein
ASCVD Atherosclerotic cardiovascular disease
ATF3 Activating transcription factor 3
CETP Cholesteryl ester transport protein
CHD Coronary heart disease
CM Chylomicron
CMR CM remnant
CVD Cardiovascular disease
DHA Docosahexaenoic acid
EPA Eicosapentaenoic acid
ER Endoplasmic reticulum
ERK Extracellular signal-regulated kinase
FA Fatty acid
FCS Familial CM syndrome
G3P Glycerol-3-phosphate
GLP-1 Glucagon-like peptide-1
GPAT G3P acyltransferase
GPIHBP1 Glycosylphosphatidylinositol-anchored HDL binding protein 1
HDL High density lipoprotein
HDL-C HDL cholesterol
HSPG Heparan sulfate proteoglycan
HTG Hypertriglyceridemia
HTGL Hepatic TG lipase
ICAM-1 Intercellular adhesion molecule-1
IDL Intermediate density lipoprotein
IL Interleukin
JNK c-Jun NH2-terminal kinase
LDL Low-density lipoprotein
LDL-C LDL cholesterol
LDLR LDL receptor
LOX-1 Lectin-like receptor for oxidized LDL
LPL Lipoprotein lipase
LRP-1 LDLR-related protein 1
MAPK Mitogen-activated protein kinase
MCP Monocyte chemoattractant protein
MEK MAPK kinase
MMP Matrix metalloproteinase
MTP Microsomal triglyceride transfer protein
NF-κB Nuclear factor-κB
NLRP1 Nucleotide binding domain like receptor family pyrrole domain containing protein 1
PCSK9 Proprotein convertase subtilisin/kexin-type 9
PKC Protein kinase C
PPAR Peroxisome proliferator activated receptor
PUFA Polyunsaturated fatty acids
SR-B1 Scavenger receptor B type 1
SREBP Sterol regulatory element binding protein
TG Triglyceride
TGRL TG-rich lipoprotein
TNF-α Tumor necrosis factor-alpha
VCAM Vascular cell adhesion molecule
VLDL Very low-density lipoprotein
VLDL-C VLDL cholesterol

frontiers | Frontiers in Molecular Biosciences

ORIGINAL RESEARCH
published: 15 June 2022
doi: 10.3389/fmolb.2022.879294

Polyethylene Glycol Loxenatide Injection (GLP-1) Protects Vascular Endothelial Cell Function in Middle-Aged and Elderly Patients With Type 2 Diabetes by Regulating Gut Microbiota

Fengwu Chen[1,2†], Lina He[3†], Jilin Li[4†], Shuhui Yang[5†], Bangzhou Zhang[6,7†], Dan Zhu[2], Zezhen Wu[1,2], Shuo Zhang[1,2], Ducheng Hou[2], Cong Ouyang[8], Jianfeng Yi[3], Chuanxing Xiao[6,7,9] and Kaijian Hou[1,2,7]**

[1]The First Affiliated Hospital of Shantou University Medical College, Shantou, China, [2]Department of Endocrine and Metabolic Diseases, Longhu People's Hospital, Shantou, China, [3]Key Laboratory for Research on Active Ingredients in Natural Medicine of Jiangxi Province, Yichun University, Yichun, China, [4]Department of Cardiology, The Second Affiliated Hospital of Shantou University Medical College, Shantou, China, [5]Department of Endocrine and Metabolic Diseases, Shantou Central Hospital, Shantou, China, [6]School of Pharmacy, Fujian University of Traditional Chinese Medicine, Fuzhou, China, [7]School of Basic Medical Science, Central South University, Changsha, China, [8]Center for Research and Development, Xiamen Treatgut Biotechnology Co., Ltd., Xiamen, China, [9]Department of Gastroenterology, The Second Affiliated Hospital of Fujian University of Traditional Chinese Medicine, Fuzhou, China

Objective: To evaluate the protective effect of Polyethylene Glycol Loxenatide Injection (Glucagon-like peptide-1, GLP-1) on endothelial cells from middle-aged and elderly patients with newly diagnosed or poorly controlled type 2 diabetes mellitus (T2DM). GLP-1 weekly formulation was analyzed for cardiovascular disease protection and correlated with intestinal flora.

Design: Stool samples were collected from middle-aged and elderly patients with new-onset or poorly controlled type 2 diabetes in Longhu People's Hospital and Shantou Central Hospital from June 2019 to November 2019. Samples were collected at week 0, 4, and 8 of treatment with GLP-1 weekly formulations. Samples were analyzed for metagenomic sequencing. Analysis was performed to compare the characteristics of the gut microbiota at week 0, 4, and 8 of GLP-1 treatment and to correlate different microbiota with characteristic clinical parameters.

Results: Statistical differences were found in blood glucose lowering, cardiovascular endothelial, and inflammation-related indices between week 0 and W4 and in blood glucose lowering and cardiovascular endothelial indices from week 0 to 8 in the newly diagnosed or poorly controlled type 2 diabetic patients treated with GLP-1. Changes in gut microbiota at week 0, 4, and 8 after using GLP-1 were not statistically different, but had an overall trend of rising and then falling, and with different bacteria, that were correlated with different clinical indicators.

OPEN ACCESS

Edited by:
Leming Sun,
Northwestern Polytechnical University, China

Reviewed by:
Barkat A. Khan,
Gomal University, Pakistan
Dong-Hua Yang,
St. John's University, United States

***Correspondence:**
Chuanxing Xiao
xiaoxx@163.com
Kaijian Hou
kaijianhou@126.com

[†]These authors have contributed equally to this work and share first authorship

Specialty section:
This article was submitted to Molecular Diagnostics and Therapeutics, a section of the journal Frontiers in Molecular Biosciences

Received: 19 February 2022
Accepted: 19 April 2022
Published: 15 June 2022

Citation:
Chen F, He L, Li J, Yang S, Zhang B, Zhu D, Wu Z, Zhang S, Hou D, Ouyang C, Yi J, Xiao C and Hou K (2022) Polyethylene Glycol Loxenatide Injection (GLP-1) Protects Vascular Endothelial Cell Function in Middle-Aged and Elderly Patients With Type 2 Diabetes by Regulating Gut Microbiota. Front. Mol. Biosci. 9:879294. doi: 10.3389/fmolb.2022.879294

Conclusion: GLP-1 improves endothelial cell function indicators in middle-aged and elderly diabetic patients, which may be related to its alteration of the population numbers of gut microbiota such as *Acinetobacter*, *Eubacterium ramulus ATCC 29099*, and *Bacteroides_faecis*. This study provides a guidance for the treatment of type 2 diabetic patients.

Keywords: GLP-1, type 2 diabetes mellitus, gut microbiota, vascular endothelial cells, middle-aged

1 INTRODUCTION

With the changes in human lifestyle, the prevalence of diabetes is increasing and has become a very serious public health problem worldwide and in China. Although the pathogenesis of diabetes is controversial, it is generally believed to be related to host genes, environment, diet structure, and gut microbiota dysbiosis. In recent years, many studies have revealed that the occurrence, development, and prognosis of diabetes may be associated with gut microbiota (Ma et al., 2019).

The human gastrointestinal tract contains normally a large number of normal microbiota, mainly composed of the Firmicutes, Bacteroidetes, Actinomycetes, Aspergillus, and Wolbachia phyla (Lozupone et al., 2012). The type and quantity of gut microbiota in the guts of diabetic patients are somewhat different compared to normal people (Jayalakshmi et al., 2009; Sedighi et al., 2017). For example, Zhang et al. found a greater number of butyric acid-producing bacteria Akkermansia muciniphila and Faecalibacterium prausnitzii in the normal population than in the pre-diabetic population, the number of anthropoid bacteria was only half of that in the pre-diabetic and the abundance of Wolbachia bacteria was significantly reduced in the diabetic population (Larsen et al., 2010). Moreover, Wu et al. (2010) respectively reported that *Bacillus* or *Bifidobacteria* was significantly decreased in T2DM compared to that of the normal healthy controls. In recent years, it has been found that human gut microbiota is involved in the development of obesity, insulin resistance, and diabetes through different mechanisms, and that many blood glucose-lowering drugs cause changes in gut microbiota. For example, a study (Cao, 2015) found a significant increase in the number and proportion of enterobacteriaceae in type 2 diabetes patients after treatment with acarposose compared with the control group, reaching 71%. Xu et al. conducted high-throughput sequencing analysis on 68 patients with type 2 Diabetes Mellitus (T2DM) (Xu et al., 2013) and found that the number of bifidobacteria in the oral acarbose treatment group increased significantly compared with the control group after 3 months. This was consistent with the results of Su, Aitken and Gerwitz's study, that is, the number of bifidobacteria in the intestinal microflora of T2DM patients treated with acarbose was significantly higher than that of the control group (Aitken and Gewirtz, 2013; Su et al., 2015). Sun, 2014 found that patients with T2DM treated with metformin showed significant changes in the community composition of their intestinal flora, with an increase in species and no significant difference in the dominant bacteria compared to healthy individuals. Burton et al. (2015) found that the diversity and composition of the gut microbiota changed significantly during metformin treatment, and the use of metformin in combination with gastrointestinal microbial modulators may increase patient tolerance to metformin. Lee and Ko (2014), using mice as experimental subjects, found that the number of *Bacteroidetes* in mice on high-fat diet was significantly reduced compared with the control group while the number of *thick-walled bacteria* was significantly increased compared with the control group, and the number of mimics in mice on high-fat diet was significantly increased after treatment with metformin and was close to that in mice on non-high-fat diet. Hwang et al. (2015) found that the application of liraglutide in diabetic rats led to decrease in the number of microbiota on top of the decrease in the number of high-fat diet microbiota, suggesting a connection between liraglutide and gut microbiota. The above experimental results suggest that some drug treatments for diabetes can cause changes in gut microbiota.

In recent years, a new class of therapeutic drugs targeting the effect of enteroglucagon has been used in clinical practice. The drugs are divided into two types according to mechanism: glucagon-like peptide 1 receptor agonists and dipeptidyl peptidase (DPP-4) inhibitors. GLP-1 agonists have been shown to not only reduce fasting blood glucose (FBG) and 2 h postprandial blood glucose (2hPG), but also reduce body weight, control eating, and protect the function of pancreatic islet B cells (Nadkarni et al., 2014) Representative GLP-1 agonists are lalutide and exenatide. DPP-4 inhibitors can limit the degradation of endogenous GLP-1 (Pratley et al., 2012), and representative drugs include sitagliptin, saxagliptin, liragliptin, and vigliptin. DPP-4 inhibitors are used to enhance glucose-dependent insulin secretion and lower blood glucose by inhibiting the degradation of GLP-1 and increasing fasting and postprandial GLP-1 levels (Nyborg et al., 2012; Xu and Jin, 2014). In terms of plasma half-life, exenatide has a short half-life and is suitable for a twice daily dosing regimen, liraglutide has a long half-life and is suitable for once daily, mainly because the self-linking effect slows down its absorption and binds to albumin and improves its stability to DPP-4 and neutral endopeptidase (NEP). Benalutide has a short half-life and is suitable for a three times daily dosing regimen. The number of doses, gastrointestinal discomfort (including diarrhea, dyspepsia, gastrointestinal reflux disease, nausea, vomiting) is more serious, while multiple injections of dosing, the painful feeling of needle injection, etc. will greatly reduce the patient's long-term compliance with the drug, thus making the drug less effective (de Moraes and Layton, 2016).

On 3 January 2018, the first glucagon-like peptide-1 receptor agonist weekly formulation in China was officially approved by the State Food and Drug Administration, providing a new

therapeutic option for improving glycemic control in patients with type 2 diabetes. The GLP-1 weekly formulation can greatly reduce the frequency of dosing, reduce gastrointestinal adverse effects, and increase the stability of the drug and improve patient compliance, which will provide a new treatment option for most Chinese patients with T2DM (Zhou et al., 2019). Currently, the GLP-1 receptor agonist weekly formulations are available in the United States, Europe, Japan, Korea, Hong Kong, Taiwan, and many other places, and the overall safety is good in the clinics. In addition, studies indicate that GLP-1 analogs, including liraglutide, reduce the risk of cardiovascular events in T2DM due to the expression of GLP-1 receptor) on different cell types, including endothelial cells and immune cells (Helmstädter et al., 2020). Other studies show that the potential cardioprotective effects of GLP-1 can be attributed to their multiple non-glycemic actions in the cardiovascular system, including weight loss, lower blood pressure, improved lipid profile, and direct effects on cardiac and vascular endothelial cells (Andrikou et al., 2019). However, its specific efficacy, safety, and effect on gut microbiota with lowering blood glucose have not been described. There is a lack of data from large-scale prospective studies in our country on the efficacy, safety, compliance, and effects on gut microbiota of GLP-1 weekly preparations in hypoglycemia. Whether the glucose-lowering index of GLP-1 weekly preparation and the protective effect on cardiovascular disease are also related to the change of gut microbiota has not been shown.

In the treatment of type 2 diabetic patients with GLP-1 weekly formulation, we found that the efficacy varied from individual to individual and that patients were accompanied by different degrees of digestive symptoms. Considering the presence of extra-islet glucose control factors, we hypothesized that gut microbiota may influence the therapeutic effect of GLP-1 weekly formulation by affecting the intestinal inflammatory response. To test this hypothesis, this study was proposed to include patients with T2DM who were newly diagnosed or had poor blood glycemic control on metformin alone, who met the enrollment criteria, in an open prospective study. Through an 8-weeks pharmacological intervention, T2DM patients were compared before and after 4, and 8 weeks of treatment for changes in gut microbiota, and related metabolic, vascular endothelial cell function, and inflammatory factors. To support the hypoglycemic effect of GLP-1 weekly preparations and the cardiovascular disease protective effect and the cardiovascular disease protective effect. The results show that GLP-1 improves endothelial cell function indicators in middle-aged and elderly diabetic patients, which may be related to its alteration of the population numbers of specific bacteria in the intestinal microbiome.

2 MATERIALS AND METHODS

2.1 Patient Recruitment

2.1.1 Clinical Patient Enrollment

Patients with T2DM who were newly diagnosed clinically or poorly controlled by metformin alone were characterized based on WHO 1999) diagnostic criteria for diabetes mellitus: typical diabetic symptoms + random blood glucose ≥ 11.1 mmol/L; diabetic symptoms + fasting blood glucose (FPG) ≥ 7.0 mmol/L; diabetic symptoms + 2 h postprandial blood glucose ≥ 11.1 mmol/L; oral 75 g anhydrous glucose loading test (OGTT), 2hPG ≥ 11.1 mmol/L confirmed the diagnosis of diabetes mellitus. Diabetic symptoms refer to irritable and excessive drinking, polyuria, polyphagia, and unexplained weight loss. For those without diabetes, only one blood glucose value meets the diagnostic criteria for diabetes, and the diagnosis must be confirmed by rechecking on another day. Random blood glucose refers to any time of the day, regardless of the time of the last meal and food intake; fasting status refers to no calorie intake for at least 8 h.

A total of 12 volunteers were recruited, and the enrolled investigators maintained records of the pre-screened subjects, or a subject screening log. The clinical study followed the Declaration of Helsinki and the official Chinese regulations for clinical research studies. Subjects were enrolled in the clinical study only after they voluntarily sign the informed consent form, and patient privacy was maintained and ensured by the investigator.

2.1.2 Patient Recruitment Standards

Subjects included in this study met the following criteria: male and female subjects were 20 to 75 years old; patients with newly diagnosed T2DM had not been treated with oral hypoglycemic agents or insulin, or patients with T2DM were being treated with metformin but exhibited poor blood glucose control; 6.3% ≤ HbA1c ≤ 10.5%; Fasting C-peptide (FCP) > 1 nmol/L.

Participation and cooperation in the study was voluntary, and all subjects signed an informed consent form.

2.1.3 Exclusion Criteria

Subjects were not included in this study if any of the following exclusion criteria were met: 1) Patients with other types of diabetes mellitus rather than T2DM; 2) Those with severe combined diabetic complications such as diabetic ketoacidosis, hyperosmolar hyperglycemic syndrome, or lactic acidosis; 3) Patients with clinically significant hepatobiliary disease, including but not limited to, chronic active hepatitis and/or severe hepatic insufficiency, cirrhosis, glutamic aminotransferase (ALT) or glutamic oxalacetic aminotransferase (AST) > 3 times the upper limit of normal (150 U/L), or serum total bilirubin (TB) > 34.2 μmol/L (>2 mg/dl); 4) Patients with the following history of renal disease or features associated with renal disease: history of unstable or rapidly progressive renal disease, patients with moderate/severe renal impairment or end-stage renal disease, glomerular filtration rate estimate (eGFR) < 60 ml/min/1.73 m^2, serum creatinine (Cr) ≥ 133 μmol/L (≥1.50 mg/dl) in male subjects and serum Cr ≥ 124 μmol/L (>1.40 mg/dl) in female subjects; 5) Any of the following cardiovascular conditions: myocardial infarction, cerebral infarction, cardiac surgery or revascularization (coronary artery bypass grafting/percutaneous transluminal coronary angioplasty), unstable angina, congestive heart failure (New York Heart Association class III or IV), transient ischemic

attack, or significant cerebrovascular disease within the last 12 weeks; 6) History of gastrointestinal disease or surgery, including intestinal obstruction, intestinal ulcer, bariatric surgery or girdle surgery, gastrointestinal anastomosis, or bowel resection; 7) Pregnant women who were breastfeeding; 8) Urinary tract infection within the last 2 weeks; 9) Subjects who are in the judgment of the investigator unlikely to comply with the protocol, or patients with serious physical or psychological illnesses that could affect the effectiveness or safety of the study.

2.2 Interventions

In 12 subjects who voluntarily participated and signed the relevant consent forms, with T2DM newly diagnosed clinically or poorly controlled by metformin alone and who met the inclusion criteria and did not meet the exclusion criteria, relevant specimens were retained before the use of the GLP-1 weekly preparation, and then the GLP-1 weekly preparation (Polyethylene Glycol Loxenatide Injection 0.2 mg each time, subcutaneously every 1 week) was started. The corresponding indices were checked again after 4 and 8 weeks. Changes in glycated hemoglobin and intestinal flora were recorded before and after 4 and 8 weeks of treatment, as well as changes in the following indicators before and after 8 weeks of treatment: fasting glucose, 2-h postprandial glucose, fasting insulin, 2-h postprandial insulin, fasting C-peptide, 2-h postprandial C-peptide, HOMA-IR index, HOMA-HBCI; weight, BMI, waist circumference, waist-to-hip ratio, body fat percentage, basal metabolic rate, etc. Inflammatory factors examined were: CRP (ultrasensitive C-reactive protein), IL-6, IL-8, MCP-1, TNF-α, IL-1β; Changes in vascular endothelial cell function were measured: peripheral blood plasma EMPs levels, markers of endothelial dysfunction associated with inflammation, including soluble intercellular adhesion molecule (sICAM-1), vascular cell adhesion molecule (VCAM-1) and P Selectin, NO, prostacyclin PGI2, and endothelin-1 (ET-1). In addition, markers of endothelial dysfunction related to thrombosis were examined: tissue factor, tissue-type fibrinogen activator, von Willebrand factor, and fibrinogen activator factor inhibitor (PAI-1) change values. The number of hypoglycemia occurrences, combined medications, and adverse events were recorded throughout the study.

2.3 Endpoints

2.3.1 Primary Endpoint

Primary endpoints were HbA1c values and changes in gut microbiota of patients before and after 4 and 8 weeks of treatment.

2.3.2 Secondary Endpoint

Secondary endpoints measured were changes in the following indexes after 4 and 8 weeks of GLP-1 weekly formulation intervention.

(1) Glucose metabolism indexes: fasting/2-h postprandial glucose, fasting/2-h postprandial insulin, fasting/2-h postprandial C-peptide, HOMA-IR index, and HOMA-HBCI.
(2) Obesity-related indicators: weight, BMI, waist circumference, hip circumference, waist-to-hip ratio, basal metabolic rate, and total energy.
(3) Inflammatory factors: CRP (hypersensitive C-reactive protein), IL-6, IL-8, MCP-1, TNF-α, and IL-1β.
(4) Vascular endothelial cell function-related indicators: changes in vascular endothelial cell function, including peripheral blood plasma EMPs levels, markers of endothelial dysfunction related to inflammation: soluble intercellular adhesion molecule, vascular cell adhesion molecule and P-selectin, Nitric Oxide (NO), prostacyclin PGI2, endothelin-1; markers of endothelial dysfunction related to thrombosis, including tissue factor, tissue-type fibrinogen activator, von Willebrand factor, fibrinogen activator factor inhibitor.
(5) The ratio of HbA1c ≤ 7.0%.
(6) The ratio of patients with hypoglycemia and gastrointestinal discomfort (blood glucose ≤ 3.9 mmol/L).

2.3.3 Follow-Up Visit Plans

Follow-up visits were performed in the hospital at W0 (week 0), W4 (weeks 4), and W8 (weeks 8), with a 1-month telephone visit at the end of the study.

2.4 Analysis of Intestinal Flora

Fecal samples from T2DM patients were collected on the day of the medical examination and stored in microbiota stabilizer EffcGut (Yang et al., 2020) untill DNA extraction. Fecal genomic DNA was extracted using the QIAamp Fast DNA Stool Mini Kit (Qiagen, CA, United States). DNA samples were fragmented to an insert size of 400 bp for library prearation and sequenced by Illumina Nova seq with PE 150 reagents. Raw reads were trimmed to filter the sequencing adapter, low-quality reads, and the human genome (based on reference hg18). Micorbial gene profiles and KEGG orthologous groups (KOs) were generated by aligning the obtained high-quality reads to the reference gene catalogue as previously described (Li et al., 2014). The taxonomic composition at genus, species and strain levels were processed using MetaPhlAn2 (Segata et al., 2012). The differences in the structural composition and functional prediction of bacterial diversity in the W0 and W4and W8 groups using GLP-1 were compared. At the same time, macro-gene sequencing was performed on some samples and sequence splicing function annotation was performed to explore the role of bacteria in the treatment of T2DM from the species level.

2.5 Statistical Analysis

Two independent sample T tests were used to compare the mean difference of HbA1c and the secondary end point indexes. For measurement data with non-normal distribution and microbial eatues, Wilcoxon rank sum test was used for comparison between groups. Spearman correlation was used to the calculate the correlation

TABLE 1 | Clinical information for patients treated with GLP-1 from W0 toW4.

Participants, *n* = 12	W0–W4 (T test)			
Clinical information	**W0_sd**	**W4_sd**	***p*-value_04t**	**p.adjust_04t**
PAI-1	61.23 ± 6.4	57.65 ± 6.52	5.40E-06	0.00019718
Tissue factor	56.69 ± 6.46	52.78 ± 5.99	3.60E-05	0.00065758
Endothelin-1 (ET-1)	96.5 ± 20.28	91.85 ± 19.82	0.000139623	0.00203849
Von willebrand factor	192.54 ± 16.03	182.98 ± 14.9	2.61E-06	0.00019078
Tissue type fibrinogen activator	16.68 ± 2	17.86 ± 1.88	2.33E-05	0.00056622
Prostacyclin PGI2	99.55 ± 19.09	106.7 ± 22.97	0.001445291	0.01758438
LDLC	3.17 ± 1.05	2.76 ± 0.87	0.002960829	0.02879347
Albumin	43.03 ± 3.49	44.21 ± 3.78	0.31165418	0.517062617
Apolipoprotein A (g/L)	1.39 ± 0.3	1.38 ± 0.24	0.896860597	0.909316994
Glucose	10.83 ± 4.32	8.83 ± 2.29	0.07037148	0.210221666
Age	62.01 ± 10.61	62.01 ± 10.61	NA	NA

Note: The data were expressed as mean ± SD.

TABLE 2 | Clinical information for patients treated with GLP-1 from W0 to W8.

Participants, *n* = 12	W0–W4 (T test)			
Clinical information	**W0_sd**	**W8_sd**	**pvalue_08t**	**p.adjust_08t**
PAI-1	61.23 ± 6.4	54.55 ± 6.15	1.64E-08	5.98E-07
Tissue factor	56.69 ± 6.46	49.45 ± 5.22	1.23E-07	2.99E-06
Endothelin-1 (ET-1)	96.5 ± 20.28	84.85 ± 17.72	3.77E-07	6.88E-06
Von willebrand factor	192.54 ± 16.03	175.77 ± 14.51	1.99E-09	1.45E-07
Tissue type fibrinogen activator	16.68 ± 2	18.89 ± 2.42	2.24E-05	0.000327513
Prostacyclin PGI2	99.55 ± 19.09	118.68 ± 31.65	0.00071005	0.007404807
LDLC	3.17 ± 1.05	2.32 ± 0.82	0.001058853	0.009662035
Albumin	43.03 ± 3.49	47 ± 2.89	0.000343558	0.004179959
Apolipoprotein A (g/L)	1.39 ± 0.3	1.47 ± 0.25	0.492811875	0.609750286
Age	62.01 ± 10.61	62.01 ± 10.61	NA	NA

Note: The data were expressed as mean ± SD.

between clinical data and microbial taxa. Data were visualized using R language (Mair et al., 2015), mainly with packages of reshape2 (Zhang, 2016), ggplot2[1], ggsignif, ape (Paradis et al., 2004), gridExtra[2].

3 RESULTS

3.1 Improvement of Clinical Indicators

In this study, a total of 36 stool samples and clinical data from 12 patients with T2DM were analyzed at W0, 4, and 8 during treatment with GLP-1. The patients had a mean age of 62 years at baseline and a mean BMI of 21.57. This study identified clinical indicators that showed significant changes between W0 and W4, and between W0 and W8. The glucose lowering indicators with significant differences in improvement at W4 compared to W0 were 2HPG, FCP; the cardiovascular endothelium-related indicators that improved were tissue factor, PAI-1, Endothelin-1, von Willebrand factor, tissue type fibrinogen activator, Prostacyclin PGI2, and LDLC. One weight-related indicator improved, BMI (kg/m2), and one inflammation-related indicator improved, IL-6 (**Table 1**). The glucose lowering indices with significant difference improvement at W8 compared with W0 were: HbA1c, islet β-cell function index [HOMA-β: 20 * FINS/(FPG-3.5)], FBG, 2HPG, and FINS. Cardiovascular endothelium related indexes improved were: tissue factor, albumin, von Willebrand factor, tissue type fibrinogen activator, and adenosine dehydrogenase (**Table 2**). These clinical indicators, which were statistically different between 0 to W4, and between 0 and W8, are markers of endothelial dysfunction associated with diabetes and thrombosis, indicating that GLP-1 has a good hypoglycemic effect on type 2 diabetic patients and a protective effect on vascular endothelial function.

3.2 Changes in Gut Microbiota in Middle-Aged and Elderly Patients With T2DM Treated With GLP-1 at 0, 4, and W8

Comparing the differences in the intestinal flora diversity and function prediction of T2DM patients after GlP-1 treatment at 0, 4, and W8. At the same time, macrogene sequencing was performed on some samples and sequence-splicing function

[1]*<ggplot2- Elegant Graphics for Data Analysis.pdf>*.
[2]*<gridExtra.pdf>*.

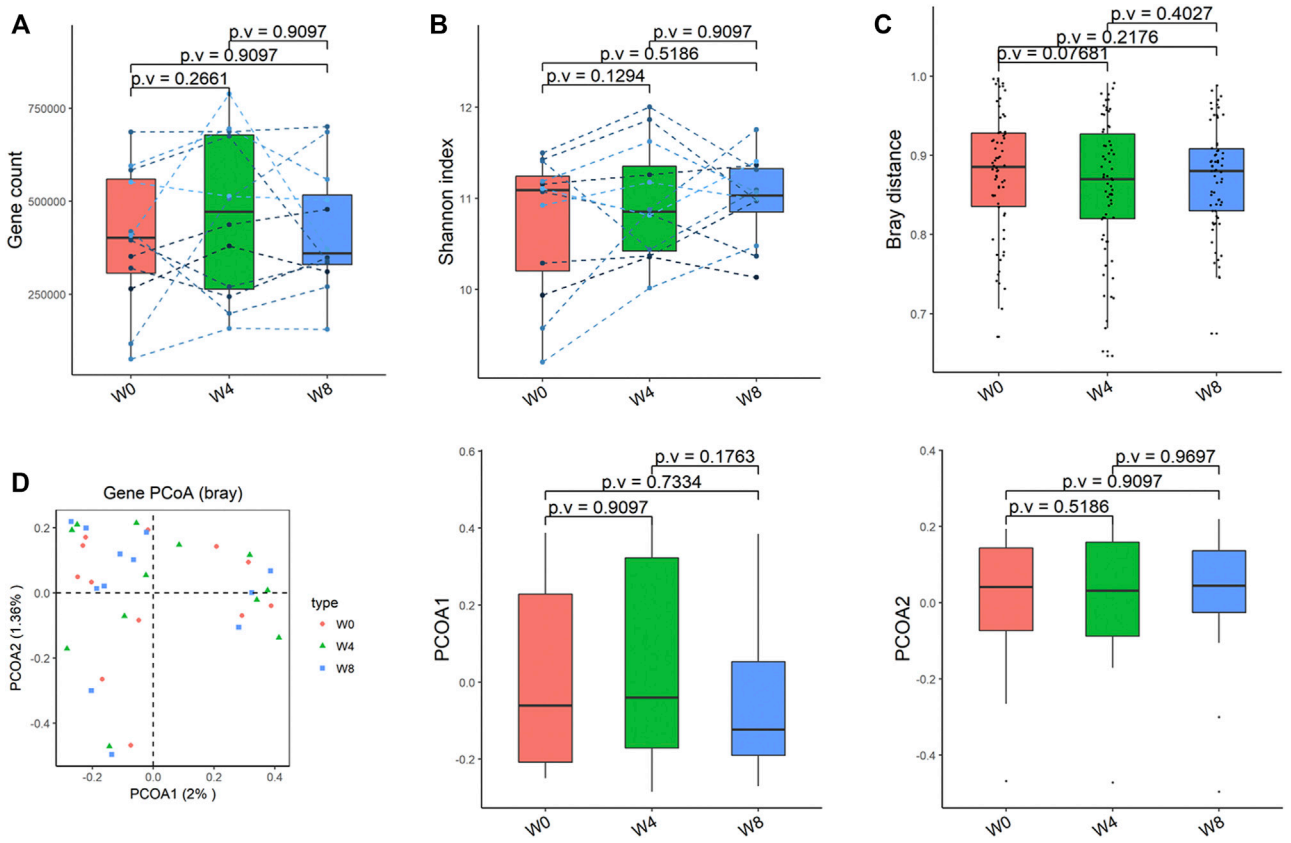

FIGURE 1 | Alpha-diversity, beta-diversity, and principal component analysis at the gene level. **(A)** Gene count detected was not significantly different in comparisons between W0 and W4, W0 and W8, and W4 and W8. **(B)** Shannon index was not significantly different in comparisons between W0 and W4, W0 and W8, and W4 and W8 **(C)** No significant difference in beta diversity based on Bray-Curtis (Bray) distance for W0 vs W4, W0 vs W8, and W4 vs W8. **(D)** PCoA analysis based on Bray distance showed that the first principal component was not significantly different in W0 vs W4, W0 vs W8, and W4 vs W8, nor the second component.

annotation was performed to explore the role of bacteria in the treatment of T2DM at the species level. Diversity analysis at the gene level, T2DM including gene stripes (A), Alpha diversity (B), Beta diversity (C), and principal component analysis (D), was performed as shown in **Figure 1**. The number of genes showed an increasing trend after W4 of GLP-1 use, but then showed a decreasing trend at W8. There was a trend of change in the number of genes in patients after GLP-1 use. Although this trend was not statistically significant ($p > 0.05$). There was also an upward and then downward trend at the genus (**Figure 2**) and species and subspecies levels (as shown in **Figures 3**, **4**). In terms of microbial diversity, the overall trend was rising and then declining (see **Figure 2**). At the genus level, one significant difference can be found for the genera atW0,W4, and W8: *Acinetobacter* ($p < 0.005$); at the species level, one significant difference can be found at W0, W 4, and W8: *Acinetobacter-unclassified* ($p < 0.005$). Two bacteria were significantly different at 0 and W8: *Acinetobacter-unclassified* ($p < 0.05$) and *Bacteroides_faecis* ($p < 0.05$); one bacteria differed significantly at W4 and W8: *Eubacterium_ramulus*. Significant difference analyses at the strain level, in W0 versus W4, W0 versus W8, and W4 versus W8, revealed the following: at W0 and W8 there was a significant difference in the strain level, *Bacteroides faecis MAJ27*; at W4 and W8 there were a significant differences in the strain level of *Clostridium bolteae* ($p < 0.05$) and *Eubacterium ramulus ATCC 29099* ($p < 0.05$) (**Figure 5**).

To verify the change of functional pathways, KO—Alpha Diversity, KO—beta Diversity, KO—Principal Coordinate Analysis PCoA (Bray) were analyzed and found that there was changes in the functions with signals, modules, pathways. The beta diversity based on Jensen-Shannon Divergence (JSD) distance was significantly different at 0 and W4 ($p = 0.001$), and 0 and W8 ($p = 0.046$) (**Figure 6**).

In addition, we also analyzed the significant differences of phenotypes in W0 and W4, W0 and W8, and W4 and W8, and found that there were 27 significantly different phenotypes in W0 and 4, 23 significantly different phenotypes in W0 and W8, and 18 significantly different phenotypes in W4 and 8. Permanova analysis of significantly different phenotypes based on the bray distance at the gene level showed that 19 phenotypes had a significant effect on gut microbes ($p < 0.05$) as shown in **Figures 7**, **8**. As clearly shown in the **Table 3** below, glucose

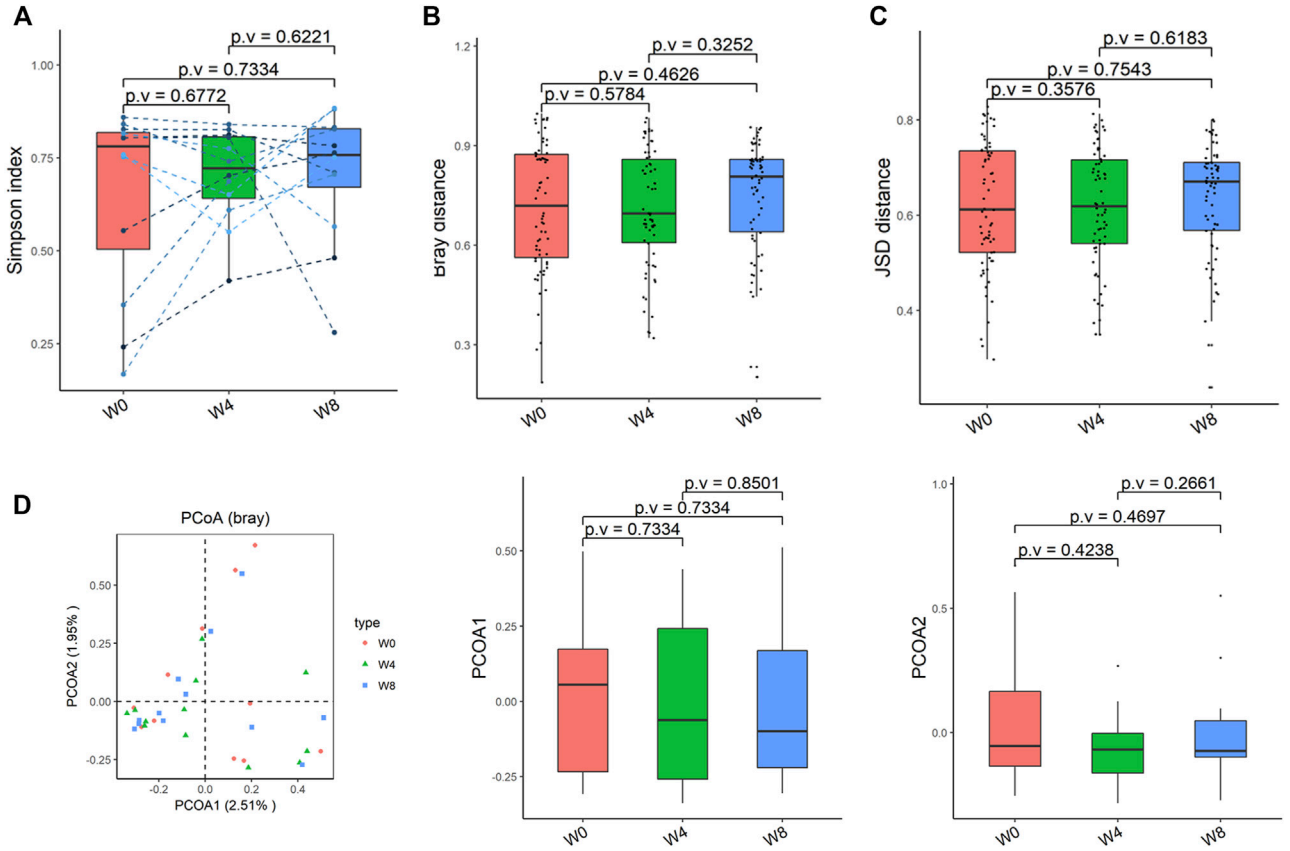

FIGURE 2 | Alpha-diversity, beta-diversity, and principal component analysis at the species level. **(A)** Simpson index was not significantly different in comparisons between W0 and W4, W0 and W8, and W4 and W8. **(B)** No significant difference in beta diversity based on Bray-Curtis (Bray) distance for W0 vs W4, W0 vs W8, and W4 vs W8. **(C)** The Jensen-Shannon Divergence (JSD) distance-based beta diversity was not significantly different in W0 vs W4, W0 vs W8, and W4 vs W8. **(D)** PCoA analysis based on Bray distance showed that the first principal component was not significantly different in W0 vs W4, W0 vs W8, and W4 vs W8, nor the second component.

lowering indices and cardiovascular disease related indices correlate with gut microbes.

With the change of time, there was a decreasing trend of body mass index and vascular damage related indexes at different time points of W0, W4, and W8 of treatment with GLP-1 in type 2 diabetes. This indicates that GLP-1 has a good effect on weight reduction and protection of vascular endothelial cells. The indicators associated with beneficial effects on cardiovascular disease showed an increasing trend, and those associated with harmful effects on cardiovascular disease showed a decreasing trend. The specific indicators of change include Prostacyclin PGI2, tissue-type fibrinogen activator with an increasing trend, while some indicators such as fibrinogen activator inhibitor-1 (PAI-1), endothelin-1 (et -1), and Tissue factor (et al.) showed a decreasing trend. Waist circumference and waist-to-hip ratio showed a decreasing trend. Cycloprost PGI2, endothelin, tissue factor, tissue-type fibrinogen activator, and vascular pseudohemophilic factor are all indicators related to vascular endothelial function, and the changes in these indicators are the main clinical results of the protective effect of GLP-1 on vascular endothelium in middle-aged and elderly diabetic patients, indicating that GLP-1 has a protective effect on vascular endothelium (**Figure 8**).

3.3 Analysis of the Correlation Between Clinical Indicators and Gut Microbiota

Correlation analysis was undertaken to examine clinical indicators with significant differences in T2DM with characteristic differences in the gut microbiota genera, where "+" indicates p-value <0.05, and "*" indicates p-value <0.001. Clinical indicators with positive correlation and significant differences in the genus *Fusobacterium* were nitric oxide and blood sedimentation. Clinical indicators that were negatively correlated and significantly different from Aphanizomenon spp. were fasting C-peptide and 2-h postprandial C-peptide. Clinical indicators that showed a positive correlation with *Aphanizomenon*. with significant differences were total bile acids, 2-h postprandial C-peptide, aspartate aminotransferase, indirect bilirubin, total bilirubin, and direct bilirubin. Clinical indicators that showed a negative correlation with *Aphanizomenon*. with significant differences were

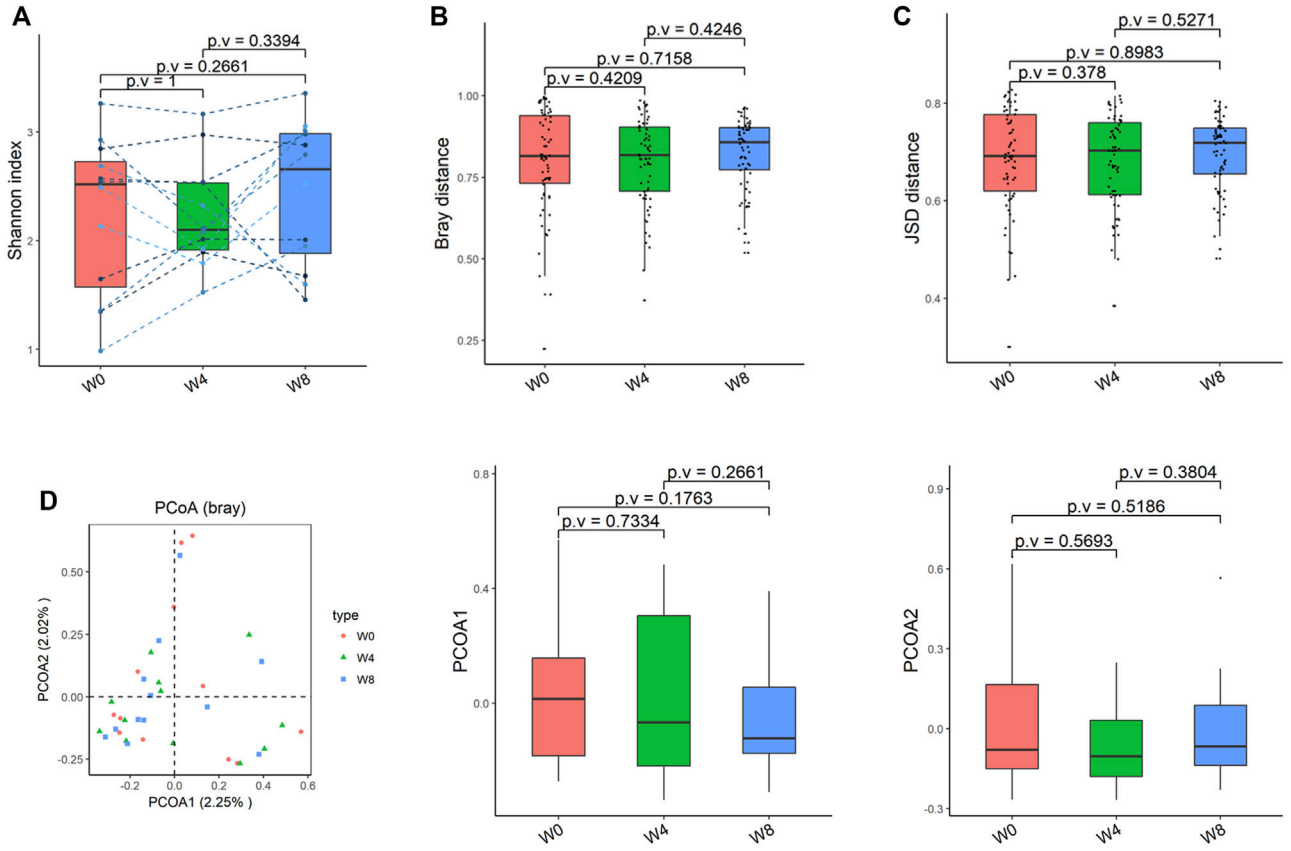

FIGURE 3 | Alpha-diversity, beta-diversity, and principal component analysis at the species level. **(A)** Shannon index was not significantly different in comparisons between W0 and W4, W0 and W8, and W4 and W8. **(B)** No significant difference in beta diversity based on Bray-Curtis (Bray) distance for W0 vs W4, W0 vs W8, and W4 vs W8. **(C)** The Jensen-Shannon Divergence (JSD) distance-based beta diversity was not significantly different in W0 vs W4, W0 vs W8, and W4 vs W8. **(D)** PCoA analysis based on Bray distance showed that the first principal component was not significantly different in W0 vs W4, W0 vs W8, and W4 vs W8, nor the second component.

homocysteine, cholinesterase, creatinine, urea nitrogen, cystatin, triglycerides, glycated hemoglobin, monocyte chemokine-1, interleukin-6, nitric oxide, and 2-h postprandial glucose (**Figure 8A**). Clinical indicators that showed a positive correlation with *Fusobacterium* with significant differences were nitric oxide. Significantly different clinical indicators that negatively correlated with *Fusobacterium* were fasting C-peptide and chloride. Clinical indicators that showed a positive correlation with *Fusobacterium* with significant differences were endothelin 1, a-L-amylase, total bilirubin, and indirect bilirubin. Clinical indicators that showed a negative association with *S. cerevisiae* with significant differences were uric acid, prostacyclin I2, body mass index, and apolipoprotein A. Clinical indicators that showed a positive association with *S. cerevisiae* with significant differences were aspartate aminotransferase, total bile acids, phosphocreatine isoenzymes, and phosphocreatine. Clinical indicators that showed negative correlation with *Acinetobacter* with significant differences were age, leukocytes, triglycerides, cysteine, creatinine, monocyte chemokine-1, total cholesterol, interleukin-6, nitric oxide, and uric acid (**Figure 8B**). The clinical indicators that showed positive correlation with *Acinetobacter* with significant differences were interleukin-6, leukocytes, triglycerides, globulin, total protein, and cysteine. Clinical indicators that showed positive correlation with *Acinetobacter* with significant differences were a-L-fucosidase, total bilirubin and indirect bilirubin (**Figure 8C**).

These results indicate that the gut microbiota and indicators related to glucose metabolism and vascular endothelial cell function were improved in T2DM patients after the use of GLP-1, suggesting that GLP-1 has a good hypoglycemic effect and protective effect on vascular endothelial function in patients with T2DM. In terms of microbial diversity, there was no significant difference among groups at 0, 4, and W8, but the overall trend was first increased and then decreased. There are individual species that are significant at the species level. The correlation analysis of clinical indicators and characteristic bacteria showed that the improvement of clinical indicators was closely related to the intestinal microflora ($p < 0.05$), suggesting that the hypoglycemic and endothelial protective effects of GLP-1 are closely related to the gut microbiota. That

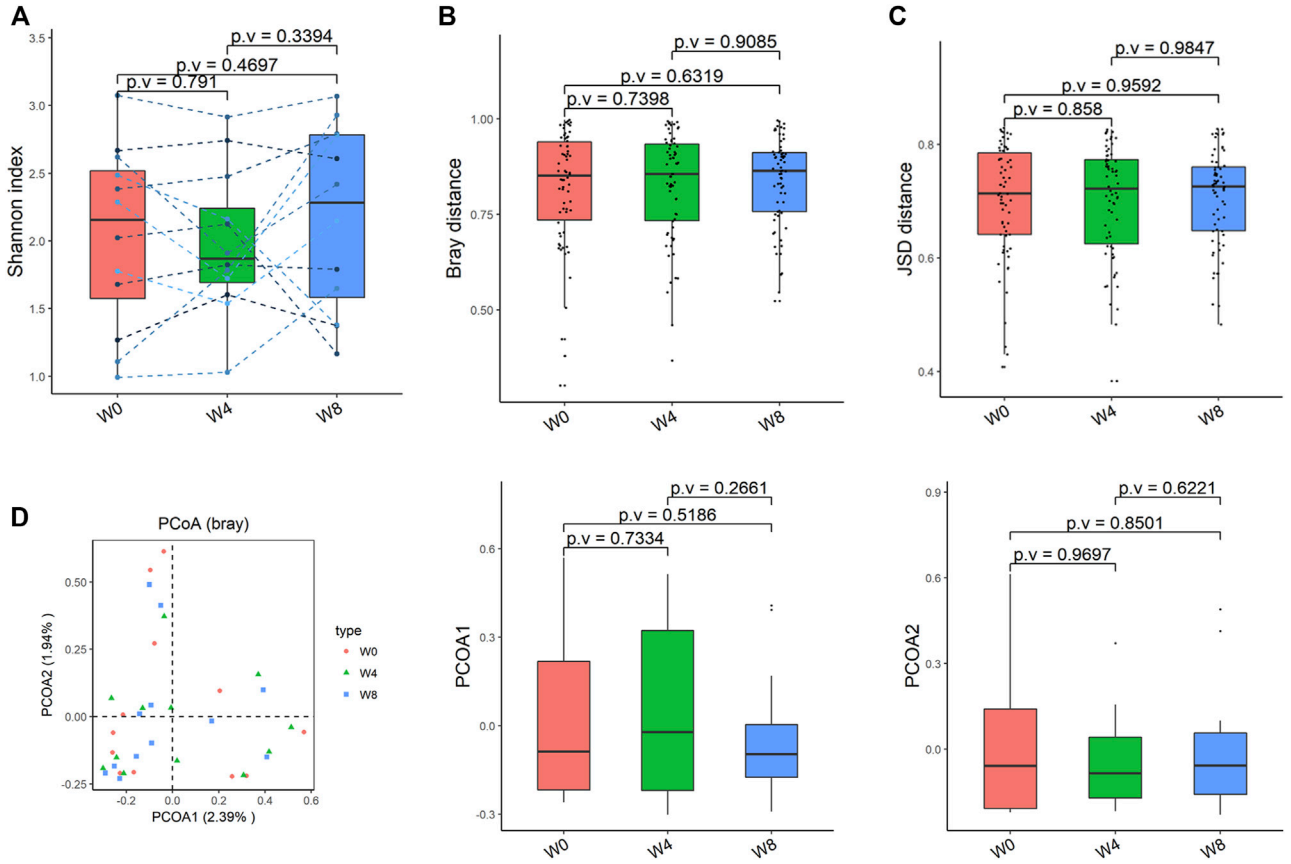

FIGURE 4 | Alpha-diversity, beta-diversity, and principal component analysis at the strain level. **(A)** Shannon index was not significantly different in comparisons between W0 and W4, W0 and W8, and W4 and W8. **(B)** No significant difference in beta diversity based on Bray-Curtis (Bray) distance for W0 vs W4, W0 vs W8, and W4 vs W8. **(C)** The Jensen-Shannon Divergence (JSD) distance-based beta diversity was not significantly different in W0 vs W4, W0 vs W8, and W4 vs W8. **(D)** PCoA analysis based on Bray distance showed that the first principal component was not significantly different in W0 vs W4, W0 vs W8, and W4 vs W8, nor the second component.

is, GLP-1 may protect vascular endothelial cell function in middle-aged and elderly patients with T2DM by regulating the gut microbiota.

4 DISCUSSION

Many studies shown that patients with T2DM led to impairment in endothelial-dependent vasodilatation, decreased expression of NO, showing a dysfunction of cardiovascular and endothelial. (Néri et al., 2021; Tay et al., 2021; Wang et al., 2021).

In our previously published article (Que et al., 2021), we found a consistent trend toward increased relative abundances of the phyla Firmicutes (class Negativicutes or family Veillonellaceae) and Actinobacteria and decreased relative abundances of Bacteroidetes (class Bacteroidia or family Bacteroidaceae) for T2DM. The relationship between T2DM-associated (enriched or depleted) genera and probiotics shows that *Clostridium* sensu stricto 1 and Blautia were positively correlated with B. breve, and that *Lactobacillus* enriched in T2DM patients was correlated negatively with B. bifidum.

The main change seen in various research is an increase in the amount of opportunistic pathogens (Qin et al., 2012; Karlsson et al., 2013; Allin et al., 2015) such as Akkermansia muciniphila (Qin et al., 2012) and four *Lactobacillus* species (Karlsson et al., 2013). And the decreased levels of the phylum Firmicutes, class Clostridia, Faecalibacterium, Roseburia, butyrate producers (Qin et al., 2012; Karlsson et al., 2013), Akkermansia muciniphila, Roseburia (Salamon et al., 2018) and species of the genus *Clostridium* and Akkermansia muciniphila (Allin et al., 2018).

The results of various studies differ from one another, but, in general, the genera negatively associated with T2D are *Bacteroides*, Bifidobacterium, Faecalibacterium, Akkermansia and Roseburia, and the genera Fusobacteria, Ruminococcus and Blautia are positively connected with this disease (Gurung et al., 2020; Bielka et al., 2022).

In this study, we found that the middle-aged and elderly diabetic patient population showed significant improvement in blood glucose lowering indices and inflammation-related indices after 8 and W4 of GLP-1 use compared to W0. Also, there were significant changes in the indicators related to vascular endothelial cell function, and this improvement was associated with the change in the populations of

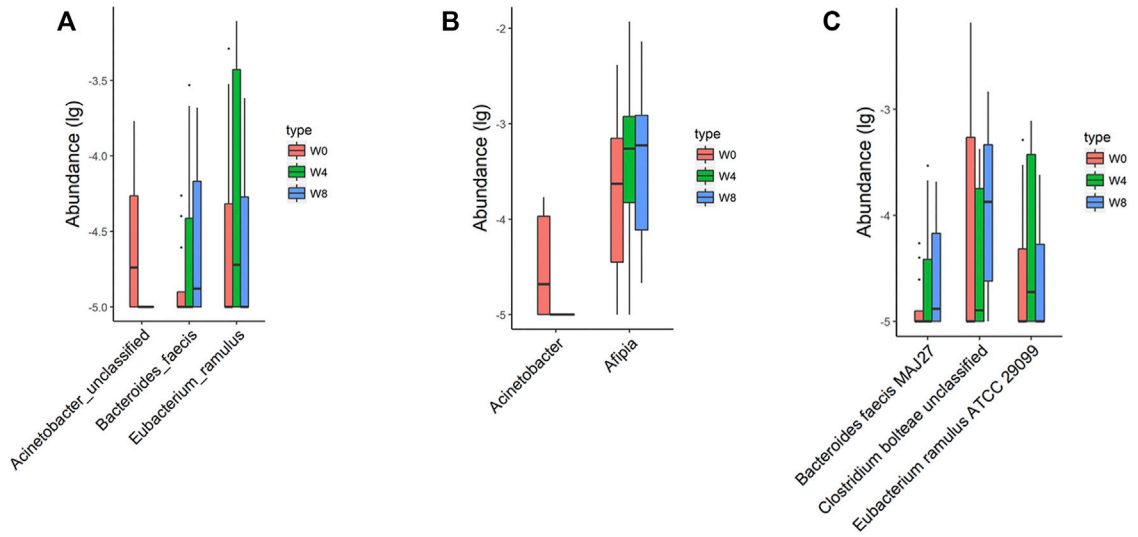

FIGURE 5 | Significantly different taxa at levels of species **(A)**, genus **(B)**, and strain **(C)** in comparisons between W0 vs W4, W0 vs W8, and W4 vs W8.

gut microbiota such as *Acinetobacter*, *afebola*, *Eubacterium twigs*, *Bacteroides*, and *Acinetobacter baumannii*. Furthermore, it was revealed that GLP-1 is not only a hypoglycemic drug, but also has a protective effect on the function of vascular endothelial cells in the middle-aged and elderly diabetic patients (Wang et al., 2013).

In our study, indicators related to vascular endothelial cell function, including Prostacyclin PGI2, tissue-type fibrinogen activator, fibrinogen activator inhibitor-1, endothelin-1, and tissue factor were improved, suggesting that GLP-1 can protect the cardiovascular system in treatment, which is consistent with the results of RCTs with large clinical data and long follow-up (Rutten et al., 2016; Ipp et al., 2017). In Leader's study, researchers found whether the GLP-1 receptor agonist liraglupeptide reduced the risk of cardiovascular death in a large clinical study of 374 elderly people at high cardiovascular risk. In T2 DM patients with a history of cardiovascular disease or cardiovascular risk factors, GLP-1 treatment significantly reduced the risk of the primary endpoint of cardiovascular death, non-fatal myocardial infarction, and stroke in diabetic patients (Ipp et al., 2017). In contrast, in the SUSTAIN-6 study, a placebo-controlled design was used to enroll a total of 3,297 patients ≥50 years of age with T2DM with the primary endpoint of first major adverse cardiovascular event (including cardiovascular death, nonfatal myocardial infarction, or nonfatal stroke). Results at W4 of follow-up showed a 26% reduction in the risk of MACE with somalutide, again showing that GLP-1 receptor agonists have cardioprotective effects (Ipp et al., 2017). It has also been shown in preclinical studies that both GLP-1 receptor agonists and DPP-4 inhibitors exhibit cardioprotective effects in animal models of myocardial ischemia and ventricular insufficiency through incompletely characterized mechanisms. At the species level, fasting blood glucose is negatively correlated with *Eubacterium ramulus*, *Roseburia inulinivorans*, *Roseburia hominis*, *Eubacterium eligens*, and *Ruminococcus callidus*. This indicates that patients with T2DM and diabetic cardiovascular complications have significant abnormal glucolipid metabolism and gut microbiota dysbiosis, and gut microbiota disorders may play an important role in the pathogenesis and progression of diabetes. In our study, the number of fine fungal bacteria was also changed in T2DM patients with GLP-1, and it was negatively correlated with prostacyclin I2. Prostacyclin I2 inhibits platelet-mediated agglutination process and has a strong vasodilatory effect, so that the production of prostacyclin I2 in the damaged vascular endothelium is reduced during coagulation, which facilitates platelet aggregation. Therefore, the vasoprotective effect of GLP-1 may be produced by regulating the number of fine branching fungi, thus affecting the production of prostacyclin I2.

In the present study we found that the gut microbiota of T2DM patients was significantly altered with the use of GLP-1, and the altered bacteria were: *Acinetobacter*, *afebola*, *Eubacterium twigs*, *Bacteroides*, *Acinetobacter baumannii*. Among them, the changes of *Acinetobacter*, *afebo*, and *Bacteroides* were correlated with NO. In this study after the use of GLP-1, NO of the patients was positively correlated with *Acinetobacter*, and negatively correlated with *afebo* and *Bacteroides*. NO is the primary endothelial regulator for local vascular tone and inhibits the production and action of other vasoactive factors, such as the vasoconstrictors prostaglandin and ET-1. In the early stages of vascular disease, when NO-mediated responses are impaired, prostacyclin and endothelium-dependent hyperpolarization are helpful in compensating for the damage. However, as the ability of endothelial cells to release NO gradually decreases, the production of endothelium-derived cyclic oxygenase-dependent contractile factor, ET-1, increases and helps vasoconstriction. At the same time, the protein expression of endothelial cell adhesion molecules (e.g., vascular cell adhesion molecule 1, intercellular adhesion molecule 1, E-selectin) is enhanced due to the diminished protective effect of NO, which promotes leukocyte adhesion and infiltration, resulting in increased E-selectin on endothelial cells and promoting leukocyte adhesion and infiltration (Vanhoutte, 2009; Vanhoutte et al., 2016; Vanhoutte et al., 2017). The elevated NO facilitates repair of endothelial injury.

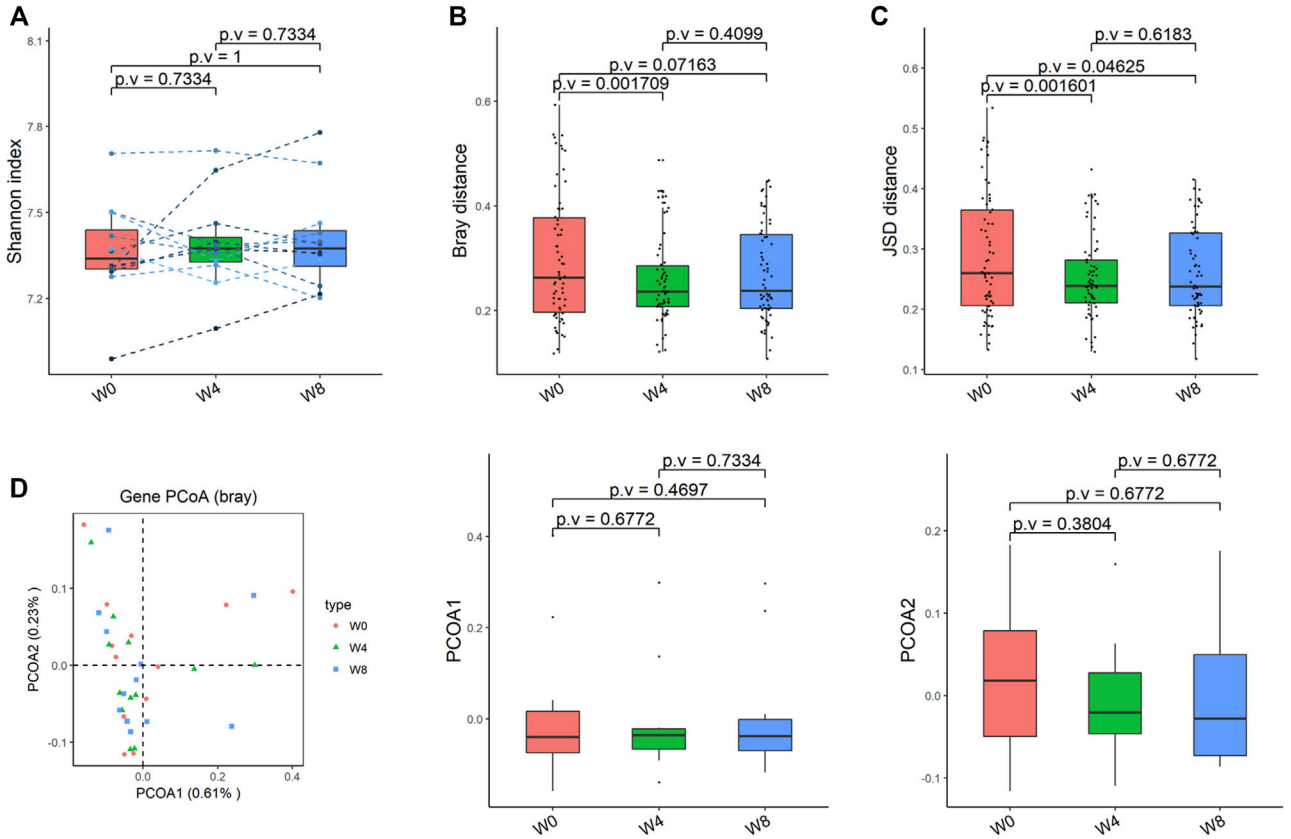

FIGURE 6 | Alpha-diversity, beta-diversity, and principal component analysis at the KO level. **(A)** Shannon index was not significantly different in comparisons between W0 and W4, W0 and W8, and W4 and W8. **(B)** Significant difference in beta diversity based on Bray-Curtis (Bray) distance for W0 vs W4, but not in W0 vs W8, norW4 vs W8. **(C)** The Jensen-Shannon Divergence (JSD) distance-based beta diversity was significantly different in W0 vs W4 and W0 vs W8, but not W4 vs W8. **(D)** PCoA analysis based on Bray distance showed that the first principal component was not significantly different in W0 vs W4, W0 vs W8, and W4 vs W8, nor the second component.

InT2DM patients in this study, NO levels were elevated after the administration of GLP-1, and the levels of NO were positively correlated with *Acinetobacter*, and negatively correlated with *afebo* and *Bacteroides*, which means the levels of *Acinetobacter* decreased while the levels of *afebo* and *Bacteroides* increased (Madsen et al., 2019). In a Japanese study of gut microbiota in obese and non-obese subjects, T-RFLP analysis showed that obese subjects had a significantly lower number of phylum *Bacteroides* and a significantly lower ratio of thick-walled phylum to phylum *Bacteroides* compared to non-obese subjects. Bacterial diversity was significantly higher in obese subjects compared to non-obese subjects (Kasai et al., 2015). In contrast, in animal experiments, we also observed an increase in SCFA-producing bacteria in experimental rats after GLP-1 (liraglutide) injection, including the genera *Anaplasma*, *Trichophyton*, and *Bifidobacterium* (Zhang et al., 2018). GLP-1 (liraglutide) significantly altered the overall composition of the intestinal microbiota, consistent with its weight loss effect (Wang et al., 2016). These reports are all consistent with our findings. It has been shown that a decrease in NO can lead to endothelium-dependent reduced vasodilatory function and affect the metabolism and function of the vascular wall, while overproduction of reactive oxygen species is one of the important factors contributing to endothelial dysfunction (Smits et al., 2021). Gut microbiota can promote atherosclerosis and vascular endothelial cell dysfunction. Vascular endothelial cell dysfunction, marked by impaired endothelium-dependent vasodilation, is an early indicator of atherosclerosis, and the expression of vascular microRNA-204 (miR-204) is remotely regulated by the flora, with miR-204 targeting downregulation of deacetylase 1, resulting in impaired endothelial cell function (Vikram et al., 2016).

In our study, type 2 diabetic patients with GLP-1 showed a decrease in BMI, an increase in *Bacteroides* levels, and a negative correlation with NO levels, suggesting that the use of GLP-1 in type 2 diabetic patients may alter the gut microbiota of patients, and that GLP-1 may exert vascular endothelial protective effects by increasing the levels of fecal *Bacteroides* in type 2 diabetic patients, regulating their body weight, causing a decrease in their BMI levels, and downregulating their NO levels, thereby inhibiting the production and effects on other vasoactive factors.

In terms of microbial alpha and beta diversity, alpha diversity is an ecological indicator of the abundance and diversity of microbiota in a sample (for example, the abundance distribution of detected microorganisms in each sample); beta diversity indicates differences

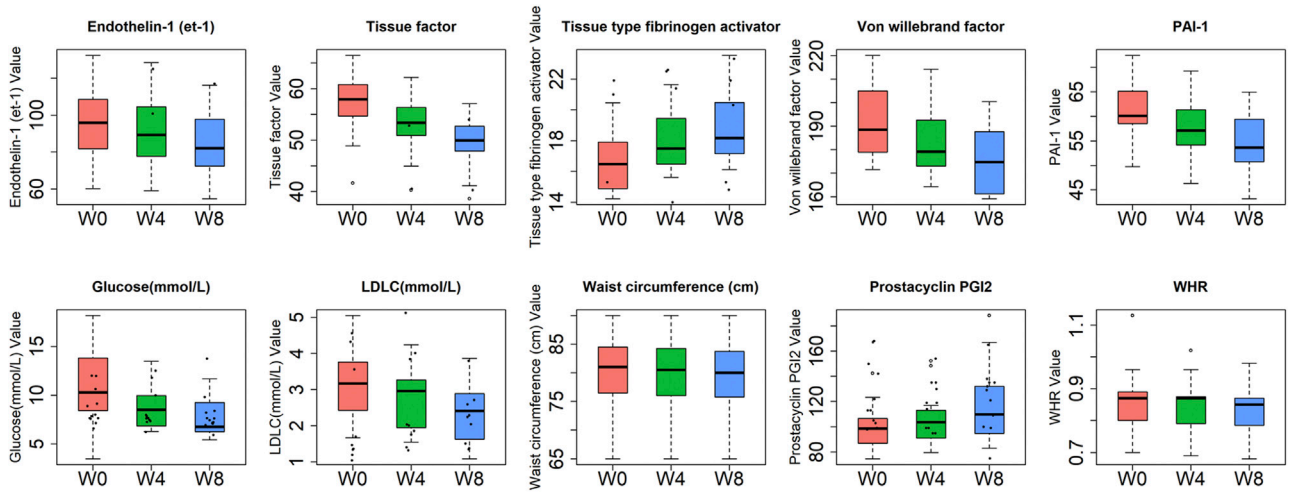

FIGURE 7 | Trends over time in clinical indicators with significant effects on gut microbes.

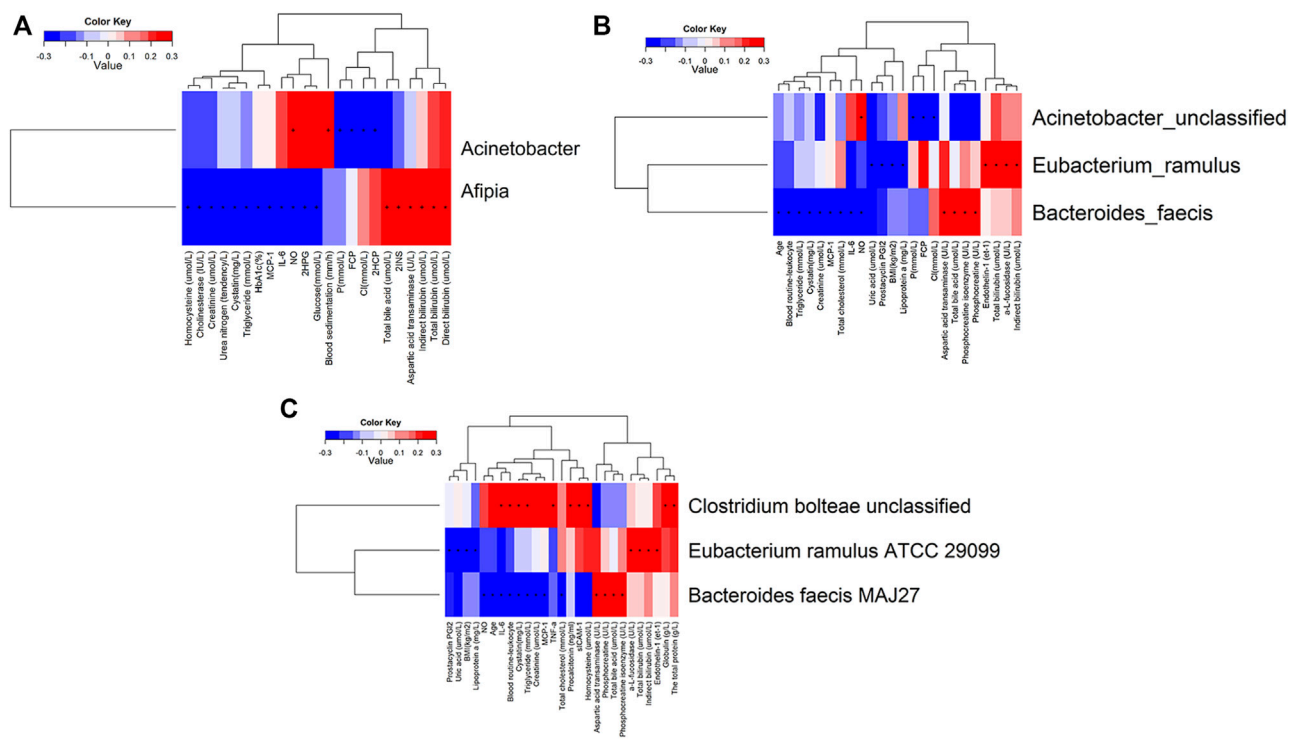

FIGURE 8 | Correlation analysis of significantly different clinical indicators and differential bacteria at levels of genus **(A)**, species **(B)** and strain **(C)** in type 2 diabetic patients.

in composition between samples (for example, the composition of microbiota in different subjects from different treatment groups). It was found that there was an overall trend of increasing and then decreasing microbial diversity. This indicates a gradual process of increasing microbiota diversity over the course of 0-W4 with GLP1. Previous animal studies have also (Li et al., 2014) shown that probiotics can significantly improve patients' blood glucose and lipid indexes, and improve morphological changes in the pancreas, liver, and kidneys. In this study, differential analysis of gut microbiota at W0, W4, and W8 with GLP-1 weekly preparations revealed significantly different genera: *Acinetobacter* (p = 0.000982716). In the present study, there was a decreasing trend in the abundance of *Acinetobacter* at 0, 4, and W8, and a decreasing trend in the indicators related to cardiovascular adverse effects and an increasing trend in the indicators related to beneficial

TABLE 3 | Clinical indicators associated with intestinal microbiota.

Phenotype	SampleNum	Df	SumsOfSqs	MeanSqs	F. Model	R2	Pr (>F)
Alkaline phosphatase (U/L)	36	1	0.732253123	0.732253123	2.03707352	0.056527163	0.0046
FBG	36	1	0.706773832	0.706773832	1.962101546	0.054560258	0.0059
HbA1c (%)	36	1	0.672513636	0.672513636	1.861782402	0.051915501	0.0098
NO	36	1	0.667862061	0.667862061	1.84820501	0.051556417	0.0099
Glucose (mmol/L)	36	1	0.648365136	0.648365136	1.791407492	0.050051328	0.0132
LDLC (mmol/L)	36	1	0.647663586	0.647663586	1.789367126	0.049997171	0.0138
FCP	36	1	0.637714707	0.637714707	1.760457113	0.049229156	0.0155
Prostacyclin PGI2	36	1	0.641743358	0.641743358	1.772158163	0.049540152	0.0172
PAI-1	36	1	0.626620928	0.626620928	1.728275213	0.048372758	0.0187
Cl (mmol/L)	36	1	0.622514811	0.622514811	1.716378478	0.048055781	0.019
Von willebrand factor	36	1	0.616806148	0.616806148	1.699851811	0.047615094	0.0203
Tissue type fibrinogen activator	36	1	0.593225856	0.593225856	1.631748259	0.045794785	0.0282
MCP-1	36	1	0.566648666	0.566648666	1.555300003	0.043743127	0.0309
Transglutaminase (U/L)	36	1	0.543817812	0.543817812	1.489889395	0.041980672	0.0353
BMI (kg/m^2)	36	1	0.574320548	0.574320548	1.577334174	0.044335367	0.0388
Tissue factor	36	1	0.567614984	0.567614984	1.558073833	0.043817723	0.0427
2INS	36	1	0.559606295	0.559606295	1.535097846	0.043199483	0.0451
Adenosine dehydrogenase (U/L)	36	1	0.56118808	0.56118808	1.539633447	0.043321591	0.0453
Homocysteine (μmol/L)	36	1	0.529575982	0.529575982	1.44920817	0.040881256	0.0512
Waist circumference (cm)	36	1	0.544807198	0.544807198	1.492719006	0.042057049	0.0583
TNF-a	36	1	0.321946367	0.321946367	0.86653943	0.024853038	0.744
IL-6	36	1	0.272752462	0.272752462	0.731282972	0.021055455	0.8728

effects, including an increasing trend in prostacyclin PGI2, tissue-type fibrinogen activator, and a decreasing trend in some indicators such as fibrinogen activator inhibitor-1 (PAI-1), ET-1, and tissue factor. PAI-1, e ET-1, and tissue factor showed a decreasing trend. This is consistent with the trend of the indicators harmful to the endothelium and opposite to the trend of the indicators beneficial to the endothelium. This leads us to speculate that the reduction of *Acinetobacter baumannii* may be an indicator of improved cardiovascular risk in elderly T2DM patients, and that the improvement of GLP-1 as an indicator of vascular endothelial function in middle-aged and elderly T2DM patients may depend on the reduction of *Acinetobacter baumannii* in the intestinal tract of patients.

To conclude, the present study shows that the hypoglycemic effect of GLP-1 as a drug in diabetic patients and the protective effect of cardiovascular disease are worthy of recognition. Most notably, we found that certain characteristic bacteria are correlated with relevant clinical indicators, such as *Acinetobacter*, *Afebola*, *Eubacterium twigs*, *Bacteroides*, *Acinetobacter baumannii*. The level of NO of the patients was positively correlated with the genus *Acinetobacter* and negatively correlated with the genus *Afebola* and *Bacteroides*. The improvement of vascular endothelial cell function index of middle-aged and old-aged diabetic patients by GLP-1 may be related to its change of the number of gut microbiota of the patients. Therefore, we suggest that the cardioprotective function of GLP-1 in diabetic patients may be correlated with the specific differential bacteria of the gut microbiota.

DATA AVAILABILITY STATEMENT

The raw sequencing data supporting the conclusions of this article were deposited in the NCBI Sequence Read Archive (SRA) database under bioproject number PRJNA809514. (https://www.ncbi.nlm.nih.gov/sra/PRJNA809514).

ETHICS STATEMENT

The studies involving human participants were reviewed and approved by Chinese clinical Trial Registry, Registration number: ChiCTR1900026514 http://www.chictr.org.cn/showprojen.aspx?proj=44112.

AUTHOR CONTRIBUTIONS

FC, LH, JL, and KH contributed conception and design of the study. DZ, ZW, SZ, and DH conducted clinical trials and data collection. CO, CX, and JY performed the statistical analysis. FC, BZ, and SY wrote the manuscript. All authors contributed to the article and approved the submitted version.

FUNDING

This study was supported by Shantou science and technology project (No: 200812225264260).

SUPPLEMENTARY MATERIAL

The Supplementary Material for this article can be found online at: https://www.frontiersin.org/articles/10.3389/fmolb.2022.879294/full#supplementary-material

REFERENCES

Aitken, J. D., and Gewirtz, A. T. (2013). Gut microbiota in 2012:Toward Understanding and Manipulating the Gut Microbiota. *Nat. Rev. Gastroenterol. Hepatol.* 10 (2), 72–74. doi:10.1038/nrgastro.2012.252

Allin, K. H., Tremaroli, V., Caesar, R., Jensen, B. A. H., Damgaard, M. T. F., et al. (2018). Aberrant Intestinal Microbiota in Individuals with Prediabetes. *Diabetologia* 61 (4), 810–820. doi:10.1007/s00125-018-4550-1

Allin, K. H., Nielsen, T., and Pedersen, O. (2015). Mechanisms in Endocrinology: Gut Microbiota in Patients with Type 2 Diabetes Mellitus. *Eur. J. Endocrinol.* 172 (4), R167–R177. doi:10.1530/eje-14-0874

Andrikou, E., Tsioufis, C., Andrikou, I., Leontsinis, I., Tousoulis, D., and Papanas, N. (2019). GLP-1 Receptor Agonists and Cardiovascular Outcome Trials: An Update. *Hellenic J. Cardiol.* 60 (6), 347–351. doi:10.1016/j.hjc.2018.11.008

Bielka, W., Przezak, A., and Pawlik, A. (2022). The Role of the Gut Microbiota in the Pathogenesis of Diabetes. *Int. J. Mol. Sci.* 23 (1), 10480. doi:10.3390/ijms23010480

Burton, J. H., Johnson, M., Johnson, J., Hsia, D. S., Greenway, F. L., and Heiman, M. L. (2015). Addition of a Gastrointestinal Microbiome Modulator to Metformin Improves Metformin Tolerance and Fasting Glucose Levels. *J. Diabetes Sci. Technol.* 9 (4), 808–814. doi:10.1177/1932296815577425

Cao, X.-H. (2015). Acarbose in Combination with Sitagliptin Phosphate for Treatment of Elderly Patients with Type 2 Diabetes Mellitus: Curative Efficacy and Effect on Intestinal Microflora. *World Chin. J. Digestology* 23 (15), 2507. doi:10.11569/wcjd.v23.i15.2507

de Moraes, G., and Layton, C. J. (2016). Therapeutic Targeting of Diabetic Retinal Neuropathy as a Strategy in Preventing Diabetic Retinopathy. *Clin. Exp. Ophthalmol.* 44 (9), 838–852. doi:10.1111/ceo.12795

ggplot2 (2009). *Elegant Graphics for Data Analysis.Pdf*.

Gurung, M., Li, Z., You, H., Rodrigues, R., Jump, D. B., Morgun, A., et al. (2020). Role of Gut Microbiota in Type 2 Diabetes Pathophysiology. *EBioMedicine* 51, 102590. doi:10.1016/j.ebiom.2019.11.051

Helmstädter, J., Frenis, K., Filippou, K., Grill, A., Dib, M., Kalinovic, S., et al. (2020). Endothelial GLP-1 (Glucagon-like Peptide-1) Receptor Mediates Cardiovascular Protection by Liraglutide in Mice with Experimental Arterial Hypertension. *Atvb* 40 (1), 145–158. doi:10.1161/atv.0000615456.97862.30

Hwang, I., Park, Y. J., Kim, Y. R., Kim, Y. N., Ka, S., Lee, H. Y., et al. (2015). Alteration of Gut Microbiota by Vancomycin and Bacitracin Improves Insulin Resistance via Glucagon-like Peptide 1 in Diet-induced Obesity. *FASEB J.* 29 (6), 2397–2411. doi:10.1096/fj.14-265983

Ipp, E., Genter, P., and Childress, K. (2017). Semaglutide and Cardiovascular Outcomes in Patients with Type 2 Diabetes. *N. Engl. J. Med.* 376 (9), 890–891. doi:10.1056/NEJMc1615712

Jayalakshmi, K., Ghoshal, U. C., Kumar, S., Misra, A., Roy, R., and Khetrapal, C. L. (2009). Assessment of Small Intestinal Permeability Using 1H-NMR Spectroscopy. *J. Gastrointestin Liver Dis.* 18 (1), 27.

Karlsson, F. H., Tremaroli, V., Nookaew, I., Bergström, G., Behre, C. J., Fagerberg, B., et al. (2013). Gut Metagenome in European Women with normal, Impaired and Diabetic Glucose Control. *Nature* 498 (7452), 99–103. doi:10.1038/nature12198

Kasai, C., Sugimoto, K., Moritani, I., Tanaka, J., Oya, Y., Inoue, H., et al. (2015). Comparison of the Gut Microbiota Composition between Obese and Non-obese Individuals in a Japanese Population, as Analyzed by Terminal Restriction Fragment Length Polymorphism and Next-Generation Sequencing. *BMC Gastroenterol.* 15, 100. doi:10.1186/s12876-015-0330-2

Larsen, N., Vogensen, F. K., van den Berg, F. W. J., Nielsen, D. S., Andreasen, A. S., Pedersen, B. K., et al. (2010). Gut Microbiota in Human Adults with Type 2 Diabetes Differs from Non-diabetic Adults. *PLoS One* 5 (2), e9085. doi:10.1371/journal.pone.0009085

Lee, H., and Ko, G. (2014). Effect of Metformin on Metabolic Improvement and Gut Microbiota. *Appl. Environ. Microbiol.* 80 (19), 5935–5943. doi:10.1128/aem.01357-14

Li, J., Jia, H., Cai, X., Zhong, H., Feng, Q., et al. (2014). An Integrated Catalog of Reference Genes in the Human Gut Microbiome. *Nat. Biotechnol.* 32 (8), 834–841. doi:10.1038/nbt.2942

Lozupone, C. A., Stombaugh, J. I., Gordon, J. I., Jansson, J. K., and Knight, R. (2012). Diversity, Stability and Resilience of the Human Gut Microbiota. *Nature* 489 (7415), 220–230. doi:10.1038/nature11550

Ma, Q., Li, Y., Li, P., Wang, M., Wang, J., Tang, Z., et al. (2019). Research Progress in the Relationship between Type 2 Diabetes Mellitus and Intestinal flora. *Biomed. Pharmacother.* 117, 109138. doi:10.1016/j.biopha.2019.109138

Madsen, M. S. A., Holm, J. B., Pallejà, A., Wismann, P., Fabricius, K., Rigbolt, K., et al. (2019). Metabolic and Gut Microbiome Changes Following GLP-1 or Dual GLP-1/GLP-2 Receptor Agonist Treatment in Diet-Induced Obese Mice. *Sci. Rep.* 9 (1), 15582. doi:10.1038/s41598-019-52103-x

Mair, P., Hofmann, E., Gruber, K., Hatzinger, R., Zeileis, A., and Hornik, K. (2015). Motivation, Values, and Work Design as Drivers of Participation in the R Open Source Project for Statistical Computing. *Proc. Natl. Acad. Sci. U.S.A.* 112 (48), 14788–14792. doi:10.1073/pnas.1506047112

Nadkarni, P., Chepurny, O. G., and Holz, G. G. (2014). Regulation of Glucose Homeostasis by GLP-1. *Prog. Mol. Biol. Transl Sci.* 121, 23–65. doi:10.1016/b978-0-12-800101-1.00002-8

Néri, A. K., da S Junior, G. B., Meneses, G. C., Martins, A. M., F Daher, E. D., da C Lino, D. O., et al. (2021). Cardiovascular Risk Assessment and Association with Novel Biomarkers in Patients with Type 2 Diabetes Mellitus. *Biomarkers Med.* 15 (8), 561–576. doi:10.2217/bmm-2020-0611

Nyborg, N. C. B., Mølck, A.-M., Madsen, L. W., and Bjerre Knudsen, L. (2012). The Human GLP-1 Analog Liraglutide and the Pancreas: Evidence for the Absence of Structural Pancreatic Changes in Three Species. *Diabetes* 61 (5), 1243–1249. doi:10.2337/db11-0936

Paradis, E., Claude, J., and Strimmer, K. (2004). APE: Analyses of Phylogenetics and Evolution in R Language. *Bioinformatics* 20 (2), 289–290. doi:10.1093/bioinformatics/btg412

Pratley, R. E., Nauck, M. A., Bailey, T., Montanya, E., Filetti, S., Garber, A. J., et al. (2012). Efficacy and Safety of Switching from the DPP-4 Inhibitor Sitagliptin to the Human GLP-1 Analog Liraglutide after 52 Weeks in Metformin-Treated Patients with Type 2 Diabetes: a Randomized, Open-Label Trial. *Diabetes Care* 35 (10), 1986–1993. doi:10.2337/dc11-2113

Qin, J., Li, Y., Cai, Z., Li, S., Zhu, J., Zhang, F., et al. (2012). A Metagenome-wide Association Study of Gut Microbiota in Type 2 Diabetes. *Nature* 490 (7418), 55–60. doi:10.1038/nature11450

Que, Y., Cao, M., He, J., Zhang, Q., Chen, Q., Yan, C., et al. (2021). Gut Bacterial Characteristics of Patients with Type 2 Diabetes Mellitus and the Application Potential. *Front. Immunol.* 12, 722206. doi:10.3389/fimmu.2021.722206

Rutten, G. E. H. M., Tack, C. J., Pieber, T. R., Comlekci, A., Ørsted, D. D., et al. (2016). LEADER 7: Cardiovascular Risk Profiles of US and European Participants in the LEADER Diabetes Trial Differ. *Diabetol. Metab. Syndr.* 8, 37. doi:10.1186/s13098-016-0153-5

Salamon, D., Sroka-Oleksiak, A., Kapusta, P., Szopa, M., Mrozińska, S., Ludwig-Słomczyńska, A. H., et al. (2018). Characteristics of Gut Microbiota in Adult Patients with Type 1 and Type 2 Diabetes Based on Next-generation S-equencing of the 16S rRNA Gene Fragment. *Pol. Arch. Intern. Med.* 128 (6), 336–343. doi:10.20452/pamw.4246

Sedighi, M., Razavi, S., Navab-Moghadam, F., Khamseh, M. E., Alaei-Shahmiri, F., Mehrtash, A., et al. (2017). Comparison of Gut Microbiota in Adult Patients with Type 2 Diabetes and Healthy Individuals. *Microb. Pathogenesis* 111, 362–369. doi:10.1016/j.micpath.2017.08.038

Segata, N., Waldron, L., Ballarini, A., Narasimhan, V., Jousson, O., and Huttenhower, C. (2012). Metagenomic Microbial Community Profiling Using Unique Clade-specific Marker Genes. *Nat. Methods* 9 (8), 811–814. doi:10.1038/nmeth.2066

Smits, M. M., Fluitman, K. S., Herrema, H., Davids, M., Kramer, M. H. H., Groen, A. K., et al. (2021). Liraglutide and Sitagliptin Have No Effect on Intestinal Microbiota Composition: A 12-week Randomized Placebo-Controlled Trial in Adults with Type 2 Diabetes. *Diabetes Metab.* 47 (5), 101223. doi:10.1016/j.diabet.2021.101223

Su, B., Liu, H., Li, J., Sunli, Y., Liu, B., Liu, D., et al. (2015). Acarbose Treatment Affects the Serum Levels of Inflammatory Cytokines and the Gut Content of Bifidobacteria in Chinese Patients with Type 2 Diabetes Mellitus. *J. Diabetes* 7 (5), 729–739. doi:10.1111/1753-0407.12232

Sun, Yu. (2014). *Effect of Metformin on Intestinal flora and Chronic Inflammatory Status in Type 2 Diabetic patients[D]*. Doctoral Dissertation from Zhengzhou University in China.

Tay, H. M., Leong, S. Y., Xu, X., Kong, F., Upadya, M., Dalan, R., et al. (2021). Direct Isolation of Circulating Extracellular Vesicles from Blood for Vascular Risk Profiling in Type 2 Diabetes Mellitus. *Lab. Chip* 21 (13), 2511–2523. doi:10.1039/d1lc00333j

Vanhoutte, P. M. (2009). How We Learned to Say NO. *Arterioscler Thromb Vasc Biol* 29 (8), 1156–1160. doi:10.1161/atvbaha.109.190215

Vanhoutte, P. M., Shimokawa, H., Feletou, M., and Tang, E. H. C. (2017). Endothelial Dysfunction and Vascular Disease - a 30th Anniversary Update. *Acta Physiol.* 219 (1), 22–96. doi:10.1111/apha.12646

Vanhoutte, P. M., Zhao, Y., Xu, A., and Leung, S. W. S. (2016). Thirty Years of Saying NO. *Circ. Res.* 119 (2), 375–396. doi:10.1161/circresaha.116.306531

Vikram, A., Kim, Y.-R., Kumar, S., Li, Q., Kassan, M., Jacobs, J. S., et al. (2016). Vascular microRNA-204 Is Remotely Governed by the Microbiome and Impairs Endothelium-dependent Vasorelaxation by Downregulating Sirtuin1. *Nat. Commun.* 7, 12565. doi:10.1038/ncomms12565

Wang, D., Luo, P., Wang, Y., Li, W., Wang, C., Sun, D., et al. (2013). Glucagon-like Peptide-1 Protects against Cardiac Microvascular Injury in Diabetes via a cAMP/PKA/Rho-dependent Mechanism. *Diabetes* 62 (5), 1697–1708. doi:10.2337/db12-1025

Wang, L., Li, P., Tang, Z., Yan, X., and Feng, B. (2016). Structural Modulation of the Gut Microbiota and the Relationship with Body Weight: Compared Evaluation of Liraglutide and Saxagliptin Treatment. *Sci. Rep.* 6, 33251. doi:10.1038/srep33251

Wang, X. L., Zhang, W., Li, Z., Han, W. Q., Wu, H. Y., Wang, Q. R., et al. (2021). Vascular Damage Effect of Circulating Microparticles in Patients with ACS Is Aggravated by Type 2 Diabetes. *Mol. Med. Rep.* 23 (6), 12113. doi:10.3892/mmr.2021.12113

Wu, X., Ma, C., Han, L., Nawaz, M., Gao, F., Zhang, X., et al. (2010). Molecular Characterisation of the Faecal Microbiota in Patients with Type II Diabetes. *Curr. Microbiol.* 61 (1), 69–78. doi:10.1007/s00284-010-9582-9

Xu, J., Su, B., and Guan, Y. (2013). Effect of Acarbose on Intestinal Bifidobacteria in Patients with Diabetes Mellitus. *J. Med. Innovation China[J]* 10 (09), 37

Xu, N., and Jin, W. (2014). Clinical Efficacy of Glucagon-like Peptide-1 Receptor Agonist and Dipeptidyl Peptidase-4 Inhibitor in the Treatment of Type 2 Diabetes Mellitus. *J. Chinses J. Diabetes[J]* 22 (08), 731

Yang, L., Hou, K., Zhang, B., Ouyang, C., Lin, A., Xu, S., et al. (2020). Preservation of the Fecal Samples at Ambient Temperature for Microbiota Analysis with a Cost-Effective and Reliable Stabilizer EffcGut. *Sci. Total Environ.* 741, 140423. doi:10.1016/j.scitotenv.2020.140423

Zhang, Q., Xiao, X., Zheng, J., Li, M., Yu, M., Ping, F., et al. (2018). Featured Article: Structure Moderation of Gut Microbiota in Liraglutide-Treated Diabetic Male Rats. *Exp. Biol. Med. (Maywood)* 243 (1), 34–44. doi:10.1177/1535370217743765

Zhang, Z. (2016). Reshaping and Aggregating Data: an Introduction to Reshape Package. *Ann. Transl Med.* 4 (4), 78. doi:10.3978/j.issn.2305-5839.2016.01.33

Zhou, L., Fang, Y., Hu, M., Long, E., and Zhou, N. (2019). Analysis of Domestic Marketing of GLP-1 Analogs and DPP-4 Inhibitors. *J. China Pharmaceuticals[j]* 28 (03), 96.

Conflict of Interest: Author CO was employed by the company Xiamen Treatgut Biotechnology Co., Ltd.

The remaining authors declare that the research was conducted in the absence of any commercial or financial relationships that could be construed as a potential conflict of interest.

Publisher's Note: All claims expressed in this article are solely those of the authors and do not necessarily represent those of their affiliated organizations, or those of the publisher, the editors and the reviewers. Any product that may be evaluated in this article, or claim that may be made by its manufacturer, is not guaranteed or endorsed by the publisher.

frontiers | Frontiers in Bioengineering and Biotechnology

ORIGINAL RESEARCH
published: 13 July 2022
doi: 10.3389/fbioe.2022.929979

Suppression of AGTR1 Induces Cellular Senescence in Hepatocellular Carcinoma Through Inactivating ERK Signaling

Houhong Wang[1†], *Yayun Cui*[2†], *Huihui Gong*[3], *Jianguo Xu*[1], *Shuqin Huang*[1] *and Amao Tang*[4*]

[1]*Department of General Surgery, The Affiliated Bozhou Hospital of Anhui Medical University, Bozhou, China,* [2]*Department of Cancer Radiotherapy, The First Affiliated Hospital of USTC, Division of Life Sciences and Medicine, (Anhui Provincial Cancer Hospital), University of Science and Technology of China, Hefei, China,* [3]*Faculty of Health and Life Sciences, Oxford Brookes University, Oxford, United Kingdom,* [4]*Department of Gastroenterology, The Affiliated Hangzhou First People's Hospital, Zhejiang University School of Medicine, Hangzhou, China*

Objective: Cellular senescence is an effective barrier against tumorigenesis. Hence, it is of significance to characterize key features of cellular senescence and the induction of senescence in hepatocellular carcinoma (HCC) cells via pharmacological interventions. Our study determined the biological roles as well as mechanisms of angiotensin II type I receptor (AGTR1) on cellular senescence in HCC.

Methods: Lentivirus vector-mediated overexpression or knockdown of AGTR1 was conducted in HCC cells, respectively. A volume of 8 μM sorafenib was used to induce cellular senescence, and ERK was activated by 30 ng/ml ERK agonist EGF. Proliferation was evaluated *via* clone formation assay. HCC cell senescence was examined by flow cytometry for cell cycle, senescence-associated β-galactosidase (SA-β-gal) staining, and senescence-associated heterochromatin foci (SAHF) analysis. AGTR1, p53, p21, extracellular signal-regulated kinase (ERK), and p-ERK expression were assessed through Western blot or immunofluorescence.

Results: AGTR1-knockout HCC cells displayed the attenuated proliferative capacity, G2-M phase arrest, increased expression of p53 and p21, and elevated percentages of SA-β-gal- and SAHF-positive cells. In sorafenib-exposed HCC cells, overexpressed AGTR1 enhanced the proliferative capacity and alleviated G2-M phase arrest as well as decreased p53 and p21 expression and the proportions of SA-β-gal- and SAHF-positive cells. Moreover, AGTR1 knockdown attenuated the activity of p-ERK in HCC cells, and ERK agonist ameliorated AGTR1 knockdown-induced cellular senescence.

Conclusion: This study demonstrates that suppression of AGTR1 induces cellular senescence in HCC through inactivating ERK signaling. The significant synergistic

OPEN ACCESS

Edited by:
Leming Sun,
Northwestern Polytechnical University, China

Reviewed by:
Chen Li,
Free University of Berlin, Germany
Xing Niu,
China Medical University, China

****Correspondence:***
Amao Tang
ynszdi@163.com

†These authors have contributed equally to this work and share first authorship

Specialty section:
This article was submitted to Preclinical Cell and Gene Therapy, a section of the journal Frontiers in Bioengineering and Biotechnology

Received: *27 April 2022*
Accepted: *06 June 2022*
Published: *13 July 2022*

Citation:
Wang H, Cui Y, Gong H, Xu J, Huang S and Tang A (2022) Suppression of AGTR1 Induces Cellular Senescence in Hepatocellular Carcinoma Through Inactivating ERK Signaling. Front. Bioeng. Biotechnol. 10:929979. doi: 10.3389/fbioe.2022.929979

Abbreviations: HCC, hepatocellular carcinoma; SASP, senescence-associated secretory phenotype; AGTR1, angiotensin II type I receptor; CXCR4, C-X-C chemokine receptor type 4; SDF-1α, stromal cell-derived factor-1α; RPMI-1640, Roswell Park Memorial Institute media 1640; shRNA, short hairpin RNA; SDS-PAGE, sodium dodecyl sulfate-polyacrylamide gel electrophoresis; SA-β-gal, senescence-associated β-galactosidase; SAHF, senescence-associated heterochromatin foci; DAPI, 4',6-diamidino-2-phenylindole; SD, standard deviation.

effect of AGTR1 suppression and sorafenib might represent a potential combination therapy for HCC.

Keywords: AGTR1, hepatocellular carcinoma, cellular senescence, sorafenib, ERK signaling

INTRODUCTION

Liver cancer remains a global health challenge, with an estimated incidence of more than one million cases by 2025 (Li et al., 2022). Hepatocellular carcinoma (HCC) represents the dominating type of liver cancer, occupying ~90% of all cases (Vogel et al., 2021; Cheng et al., 2022). Due to late diagnosis and damaged liver function, the five-year survival rate remains about 15% (Galle et al., 2021). Sorafenib is a multiple-target tyrosine kinase inhibitor, which has been approved as the only first-line therapeutic targeted drug against advanced HCC (Benson et al., 2021). It inhibits HCC cell proliferation via inactivating Ras/Raf/MEK/ERK signaling as well as targets PDGFR-β, VEGFR2, and c-KIT, etc., to weaken angiogenesis (Sun et al., 2021). Regrettably, only about 30% of HCC patients benefit from sorafenib and often typically experience resistance within 6 months (Finn et al., 2020; Qin et al., 2021). Additionally, some patients cannot tolerate sorafenib toxicity. Hence, it is imperative to discover more effective combination therapies to enhance the sensitivity of HCC cells to sorafenib as well as improve the efficacy.

Cellular senescence is a key process that modulates distinct pathophysiological processes from embryonic development to aging (Ziegler et al., 2021), which is not just a cell arrest but rather an active mechanism regulating cellular homeostasis, fibrotic process, and microenvironment through hindering the proliferation of abnormal cells (Duan et al., 2022). Evidence demonstrates that cellular senescence prevents tumorigenesis via suppressing the proliferation of tumor cells (Chini et al., 2020). Additionally, senescent cells that express markers (p53 and p21, etc.) result in tissue repair via secreting the senescence-associated secretory phenotype (SASP) (Chini et al., 2020). Recently, inducing cellular senescence as a tumor suppressor mechanism has emerged as a promising strategy to suppress tumor growth (Prasanna et al., 2021). Several intrinsic and extrinsic inducers of cellular senescence have been discovered such as oncogene activation and chemotherapeutics (sorafenib, etc.) (Alimirah et al., 2020). Angiotensin II type I receptor (AGTR1) is a potent vasopressor hormone and the main regulator of aldosterone secretion, which is a key effector in controlling blood pressure and volume in the cardiovascular system (Qiao et al., 2021). Previous evidence demonstrates that AGTR1 exerts a crucial role in facilitating cancer progression. AGTR1 triggers ovarian cancer spheroid formation and metastases through upregulating lipid desaturation as well as suppressing endoplasmic reticulum stress (Zhang Q et al., 2019). Overexpressed AGTR1 defines a subset of breast cancer and may confer sensitivity to AGTR1 antagonist losartan (Rhodes et al., 2009). Also, it facilitates lymph node metastases of breast cancer via activating C-X-C chemokine receptor type 4 (CXCR4)/stromal cell-derived factor-1α (SDF-1α) as well as triggering cellular migration and invasion (Ma et al., 2019). Targeting AGTR1 attenuates oncogenicity of glioblastoma via disrupting NF-κB/CXCR4 signaling (Singh et al., 2020). Telmisartan, an AGTR1 inhibitor, triggers melanoma cell apoptosis and can synergize with vemurafenib through affecting cell bioenergetics (Jelena et al., 2019). Moreover, AGTR1 blocker candesartan attenuates proliferation and fibrosis in gastric cancer (Okazaki et al., 2014). Suppression of AGTR1 inhibits cell growth and invasion in pancreatic cancer (Guo et al., 2015). AGTR1 results in intratumoral immunosuppression through inducing PD-L1 expression in non-small cell lung carcinoma (Zhu et al., 2019; Yang et al., 2020). Although AGTR1 has been recognized as an oncogene in several cancer types, the role in HCC remains to be fully explored. Furthermore, the underlying mechanisms of its upregulation in HCC are unclear and required to be further elucidated.

In the present study, we sought to determine the biological roles and mechanisms of AGTR1 on cellular senescence in HCC. We first demonstrated the functions of AGTR1 in attenuating HCC cell senescence through ERK signaling, providing a novel potential target as well as a potential combination therapy of AGTR1 suppression with sorafenib for HCC.

MATERIALS AND METHODS

Cell Culture and Administration

Human normal hepatocyte line L-02 (Chinese Academy of Sciences) and HCC cell lines HepG2 and Huh7 (Chinese Academy of Sciences) were cultured in Roswell Park Memorial Institute Media 1640 (RPMI-1640) (Gibco, United States) with 10% fetal bovine serum (FBS; Gibco) and 1% penicillin–streptomycin and incubated at 37°C in a humidified incubator with 5% CO_2. To induce cell senescence by sorafenib (TargetMol, China), HCC cells were exposed to 8 μM sorafenib and grown in RPMI-1640 plus 10% FBS lasting 4 days. HCC cells were exposed to 30 ng/ml ERK agonist EGF (PeproTech, United States) to activate ERK.

Virus Production and Target Cell Transduction

Human HEK293T cells (Chinese Academy of Sciences) were seeded onto a six-well plate. When the confluence was 80%, the cells were transfected with 2 μg lentiviral vector that expressed full-length human AGTR1 or short hairpin RNA (shRNA) lentivirus vector of AGTR1 (GenePharma, China) utilizing Lipofectamine 3000 (Invitrogen, United States). Afterward, the cells were maintained in RPMI-1640 with 10% FBS. The supernatant with lentivirus was collected at 48 h. HCC cells

were maintained in RPMI-1640, followed by a mixture of 2×10^5 cells with 450 μl lentivirus-containing supernatants along with 4 μg/ml polybrene (Sigma-Aldrich, United States). Afterward, they were seeded onto a six-well plate, with replacement of RPMI-1640 after half an hour. After 2 days, the transduced cells were planted onto a 10-cm culture dish plus 4 μg/ml puromycin. Finally, we harvested the stably transduced cells.

Western Blot

HCC cells were collected in a 1.5-ml centrifuge tube and centrifuged at 1500 rpm for 5 min. After removal of the supernatant, an appropriate amount of cell lysis buffer (Takara, China) was added containing PMSF, protease inhibitor, and phosphatase inhibitor. Then, the cells were lysed on ice for 30 min and then sonicated for 5 s. After centrifugation at 12,000 rpm for 10 min at 4°C, the supernatant was transferred to a freshly labeled 1.5-ml centrifuge tube. BCA kit was applied for quantification, and the remaining protein was added with 1/4 of the sample volume of 5× protein loading buffer. After blowing using a pipette, they were placed in a metal bath heater and heated at 100°C for 10 min. For denaturation, the denatured samples can be stored in a −80°C freezer. The protein was separated with sodium dodecyl sulfate-polyacrylamide gel electrophoresis (SDS-PAGE), along with transference onto a polyvinylidene difluoride membrane (Millipore, United States). The membrane was sealed by 5% skim milk, along with incubation with primary antibody of AGTR1 (1:500; 25343-1-AP; Proteintech, China), p53 (1:5000; 60283-2-Ig; Proteintech), p21 (1:3000; 10355-1-AP; Proteintech), p-p53 (1:4000; 28961-1-AP; Proteintech), p-p21 (1:1000; ab47300; Abcam, United States), ERK (1:1000; 51068-1-AP; Proteintech), p-ERK (1:1000; 28733-1-AP; Proteintech), or GAPDH (1:5000; HRP-60004; Proteintech). Being incubated with secondary antibodies, signals were visualized using ECL reagents (Takara). The gray value was quantified with ImageJ software.

Clone Formation Assay

HCC cells were inoculated onto a six-well plate (600 cells per well) with a culture medium for two weeks. Afterward, the clones were fixed with 4% paraformaldehyde (Sangon Biotech, China) as well as dyed with crystal violet (Sigma-Aldrich). The number of clones (≥ 50 cells) was counted microscopically.

Flow Cytometry

HCC cells were digested with 0.25% trypsin, along with centrifugation at 800 rpm lasting 5 min to prepare a cell suspension. The cell suspension was inoculated onto a six-well plate (20,000 cells per well) lasting 8 h. After waiting for the cells to adhere, the serum-free culture was continued for 12 h. After processing as intended, the cells were harvested into 15-ml centrifuge tubes. The supernatants were removed, along with being washed twice utilizing pre-chilled PBS. Afterward, digestion and centrifugation at 1200 rpm lasting 5 min were carried out. Being washed with PBS to remove cellular debris and residual impurities, the prepared pre-cooled 70% alcohol was added to the cells and placed at 4°C overnight to achieve the immobilization effect. The fixed cells were centrifuged and washed with PBS to remove residual alcohol. The PI staining solution was added to the cells, and the cell cycle was measured through flow cytometry (BD, United States) within 30 min after staining in the dark.

Senescence-Associated β-Galactosidase Staining

HCC cells were inoculated onto a six-well plate and fixed with 4% paraformaldehyde for 5 min at room temperature. Being washed with PBS, the cells were incubated with fresh SA-β-gal staining reagent (Cell Biolabs, United States) supplemented with 1.0 mg/ml X-galactosidase at 37°C lasting 18 h for visualizing SA-β-gal staining. The senescent cells were photographed under a microscope. The SA-β-gal-positive percentage was quantified with ImageJ software.

Senescence-Associated Heterochromatin Foci Assay

SAHF are specialized domains of facultative heterochromatin senescent cells. HCC cells were inoculated onto a 15-mm confocal dish (2×10^4 cells per well). The cells were fixed in 4% paraformaldehyde, and dyed utilizing 4',6-diamidino-2-phenylindole (DAPI) staining (Solarbio, China) lasting 10 min to investigate SAHF. The images were captured under a confocal microscope (Leica, Germany). The SAHF-positive percentage was quantified with ImageJ software.

Immunofluorescent Staining

The sterilized cell slides were placed in a 12-well plate, along with being washed utilizing PBS. HCC cells were evenly inoculated onto the slides, and the cell density on the slides was about 40%. After treating the cells according to the experimental purpose, the cells were investigated under a microscope to achieve the ideal density. After the cells became elliptical, they were removed using curved tweezers and placed them face upward on the wet box. Following removal of PBS buffer on the cell slides, 200 μl of 4% paraformaldehyde was added, and the cells were fixed for 10 min. Then, the climbing piece was placed in 0.5% Triton penetrating solution for 20 min. PBS was aspirated, along with blocking utilizing 3% BSA lasting 1 h. The primary antibody diluent of p-ERK (1:100; 28733-1-AP; Proteintech) was slowly covered with the cell slides and kept in a refrigerator at 4°C overnight. In the dark, 200 μl of secondary antibody was dropped on the cell slide and incubated for 60 min at room temperature in the dark. Nuclei were stained by DAPI staining for 10 min. The fluorescence quencher was dropped on a clean glass slide and gently covered the cell surface of the cell slide. The capture of images was implemented utilizing a confocal microscope (Leica, Germany) and quantified with ImageJ software.

Statistical Analysis

GraphPad Prism 8.0.1 was applied for data analysis. Data were displayed as mean ± standard deviation (SD). Comparison of two groups was evaluated with Student's t-test. Comparison of multiple groups was conducted with one-way analysis of

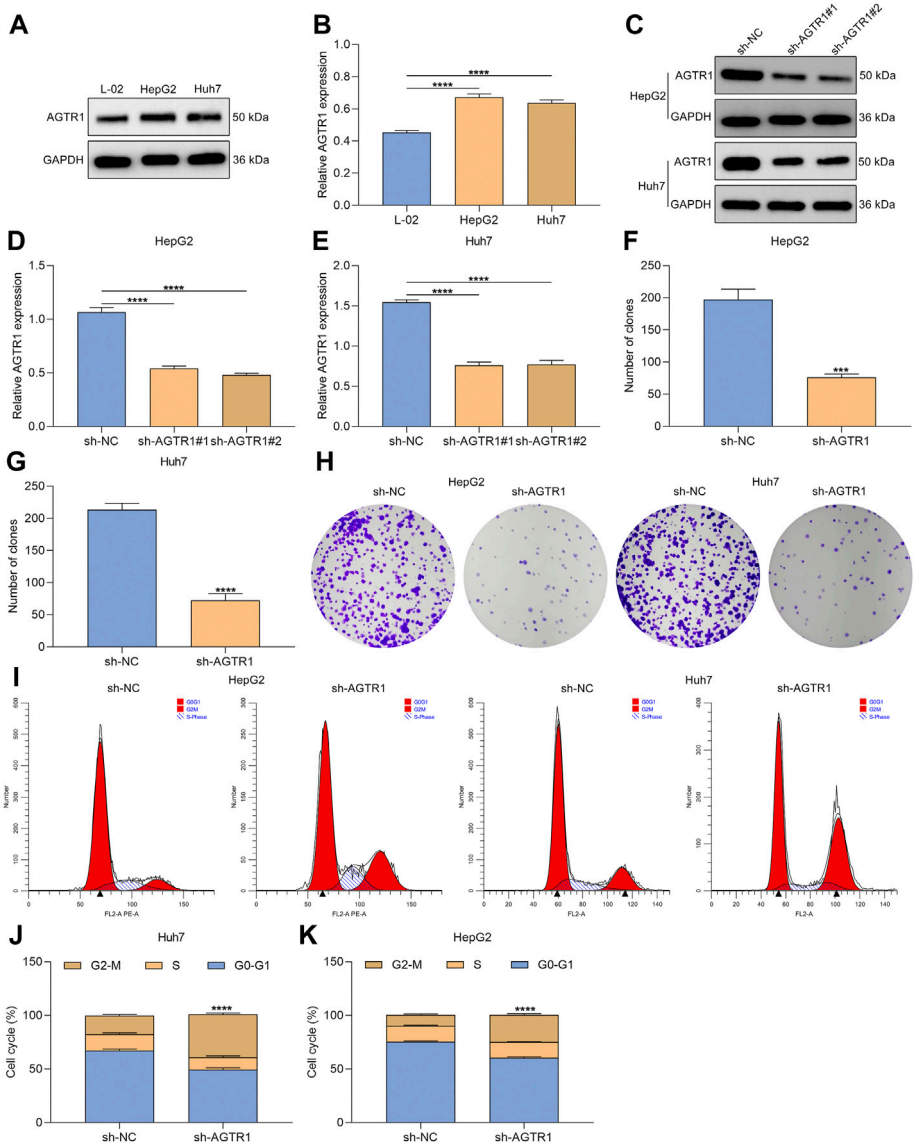

FIGURE 1 | AGTR1 knockdown alleviates proliferation and induces growth arrest for HCC cells. **(A,B)** AGTR1 protein expression in L-02, HepG2 along with Huh7 cell lines. **(C–E)** AGTR1 protein expression in HepG2 and Huh7 cell lines with sh-AGTR1 lentivirus transduction. **(F–H)** Number of colonies in HCC cell lines with sh-AGTR1 lentivirus transduction. **(I–K)** Cell cycle distribution of HCC cell lines with sh-AGTR1 lentivirus transduction.

variance along with Bonferroni *post hoc* tests. p values < 0.05 were considered statistically significant. Significance was determined as follows: $^{*}p \leq 0.05$, $^{**}p \leq 0.01$; $^{***}p \leq 0.001$; $^{****}p \leq 0.0001$.

RESULTS

Angiotensin II Type I Receptor Knockdown Alleviates Proliferation and Induces Growth Arrest for Hepatocellular Carcinoma Cells

We first determined the expression of AGTR1 in human normal hepatocyte line L-02 and human HCC cell lines HepG2 and Huh7. Compared with L-02 cells, high AGTR1 expression was investigated in HCC cells (**Figures 1A,B**). For determining the functional role of AGTR1 in HCC, this study utilized sh-AGTR1 lentivirus for stable knockdown of AGTR1 in HepG2 and Huh7 cells. Following validation, sh-AGTR1 stably attenuated AGTR1 expression in HCC cells (**Figures 1C–E**). Afterward, we investigated whether suppression of AGTR1 prevented the proliferation of HCC cells. As a result, sh-AGTR1 dramatically restrained the cellular growth of HCC cells (**Figures 1F–H**). Cell cycle profiles were examined with flow cytometry. G2-M cell phase arrest was triggered by sh-AGTR1 (**Figures 1I–K**). Thus, suppression of AGTR1 enabled to alleviate proliferation and aggravate growth arrest for HCC cells.

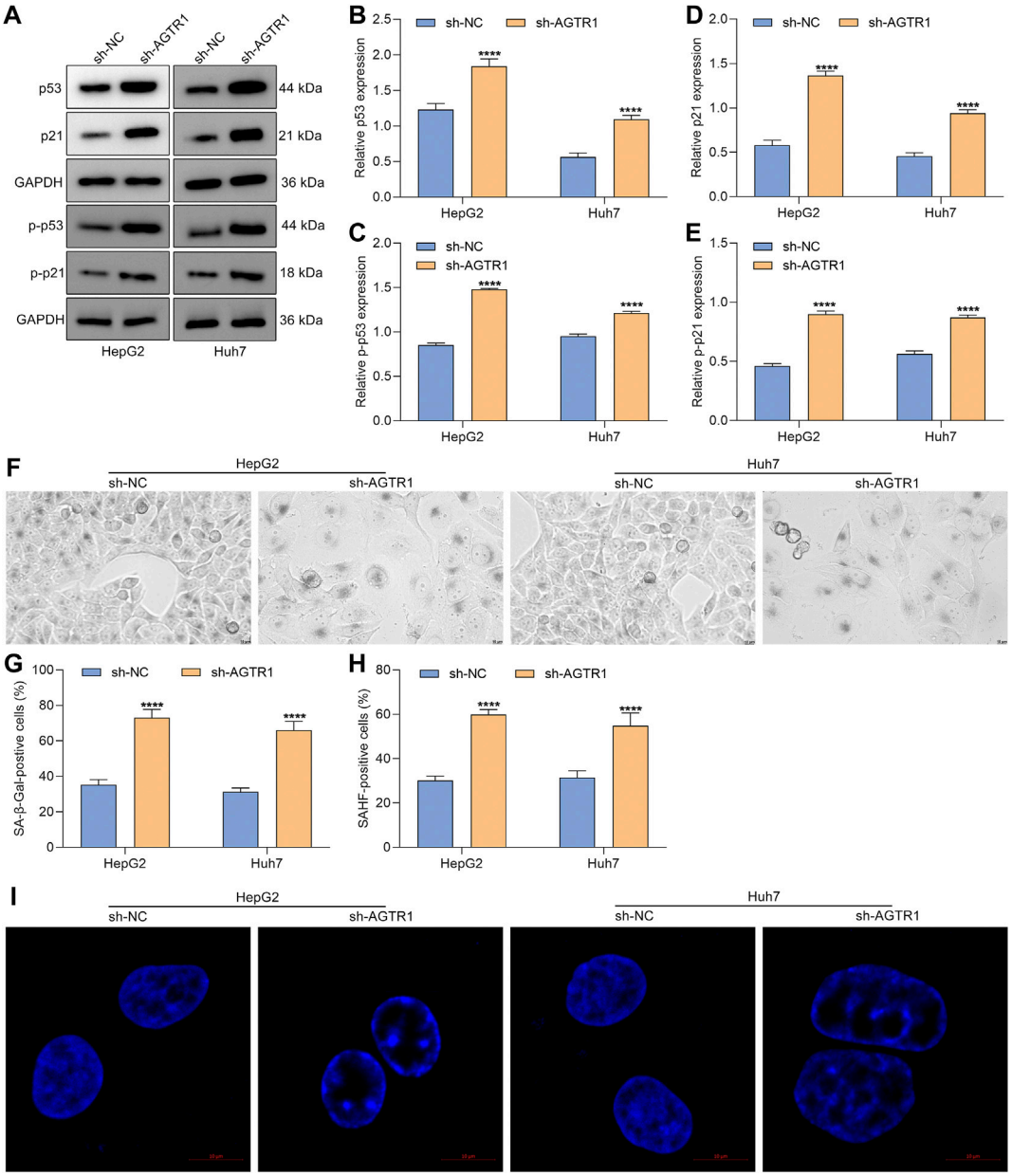

FIGURE 2 | Suppression of AGTR1 triggers cellular senescence of HCC cells *via* p53/p21 signaling. **(A–E)** Expression of p53, p-p53, p21, and p-p21 in HepG2 and Huh7 cell lines with sh-AGTR1 lentivirus transduction. **(F,G)** SA-β-Gal activity of HCC cell lines with sh-AGTR1 lentivirus transduction. Scale bar, 10 μm. **(H,I)** SAHF activity of HCC cell lines with sh-AGTR1 lentivirus transduction. Scale bar, 10 μm.

Angiotensin II Type I Receptor Knockdown Triggers Cellular Senescence of Hepatocellular Carcinoma Cells *via* p53/p21 Signaling

Senescence is an antiproliferative mechanism, which enables inhibition of tumor development (Trayssac et al., 2021). Except for cell cycle arrest, cellular senescence was characterized by secretion of SASP and genetic alterations, etc. Here, we further determined whether AGTR1 affected cellular senescence of HCC cells. Senescence markers p53 and p21 were first examined. Under AGTR1 knockout, HepG2 and Huh7 cells, p53, p-p53, p21, and p-p21 expressions were remarkably increased (**Figures 2A–E**). SA-β-Gal staining that reflects enhanced lysosomal functions and lipofuscin induced by protein and lipid changes was conducted for evaluating cellular senescence. The percentages of SA-β-Gal-positive cells were markedly elevated in sh-AGTR1 lentivirus-transduction HCC cells (**Figures 2F,G**). We also noted that AGTR1 knockout HCC cells displayed striking phenotypic

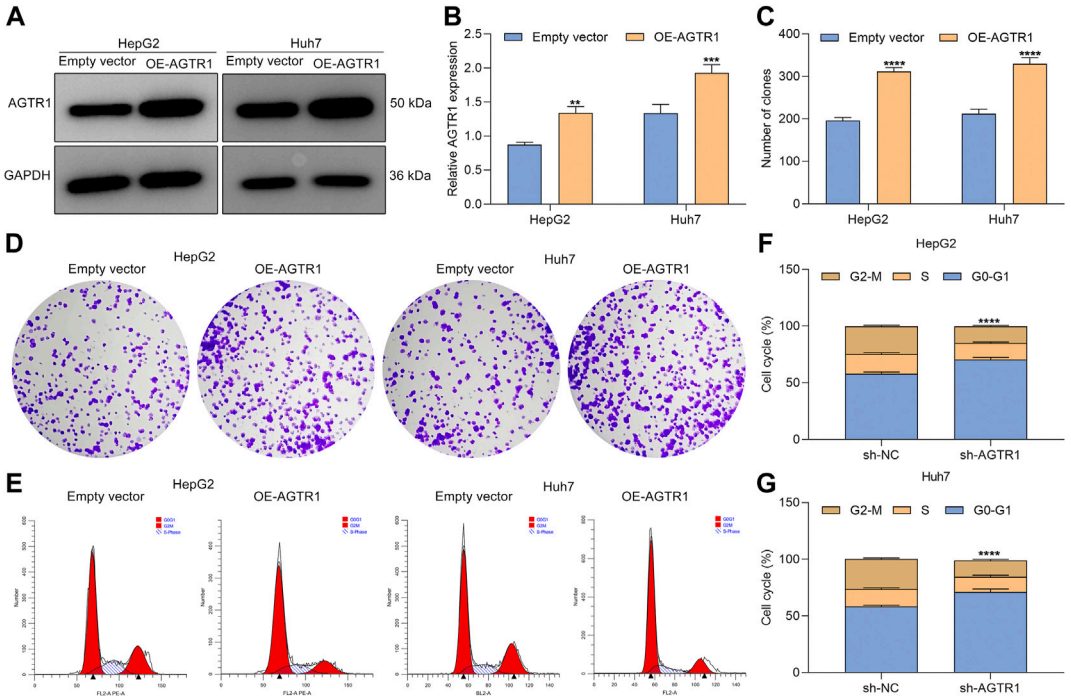

FIGURE 3 | Upregulated AGTR1 increases proliferation and weakens growth arrest for sorafenib-treated HCC cells. **(A,B)** AGTR1 protein expression in sorafenib-treated HepG2 and Huh7 cell lines under AGTR1 lentivirus transduction. **(C,D)** Number of colonies of sorafenib-treated HCC cells with AGTR1 lentivirus transduction. **(E–G)** Cell cycle of sorafenib-treated HCC cells with AGTR1 lentivirus transduction.

alterations (increased cell size and flattened morphology, etc.). Additionally, AGTR1 knockdown dramatically increased the percentage of SAHF-positive HCC cells (**Figures 2H,I**). On the basis of the obtained data, we concluded that suppression of AGTR1 was capable of triggering cellular senescence of HCC cells via p53/p21 signaling.

Overexpressed Angiotensin II Type I Receptor Increases Proliferation and Weakens Growth Arrest for Sorafenib-Treated Hepatocellular Carcinoma Cells

Evidence demonstrates that cellular senescence of HCC cells can be induced by chemotherapeutics (including sorafenib) (Leung et al., 2020). To investigate whether AGTR1 affected the therapeutic effect of sorafenib in HCC cells, AGTR1-overexpressed HepG2 and Huh7 cells (**Figures 3A,B**) were administrated with 8 μM sorafenib lasting 4 days. We found that AGTR1 overexpression reinforced the proliferative ability of sorafenib-treated HCC cells (**Figures 3C,D**). Senescence-associated cell cycle arrest in cancer cells is regarded as an effective therapeutic strategy, notably those with apoptosis resistance. We investigated that G2-M phase arrest of sorafenib-exposed HCC cells was alleviated by AGTR1 overexpression (**Figures 3E–G**). By reason of the foregoing, AGTR1 strengthened proliferation as well as weakened growth arrest for sorafenib-treated HCC cells.

Overexpressed Angiotensin II Type I Receptor Weakens Cellular Senescence of Sorafenib-Treated Hepatocellular Carcinoma Cells

Further analysis was conducted for determining the functional roles of AGTR1 in sorafenib-induced cellular senescence in HepG2 and Huh7 cells. The data showed that AGTR1 upregulation dramatically reduced p53 and p21 expression in sorafenib-treated HCC cells (**Figures 4A–C**). Moreover, the percentages of SA-β-Gal-positive sorafenib-treated HCC cells were markedly decreased by AGTR1 overexpression (**Figures 4D,E**). Meanwhile, upregulated AGTR1 reduced the percentage of SAHF-positive sorafenib-treated HCC cells (**Figures 4F,G**). On the basis of aforementioned data, we drew a conclusion that AGTR1 enabled alleviation of cellular senescence of sorafenib-treated HCC cells.

Suppression of Angiotensin II Type I Receptor Weakens ERK Activity in Hepatocellular Carcinoma Cells

Evidence demonstrates the crucial role of ERK signaling in cellular senescence (Yan et al., 2019). In HepG2 and Huh7 cells, suppression of AGTR1 did not affect ERK expression but dramatically lowered p-ERK levels (**Figures 5A–C**). Immunofluorescent staining also confirmed the down-

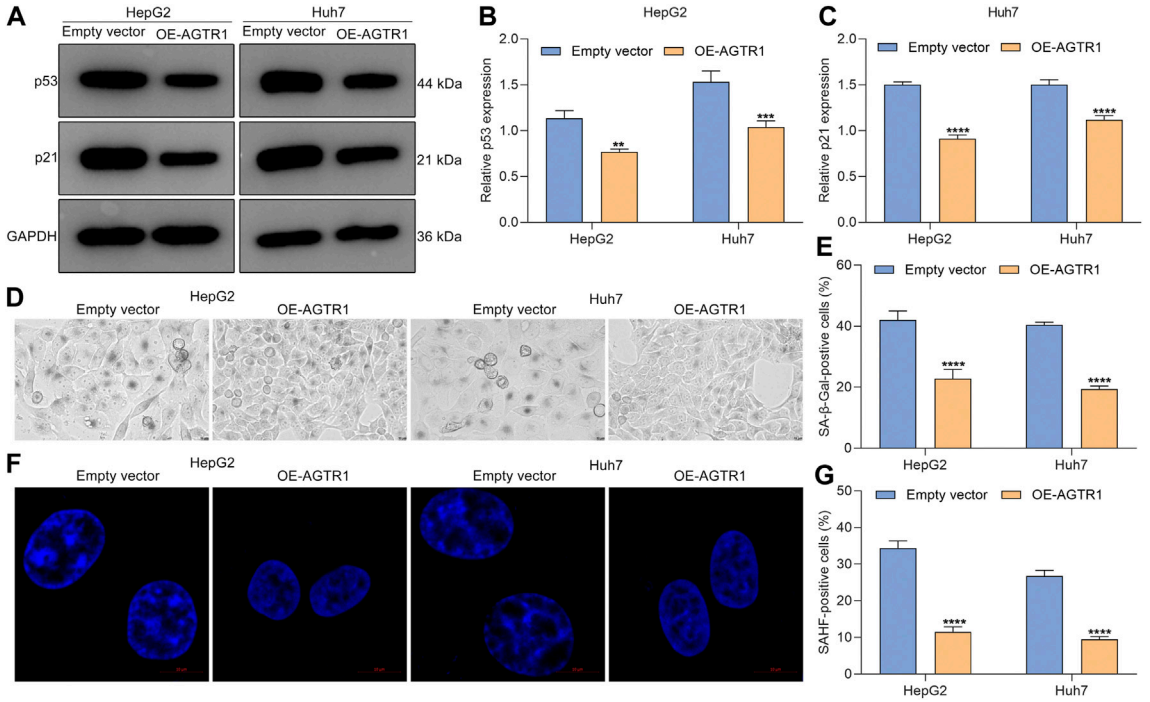

FIGURE 4 | Upregulated AGTR1 weakens cellular senescence of sorafenib-treated HCC cells. **(A–C)** p53 and p21 protein expression in sorafenib-treated HepG2 along with Huh7 cell lines under AGTR1 lentivirus transduction. **(D,E)** SA-β-Gal activity of HCC cell lines with AGTR1 lentivirus transduction. Scale bar, 10 μm. **(F,G)** SAHF activity of HCC cell lines with AGTR1 lentivirus transduction. Scale bar, 10 μm.

regulation of p-ERK in HCC cells with AGTR1 knockdown (**Figures 5D,E**). Hence, suppression of AGTR1 was capable of weakening ERK activity in HCC cells.

Angiotensin II Type I Receptor Knockdown Suppresses Proliferation and Triggers Growth Arrest for Hepatocellular Carcinoma Cells Through ERK Signaling

Further analysis was carried out for evaluating whether AGTR1 induced cellular senescence of HCC cells through modulating ERK activity. The data showed that ERK agonist EGF improved the colonies of AGTR1-knockout HepG2 and Huh7 cells (**Figures 6A–C**). This indicated that the proliferative capacity of AGTR1-knockout HCC cells was improved by activated ERK. Moreover, G2-M phase arrest of AGTR1-knockout HCC cells was alleviated by ERK agonist EGF (**Figures 6D–F**). Based on these, we concluded that suppression of AGTR1 suppressed proliferation as well as triggered growth arrest for HCC cells *via* ERK signaling.

Angiotensin II Type I Receptor Knockdown Triggers Cellular Senescence of Hepatocellular Carcinoma Cells in an ERK-dependent Pathway

As depicted in **Figures 7A–E**, ERK agonist EGF dramatically improved the expression of p53 and p21 in AGTR1-knockout HepG2 and Huh7 cells. Moreover, the percentage of SA-β-Gal-positive AGTR1-knockout HCC cells was increased by ERK agonist EGF (**Figures 7F–H**). Meanwhile, we investigated that ERK agonist EGF markedly improved the percentage of SAHF-positive AGTR1-knockout HCC cells (**Figures 7I–K**). Thus, suppression of AGTR1 enabled to trigger cellular senescence of HCC cells in an ERK-dependent pathway.

DISCUSSION

In the present study, our evidence suggested that AGTR1 attenuated cellular senescence of HCC cells through activating ERK signaling, indicating AGTR1 as a drug target against HCC. HCC is still difficult to treat due to a lack of drugs targeting key dependencies (Gao et al., 2021), and broad-spectrum kinase antagonists (especially sorafenib) have little benefit in HCC patients (Kelley et al., 2021; Ren et al., 2021; Wen et al., 2021). Experimental evidence suggests that sorafenib enables to facilitate cellular apoptosis and senescence and mitigates angiogenesis as well as suppresses proliferation in cancer cells (Ding et al., 2021; Ryoo et al., 2021). Overexpressed AGTR1 weakened sorafenib-induced cellular senescence in HCC cells, indicating that AGTR1 suppression and sorafenib as a potential combination therapy might synergistically inhibit HCC progression.

Upregulated AGTR1 was found in human HCC cell lines HepG2 and Huh7 in comparison to human normal hepatocyte

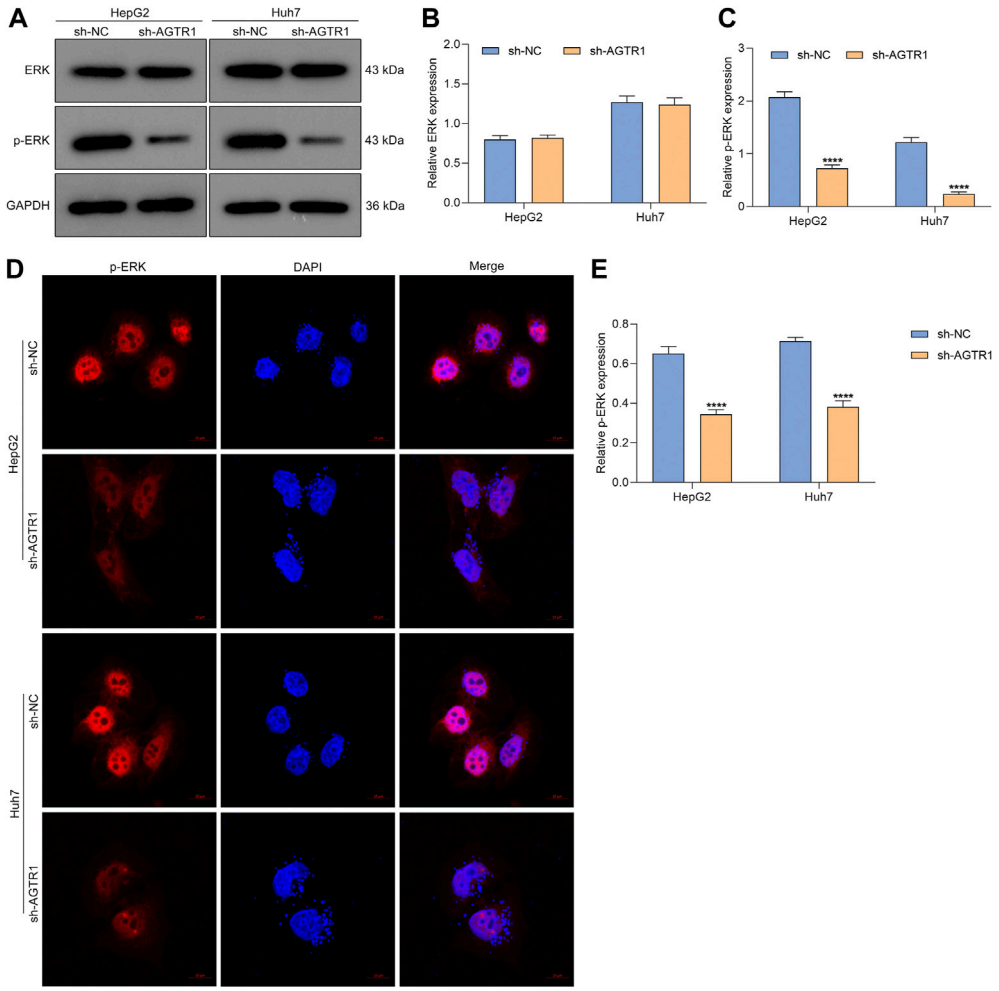

FIGURE 5 | Suppression of AGTR1 weakens ERK activity in HCC cells. **(A–C)** ERK and p-ERK levels in HepG2 and Huh7 cell lines with sh-AGTR1 lentivirus transduction. **(D,E)** Immunofluorescent staining of p-ERK in HCC cell lines with sh-AGTR1 lentivirus transduction. Scale bar, 10 μm.

line L-02. Previous studies have demonstrated the upregulation of AGTR1 in other cancer types (breast cancer, etc.) (Qiao et al., 2021). Lentivirus vector-mediated sh-AGTR1 was utilized for stably silencing AGTR1 in HCC cells. Our data demonstrated the inhibitory effect of AGTR1 knockdown on the proliferative ability of HCC cells. Additionally, AGTR1-knockout HCC cells presented G2-M cell phase arrest. Senescence is a status in which stable cell cycle arrest is triggered by intrinsic or extrinsic damage (Innes et al., 2018). Senescent cells have the key features of persistent cell cycle arrest, elevated lysosomal contents called SA-β-Gal activity, markedly increased expression of cyclin-dependent kinase inhibitors, persistent DNA damage response, the abnormal changes in the structure of condensed chromatin called SAHF, and secretion of SASP (Zhang et al., 2021). Evidence suggests that cellular senescence is a key tumor suppression mechanism, which may prevent oncogenic activation and genetic instability as well as damaged cells. Inducing cellular senescence of tumor cells is an underlying mechanism by which cancer therapies exert antitumor activity (Birch and Gil, 2020). The tumor suppressor p53 is capable of restricting malignant transformation through inducing a cell-autonomous program of cell cycle arrest as well as apoptosis (Wang et al., 2021). Additionally, p53 enables facilitation of cellular senescence, involving stable cell cycle arrest as well as secretion of factors that alter the tissue microenvironment (Lujambio et al., 2013). In HCC, cellular senescence is primarily controlled by p53-dependent or -independent signaling (Xiang et al., 2021). Understanding the molecular signaling that mediates cancer cell senescence enables to yield new insights into guiding the discovery of unique antitumor agents as well as molecular biomarkers (Qiu et al., 2020). In our study, cellular senescence of HCC cells was triggered by AGTR1 knockdown in accordance with weakened proliferative ability, G2-M phase arrest, and increased expression of p53 and p21 as well as the proportions of SA-β-Gal- and SAHF-positive cells, indicating that

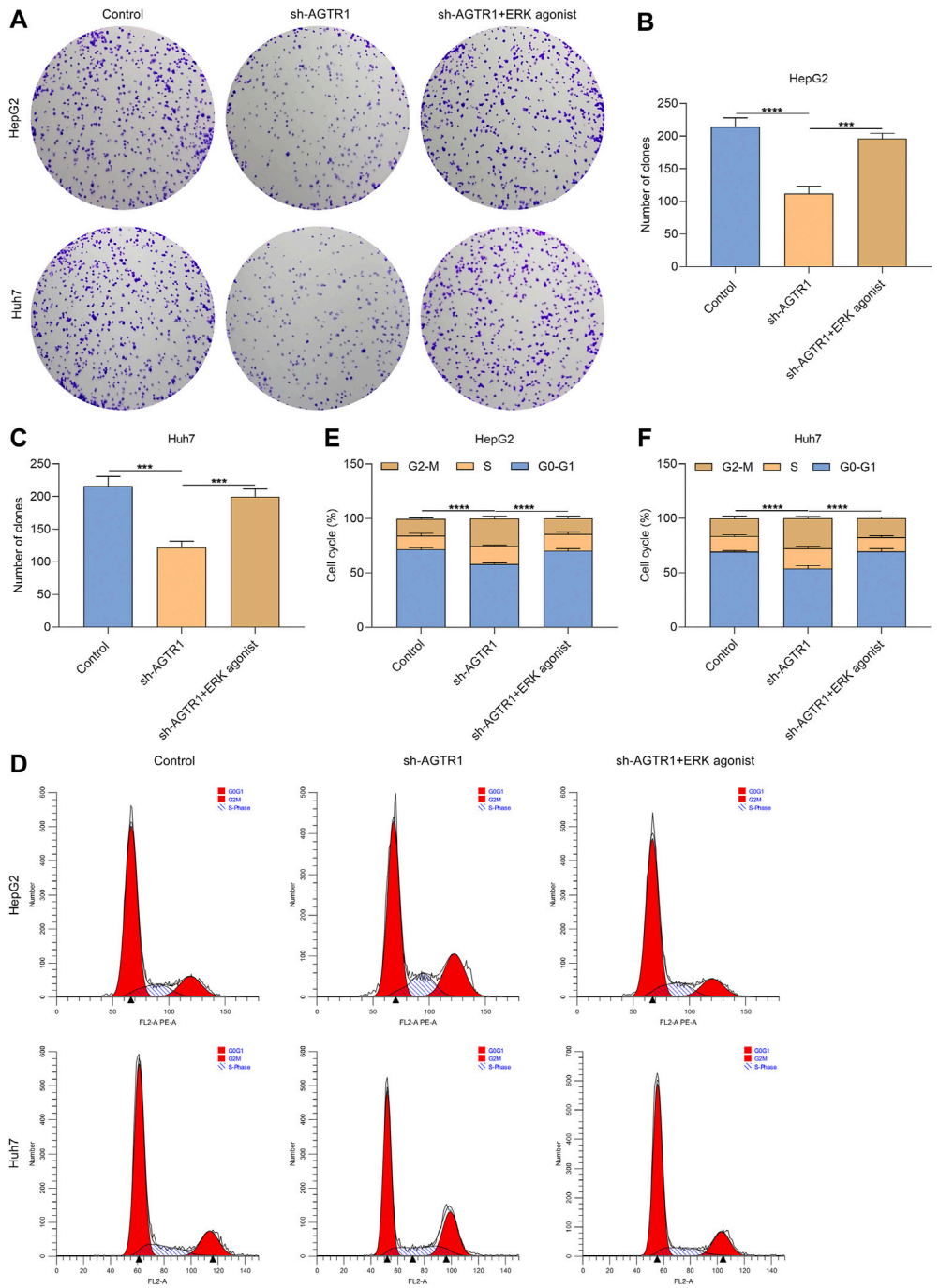

FIGURE 6 | AGTR1 knockdown suppresses proliferation and triggers growth arrest for HCC cells through inactivating ERK signaling. **(A–C)** Number of colonies of HepG2 and Huh7 cell lines with sh-AGTR1 lentivirus transduction or ERK agonist EGF. **(D–F)** Cell cycle of HCC cell lines with sh-AGTR1 lentivirus transduction or ERK agonist EGF.

AGTR1 attenuated tumor cellular senescence during HCC progression.

Senescence occurs following chemotherapies (sorafenib, etc.), called therapy-induced senescence through inducing DNA double-strand breaks (Tang et al., 2020). We found that overexpressed AGTR1 heightened proliferation as well as alleviated G2-M cell phase arrest for sorafenib-treated HCC cells. Additionally, AGTR1 upregulation decreased p53 and p21 expressions as well as the proportions of SA-β-gal- and SAHF-positive cells for sorafenib-exposed HCC cells. Several therapeutic options, notably sorafenib, offer only modest survival benefits to patients with HCC (Lyu et al.,

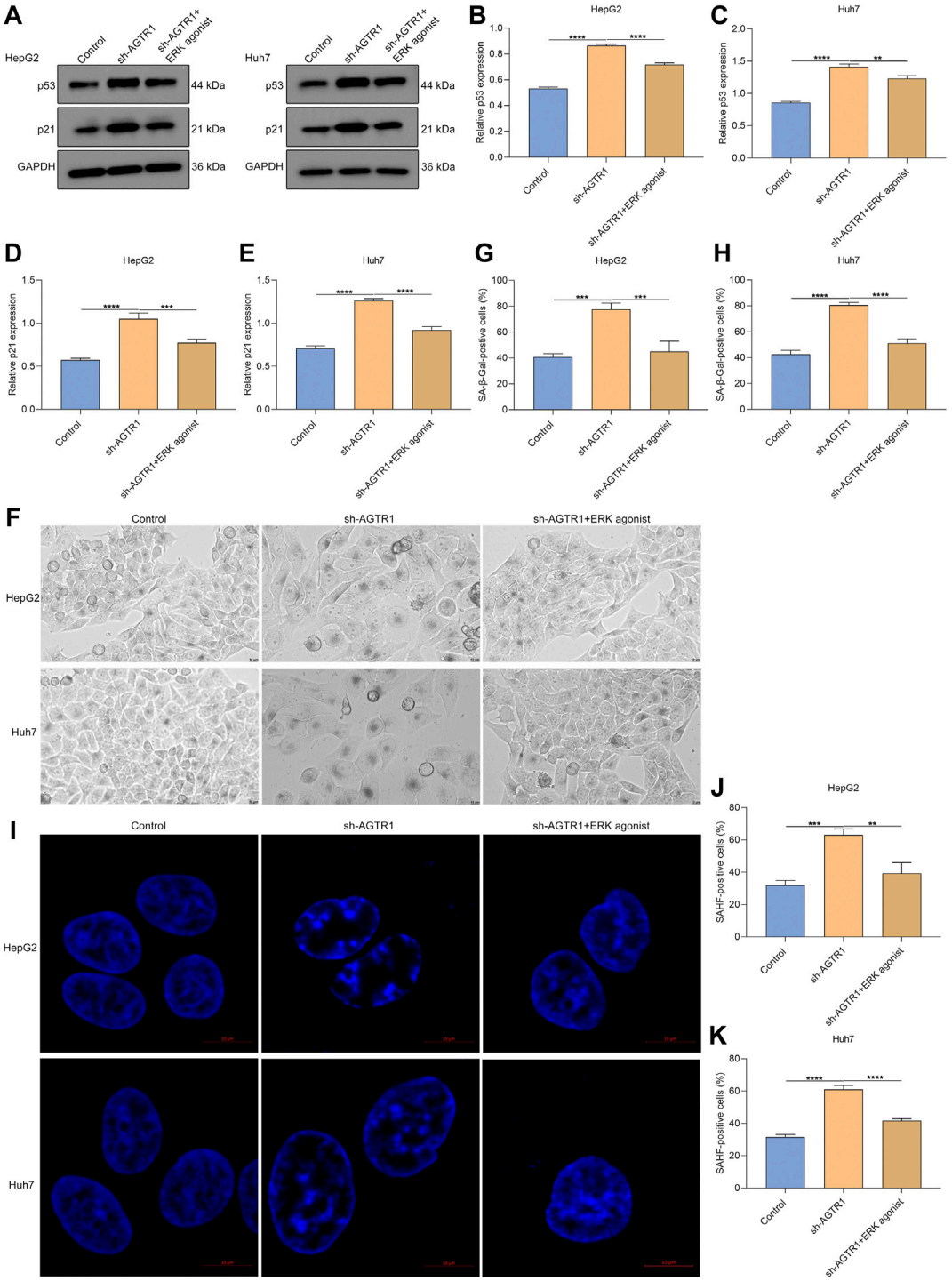

FIGURE 7 | AGTR1 knockdown triggers cellular senescence of HCC cells in an ERK-dependent pathway. **(A–E)** p53 and p21 protein expressions in HepG2 along with Huh7 cell lines with sh-AGTR1 lentivirus transduction or ERK agonist EGF. **(F–H)** SA-β-Gal activity of HCC cell lines with sh-AGTR1 lentivirus transduction or ERK agonist EGF. Scale bar, 10 μm. **(I–K)** SAHF activity of HCC cell lines with sh-AGTR1 lentivirus transduction or ERK agonist EGF. Scale bar, 10 μm.

2022; Öcal et al., 2022). A combination of AGTR1 suppression and sorafenib might be a potential therapeutic regimen to synergistically restrain HCC progression.

The ERK signaling pathway exerts a key in nearly all cellular functions (especially proliferation and senescence) (Berger et al., 2017). Evidence indicates that AGTR1 mediates ERK activity in prostate cancer (Zhang D et al., 2019). In HCC cells, suppression of

AGTR1 enabled weakening of ERK activity. ERK agonist EGF improved the proliferative ability as well as decreased G2-M cell phase arrest in HCC cells. Additionally, the expression of p53 and p21 as well as the proportions of SA-β-gal- and SAHF-positive cells for AGTR1-knockout HCC cells was ameliorated by ERK agonist EGF in HCC cells. Hence, suppression of AGTR1 induced cellular senescence in HCC through inactivating ERK signaling. Despite this, the effect and mechanisms of AGTR1 inhibition on cellular senescence of HCC should be investigated *in vivo* in our future studies.

CONCLUSION

Our study offered comprehensive evidence that AGTR1 exerted a key role in cellular senescence of HCC cells. Following exposure to sorafenib, overexpressed AGTR1 enabled to resist cellular senescence of HCC. Additionally, AGTR1 inhibition induced cellular senescence of HCC in an ERK-dependent pathway. Collectively, our findings highlighted the therapeutic implications of AGTR1 in HCC patients.

DATA AVAILABILITY STATEMENT

The original contributions presented in the study are included in the article/Supplementary Material; further inquiries can be directed to the corresponding author.

AUTHOR CONTRIBUTIONS

AT conceived and designed the study. HW, YC, and HG conducted most of the experiments and data analysis and wrote the manuscript. JX and SH participated in collecting data and helped to draft the manuscript. All authors reviewed and approved the manuscript.

FUNDING

This work was funded by the Fundamental Research Funds for the Central Universities (WK9110000071).

REFERENCES

Alimirah, F., Pulido, T., Valdovinos, A., Alptekin, S., Chang, E., Jones, E., et al. (2020). Cellular Senescence Promotes Skin Carcinogenesis through p38MAPK and p44/42MAPK Signaling. *Cancer Res.* 80 (17), 3606–3619. doi:10.1158/0008-5472.Can-20-0108

Benson, A. B., D'Angelica, M. I., Abbott, D. E., Anaya, D. A., Anders, R., Are, C., et al. (2021). Hepatobiliary Cancers, Version 2.2021, NCCN Clinical Practice Guidelines in Oncology. *J. Natl. Compr. Canc Netw.* 19 (5), 541–565. doi:10.6004/jnccn.2021.0022

Berger, M. D., Stintzing, S., Heinemann, V., Yang, D., Cao, S., Sunakawa, Y., et al. (2017). Impact of Genetic Variations in the MAPK Signaling Pathway on Outcome in Metastatic Colorectal Cancer Patients Treated with First-Line FOLFIRI and Bevacizumab: Data from FIRE-3 and TRIBE Trials. *Ann. Oncol.* 28 (11), 2780–2785. doi:10.1093/annonc/mdx412

Birch, J., and Gil, J. (2020). Senescence and the SASP: Many Therapeutic Avenues. *Genes. Dev.* 34 (23-24), 1565–1576. doi:10.1101/gad.343129.120

Cheng, A.-L., Qin, S., Ikeda, M., Galle, P. R., Ducreux, M., Kim, T.-Y., et al. (2022). Updated Efficacy and Safety Data from IMbrave150: Atezolizumab Plus Bevacizumab vs. Sorafenib for Unresectable Hepatocellular Carcinoma. *J. Hepatology* 76 (4), 862–873. doi:10.1016/j.jhep.2021.11.030

Chini, C. C. S., Peclat, T. R., Warner, G. M., Kashyap, S., Espindola-Netto, J. M., de Oliveira, G. C., et al. (2020). CD38 Ecto-Enzyme in Immune Cells Is Induced during Aging and Regulates NAD+ and NMN Levels. *Nat. Metab.* 2 (11), 1284–1304. doi:10.1038/s42255-020-00298-z

Ding, X., Sun, W., Li, W., Shen, Y., Guo, X., Teng, Y., et al. (2021). Transarterial Chemoembolization Plus Lenvatinib versus Transarterial Chemoembolization Plus Sorafenib as First-Line Treatment for Hepatocellular Carcinoma with Portal Vein Tumor Thrombus: A Prospective Randomized Study. *Cancer* 127 (20), 3782–3793. doi:10.1002/cncr.33677

Duan, J. L., Ruan, B., Song, P., Fang, Z. Q., Yue, Z. S., Liu, J. J., et al. (2022). Shear Stress-Induced Cellular Senescence Blunts Liver Regeneration through Notch-Sirtuin 1-P21/P16 axis. *Hepatology* 75 (3), 584–599. doi:10.1002/hep.32209

Finn, R. S., Ryoo, B.-Y., Merle, P., Kudo, M., Bouattour, M., Lim, H. Y., et al. (2020). Pembrolizumab as Second-Line Therapy in Patients with Advanced Hepatocellular Carcinoma in KEYNOTE-240: A Randomized, Double-Blind, Phase III Trial. *J. Clin. Oncol.* 38 (3), 193–202. doi:10.1200/jco.19.01307

Galle, P. R., Finn, R. S., Qin, S., Ikeda, M., Zhu, A. X., Kim, T.-Y., et al. (2021). Patient-reported Outcomes with Atezolizumab Plus Bevacizumab versus Sorafenib in Patients with Unresectable Hepatocellular Carcinoma (IMbrave150): an Open-Label, Randomised, Phase 3 Trial. *Lancet Oncol.* 22 (7), 991–1001. doi:10.1016/s1470-2045(21)00151-0

Gao, G., Li, C., Fan, W., Zhang, M., Li, X., Chen, W., et al. (2021). Brilliant Glycans and Glycosylation: Seq and Ye Shall Find. *Int. J. Biol. Macromol.* 189, 279–291. doi:10.1016/j.ijbiomac.2021.08.054

Guo, R., Gu, J., Zhang, Z., Wang, Y., and Gu, C. (2015). MicroRNA-410 Functions as a Tumor Suppressor by Targeting Angiotensin II Type 1 Receptor in Pancreatic Cancer. *IUBMB Life* 67 (1), 42–53. doi:10.1002/iub.1342

Innes, K. E., Selfe, T. K., Brundage, K., Montgomery, C., Wen, S., Kandati, S., et al. (2018). Effects of Meditation and Music-Listening on Blood Biomarkers of Cellular Aging and Alzheimer's Disease in Adults with Subjective Cognitive Decline: An Exploratory Randomized Clinical Trial. *J. Alzheimers Dis.* 66 (3), 947–970. doi:10.3233/jad-180164

Jelena, G., Tatjana, S.-R., Juan, F. S., Marijana, P., Milena, Č., and Siniša, R. (2019). Telmisartan Induces Melanoma Cell Apoptosis and Synergizes with Vemurafenib *In Vitro* by Altering Cell Bioenergetics. *Cancer Biol. Med.* 16 (2), 247–263. doi:10.20892/j.issn.2095-3941.2018.0375

Kelley, R. K., Sangro, B., Harris, W., Ikeda, M., Okusaka, T., Kang, Y.-K., et al. (2021). Safety, Efficacy, and Pharmacodynamics of Tremelimumab Plus Durvalumab for Patients with Unresectable Hepatocellular Carcinoma: Randomized Expansion of a Phase I/II Study. *J. Clin. Oncol.* 39 (27), 2991–3001. doi:10.1200/jco.20.03555

Leung, C. O. N., Tong, M., Chung, K. P. S., Zhou, L., Che, N., Tang, K. H., et al. (2020). Overriding Adaptive Resistance to Sorafenib through Combination Therapy with Src Homology 2 Domain-Containing Phosphatase 2 Blockade in Hepatocellular Carcinoma. *Hepatology* 72 (1), 155–168. doi:10.1002/hep.30989

Li, Q.-J., He, M.-K., Chen, H.-W., Fang, W.-Q., Zhou, Y.-M., Xu, L., et al. (2022). Hepatic Arterial Infusion of Oxaliplatin, Fluorouracil, and Leucovorin versus Transarterial Chemoembolization for Large Hepatocellular Carcinoma: A Randomized Phase III Trial. *J. Clin. Oncol.* 40 (2), 150–160. doi:10.1200/jco.21.00608

Lujambio, A., Akkari, L., Simon, J., Grace, D., Tschaharganeh, D. F., Bolden, J. E., et al. (2013). Non-cell-autonomous Tumor Suppression by P53. *Cell* 153 (2), 449–460. doi:10.1016/j.cell.2013.03.020

Lyu, N., Wang, X., Li, J.-B., Lai, J.-F., Chen, Q.-F., Li, S.-L., et al. (2022). Arterial Chemotherapy of Oxaliplatin Plus Fluorouracil versus Sorafenib in Advanced Hepatocellular Carcinoma: A Biomolecular Exploratory, Randomized, Phase III Trial (FOHAIC-1). *J. Clin. Oncol.* 40 (5), 468–480. doi:10.1200/jco.21.01963

Ma, Y., Xia, Z., Ye, C., Lu, C., Zhou, S., Pan, J., et al. (2019). AGTR1 Promotes Lymph Node Metastasis in Breast Cancer by Upregulating CXCR4/SDF-1α and Inducing Cell Migration and Invasion. *Aging* 11 (12), 3969–3992. doi:10.18632/aging.102032

Öcal, O., Schütte, K., Kupčinskas, J., Morkunas, E., Jurkeviciute, G., de Toni, E. N., et al. (2022). Baseline Interleukin-6 and -8 Predict Response and Survival in Patients with Advanced Hepatocellular Carcinoma Treated with Sorafenib Monotherapy: an Exploratory Post Hoc Analysis of the SORAMIC Trial. *J. Cancer Res. Clin. Oncol.* 148 (2), 475–485. doi:10.1007/s00432-021-03627-1

Okazaki, M., Fushida, S., Harada, S., Tsukada, T., Kinoshita, J., Oyama, K., et al. (2014). The Angiotensin II Type 1 Receptor Blocker Candesartan Suppresses Proliferation and Fibrosis in Gastric Cancer. *Cancer Lett.* 355 (1), 46–53. doi:10.1016/j.canlet.2014.09.019

Prasanna, P. G., Citrin, D. E., Hildesheim, J., Ahmed, M. M., Venkatachalam, S., Riscuta, G., et al. (2021). Therapy-Induced Senescence: Opportunities to Improve Anticancer Therapy. *J. Natl. Cancer Inst.* 113 (10), 1285–1298. doi:10.1093/jnci/djab064

Qiao, Z.-w., Jiang, Y., Wang, L., Wang, L., Jiang, J., Zhang, J.-r., et al. (2021). LINC00852 Promotes the Proliferation and Invasion of Ovarian Cancer Cells by Competitively Binding with miR-140-3p to Regulate AGTR1 Expression. *BMC Cancer* 21 (1), 1004. doi:10.1186/s12885-021-08730-7

Qin, S., Bi, F., Gu, S., Bai, Y., Chen, Z., Wang, Z., et al. (2021). Donafenib versus Sorafenib in First-Line Treatment of Unresectable or Metastatic Hepatocellular Carcinoma: A Randomized, Open-Label, Parallel-Controlled Phase II-III Trial. *J. Clin. Oncol.* 39 (27), 3002–3011. doi:10.1200/jco.21.00163

Qiu, X.-T., Song, Y.-C., Liu, J., Wang, Z.-M., Niu, X., and He, J. (2020). Identification of an Immune-Related Gene-Based Signature to Predict Prognosis of Patients with Gastric Cancer. *World J. Gastrointest Oncol.* 12 (8), 857–876. doi:10.4251/wjgo.v12.i8.857

Ren, Z., Xu, J., Bai, Y., Xu, A., Cang, S., Du, C., et al. (2021). Sintilimab Plus a Bevacizumab Biosimilar (IBI305) versus Sorafenib in Unresectable Hepatocellular Carcinoma (ORIENT-32): a Randomised, Open-Label, Phase 2-3 Study. *Lancet Oncol.* 22 (7), 977–990. doi:10.1016/s1470-2045(21)00252-7

Rhodes, D. R., Ateeq, B., Cao, Q., Tomlins, S. A., Mehra, R., Laxman, B., et al. (2009). AGTR1 Overexpression Defines a Subset of Breast Cancer and Confers Sensitivity to Losartan, an AGTR1 Antagonist. *Proc. Natl. Acad. Sci. U.S.A.* 106 (25), 10284–10289. doi:10.1073/pnas.0900351106

Ryoo, B. Y., Merle, P., Kulkarni, A. S., Cheng, A. L., Bouattour, M., Lim, H. Y., et al. (2021). Health-related Quality-Of-Life Impact of Pembrolizumab versus Best Supportive Care in Previously Systemically Treated Patients with Advanced Hepatocellular Carcinoma: KEYNOTE-240. *Cancer* 127 (6), 865–874. doi:10.1002/cncr.33317

Singh, A., Srivastava, N., Yadav, A., and Ateeq, B. (2020). Targeting AGTR1/NF-Kb/cxcr4 axis by miR-155 Attenuates Oncogenesis in Glioblastoma. *Neoplasia* 22 (10), 497–510. doi:10.1016/j.neo.2020.08.002

Sun, J., Zhou, C., Zhao, Y., Zhang, X., Chen, W., Zhou, Q., et al. (2021). Quiescin Sulfhydryl Oxidase 1 Promotes Sorafenib-Induced Ferroptosis in Hepatocellular Carcinoma by Driving EGFR Endosomal Trafficking and Inhibiting NRF2 Activation. *Redox Biol.* 41, 101942. doi:10.1016/j.redox.2021.101942

Tang, W., Chen, Z., Zhang, W., Cheng, Y., Zhang, B., Wu, F., et al. (2020). The Mechanisms of Sorafenib Resistance in Hepatocellular Carcinoma: Theoretical Basis and Therapeutic Aspects. *Sig Transduct. Target Ther.* 5 (1), 87. doi:10.1038/s41392-020-0187-x

Trayssac, M., Clarke, C. J., Stith, J. L., Snider, J. M., Newen, N., Gault, C. R., et al. (2021). Targeting Sphingosine Kinase 1 (SK1) Enhances Oncogene-Induced Senescence through Ceramide Synthase 2 (CerS2)-Mediated Generation of Very-Long-Chain Ceramides. *Cell Death Dis.* 12 (1), 27. doi:10.1038/s41419-020-03281-4

Vogel, A., Qin, S., Kudo, M., Su, Y., Hudgens, S., Yamashita, T., et al. (2021). Lenvatinib versus Sorafenib for First-Line Treatment of Unresectable Hepatocellular Carcinoma: Patient-Reported Outcomes from a Randomised, Open-Label, Non-inferiority, Phase 3 Trial. *Lancet Gastroenterology Hepatology* 6 (8), 649–658. doi:10.1016/s2468-1253(21)00110-2

Wang, X., Cheng, G., Miao, Y., Qiu, F., Bai, L., Gao, Z., et al. (2021). Piezo Type Mechanosensitive Ion Channel Component 1 Facilitates Gastric Cancer Omentum Metastasis. *J. Cell Mol. Med.* 25 (4), 2238–2253. doi:10.1111/jcmm.16217

Wen, F., Zheng, H., Zhang, P., Liao, W., Zhou, K., and Li, Q. (2021). Atezolizumab and Bevacizumab Combination Compared with Sorafenib as the First-Line Systemic Treatment for Patients with Unresectable Hepatocellular Carcinoma: A Cost-Effectiveness Analysis in China and the United states. *Liver Int.* 41 (5), 1097–1104. doi:10.1111/liv.14795

Xiang, X., Fu, Y., Zhao, K., Miao, R., Zhang, X., Ma, X., et al. (2021). Cellular Senescence in Hepatocellular Carcinoma Induced by a Long Non-coding RNA-Encoded Peptide PINT87aa by Blocking FOXM1-Mediated PHB2. *Theranostics* 11 (10), 4929–4944. doi:10.7150/thno.55672

Yan, Z., Ohuchida, K., Fei, S., Zheng, B., Guan, W., Feng, H., et al. (2019). Inhibition of ERK1/2 in Cancer-Associated Pancreatic Stellate Cells Suppresses Cancer-Stromal Interaction and Metastasis. *J. Exp. Clin. Cancer Res.* 38 (1), 221. doi:10.1186/s13046-019-1226-8

Yang, K., Zhou, J., Chen, Y., Chen, Y., Chen, L., Zhang, P., et al. (2020). Angiotensin II Contributes to Intratumoral Immunosuppression via Induction of PD-L1 Expression in Non-small Cell Lung Carcinoma. *Int. Immunopharmacol.* 84, 106507. doi:10.1016/j.intimp.2020.106507

Zhang, D., Liu, H., Yang, B., Hu, J., and Cheng, Y. (2019). L-securinine Inhibits Cell Growth and Metastasis of Human Androgen-independent Prostate Cancer DU145 Cells via Regulating Mitochondrial and AGTR1/MEK/ERK/STAT3/PAX2 Apoptotic Pathways. *Biosci. Rep.* 39 (5), BSR20190469. doi:10.1042/bsr20190469

Zhang, J.-W., Zhang, D., and Yu, B.-P. (2021). Senescent Cells in Cancer Therapy: Why and How to Remove Them. *Cancer Lett.* 520, 68–79. doi:10.1016/j.canlet.2021.07.002

Zhang, Q., Yu, S., Lam, M. M. T., Poon, T. C. W., Sun, L., Jiao, Y., et al. (2019). Angiotensin II Promotes Ovarian Cancer Spheroid Formation and Metastasis by Upregulation of Lipid Desaturation and Suppression of Endoplasmic Reticulum Stress. *J. Exp. Clin. Cancer Res.* 38 (1), 116. doi:10.1186/s13046-019-1127-x

Zhu, X., Chen, L., Liu, L., and Niu, X. (2019). EMT-mediated Acquired EGFR-TKI Resistance in NSCLC: Mechanisms and Strategies. *Front. Oncol.* 9, 1044. doi:10.3389/fonc.2019.01044

Ziegler, D. V., Vindrieux, D., Goehrig, D., Jaber, S., Collin, G., Griveau, A., et al. (2021). Calcium Channel ITPR2 and Mitochondria-ER Contacts Promote Cellular Senescence and Aging. *Nat. Commun.* 12 (1), 720. doi:10.1038/s41467-021-20993-z

Conflict of Interest: The authors declare that the research was conducted in the absence of any commercial or financial relationships that could be construed as a potential conflict of interest.

Publisher's Note: All claims expressed in this article are solely those of the authors and do not necessarily represent those of their affiliated organizations, or those of the publisher, the editors, and the reviewers. Any product that may be evaluated in this article, or claim that may be made by its manufacturer, is not guaranteed or endorsed by the publisher.

frontiers | Frontiers in Bioengineering and Biotechnology

TYPE Mini Review
PUBLISHED 23 September 2022
DOI 10.3389/fbioe.2022.943915

OPEN ACCESS

EDITED BY
Leming Sun,
Northwestern Polytechnical University, China

REVIEWED BY
Huang Jiangang,
Xiamen University, China

*CORRESPONDENCE
YiBin Ma,
mybzlj1973@163.com

SPECIALTY SECTION
This article was submitted to Preclinical Cell and Gene Therapy, a section of the journal Frontiers in Bioengineering and Biotechnology

RECEIVED 14 May 2022
ACCEPTED 05 August 2022
PUBLISHED 23 September 2022

CITATION
Song D, Liu P, Shang K and Ma Y (2022), Application and mechanism of anti-VEGF drugs in age-related macular degeneration.
Front. Bioeng. Biotechnol. 10:943915.
doi: 10.3389/fbioe.2022.943915

Application and mechanism of anti-VEGF drugs in age-related macular degeneration

Dawei Song, Ping Liu, Kai Shang and YiBin Ma*

Tai'an City Central Hospital, Taian, China

Age-related macular degeneration (AMD) is the leading cause of blindness in the elderly. The incidence rate increases with age in people over 50 years of age. With the advent of China's aging society, the number of patients is increasing year by year. Although researchers have done a lot of basic research and clinical research on the pathogenesis and treatment of AMD in recent years, the pathogenesis of AMD is still controversialdue to the complexity of the disease itself. AMD is the primary cause of blindness in the elderly over 50 years old. It is characterized by the formation of choroidal neovascularization (CNV) and the over secretion of vascular endothelial growth factor (VEGF) as its main mechanism, which can eventually lead to vision loss or blindness. The occurrence and development of AMD is an extremely complex process, in which a large number of regulatory factors and cytokines are involved. Most of the existing treatments are for its concomitant CNV. Targeted VEGF drugs for neovascularization, such as Lucentis and Aflibercept, are the first-line drugs for AMD. Their application has greatly reduced the blinding rate of patients. However, there are still some patients who have no response to treatment or cannot maintain their vision after long-term treatment. Frequent injection also increases the risk of complications and economic burden. In order to further improve the quality of life and long-term prognosis of AMD patients, a variety of new treatmentshave been or will be applied in clinic, including combined treatment with the same or different targets to improve the curative effect, change or simplify the mode of medication, inhibit VEGF receptor tyrosine protein kinase and so on. This article provides a brief review of the research progress of anti-VEGF drugs and their mechanisms for the treatment of AMD, it is expected to provide a better treatment plan for AMD treatment.

KEYWORDS

mechanism, anti-VEGF drugs, age-related macularde, treatment, choroidal neovascularization

Introduction

Age-related macular degeneration (AMD) is a disease that causes progressive and irreversible loss of central vision and poses a serious threat to the vision of the elderly. There are more than 5 million AMD patients in China. With the improvement of my country's economy, medical level and average life expectancy, the prevalence of AMD has been rising (Ambati, 2011; Vogl et al., 2021). According to the fundus

manifestations, AMD is divided into exudative AMD and atrophic AMD. Exudative AMD accounts for about 10% of AMD, but the damage to vision is much greater than atrophic AMD (Zhang et al., 2003; Mettu et al., 2020a; Arjunan et al., 2021). Atrophic AMD is characterized by geographic atrophy in the macular region. According to the pathological changes, AMD can be divided into two categories: wet and dry. Wet AMD is mainly characterized by choroidal neovascularization (CNV) formation, retinal pigment epithelium (RPE) detachment, macular hemorrhage and edema, also known as exudative or neovascular AMD. Wet AMD accounts for only 10% of AMD, but the harm is much greater than dry AMD (Montorio et al., 2021). With the aging population intensifies, the harm of AMD will further increase. At present, the treatment of wet AMD mainly targets CNV, and the treatment methods are mainly drug treatment, photodynamic therapy (PDT) and surgery.

PDT is the main treatment before anti-VEGF drugs are used in wet AMD. It destroys CNV while preserving function of RPE cells and neural retina without causing central visual impairment and visual field defect (Stenirri et al., 2012; Wei and Li, 2020; Hu et al., 2021). However, PDT is often accompanied by complications such as necrosis and apoptosis of corneal cells, temporary visual impairment, photosensitivity reactions, and has disadvantages such as easy recurrence and high price. Surgical treatment is highly invasive and postoperative visual recovery is affected to some extent (Yildirim et al., 2004). Intravitreal injection of anti-VEGF is widely used as the first-line drug in clinicfor the treatment of AMD because of its low visual impairment and few adverse effects, but there are still problems such as the need for repeated multiple treatments, the lack of response to treatment in some patients, and the increased risk of repeated intravitreal injection (Gale et al., 2003; Tavakoli et al., 2020; Wei et al., 2020). The development of new drugs, improvements in dosage forms and medication methods are expected to improve these deficiencies, such as the application of eye drops, oral preparations and anti VEGF drug extended-release devices, which brings hope to reduce the use of anti-VEGF drugs (Zhang et al., 2014; ClearkinLRamasamy et al., 2019). This article provides a brief review of the research progress of anti-VEGF drugs and their mechanisms for the treatment of AMD.

Characteristics of vascular endothelial growth factor

VEGF is a kind of homodimeric glycoprotein linked by disulfide bonds. It has heparin binding activity, which promotes the mitosis of vascular endothelial cells to promote angiogenesis. VEGF is widely distributed in the brain, kidney, liver, eye and other tissues and organs of the human body. The retinal pericytes, pigment epithelial cells, endothelial cells and ganglion cells in the eyes can express VEGF, which plays an important role in maintaining the integrity of ocular blood vessels, but overexpression will promote the abnormal proliferation of blood vessels (Weber et al., 1994; Ma et al., 2021). Its gene family members mainly include VEGF-A, VEGF-B, VEGF-C, VEGF-D, VEGF-E and placental growth factor. Among them, VEGF-A plays an important role in neovascularization and increasing vascular permeability (Bhisitkul, 2006). The intrinsic biological characteristics of VEGF include: 1) Promoting endothelial cell mitosis and angiogenesis. 2) Increasing the permeability of vascular endothelium, making plasma protein overflow out of blood vessels, causing fibrin coagulation, and forming a temporary matrix for angiogenesis. Meanwhile, promoting stromal cells to further form mature vascular matrix, so as to promote angiogenesis. Changing the extracellular matrix and indirectly promoting angiogenesis. 3) Having neuroprotective effectby inhibiting neuronal apoptosis, promoting the proliferation of nerve cells and protecting retinal nerve fibers. Having vascular protective effect by antithrombotic effect (DorY and Keshet, 2001).

Pathogenesis

The risk factors for AMD are mainly age, race, smoking, drinking, sunlight exposure, inner eye surgery and genetic factors, etc. Most scholars believe that the joint action of environmental factors and genetic factors leads to the occurrence of AMD (Arjunan et al., 2021). The pathogenesis of AMD is complex and controversial. Now we mainly introduce the following pathogenesis.

Aging and metabolic changes of retinal pigment epithelium

With the decline of systemic function in the elderly, RPE also changes. Mettu et al. (2020a) found that apoptosis of RPE cells in the macula region increases with age, and the activity of lysosomal system in RPE cells is positively correlated with age. Aging initiates the lysosomal system, which leads todamage of RPE cells. RPE cells in human eyes are able to provide metabolic support for retinal photoreceptor cells. The outer segments of retinal photoreceptor cells renew periodically, and the shed substances are swallowed and cleared by RPE cells. The apoptosis and damage of RPE cells reduce their “cleaning” ability. Metabolites accumulate in the inner layer of Bruch’s membrane, forming vitreousmembrane warts that damage the adjacent retinal tissue and lead to retinal tissue atrophy, forming a vicious cycle that eventually causes calcification and rupture of Bruch’s membrane, resulting in the formation of CNV (Montorio

et al., 2021). The aging of RPE cells also breaks the balance of enzymes in its extracellular matrix, causing the local RPE extracellular matrix in the macular region to gather on the Bruch's membrane, resulting in the thickening of Bruch's membrane, reducing retinal blood supply, stimulating phagocytes to produce angiogenic factors, resulting in the formation of CNV, which is seriously harmful to vision.

Light damage and oxidative damage

When looking at objects, the macula is always under light, so some scholars have proposed the mechanism of light damage (Wei and Li, 2020). Studies have shown that long-term irradiation of light will increase the concentration of free radicals in the eye. The original physiological balance is broken and the outer segments of photoreceptors are the first to be attacked by free radicals (Wei and Li, 2020). Light damage and oxidative damage cause retinal cell damage and apoptosis, which in turn lead to the occurrence and development of AMD. Research have (Hu et al., 2021) reported that hydrogen peroxide was used to induce the expression of recombinant ferritin, mitochondrial (FtMt) in acute retinal pigment epithelium (ARPE) cells, and then the overexpression of FtMt induced by oxidative stress was detected by flow cytometry and MTT method, and the damage and apoptosis of the two cell lines were observed. The results showed that the highly expressed FtMt had a protective effect on the cells against oxidative stress. Stenirri et al. (2012) found that there are mutant FtMt in some AMD patients. The conformation of mutant FtMt changes, which weakens the original antioxidant stress ability and causes oxidative damage to cells. Malondialdehyde level is a marker of oxidative stress level. Yildirim et al. (2004) detected the plasma malondialdehyde level in 30 patients with AMD and 60 healthy people. It was found that the plasma malondialdehyde level in patients with AMD is significantly higher than that in healthy people. The macular region of healthy people is rich in lutein, which can filter harmful light and reduce oxidative damage. This suggests that the occurrence of AMD is related to the decrease of lutein in macula. Gale et al. (2003) found that the pigment in the macular area of AMD patients decreased. It has also been reported that high-dose intake of lutein can help delay the loss of vision in patients with atrophic AMD, which proves that the development of AMD is related to the reduction of lutein (Yildirim et al., 2004).

Immune inflammation

Recently, studies have shown that fundus inflammation leads to the production of vitreous membrane wart and the occurrence and development of AMD (Gale et al., 2003). Immunohistochemical study on vitreousmembrane wart showed that its components mainly include RPE cells, factors involved in complement pathway, acute phase molecules, main tissue soluble type II antigen complex, etc., (Wei et al., 2020). Some pathological components of atherosclerosis, Alzheimer's disease and type 2 membranoproliferative glomerulonephritisare the same as thatofvitreous membrane warts, suggesting that the pathogenesis of these diseases may be similar to AMD. Some scholars believe that AMD may be a chronic persistent inflammatory disease. Local cell tissue damage leads to the damage of inner and outer retinal barriers and the release of inflammatory factors (Tavakoli et al., 2020). Wei et al. (2020) observed the vitreous membrane wart under the electron microscope and found that dendritic cells could be seen in the center of most vitreous membrane warts. Zhang et al. (2014) measured monocyte chemoattractant protein 1 and transforming growth factorβ1and interleukin-6 in venous blood of 55 patients with exudative AMD and 33 patients with age-related cataract by enzyme-linked immunosorbent assay (ELISA). The results showed that the levels of transforming growth factor β1 and interleukin-6 in venous blood of patients with exudative AMD are significantly higher than those of patients with age-related cataract. The level of interleukin-6 is significantly higher than that in age-related cataract patients. Studies have shown that macrophages are abundant in the choroid of AMD patients and isolated CNV tissues (ClearkinLRamasamy et al., 2019). ClearkinLRamasamy et al. (2019) found that in mice with reduced macrophages induced by laser, the expression of vascular endothelial growth factor (VEGF) is decreased due to the decrease of macrophages, which lead to the decrease of CNV production.

Heredity and gene mutation

Ma et al. (2021) confirmed that heredity is related to the occurrence of AMDby studying on 840 elderly male twins. The early clinical manifestation of Sorsby macular dystrophy (SDF) is the thickening of Bruch's membrane in the macular region and the deposition of lipid like substances. In the late stage, there are scars, neovascularization and hemorrhage in the macular region. SDF has many similarities with AMD and has become an important model to study the mechanism of AMD. As early as 1994, Weber et al. (1994) found that the gene causing AMDis located on chromosome 22q13.1 when studying a Canadian SDF family. Gene abnormalities in this region will lead to the disruption of the stability of extracellular matrix, the damage of retinal tissue and the generation of CNV. Studies have shown that a variety of complement factors in the complement system are related to the occurrence of AMD, including complement 3 (C3), complement factor H (CFH) and complement factor I (CFI) (Bhisitkul, 2006). Bhisitkul (2006) extracted DNA from venous blood of 119 patients with exudative AMD, 120 patients with early AMD and 140 healthy controls, and detected CFI gene by polymerase chain reaction (PCR) combined with restriction enzyme digestion analysis and DNA sequencing. The results showed that CFI is

associated with the occurrence of AMD, and the CFI variant alleles in exudative AMD are less than those in the control group. Thus, CFI variant allele is a protective factor. Ithas been demonstratedby many studiesthatAMDis related to gene mutation, while the occurrence of AMD may also be related to the imbalance between inhibitory genes and regulatory genes (DorY and Keshet, 2001). The pathogenic gene of AMDisstill unclear, and further studies are needed to verify it.

Hemodynamic changes

AMD patients, especially exudative AMD patients, have decreased choroidal blood flow and blood perfusion in the macular areaof the affected eye. RPE cells suffer from hypoxia and injurydue to insufficient perfusion, whichin turn leads to the formation of CNV and vascular exudation. Due to blood lipid deposition, arteriosclerosis and other reasons, it often leads to thickening of vascular wall, narrowing of vascular cavity and reduction of vascular wall compliance in the elderly, which leads to changes in hemodynamics and affects fundus blood perfusion. Sharma et al. (2021) used Doppler ultrasound to detect the hemodynamic changes of ophthalmic artery, central retinal artery and posterior ciliary artery ofthe affected eyes in 47 patients with AMD. It was found that theocular artery peak systolic velocity (PSV) of blood flowdecreased significantly, especially in patients with exudative AMD. With the aggravation of the disease, the ocular arterial resistance index (RI) also increased significantly. Abnormal perfusion of the choroid can lead to calcification and damage of Bruch's membrane, accelerating lipid deposition, further impairing the function of RPE cells, and ultimately inducing AMD (ArjamaaONikinmaa et al., 2009). Cigarette smoke contains a large number of substances harmful to blood vessels, which is an important risk factor for inducing AMD. At the same time, smoking can promote the transformation of atrophic AMD into exudative AMD. Mei et al. (2009) analyzes the carotid hemodynamics of 50 active smokers, 44 passive smokers and 44 normal controls by vascular echo tracking (ET)technology. The results showed that the carotid pressure-strain elastic coefficient and stiffness of active smokers and passive smokers are higher than those of normal controls, while the carotid compliance of active smokers and passive smokers is significantly lower than that of normal controls.

Vascular endothelial growth factor and age-related macular degeneration

The pathogenesis of AMD is not fully understood, and epidemiology shows that ethnicity, age, and smoking are definite risk factors, with a high prevalence in Caucasians and a low prevalence in Blacks, and no difference in prevalence between men and women (ArjamaaONikinmaa et al., 2009; Sharma et al., 2021). Numerous studies have shown that the VEGF/VEGFR pathway induces neovascularization and is an important pathogenesis of AMD. VEGF is a glycoprotein isolated from bovine pituitary follicular cells by Ferrara et al., in 1989, and seven kinds have been identified to date: VEGF (VEGF-A), VEGF-B to E, spinal cord-derived growth factor, and placental growth factor (PIGF). VEGF receptors include fms-like tyrosine kinase 1 (i.e., vascular endothelial growth factor receptor l, VEGFR1), fetal liver kinase insertion domain receptor (i.e., VEGFR2), VEGFR3, Neuropillin-1 (Npn-1) and Npn-2 (Mei et al., 2009). VEGF promotes neovascularization mainly by binding to ligand families which containing one or both VEGFR1 and VEGFR2.

VEGF-A is the strongest pro-angiogenic growth factor known at present. Its role is mainly to promote angiogenesis, proliferation and survival, and increase microvascular permeability, while VEGFR2 is the main mediator of angiogenesis (Mei et al., 2009). PIGF can selectively bind to VEGFR1 and be abundantly expressed in endothelial cells, thus accelerating VEGF-A-induced endothelial cell proliferation. In addition to directly mediating angiogenesis, VEGF can also stimulate the expression of matrix metalloproteinases in vascular endothelial cells, help neovascularization invade tissues by degrading extracellular matrix, make CNV grow continuously, and promote the chemotaxis of monocytes and macrophages (Wang et al., 2013a; Mohan et al., 2013).

In the early stage of exudative AMD, theincreased VEGF expression can be detected in both the RPE and the outer nuclear layer of the macula, and elevated VEGF levels are also seen in surgically resected CNV lesions by immunohistochemical methods, all of which suggest an important role for VEGF in exudative AMD. With the development of AMD, choroidal microcirculation is often impaired, leading to tissue ischemia and hypoxia. Shibuya and claesson-welsh (2006) showed that VEGF mRNA transcript levels are upregulated under the condition of retinal hypoxia, and correspondingly the expressionsof VEGFR1 and VEGFR2 are increased. In the normal physiological state, VEGFR1 inhibits the over-phosphorylated expression of VEGFR2, whereas it exhibits a promoting effect in the pathological state and increases vascular permeability. The two interact to promote neovascularization.

Anti-vascular endothelial growth factor drugs for age-related macular degeneration

At present, anti-VEGF drugs used in clinic and R&D are roughly divided into drugs that block the binding of VEGF and VEGFR (such as anti-VEGF aptamer and anti-VEGF monoclonal antibody or antibody fragment), drugs that block important kinases

downstream of VEGF pathway signal transduction and drugs that inhibit VEGF gene expression (Peng, 2021; ZarbinMAHill et al., 2021). By blocking the activation of VEGF downstream pathway, anti-VEGF drugs can reduce the increase of vascular permeability caused by the increase of VEGF, inhibit the growth of CNV, alleviate macular edema and improve the visual acuity of patients with exudative AMD. However, a number of clinical trials of several anti-VEGF drugs currently used in clinic show that 1/4 of patients still have no response to treatment, and even their vision continues to decline after treatment, eventually becoming blind (Mettu et al., 2020b). Meanwhile, anti-VEGF drugs often need to be injected repeatedly on a monthly basis, which increases the risk of complications.

At present, there is no specific treatment for AMD, especially for atrophic AMD. Most treatments are for CNV associated with exudative AMD. The formation mechanism of CNV is not very clear. The current research have showed that inflammation plays an important role in the occurrence and development of AMD (ArjunanPSwaminathan et al., 2021). Inflammatory reaction promotes the over-regulation of cells and a variety of growth factors, leading to pathological vascular proliferation and CNV. Among the growth factors, VEGF is the most powerful promoter of ocular neovascularization (ZhuLParker et al., 2020). The continuous research on the mechanism of CNV for AMD and the R&D of anti-VEGF drugs, that is, applying anti-VEGF drugs to prevent choroidal neovascularization in the treatment of wet or neovascularAMD (Wang et al., 2013b), shows that the level of VEGF in aqueous humor of AMD patients is significantly higher than that of normal people. VEGF is an important factor to promote the formation of CNV. Inhibiting VEGF can effectively inhibit the formation of CNV and reduce vascular exudation. Anti-VEGF drugs are the main method to treat exudative AMD. At present, anti-VEGF drugs mainly include the following:

Avastin

Avastin, a recombinant human VEGF monoclonal antibody, was approved by the U.S. Food and Drug Administration (FDA) in February 2004 and is the first drug approved for marketing in the United States to inhibit tumor angiogenesis. Because of its structural similarity to Lucentis, it has been applied by some clinicians to ophthalmic neovascular diseases and has shown good safety and efficacy. Hong et al. (2020) showed that intravitreal injection of Avastin in 22 patients (22 eyes) is safe and effective in treating exudative AMD, significantly reducing macular edema and improving visual acuity at a 6-months follow-up.

Lucentis

Lucentis is the second generation of recombinant human VEGF monoclonal antibody, which can specifically bind VEGF-A and has higher affinity than Avastin. As one of the anti-VEGF drugs, clinical studies have shown that Lucentis can effectively reduce neovascular exudation, reduce macular edema, and improve or maintain the existing visual acuity (Hong and Liu, 2010). Chu et al. (2015) analyzed the clinical data of 46 patients (47 eyes) with exudative AMD who received intravitreal injection of Lucentis and the best corrected visual acuity are <0.05. It was found that after treatment, 61.7% (29/47) of the patients had improved visual acuity, 31.9% (15/47) of the patients had stable visual acuity, and the retinal thickness in the macular center decreased significantly compared with that before treatment.

Aflibercept

Aflibercept, marketed in 2011, is a recombinant VEGF receptor fusion protein consisting of Domain2 of VEGF-R1 and Domain3 of VEGF-R2 and the Fc segment of IgG1, which can specifically bind VEGF-A, VEGF-B, and platelet-derived growth factor (PDGF). Some studies have shown that treatment with Aflibercept in patients with exudative AMD, who were poorly treated with other anti-VEGF drugs, can improve visual acuity and reduce macular edema in the short term (Singh et al., 2014). Heier et al. (2012) treated 2419 subjects with intravitreal injection of Lucentis and Aflibercept, and compared their efficacy and safety. The results showed that Aflibercept and Lucentis have similar efficacy and safety.

Conbercept

Conbercept is the first independently developed anti-VEGF drug in China, a novel receptor fusion protein, which was approved by ChinaNational Medical Products Administration in 2013 for the treatment of exudative AMD. Conbercept specifically binds VEGF-A, VEGF-B, VEGF-C and human placental factor (PIGF). Zhang et al. (2008) applied Biacore and ELISA assays to compare the affinity of Conbercept and Avastin for VEGF-A and PIGF. It was found that Conbercept had higher affinity for VEGF-A than Avastin, and Avastin did not have affinity for PIGF, suggesting that Conbercept has better efficacy and safety in the treatment of exudative AMD. Yu et al. (2015) treated 20 patients with exudative AMD with intravitreal injection of Conbercept once/month for 3 consecutive injections, and after 6 months of follow-up, the patients had significantly improved visual acuity and reduced macular central recess thickness, and no serious adverse effects were observed.

Pegaptanib

Pegaptanib, the first anti-VEGF drug used in ophthalmology, is an RNA aptamer consisting of 28 bases which specifically binds

VEGF-A165. Gragoudas et al. (2004) found that Pegaptanib stabilized but did not improve visual acuity in patients with exudative AMD.

Other drugs

Vatalanib (PTK787) is a potent inhibitor of all known VEGF receptor tyrosine kinases, including VEGFR1, VEGFR2 and VEGFR3. The bioavailability of Vatalanib is high. Preclinical trials and phase I clinical trials showed that Vatalanib has inhibitory effect on CNV and good safety. At present, a trial combined Vatalanibwith PDT is under way. Regorafanib mainly targets VEGF1/3, PDGF-B and fibroblast growth factor receptor 1. The eye drops made from this drug have proved their safety in phase I clinical trials and are now in phase II clinical trials (Hong et al., 2020). As a small molecule preparation, RTKIhas the advantages of easy absorption, simple synthesis and suitable for long-term medication. However, due to its inhibitory effect on a variety of kinases in human body, its specificity is poor and may cause serious adverse reactions. Its clinical efficacy still needs to be further studied. With the approval of anti-VEGF drugs for ophthalmology, AMD patients have ushered in the dawn of hope (Schopf et al., 2013). In order to improve the long-term prognosis and quality of life of patients to the greatest extent, reducing the number of intraocular injections, prolonging the treatment interval, enhancing the efficacy and simplifying the mode of administration are still the hot and difficult areas of concern in the treatment of wet AMD. Although new drugs have been developed to improve at different levels, better treatment schemes still need to be explored in the future.

Prospect

The occurrence and development of AMD is an extremely complex process, in which a large number of regulatory factors and cytokines are involved. Most of the existing treatments are for its concomitant CNV (Yla et al., 2021). Especially, the anti-VEGF drugs have shown good efficacy and application prospect, and have becomea recognized first-line clinical treatment drug (Kc et al., 2020). However, the commonly used anti-VEGF drugs need frequent intravitreal injection, which may be accompanied by serious adverse reactions, thus bringing huge economic burden to patients. In order to improve these problems, researchers have made major breakthroughs in exploring new anti-neovascularization targets, multi-path combination drugs and new administration methods, such as Lucentisextended-release device, combinationwith PDGF target inhibitors, and various drugs developed, such as oral preparation X-82, small molecule preparation brolucizumab, apiciparpegol and eye drops made of VEGF receptor tyrosinase inhibitor pazopanib, have successively entered phase IIand Phase III clinical trials (Waters et al., 2021). However, just as the drug extended-release devices need to overcome the compatibility with tissue and pharmacological and toxicological reactions, and the phase III clinical trial of fovista combined with Lucentis and the phase II clinical trial of pazopanib ended in failure (Wu et al., 2019; Mettu et al., 2020c). The pharmacodynamics, pharmacokinetics and safety of these emerging drugs or administration methods need to be further studied. With the further understanding of the pathogenesis of AMD and the development of genetic technology and bioscience, it is expected that more effective, safer, more lasting and simplified drugs or treatments will be used in clinic as soon as possible and the combination of multiple methods is the main trend in the treatment of AMD in the future.

Author contributions

DS, PL, KS, and YM wrote the paper.

Conflict of interest

The authors declare that the research was conducted in the absence of any commercial or financial relationships that could be construed as a potential conflict of interest.

Publisher's note

References

Ambati, J. (2011). Age-related macular degeneration and the other double helix. the cogan lecture. *Invest. Ophthalmol. Vis. Sci.* 52 (5), 2165–2169. doi:10.1167/iovs.11-7328

Olli Arjamaa, O., Nikinmaa, M., Salminen, A., and Kaarniranta, K. (2009). Regulatory role of hif-1α in the pathogenesis of age-related macular degeneration (AMD). *Ageing Res. Rev.* 8 (4), 349–358. doi:10.1016/j.arr.2009.06.002

Arjunan, P., Swaminathan, R., Yuan, J., Elashiry, M., Tawfik, A., Al-Shabrawey, M., et al. (2021). Exacerbation of amd phenotype in lasered cnv murine model by dysbiotic oral pathogens. *Antioxidants* 10 (2), 309. doi:10.3390/antiox10020309

ArjunanPSwaminathan, R., Yuan, J., Elashiry, M., Tawfik, A., Al-Shabrawey, M., et al. (2021). Exacerbation of amd phenotype in lasered cnv murine model by dysbiotic oral pathogens. *Antioxidants* 10 (2), 309. doi:10.3390/antiox10020309

Bhisitkul, R. B. (2006). Vascular endothelial growth factor biology:clinical implications for ocular treatments. *Br. J. Ophthalmol.* 90 (12), 1542–1547. doi:10.1136/bjo.2006.098426

Chu, S. J., Wang, H. H., Wang, M., et al. (2015). The efficacy of ranibizumab onpatients with exudative age-related macular degeneration and severevisual impairment. *J. Clin. Ophthalmol.* 23 (1), 24–27.

Clearkin, L., Ramasamy, B., Wason, J., and Tiew, S. (2019). Anti-VEGF intervention in neovascular amd: benefits and risks restated as natural frequencies. *BMJ Open Ophthalmol.* 4 (1), e000257–391. doi:10.1136/bmjophth-2018-000257

Dor, Y., and Keshet, E. (2001). Vascular endothelial growth factor and vascular adjustments to perturbations in oxygen homeostasis. *Am. J. Physiology-Cell Physiology* 280 (6), 1367–1374. doi:10.1152/ajpcell.2001.280.6.c1367

Gale, C. R., Hall, N. F., Phillips, D. I., and Martyn, C. N. (2003). Lutein and zeaxanthin status and risk of age-related macular degeneration. *Invest. Ophthalmol. Vis. Sci.* 44 (6), 2461–2465. doi:10.1167/iovs.02-0929

Gragoudas, E. S., Adamis, A. P., Cunningham, E. T., Feinsod, M., and Guyer, D. R. (2004). Pegaptanib for neovascular age related macular degeneration. *N. Engl. J. Med. Overseas. Ed.* 351 (7), 2805–2816. doi:10.1056/nejmoa042760

Heier, J. S., Brown, D. M., Chong, V., Korobelnik, J. F., Kaiser, P. K., Nguyen, Q. D., et al. (2012). Intravitreal aflibercept(VEGF Trap - Eye) in wet age - related macular degeneration. *Ophthalmology* 119 (12), 2537–2548. doi:10.1016/j.ophtha.2012.09.006

Hong, H. K., Park, Y. J., Kim, D. K., Ryoo, N. K., Ko, Y. J., Park, K. H., et al. (2020). Preclinical efficacy and safety of vegf-grab, a novel anti-vegf drug, and its comparison to aflibercept. *Invest. Ophthalmol. Vis. Sci.* 61 (13), 22. doi:10.1167/iovs.61.13.22

Hong, H., and Liu, Q. H. (2010). Clinical observation of intravitreous injections of bevacizumab(avastin) for exudative age - related macular degeneration. *Int. J. Ophthalmol.* 10 (11), 2176–2178.

Hu, Y. C., Chen, Y. L., Chen, Y. C., and Chen, S. N. (2021). 3-year Follow-up of half-dose verteporfin photodynamic therapy for central serous chorioretinopathy with oct-angiography detected choroidal neovascularization. *Sci. Rep.* 11 (1), 13286. doi:10.1038/s41598-021-92693-z

Kc, A., Jian, L. B., Lh, C., et al. (2020). Andrographolide attenuates choroidal neovascularization by inhibiting the hif-1α/vegf signaling pathway - sciencedirect. *Biochem. Biophysical Res. Commun.* 530 (1), 60–66.

Ma, R., Xie, Q., Li, H., Guo, X., Wang, J., Li, Y., et al. (2021). l-Borneol exerted the neuroprotective effect by promoting angiogenesis coupled with neurogenesis via ang1-vegf-bdnf pathway. *Front. Pharmacol.* 12, 641894. doi:10.3389/fphar.2021.641894

Mei, L. X., Zhang, X. L., Bai, L., et al. (2009). E-Tracking technology in evaluating carotid artery elasticity function in passive smokers. *Chin. J. Med. Imaging Technol.* 25 (5), 813–815.

Mettu, P. S., Allingham, M. J., and Cousins, S. W. (2020). Incomplete response to anti-vegf therapy in neovascular amd: exploring disease mechanisms and therapeutic opportunities. *Prog. Retin. Eye Res.* 82, 100906. doi:10.1016/j.preteyeres.2020.100906

Mettu, P. S., Allingham, M. J., and Cousins, S. W. (2020). Incomplete response to anti-vegf therapy in neovascular amd: exploring disease mechanisms and therapeutic opportunities. *Prog. Retin. Eye Res.* 82, 100906. doi:10.1016/j.preteyeres.2020.100906

Mettu, P. S., Allingham, M. J., and Cousins, S. W. (2020). Incomplete response to anti-vegf therapy in neovascular amd: exploring disease mechanisms and therapeutic opportunities. *Prog. Retin. Eye Res.* 82, 100906. doi:10.1016/j.preteyeres.2020.100906

Mohan, R. R., Tovey, J., Sharma, A., et al. (2013). *Representative stereomicroscopy images showing vegf-induced cnv in no decorin-delivered control (a, c and e) and decorin-delivered (b, d and f) rabbit corneas*. 145–148.

Montorio, D., D'Andrea, L., Mirto, N., and Cennamo, G. (2021). The role of optical coherence tomography angiography in reticular pseudodrusen. *Photodiagnosis Photodyn. Ther.* 33 (5), 102094. doi:10.1016/j.pdpdt.2020.102094

Peng, C. L. (2021). Combination of fish oil and selenium enhances anticancer efficacy and targets multiple signaling pathways in anti-vegf agent treated-tnbc tumor-bearing mice. *Mar. Drugs* 19 (88), 109–117.

Schopf, L., EnlowE, E., Popov, A., et al. (2013). Enhanced topical delivery of a small molecule receptor tyrosine kinase inhibitor (rtki) via mucosal-penetrating particle technology. *Invest. Ophthalmol. Vis.* 84 (5), 922–933.

Sharma, K., Tyagi, R., Battu, P., et al. (2021). *The contribution of rare allele and junk genome in amd pathogenesis*.

Shibuya, M., and claesson-welsh, L. (2006). Signal transduction by vegf receptors in regulation of angiogenesis and lymphangiogenesis. *Exp. Cell. Res.* 312 (5), 549–560. doi:10.1016/j.yexcr.2005.11.012

Singh, R. P., Srivastava, S., Ehlers, J. P., Bedi, R., Schachat, A. P., and Kaiser, P. K. (2014). A single-arm, investigator-initiated study of the efficacy, safety and tolerability ofintravitrealaflibercept injection in subjects with exudative age-related maculardegeneration, previously treated withranibizumaborbevacizumab; 6-month interim analysis. *Br. J. Ophthalmol.* 98, i22–27. doi:10.1136/bjophthalmol-2013-304798

Stenirri, S., Santambrogio, P., Setaccioli, M., Erba, B. G., Pia Manitto, M., Rovida, E., et al. (2012). Study of FTMT and ABCA4 genes in a patient affected by age - related macular degeneration:identification and analysis of new mutations. *Clin. Chem. Lab. Med.* 50 (6), 1021–1029. doi:10.1515/cclm-2011-0854

Tavakoli, Z., Yazdian, F., Tabandeh, F., and Sheikhpour, M. (2020). Regenerative medicine as a novel strategy for amd treatment: A review. *Biomed. Phys. Eng. Express* 6 (1), 012001. doi:10.1088/2057-1976/ab269a

Vogl, W. D., Bogunovi, H., Waldstein, S. M., Riedl, S., and Schmidt-Erfurth, U. (2021). Spatio-temporal alterations in retinal and choroidal layers in the progression of age-related macular degeneration (amd) in optical coherence tomography. *Sci. Rep.* 11 (1), 5743. doi:10.1038/s41598-021-85110-y

Wang, J. L., Xi, Y., Liu, Y. L., Wang, Z. h., and Zhang, Q. (2013). Combination of targeted pdt and anti-vegf therapy for rat cnv by rgd-modified liposomal photocyanine and sorafenib. *Invest. Ophthalmol. Vis. Sci.* 54 (13), 7983–7989. doi:10.1167/iovs.13-13068

Wang, J. L., Xi, Y., Liu, Y. L., Wang, Z. h., and Zhang, Q. (2013). Combination of targeted PDT and anti-VEGF therapy for Rat CNV by RGD-modified liposomal photocyanine and sorafenib. *Invest. Ophthalmol. Vis. Sci.* 54 (13), 7983–7989. doi:10.1167/iovs.13-13068

Waters, S. B., Zhou, C., Nguyen, T., Zelkha, R., Lee, H., Kazlauskas, A., et al. (2021). VEGFR2 trafficking by KIF13B Is a novel therapeutic target for wet age-related macular degeneration. *Invest. Ophthalmol. Vis. Sci.* 62 (2), 5. doi:10.1167/iovs.62.2.5

Weber, B. H., Vogt, G., Wolz, W., Ives, E. J., and Ewing, C. C. (1994). Sorsby's fundus dystrophy is genetically linked to chromosome 22q13–Qter. *Nat. Genet.* 7 (2), 158–161. doi:10.1038/ng0694-158

Wei, C., and Li, X. (2020). The role of photoactivated and non-photoactivated verteporfin on tumor. *Front. Pharmacol.* 11, 557429. doi:10.3389/fphar.2020.557429

Wei, Y., Hsu, J. C., Chen, W., et al. (2020). *A simultaneous inference procedure to identify subgroups from rcts with survival outcomes: application to analysis of amd progression studies*. 105–108.

Wu, M., Liu, Y., Zhang, H., Lian, M., Chen, J., Jiang, H., et al. (2019). Intravenous injection of l-aspartic acid β-hydroxamate attenuates choroidal neovascularization via anti-vegf and anti-inflammation. *Exp. Eye Res.* 182, 93–100. doi:10.1016/j.exer.2019.03.018

Yildirim, O., Tamer, L., Tamer, L., Muslu, N., Ercan, B., Atik, U., et al. (2004). Changes in antioxidant enzyme activity and malondialdehyde level in patients with age-related macular degeneration. *Ophthalmologica* 218 (3), 202–206. doi:10.1159/000076845

Yla, B., Mfa, B., Jca, B., Li, S., Dai, X., Shan, G., et al. (2021). Repurposing bortezomib for choroidal neovascularization treatment via antagonizing vegf-a and pdgf-d mediated signaling. *Exp. Eye Res.* 204, 108446. doi:10.1016/j.exer.2021.108446

Yu, L., Chen, C. Z., Yi, Z. H. Z., et al. (2015). Clinical observation of intravitrealinjection of conbercept treating exudative age - related maculardegeneration chinese. *J. Ocular Fundus Dis.* 31 (3), 256–259.

ZarbinMAHill, L., Maunz, A., Gliem, M., and Stoilov, I. (2021). Anti-VEGF-resistant subretinal fluid is associated with better vision and reduced risk of macular atrophy. *Br. J. Ophthalmol.* 87 (5), 8688. doi:10.1136/bjophthalmol-2020-318688

Zhang, C. F., Li, Z. Q., Du, H., and Han, B. l. (2003). Natural course and prognosis of visual acuity in patients of age-related macular degeneration with occult choroidal neovascularization. *Zhonghua. Yan Ke Za Zhi.* 39 (7), 415–418.

Zhang, M., Zhang, J., Yan, M., Li, H., Yang, C., and Yu, D. (2008). Recombinant anti-vascular endothelial growth factor fusion protein efficiently suppresses choridal neovasularization in monkeys. *Mol. Vis.* 10, 37–49.

Zhang, W., Xiao, Y., and Gao, X. W., (2014). A study of the association about serum TGF- B1 and IL-6 in wet age-related macular degeneration. *Chin. J. Pract. Ophthalmol.* 32 (4), 428–431.

Zhu, L., Parker, M., Enemchukwu, N., Shen, M., Zhang, G., Yan, Q., et al. (2020). Combination of apolipoprotein-a-i/apolipoprotein-a-i binding protein and anti-vegf treatment overcomes anti-vegf resistance in choroidal neovascularization in mice. *Commun. Biol.* 3 (1), 386. doi:10.1038/s42003-020-1113-z

Frontiers in
Molecular Biosciences

Explores biological processes in living organisms on a molecular scale

Focuses on the molecular mechanisms underpinning and regulating biological processes in organisms across all branches of life.

Discover the latest Research Topics

See more →

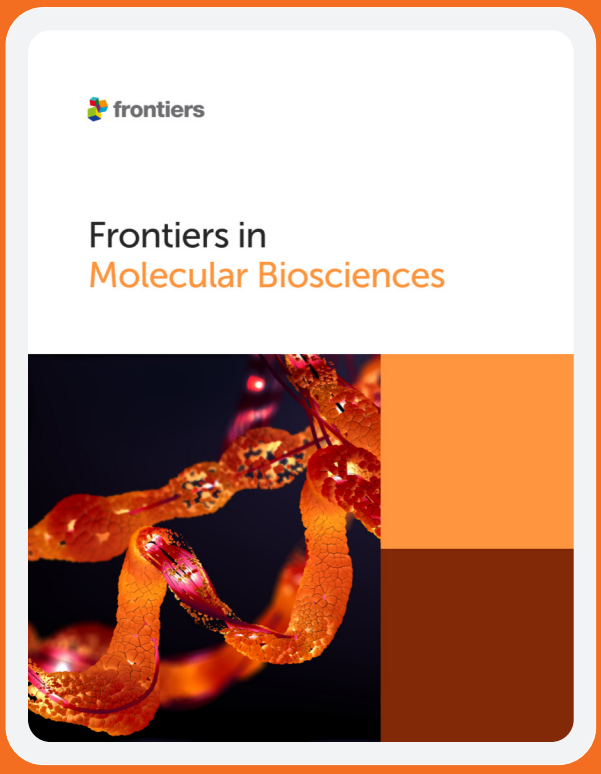

Frontiers

Avenue du Tribunal-Fédéral 34
1005 Lausanne, Switzerland
frontiersin.org

Contact us

+41 (0)21 510 17 00
frontiersin.org/about/contact